

**Cytotoxicity evaluation of methylglyoxal in HepG2 and H9c2 cells with emphasis on oxidative stress, cancer promotion and general metabolism**

By

**Sruthi C R**

**AcSIR Registration Number: 10BB17J39012**

A Thesis submitted to the  
Academy of Scientific and Innovative Research  
for the award of the degree of

**DOCTOR OF PHILOSOPHY**

in

**SCIENCE**

Under the supervision of

**Dr. K G Raghu**

Chief Scientist



**CSIR- National Institute for Interdisciplinary Science and Technology  
(CSIR-NIIST), Thiruvananthapuram**



Academy of Scientific and Innovative Research  
AcSIR Headquarters, CSIR-HRDC campus  
Sector 19, Kamla Nehru Nagar,  
Ghaziabad, U.P. – 201 002, India

**April 2023**

## CERTIFICATE

This is to certify that the work incorporated in this Ph.D. thesis entitled, "Cytotoxicity evaluation of methylglyoxal in HepG2 and H9c2 cells with emphasis on oxidative stress, cancer promotion and general metabolism", submitted by Sruthi C R to the Academy of Scientific and Innovative Research (AcSIR) in partial fulfilment of the requirements for the award of the Degree of Doctor of Philosophy in Sciences, embodies original research work carried out by the student. We further certify that this work has not been submitted to any other University or Institution in the part or full for the award of any degree or diploma. Research materials obtained from other sources and used in this research work have been duly acknowledged in the thesis. Images, illustrations, figures, tables etc., used in the thesis from other sources, have also been duly cited and acknowledged.

  
Sruthi C R

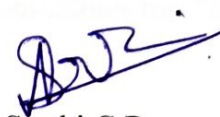
  
10/04/2023

Dr. K G Raghu (Retd.)

(Thesis Supervisor)

## STATEMENTS OF ACADEMIC INTEGRITY

I, Sruthi C R, a Ph.D. student of Academy of Scientific and Innovative Research (AcSIR) with Registration No. 10BB17J39012 hereby undertake that, the thesis entitled **“Cytotoxicity evaluation of methylglyoxal in HepG2 and H9c2 cells with emphasis on oxidative stress, cancer promotion and general metabolism”** has been prepared by me and that the document reports original work carried out by me and is free of any plagiarism in compliance with the UGC Regulations on *“Promotion of Academic Integrity and Prevention of Plagiarism in Higher Educational Institutions (2018)”* and the CSIR Guidelines for *“Ethics in Research and in Governance (2020).”*



Sruthi C R

Date 10-04-2023

Thiruvananthapuram

---

It is hereby certified that the work done by the student, under my/ our supervision, is plagiarism-free in accordance with the UGC Regulations on *“Promotion of Academic Integrity and Prevention of Plagiarism in Higher Educational Institutions, (2018)”* and the CSIR Guidelines for *“Ethics in Research and in Governance (2020).”*



Dr. K.G. Raghu

Date

Thiruvananthapuram

## DECLARATION

I, **Sruthi C R**, bearing ACSIR Registration No. 10BB17J39012 declare: that my thesis entitled, **“Cytotoxicity evaluation of methylglyoxal in HepG2 and H9c2 cells with emphasis on oxidative stress, cancer promotion and general metabolism”** is plagiarism free in accordance with the UGC Regulations on *“Promotion of Academic Integrity and Prevention of Plagiarism in Higher Educational Institutions (2018)”* and the CSIR Guidelines for *“Ethics in Research and in Governance (2020)”*.

I would be solely held responsible if any plagiarised content in my thesis is detected, which is violative of the UGC regulations 2018.



**Sruthi C R**

Thiruvananthapuram

10th April 2023

## Acknowledgements

*I've encountered a world of excitement, joy, surprises, and hardships during my time as a PhD student. It was difficult to develop independently and carve out a niche for oneself on this voyage. This was made possible by the unwavering support of several people.*

*My profound gratitude goes out to Dr K.G. Raghu, Chief Scientist (Rtd), CSIR-NIIST, for giving me a chance to pursue a Doctorate under his direction and for his ongoing support, tolerance, inspiration, and motivation. His vast knowledge and wealth of experience have inspired me throughout my whole academic career and daily life. His thoughtful criticism inspired me to think more clearly and elevated the quality of my work. His advice has been helpful to me in all of my research and writing. I also thank him for giving me access to the lab equipment needed for this project. I could not have asked for a more fabulous mentor and supervisor for my Doctorate study.*

*I am very grateful to Dr C. Anandharamakrishnan, Director, and Dr A. Ajayaghosh, former Director of CSIR-NIIST, Trivandrum, who provided the facilities needed to finish the research work.*

*Also, I want to thank Mr V.V. Venugopal and Dr Dileep Kumar BS, the current and former heads of the Agro-processing and Technology Division, for their support and words of encouragement. I sincerely appreciate the informative remarks and recommendations from the Doctoral Advisory Committee, which consists of Dr Dileep Kumar BS, Dr Binod Parameshwaran, and Dr Kaustabh Kumar Maiti. I also want to express my gratitude to the AcSIR coordinators Dr Luxmi Verma, Dr Suresh C.H., and Dr K. Karunakaran, for their assistance in ensuring I met all of the AcSIR standards.*

*I want to thank Dr P. Jayamurthy, Dr Priya S, Dr M. V. Reshma, Dr P. Nisha, Dr Anjineyulu Kothakota, Dr Venkatesh R, Mr Venkatesh T, Dr Tripti Mishra, Dr Beena Joy, Mr D.R. Soban*

*Kumar, and Mrs Divya Mohan for their help and support. I sincerely appreciate all of the assistance and cooperation from both past and present members of the Agro-processing and Technology Division.*

*I want to thank all of my senior labmates, Dr Sindhu G, Dr Shyni G L, Dr Soumya R.S, Dr Genu George, Dr Salin Raj, Dr Anupama Nair, Dr Preetha Rani M R, Dr Sreelekshmi Mohan and Dr Swapna Sasi U S for their invaluable help, and support during all stages of my research activities.*

*My friends, Ms Eveline M Anto, Ms Poornima M S, Ms Lekshmi Sundar and Ms Suryalekshmi V A who, have always been a significant source of support and happiness and with whom I have made many beautiful memories both in and outside of the lab, deserve a particular word of gratitude.*

*It gives me great pleasure to thank Ms Lekshmi Krishnan, Ms Sannya, Ms Shini, Ms Nidhina, Ms Taniya M. S., Ms Anagha Nair, Ms Anusha, Mr Ashin, Mr Billu Abraham, and all the members of APTD, I'm grateful and humbled by everything you've done for me. I am extremely thankful to Mr Vinit Singh, MSc project student, for his helping hands and motivation. Special thanks to Mr Pratheesh and Mr Sreejith for their irreplaceable assistance in the technical and official formalities. I would also like to express my gratitude to each and every member of the NIIST technical, administrative, academic programme committee, and library personnel who has assisted with this project in some way. I owe the University Grants Commission in New Delhi for their financial support in the form of research fellowships.*

*This work could have never been done without many sacrifices made by my most special people. Sacrifices made by my parents, Mr Rajan K G and Mrs Sujatha B, from the beginning of my life, hold the strongest pillar that shaped me into what and where I am today. It is my pleasure to thank my parents, my brother and my whole family for their support throughout this life. My life with PhD and my life partner both started together; without the sacrifices made by my husband, this work would never have met completion. His keen interest in my academic achievements and*

*support in fulfilling my dreams and ambitions are unbeatable. I am incredibly grateful for the tremendous understanding and motivation given by my husband, Mr Murukaraj R, and my family, especially my mother-in-law, Mrs V K Vijayamma, throughout these years. My son, Master Hayaan M S, needs remarkable words of gratitude for sacrificing the need of a mother at the most important phases of his first five years in the world. This achievement in my life is dedicated to my dearest son.*

*Above all, I profoundly thank and worship the Almighty for all of his favours and for granting me the fortitude and perseverance to attain this important academic milestone.*

Sruthi C R

# Table of Contents

## Chapter 1: Introduction

1.1	What is diabetes mellitus? .....	1
1.2	Diabetic complications .....	2
1.3	Advanced glycation end products .....	3
1.3.1	Formation of AGEs .....	4
1.3.2	Other pathways involved in AGEs formation .....	5
1.3.3	Pathophysiological impacts of AGEs .....	5
1.3.4	Mechanisms of Action .....	6
1.4	Receptor for advanced glycation end products (RAGE) .....	6
1.4.1	Many isoforms of RAGE have been widely reported: .....	7
1.4.1.1	Full-length RAGE .....	7
1.4.1.2	Soluble forms of RAGE.....	7
1.4.1.3	Dominant-negative RAGE (DN-RAGE).....	7
1.4.1.4	$\Delta$ N RAGE .....	8
1.4.2	RAGE activation by AGEs .....	8
1.5	Methylglyoxal (MGO).....	9
1.5.1	MGO regulation .....	9
1.5.1.1	MGO detoxification by glyoxalase system .....	10
1.5.1.2	MGO detoxification by reduction.....	10
1.5.1.3	MGO detoxification by oxidation .....	11
1.5.3	MGO-protein adduct formation .....	12
1.5.4	Physiological Impact of MGO and MG-AGEs.....	14
1.5.4.1	The Role of MGO and MGO-AGES in diabetes.....	14
1.5.4.2	The Role of MGO and MGO-AGES in liver disease.....	15
1.5.4.3	The Role of MGO and MGO-AGES in cancer .....	16
1.5.4.4	The Role of MGO and MGO-AGES in cardiovascular diseases .....	19
1.6	Aim and Objectives .....	20
1.7	References.....	21

## **Chapter 2: Alterations on glyoxalase pathway and redox status by methylglyoxal in HepG2 cells**

<b>2.1 Introduction.....</b>	<b>37</b>
<b>2.2 Materials and methods .....</b>	<b>39</b>
2.2.1 Reagents .....	39
2.2.2 Cell culture and treatment.....	40
2.2.3 Cell viability analysis.....	40
2.2.4 ROS generation analysis.....	40
2.2.5 Protein carbonyl assay.....	41
2.2.6 Western blotting analysis.....	42
2.2.7 Statistics.....	42
<b>2.3 Results.....</b>	<b>42</b>
2.3.1 Effects of MGO on the viability of HepG2 cells .....	42
2.3.2 MGO impairs the glyoxalase system.....	43
2.3.3 MGO-induced accumulation of MGO-adducts.....	43
2.3.4 MGO stimulated the expression RAGE and AGE-R1.....	44
2.3.5 MGO stimulates ROS generation and protein carbonyl formation.....	45
2.3.6 MGO alters innate antioxidants protein expression.....	46
<b>2.4 Discussion.....</b>	<b>47</b>
<b>2.5 Summary and Conclusion .....</b>	<b>50</b>
<b>2.6 References.....</b>	<b>51</b>

## **Chapter 3: The alterations in glucose metabolism and genesis of the Warburg effect in HepG2 cells by methylglyoxal**

<b>3.1 Introduction.....</b>	<b>56</b>
<b>3.2 Materials and methods .....</b>	<b>58</b>
2.2.1 Reagents.....	58
3.2.2 Cell culture and treatment .....	59
3.2.3 Glucose uptake analysis.....	59
3.2.3.1 Analysis of glucose uptake by flow cytometry .....	59
3.2.3.2 Analysis of glucose uptake.....	59
3.2.4 Western blotting analysis .....	60
3.2.5 Measurement of hexokinase activity (HK) .....	61

3.2.6 Analysis of lactate production.....	61
3.2.7 Oxygen consumption rate assay.....	61
3.2.8 Statistics .....	62
3.3 Results.....	62
3.3.1 MGO enhanced glucose uptake in HepG2 cells .....	62
3.3.2 Effect of MGO on glucose transporters (GLUT 1 and GLUT 2) .....	63
3.3.3 Effect of MGO on glycolytic enzymes .....	64
3.3.4 MGO facilitates metabolic flux toward aerobic glycolysis in HepG2 cells .....	65
3.3.5 Effect of MGO on oxygen consumption rate (OCR).....	66
3.3.6 MGO mediated induction of HIF-1 $\alpha$ expression.....	67
3.3.7 Effect of MGO on Hippo pathway.....	68
3.3.8 MGO induced c-Myc expression .....	68
3.4 Discussion.....	69
3.5 Summary and Conclusion .....	73
3.6 References.....	74

## **Chapter 4: Alterations in fatty acid metabolism by methylglyoxal via the amendment of autophagy, mitochondrial dynamics and endoplasmic reticulum stress in HepG2 cells**

4.1 Introduction.....	80
4.2 Materials and Methods .....	81
4.2.1 Reagents .....	81
4.2.2 Cell culture and treatment.....	83
4.2.3 Oil-red-O staining .....	83
4.2.4 Western Blotting analysis .....	83
4.2.5 Detection of autophagy .....	84
4.2.6 Determination of the mitochondrial mass .....	84
4.2.7 Determination of the mitochondrial transmembrane potential ( $\Delta\Psi$ M) in HepG2 cells .	84
4.2.8 Statistics .....	85
4.3 Results .....	85
4.3.1 Effect of MGO on lipid accumulation .....	85
4.3.2 Effect of MGO on lipid metabolism .....	86
4.3.4 MGO regulates PTEN/ Akt pathway .....	89
4.3.5 MGO regulated ERK pathway .....	89

4.3.6 Effect of MGO on the p38 pathway .....	91
4.3.7 MGO induced ER stress in HepG2 cells .....	91
4.3.7 Effect of MGO on mitochondrial mass .....	92
4.3.8 MGO causes the dissipation of $\Delta\Psi$ M. ....	93
4.3.9 Effect of MGO on mitochondrial dynamics .....	95
4.4 Discussion .....	95
4.5 Summary and Conclusion .....	100
4.6 References.....	101

## **Chapter 5: Variation in redox status via modification in glyoxalase pathway by methylglyoxal in H9c2 cells**

5.1 Introduction.....	105
5.2 Materials and Methods .....	106
5.2.1 Reagents .....	106
5.2.2 Cell culture and treatment.....	107
5.2.3 Cell viability analysis .....	107
5.2.4 ROS generation analysis.....	107
5.2.5 Western blotting analysis.....	108
5.2.6 Glucose uptake analysis.....	108
5.2.7 Determination of the mitochondrial transmembrane potential ( $\Delta\Psi$ M) in H9c2 cells ...	108
5.2.8 Determination of the mitochondrial Superoxide production in H9c2 cells .....	109
5.2.9 Immunofluorescence .....	109
5.2.10 Statistics .....	110
5.3 Results.....	110
5.3.1 Effects of MGO on the viability of H9c2 cells .....	110
5.3.2 MGO impairs the glyoxalase system.....	111
5.3.3 MGO-induced accumulation of MG-adducts.....	111
5.3.4 MGO stimulated the expression RAGE and AGE-R1.....	112
5.3.5 Effect of MGO in ROS generation in H9c2 cells .....	113
5.3.6 Effect of MGO on glucose uptake in H9c2 cells .....	114
5.3.7 MGO causes alteration of mitochondrial transmembrane potential ( $\Delta\Psi$ M) .....	114
5.3.8 MGO induced mitochondrial superoxide production in H9c2 cells.....	116
5.3.9 Effect of MGO on Hsp60 and Hsp70 .....	117
5.3.10 Nf- $\kappa$ B translocation during MGO exposure.....	117

<b>5.4 Discussion.....</b>	<b>119</b>
<b>5.5 Summary and Conclusion .....</b>	<b>121</b>
<b>5.6 References.....</b>	<b>121</b>
<b>Chapter 6: Summary and conclusion.....</b>	<b>126</b>

## List of figures

Figure No.	Captions	Page No.
1.1	Structure of methylglyoxal	9
1.2	Different ways to detoxify MGO	11
1.3	Chemical structures of nucleic and amino acids that have been modified by MGO	13
1.4	Molecular interplay between RAGE and its ligands directing the subsequent cellular events towards the execution of Hallmarks of Cancer.	18
2.1	Effect of various concentrations of MGO on cell viability in HepG2 cells.	43
2.2	Effect of MGO on glyoxalase system and intracellular adducts formation.	44
2.3	Effect of MGO receptors for AGEs	45
2.4	Genesis of oxidative stress with MGO in HepG2 cells.	46
2.5	Antioxidant status MGO treated HepG2 cells.	47
2.6	Schematic representation of altered glyoxalase pathway and redox status by MGO	50
3.1	Determination of glucose uptake in HepG2 cells.	63
3.2	Effect of MGO on GLUTs expression.	64
3.3	Effect of MGO on Glycolytic enzymes	65
3.4	Effect of MGO on aerobic glycolysis	66
3.5	Determination of oxygen consumption rate	67
3.6	Effect of MGO on HIF-1 $\alpha$ expression	68
3.7	Effect of MGO on the expression of pYAP/YAP and c-Myc	69
3.8	Schematic representation of MGO-induced Warburg effect	73
4.1	Analysis of lipid droplet formation using oil red O staining	86
4.2	MGO induces aberrant lipid metabolism in HepG2 cells	87
4.3	MGO induces AMPK activation for the initiation of autophagy	88
4.4	MGO induces AKT activation via PTEN inhibition	89
4.5	MGO induces RAF/ERK pathway	90

4.6	Effect of MGO on p38 expression	91
4.7	MGO induces initiation of ER stress	92
4.8	Effect of MGO on mitochondrial content	93
4.9	MGO causes dissipation of $\Delta\Psi$ M	94
4.10	Effect of MGO on mitochondrial dynamics	95
4.11	Schematic representation of MGO-induced tumour cell survival, growth and poliferation	100
5.1	Effect of various concentrations of MGO in H9c2 cells	110
5.2	Effect of MGO on glyoxalase system and intracellular adducts formation	111
5.3	Effect of MGO AGEs stimulated receptors	112
5.4	Effect of MGO in induction of oxidative stress	113
5.5	Determination of glucose uptake in H9c2 cells	114
5.6	MGO causes dissipation of $\Delta\Psi$ M in H9c2 cells	115
5.7	Mitochondrial superoxide generation in H9c2 cells	116
5.8	Alteration in expression of heat shock proteins	117
5.9	Alteration of NF- $\kappa$ B signaling pathway in H9c2 cells	118
5.10	Schematic representation of MGO induced cellular dysfunction in H9c2	121
6.1	Schematic representation of MGO-induced toxicity in HepG2 and H9c2 cells.	130

## ABBREVIATIONS

2-DG	:	2-deoxy-D-glucose
2-NBDG	:	2-[N-(7-nitrobenz-2-oxa-1,3-diazol-4-yl) amino]-2-deoxy-D-glucose
3DG	:	3-deoxyglucosone
ACC	:	Acetyl CoA carboxylase
ACOX	:	Peroxisomal acyl-coenzyme A oxidase 1
AGE	:	Advanced glycated end products
AGE-R1	:	Advanced glycation end products-receptor 1
AGEs	:	Advanced glycation end products
AKT	:	Protein kinase B
AMPK	:	Activated protein kinase
ANOVA	:	One-way analysis of variance
BCA	:	Bicinchoninic acid
BSA	:	Bovine serum albumin
Ca <sup>2+</sup>	:	Calcium
CD36	:	Cluster of differentiation 36
CVDs	:	Cardiovascular diseases
DAPI	:	4', 6 diamidino-2-phenylindole
DCF	:	2,7 dichlorofluorescein
DCFH DA	:	2', 7' dichlorodihydrofluorescein diacetate
DM	:	Diabetes Mellitus
DMEM	:	Dulbecco's modified eagle's medium

DMSO	:	Dimethyl sulfoxide
DNPH	:	2,4-Dinitrophenylhydrazine
DRP1	:	Dynamin-1-like protein
DTT	:	Dithiothreitol
ECL	:	Chemiluminescence
ECM	:	Extracellular matrix
EDTA	:	Ethylene diamene tetraacetic acid
ER	:	Endoplasmic reticulum
ERK	:	Extracellular signal-regulated kinase ½
ETC	:	Electron transport chain
FASN	:	Fatty acid synthase
FBS	:	Fetal bovine serum
GAPDH	:	Glyceraldehyde 3-phosphate dehydrogenase
GLO 1	:	Glyoxalase 1
GLO 2	:	Glyoxalase 2
GLUT	:	Glucose transporter
GSH	:	Reduced glutathione
HBSS	:	Hanks balanced saline solution
HCL	:	Hydrochloride
HEPES	:	4-(2-hydroxyethyl)-1-piperazineethanesulfonic acid
HGP	:	Hepatic glucose production
HIF-1 $\alpha$	:	Hypoxia-inducible factor
HK II	:	Hexokinase II

HMGCR	:	3-hydroxy-3-methylglutaryl-CoA reductase
HO-1	:	Heme oxygenase 1
HRP	:	Horseradish peroxidase
IGF	:	Impaired Fasting Glycaemia
IGT	:	Impaired Glucose Tolerance
JNK	:	c-Jun N-terminal kinases
LDH-A	:	Lactate dehydrogenase-A
MEME	:	Minimal essential media Eagles
MGO	:	Methylglyoxal
MTT	:	3-(4,5-dimethylthiazol-2-yl)-2,5-diphenyl tetrazolium bromide
NF- $\kappa$ b	:	Nuclear transcription factor kappa-B
Nrf2	:	Nuclear factor E2-related factor 2
PBS	:	Phosphate buffered saline
PDK1	:	Pyruvate dehydrogenase lipamide kinase isozyme 1
PFK 1	:	Phosphofructokinase 1
pIRE-1 $\alpha$	:	Phosphorylated IRE1 $\alpha$
PKC	:	Protein kinase C
PTEN	:	Phosphatase and tensin homolog
PVDF	:	Polyvinylidene di fluoride
RAC1	:	Ras-related C3 botulinum toxin substrate 1
RAF1	:	proto-oncogene c-RAF
RAGE	:	Receptors for advanced glycation end products
RIPA	:	Radio immunoprecipitation assay

ROS	:	Reactive oxygen species
SCD1	:	Stearoyl-CoA desaturase 1
SDS	:	Sodium dodecyl sulphate
SOD 1	:	Superoxide dismutase 1
SOD 2	:	Superoxide dismutase 2
T1DM	:	Insulin dependent diabetes mellitus (Type 1DM)
T2DM	:	Insulin independent diabetes mellitus (Type 2DM)
TCA	:	Trichloroacetic acid
UPR	:	Unfolded protein responses
VEGF	:	Vascular endothelial growth factor
XBP1	:	X-box binding protein 1
YAP	:	Yes Associated Protein

# Chapter 1

## Introduction

---

---

### 1.1 What is diabetes mellitus?

Diabetes, or diabetes mellitus (D.M.), is a critical, long-term (or "chronic") disorder that manifests as elevated blood glucose levels when the body is unable to make any sufficient amounts of or utilise the insulin that is produced (Sapra & Bhandari, 2022). Insulin enables circulatory glucose to enter the body's cells, which can be stored or transformed into energy. Furthermore, the metabolism of fat and protein relies on insulin. Hyperglycemia, the clinical manifestation of diabetes, is characterised by high blood glucose levels, which develop when insufficient insulin is produced, or cells fail to respond to it (Sapra & Bhandari, 2022).

Two significant mechanisms have been put forth in relation to the disease's pathophysiology. The two main factors contributing to persistent hyperglycemia associated with D.M. are innate resistance of body cells to insulin action and autoimmune death of pancreatic beta-cells, which results in insufficient insulin production (Toren et al., 2021).

Suppose an insulin deficiency is allowed to persist over an extended period; in that case, it can harm many of the body's organs and result in potentially fatal and disabling health issues like cardiovascular diseases (CVD), nerve damage (neuropathy), kidney damage (nephropathy), lower limb amputations, and eye disease (primarily affecting the retina) that cause vision loss and even blindness (Tomic et al., 2022). However, these dangerous problems can be postponed or avoided if diabetes is adequately managed.

Type 1 D.M. (T1DM), type 2 D.M. (T2DM), and gestational D.M. (GDM) are the three primary kinds of the disease (Sapra & Bhandari, 2022). The first kind, sometimes referred to as "juvenile/childhood-onset diabetes" or "insulin-dependent diabetes," is characterised by an insufficient amount of insulin produced by the human body. It is treated by routinely administering insulin analogues. T1DM's precise cause has not yet been identified. The scientific community does, however, believe that a complex interaction of genetic and environmental variables causes the early stages of T1DM.

The key feature of T2DM, often known as "adult-onset diabetes" or "non-insulin dependent diabetes," is insulin resistance. In other words, it results from the body's inefficient response to the generated insulin. Insulin insufficiency may develop as the illness worsens (Wondmkun, 2020). T2DM is mainly driven by ethnicity, family history of diabetes and obesity, bad eating habits, and insufficient exercise (Galicia-Garcia et al., 2020). It is frequently referred to as the transition stage between normoglycaemia and diabetes as having "Impaired Glucose Tolerance" (IGT) or "Impaired Fasting Glycaemia" (IFG). Since it is predicted that one in four people with IGT/IFG will develop D.M. within a time frame of three to five years, the last two symptoms are typically recognised as T2DM precursors (Genuth et al., 2018).

Finally, gestational diabetes mellitus (GDM) is the term for high blood sugar levels in pregnant women who have never had the disease (Mumtaz, 2000). In this instance, the infant has a high probability of acquiring D.M. as an adult (Clausen et al., 2008).

## **1.2 Diabetic complications**

Over time, diabetes can cause major problems that can damage many different organ systems in the body. Microvascular and macrovascular complications of diabetes are distinct

categories. Retinopathy, neuropathy, and nephropathy are examples of microvascular problems, while peripheral vascular disease, cardiovascular disease, and stroke are examples of macrovascular complications (Cade, 2008). Amputation may eventually result from peripheral vascular disease, a condition that can cause damage or wounds that do not heal. For people with type 1 and type 2 diabetes, the types of complications are similar, but the frequency or timing of their onset can differ (Deshpande et al., 2008).

Through a number of proposed mechanisms, including inflammation, oxidative stress, endoplasmic reticulum stress, and apoptosis, the persistent hyperglycemia of diabetes drives the progression of both macro- and microvascular complications in the neurons, eyes, kidneys, heart, liver, and other key organs. The development of diabetic complications is mediated by oxidative stress, inflammatory cytokines, transcription factors, enzymes, activation of protein kinase-c (PKC), accumulation of intracellular sorbitol and tissue advanced glycation end products (AGEs), the polyol pathway, and the production of superoxide in the mitochondria (Sruthi & Raghu, 2021). Non-enzymatic glycosylation of proteins or lipids occurs upon prolonged exposure to glucose and produces advanced glycation end products (Tamura et al., 2003). Through their interaction with their receptor, which primarily activates NADPH oxidase and the nuclear transcription factor kappa-B (NF- $\kappa$ B) pathway, AGE formation contributes to oxidative stress in a variety of cell types. This results in inflammatory and thrombogenic alterations that promote in the pathogenesis of vascular diabetic complications (Brownlee, 2005; Giacco and Brownlee, 2010; Yamagishi et al., 2012).

### **1.3 Advanced glycation end products**

AGEs are nucleic acids, lipids, or proteins that have been chemically modified. AGEs build up in tissues at a steady, gradual rate and are highly stable and irreversible. However,

hyperglycemia hastens the production of AGEs (Fleming et al., 2011). AGEs can also develop through smoking (Cerami et al., 1997) or from eating food that has been overheated (Uribarri et al., 2010). These are produced by many methods, such as a string of chemical reactions, and they affect or impair the functioning of macromolecules. AGEs are created through non-enzymatic interactions between the free amino groups in these macromolecules and non-reducing carbohydrates. Age and hyperglycemic circumstances speed up the process of AGEs development. Receptors for advanced glycation end products (RAGE) interaction with AGEs have been linked to the emergence of macrovascular and microvascular problems (Galicia-Garcia et al., 2020). Due to AGEs' high degree of stability, they build up in tissues and disrupt cellular processes, which leads to a number of pathophysiological disorders, most notably diabetic complications, cardiovascular diseases (CVDs), Alzheimer's disease, and cancer (Sorci et al., 2013).

### **1.3.1 Formation of AGEs**

The Maillard reaction, first described by Louis Camille Maillard in 1912, is a complex multistep nonenzymatic process that leads to the formation of AGEs (Maillard & LC., 1912). Hodge published the first description of the Maillard reaction's underlying chemical processes in 1953. Early, intermediate, and late stages are the different divisions of the non-enzymatic process (Hodge & E., 1953). The reaction between the carbonyl groups of reducing sugars and the amine residues on proteins, nucleic acids, and lipids initiates the process. A Schiff base, an unstable molecule, is the first by-product created in this process. The more stable Amadori products, also known as early glycation products, are created after a rearrangement of this labile Schiff base (Gerrard, 2005). This unstable Schiff base then proceeds through a rearrangement to generate Amadori products, which are also known as early glycation products (Gerrard, 2005).

These Amadori products fragment into extremely reactive dicarbonyl compounds as methylglyoxal (MGO), glyoxal (G.O.), or deoxyglucosone (1deoxyglucosone [1DG] and 3-deoxyglucosone [3DG]) at the intermediate stage after a sequence of reactions, rearrangements, and dehydration (Gerrard, 2005). "Carbonyl stress" is a state brought on by an accumulation of dicarbonyl molecules. Protein residues containing lysine, histidine, arginine, or cysteine can be attacked by carbonyl compounds (Negre-Salvayre et al., 2009). At a later stage, these dicarbonyl compounds can interact with biological components and go through additional oxidation, dehydration, and cyclisation events to create highly irreversible brownish molecules known as AGEs (Lapolla et al., 2005).

### **1.3.2 Other pathways involved in AGEs formation**

The oxidative stress-mediated oxidation of glucose and the production of dicarbonyl derivatives from lipid peroxidation are two additional mechanisms implicated in the AGEs creation process (Vistoli et al., 2013). Another recognised method for the generation of AGEs is the polyol pathway. Here, sorbitol dehydrogenase transforms sorbitol into fructose after glucose is first converted to sorbitol by aldose reductase. Fructose metabolites are derivatives of dicarbonyls that contribute to the production of AGEs (Lorenzi, 2007).

### **1.3.3 Pathophysiological impacts of AGEs**

The following pathways may be used by AGEs to trigger a response:

- Proteins, including enzymes, can be glycosylated by glycosylating agents, changing or terminating their function (Ulrich & Cerami, 2001).
- Glycosylated proteins can establish crosslinks with other proteins, stiffening tissues that would otherwise be elastic or pliable (Willett et al., 2012).

- Glycated proteins have the ability to function as ligands, activate particular cell membrane receptors (such as RAGE), and trigger cellular responses (Sparvero et al., 2009).

### **1.3.4 Mechanisms of Action**

There are two primary mechanisms by which AGEs cause diseases and disorders: (i) covalent crosslinking of serum and extracellular matrix (ECM) proteins, lipids, and DNA, which results in biochemical impairment and cell disruption; and (ii) interaction of AGEs with their receptors, especially on the AGE-RAGE axis, which triggers a cascade reaction and signaling pathways, resulting in proliferation, autophagy, and apoptosis (Jung et al., 2008). Chen and Guo also found four additional modes: (i) oxidative stress; (ii) mitochondrial dysfunction; (iii) AGEs functioning as antigens and inducing immunological responses; and (iv) AGE-induced allergies (Abdrakhmanov et al., 2020).

## **1.4 Receptor for advanced glycation end products (RAGE)**

The multiligand receptor, known as the receptor for advanced glycation end products (RAGE) is a member of the immunoglobulin superfamily. RAGE is regarded as a pattern-recognition receptor (PRR) since it can recognise a wide variety of ligands that do not have any sequence similarity (Fritz, 2011).

RAGE is a protein with 404 amino acid residues and a molecular mass of approximately 55 kDa (Neeper et al., 1992). One V (variable) and two C (constant) type Ig domains are projected to be present as extracellular domains, followed by a transmembrane spanning domain and a brief cytoplasmic domain with around 50 amino acids (Ramasamy et al., 2011)

All tissues, including the lungs, heart, liver, skeletal muscle, and kidney, express RAGE to varying degrees (Brett et al., 1993). Except for the lungs, where it is expressed more

abundantly, particularly in alveolar epithelial cells, RAGE is expressed at low levels in the majority of tissues. Furthermore, innate and adaptive immune cells have been found to express it (Narumi et al., 2015; Schmidt, 2017).

### **1.4.1 Many isoforms of RAGE have been widely reported:**

#### **1.4.1.1 Full-length RAGE**

Three extracellular domains (variable domain, C1 domain, and C2 domain) make up the complete structure of RAGE. These are followed by a transmembrane and an intracellular or cytoplasmic domain for signal transduction (Bongarzone et al., 2017; Yatime & Andersen, 2013).

#### **1.4.1.2 Soluble forms of RAGE**

RAGE ligands are lured in by circulating versions of RAGE called soluble RAGEs (sRAGE). These lack the cytoplasmic and transmembrane domains necessary for ligand binding and signal transduction, which could have caused cellular harm.

Two types of sRAGE include:

- Endogenous secretory RAGE (esRAGE) is one of the described splice variants. Pre-mRNA undergoes alternative splicing to produce esRAGE (Jules et al., 2013), and
- Cleaved RAGE (cRAGE): The extracellular domain of RAGE can be broken down by metalloproteases such as matrix metalloproteinase-9 (MMP-9) and a disintegrin and metalloproteinase 10 (ADAM10), resulting in cleaved RAGE (cRAGE) (Raucci et al., 2008).

#### **1.4.1.3 Dominant-negative RAGE (DN-RAGE)**

Another RAGE variant has been described that lacks an intracellular domain and cannot participate in signaling pathways (Oliveira et al., 2013).

#### 1.4.1.4 $\Delta N$ RAGE

It is less able to bind ligands because it lacks a V domain (Oliveira et al., 2013).

### 1.4.2 RAGE activation by AGEs

Only one of the many ligands that bind RAGE and trigger a cascade of cellular signals are AGEs. These ligands all share several sheets in their structural make up, which allows RAGE to recognise them (Chaudhuri et al., 2018; Ramasamy et al., 2011; Yan et al., 2010). Numerous diseases have been linked to AGE-RAGE signaling cascades. In particular, AGE-RAGE signaling has a significant impact on diabetes and the difficulties that are related to it (Kay et al., 2016). Vascular endothelial growth factor (VEGF) and TNF- $\alpha$  are known to lower vascular barrier properties and promote permeability in diabetic nephropathy, and AGE-RAGE interaction signals their over expression (Connolly, 1991). Cellular activity and metabolism are directly impacted by the signal cascade that has been triggered. Inflammation and oxidative stress are the key culprits in the damaging process.

The JAK/STAT pathway, MAPK/ERK pathway, Src/RhoA route, PI3K/Akt pathway, activation of PKC, and NADPH oxidase are among the cell signaling pathways that are activated by interactions with RAGE ligands (Asadipooya & Uy, 2019; Negre-Salvayre et al., 2009). These intricate signaling cascades are activated by the generation of ROS and the activation of transcription factors, primarily Nf- $\kappa$ B, AP-1, and Egr-1 (Asadipooya & Uy, 2019).

The expression and secretion of numerous inflammatory response molecules, including COX-2, IL-6, VCAM, ICAM, and TNF- $\alpha$ , are stimulated by NF- $\kappa$ B activation, which controls the AGE-RAGE driven inflammatory pathway (Xie et al., 2013). Additionally, iNOS and NADPH oxidase expression is mediated by NF- $\kappa$ B activation, which results in the production of oxidative stress and ONOO (Negre-Salvayre et al., 2009). According to Rasheed and Haqqi, the NF- $\kappa$ B mediated ROS production degrades mitochondrial function (Rasheed & Haqqi,

2012), and the AGE/RAGE axis also causes E.R. stress (Yu et al., 2017). Sirtuin 1 (SIRT1) expression has been demonstrated to decrease as a result of RAGE activation, which impairs mitochondrial biogenesis (Teissier & Boulanger, 2019).

## 1.5 Methylglyoxal (MGO)

The late 19<sup>th</sup> century saw the discovery of methylglyoxal (MGO; 2-oxopropanal or pyruvaldehyde) as a by-product of the metabolism of glucose, proteins, and lipids (Chakraborty et al., 2014). MGO is a reactive  $\alpha$ -oxoaldehyde. It has a molecular weight of 72 kDa (Leone et al., 2021). Figure 1.1 depicts the ketone group and aldehyde moiety that make up MGO. The ketone group is less reactive than the aldehyde group. MGO is a yellow liquid with a really strong smell. In aqueous solution, it exists in three forms that are in rapid equilibrium: unhydrated (1%), monohydrate (71%) and dehydrated (28%) (Thornalley et al., 2000).

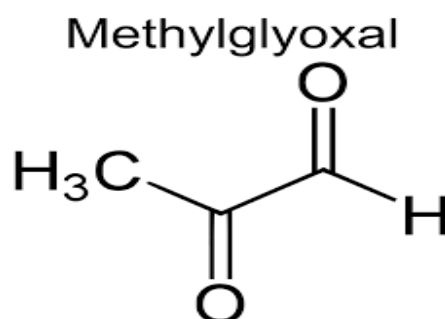


**Figure 1.1:** Structure of methylglyoxal

### 1.5.1 MGO regulation

Since MGO is reactive and can impair cellular function, it is detoxified in a variety of ways.

### 1.5.1.1 MGO detoxification by glyoxalase system

The glyoxalase pathway, which involves the activities of two enzymes: glyoxalase 1 (GLO 1) and glyoxalase 2 (GLO 2), is one of the most notable ways of detoxification of MGO (Aragonès et al., 2020). Non-enzymatically, MGO interacts with glutathione (GSH) to create hemithioacetal, which is recognised by GLO 1 and transformed into S-D-lactoylglutathione. GLO2 then converts S-o-lactoylglutathione to D-lactate, thereby replenishing GSH (Figure 1.2 (A)) (Lai et al., 2022). This pathway's rate-limiting step is GLO 1 identification of the hemithioacetal. MGO detoxification is highly dependent on the availability of GSH. GSH deficiency restricts hemithioacetal synthesis, resulting in MGO buildup (Abordo et al., 1999). The glyoxalase system catalyses irreversible processes. Glyoxalase 1 and 2 are both metalloproteins that rely on zinc in their active sites (Cameron et al., 1999)

### 1.5.1.2 MGO detoxification by reduction

In the presence of GSH, aldose reductase catalyses the NADPH-dependent reduction of MGO into lactaldehyde and subsequently to propanediol (Figure 1.2 (B & C)) (Lai et al., 2022). However, at low GSH concentrations, MGO is converted to acetol, and acetol eventually accumulates. Some diabetic people have been known to accumulate acetol to millimolar levels (Reichard et al., 1986). Acetol can also be transformed back to MGO via CYP2E1-mediated oxidation or disproportionation in the presence of copper ions without the catalysis of any enzymes (Vander Jagt et al., 2001).

The glyoxalase system is the primary metabolic mechanism for detoxifying MGO in the liver, where GSH levels are highest, and aldose reductase is almost non-existent (Vander Jagt et al., 2001). Aldose reductase contributes to MGO breakdown in tissues with high amounts of aldose reductase, such as the eyes, neurons, kidneys, and vasculature (Kador & Kinoshita, 1985).

### 1.5.1.3 MGO detoxification by oxidation

Aldehyde dehydrogenase is crucial for the NAD-dependent oxidation of MGO to pyruvate (Figure 1.2 (D)) (Lai et al., 2022). The aldehyde dehydrogenase family is made up of three isoforms, the names of which are determined by their intracellular location (Izaguirre et al., 1998). The most abundant isozymes are aldehyde dehydrogenase 1 (cytosolic) and aldehyde dehydrogenase 2 (mitochondrial), while aldehyde dehydrogenase 3 (cytosolic) is the least abundant (Hsu et al., 1985; Kurys et al., 1989). According to reports, these three isoforms of aldehyde dehydrogenase can completely hydrate MGO into pyruvate (Izaguirre et al., 1998).

2-oxoaldehyde dehydrogenase, 2-ODH, is also involved in the oxidation of MGO to pyruvate (Figure 1.2 (E)) (Lai et al., 2022). This enzyme was isolated from the liver of a sheep. It is only found in the metabolism of -oxoaldehydes. As a cofactor, it requires NAD or NADPH.

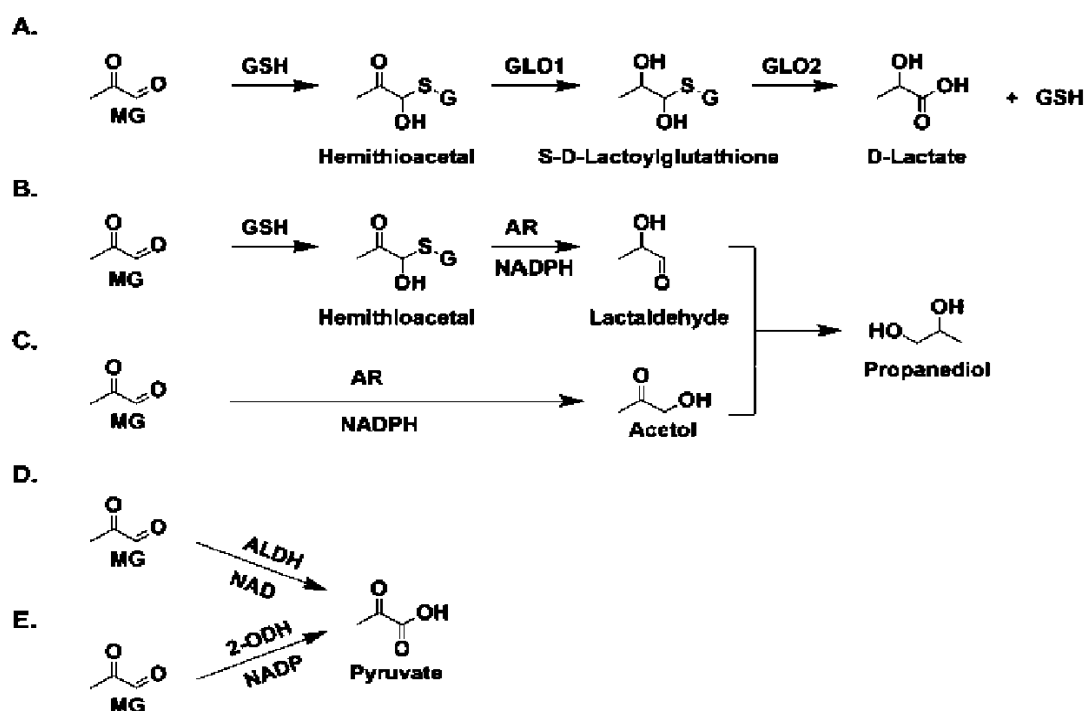


**Figure 1.2:** Different ways to detoxify MGO: (A) System of glyoxalase. MGO reacts with GSH without enzymes to make a hemithioacetal that GLO1 can recognise. GLO1 changes the hemithioacetal into S-d-lactoylglutathione. GLO2 then uses S-d-lactoylglutathione to make d-

lactate. (B) In addition to recognising GLO1, AR also recognises hemithioacetal, which is made when MGO reacts with GSH to make lactaldehyde in an NADPH-dependent reaction. Lactaldehyde can be broken down, which makes propanediol. (C) A.R. can also recognise MGO directly through a process that does not involve GSH. This makes acetol, which is then broken down to make propanediol. A.R. can get rid of MGO without GSH. (D) Pyruvate is made when ALDH oxidises MGO in a way that needs NAD. (E) Pyruvate is made when 2-ODH oxidises MGO in a way that needs NADP. PC: (Lai et al., 2022).

### 1.5.3 MGO-protein adduct formation

The amino acids lysine, arginine, and cysteine are modified by MGO to generate protein adducts that can affect the structure and function of the protein (Figure 1.3). Takahashi first discovered that free amine-containing amino acids, notably lysine and arginine, were affected by high MGO concentrations (Takahashi, 1968). He then assumed that thiol-containing amino acids might also be modified. Later, this was confirmed true; MGO modifies cysteine to produce carboxyethyl cysteine (CEC), a reversible hemithioacetal (Lo et al., 1994). Proteins, particularly BSA, are altered by physiological MGO concentrations, resulting in the formation of MG-H1 (N  $\delta$ -(5-hydro-5-methyl-4-imidazol-2-yl) ornithine). MG-H1 is the most frequent adduct, but MG-H2 and the considerably less frequent MG-H3, can also form (Ahmed et al., 2003). MG-H2 is 2-amino-5-(2-amino-5-hydro-5-methyl-4-imidazol-1-yl) pentanoic acid. Carboxyethyl arginine (CEA) can be produced via the hydrolysis of MG-H3 (CEA) (Klöpfer et al., 2010). MG-H1 can be hydrolysed to generate CEA (McEwen et al., 2021). Additionally, MGO transforms N-acetyllysine into N $\epsilon$ -carboxyethyllysine (CEL), a glycosylamine (Figure 1.3 (C)) (Lo et al., 1994). Lens protein contains CEL, which is linked to ageing. The most prevalent amino acid adduct in clinical samples is MG-H1, which is about ten times more common than CEL (Lai et al., 2022).

A subsequent change that adducted amino acids can experience can lead to macromolecule crosslinking. The protein dimers lysine-lysine (MOLD) and lysine-arginine (MODIC) are created by MGO (Figure 1.3 (D)). It has been suggested that a dG-lysine bond mediates the crosslinking that takes place between DNA and polymerases (Lai et al., 2022).

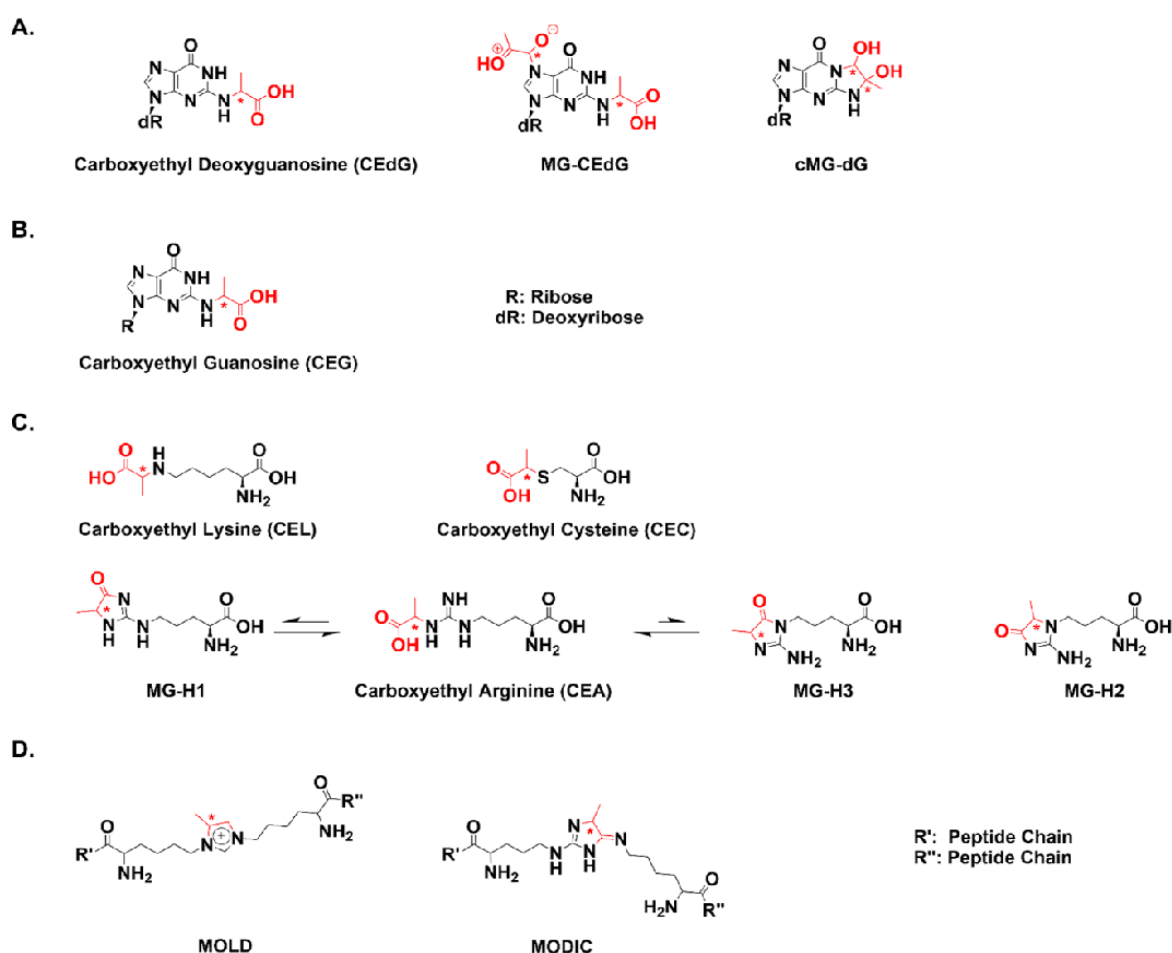


**Figure 1.3:** Chemical structures of nucleic and amino acids that have been modified by MGO.

(A) When MGO is added to dG, three primary adducts are made: CEEdG, cMG-dG, and MG-CEdG. Asterisks show where the stereocenters are, and the MGO addition is displayed in red. dR stands for sugar deoxyribose. (B) A proposed structure for MGO-modified RNA adduct CEG. R stands for sugar ribose. (C) Arginine, lysine, and cysteine are the primary amino acids that MGO changes. When lysine is changed, it makes CEL. When arginine is changed, it makes MG-H1, MG-H2, and MG-H3. When MG-H1 and MG-H3 are broken down by the water, CEA

is made. (D) Lysine dimers MOLD and MODIC can be made from MGO. P.C: (Lai et al., 2022)

### **1.5.4 Physiological Impact of MGO and MG-AGEs**

The development of several illnesses, such as cancer, diabetes, and cardiac disease, is linked to MGO and MG-AGEs. Following the findings that T1DM and T2DM both have higher plasma levels of MGO and MGO-derived AGEs, high glucose concentrations trigger the formation of MGO. Later studies have backed up the significance of MGO in diabetes and issues linked to diabetes.

#### **1.5.4.1 The Role of MGO and MGO-AGES in diabetes**

Given that MGO production depends on glucose metabolism, particularly in T1DM and T2DM, MGO is closely linked to conditions when blood glucose levels are increased. Specifically, with ERK1/2 and AKT, a signaling pathway crucial for regulating insulin sensitivity and glucose uptake, higher intracellular MGO levels reduced cellular responses to insulin in addition to generating oxidative stress and inflammation via AGE/RAGE signaling (Riboulet-Chavey et al., 2006). Therefore, too much MGO adds to insulin resistance, a T2DM symptom. People with T1DM and T2DM had significantly higher serum MGO and MG-AGEs (Ahmed et al., 2005). Serum MGO levels were found to be considerably greater in young T1DM patients without problems than in control non-diabetic individuals (Han et al., 2007). These findings, which show a connection between high MGO levels and the onset of either T1DM or T2DM, have been replicated in newly diagnosed T2DM patients (Kong et al., 2014). Secondary complications are a serious risk for those with T1D or T2D. These issues are linked to poor glycemic control, and it is claimed that MGO and MG-AGEs are connected to and may even cause them through RAGE-dependent processes. It has been thoroughly discussed above how MGO and MG-AGEs are linked to diabetic consequences like nephropathy,

cardiovascular issues, cancer, and skeletomuscular illness. In addition to these, MG-AGEs are linked to retinopathy, neuropathy, and vascular problems (Lai et al., 2022).

#### **1.5.4.2 The Role of MGO and MGO-AGES in liver disease**

When compared to untreated control rats, liver MGO levels and D-lactate were higher in rats given carbon tetrachloride (CCl<sub>4</sub>) to cause early-stage hepatitis (Wang et al., 2018). In a similar vein, a study by Michel et al. found a link between increased serum MGO levels, liver cirrhosis, and generalised inflammation (Michel et al., 2021). Elevated levels of serum and circulating MGO were associated with a worsened prognosis for liver illness and a higher chance of developing additional liver-related problems, such as ascites (Michel et al., 2021). In HepG2 cells, MGO disrupted the mitochondria, triggered apoptosis, increased the formation of ROS, and decreased GSH levels, which are a crucial part of the glyoxalase detoxifying system (Seo et al., 2014). Elevated levels of the liver health markers aspartate aminotransferase and alanine aminotransferase, which are both produced by the liver, showed that MGO treatment caused acute liver damage in vivo. All of this shows that MGO causes liver illness through increasing oxidative stress and mitochondrial dysfunction as a result of excessive ROS generation (Seo et al., 2014).

Rats were subjected to CCl<sub>4</sub> therapy to induce liver MGO buildup, which downregulation of GLO1 expression, increased the formation of MG-AGEs, and activated RAGE, resulting in inflammation and stress (Hollenbach et al., 2017). This was done to find out how inflammation affects MGO regulation. A positive feedback loop in which high MGO hinders its own detoxification while continuing to produce hepatic impairment is suggested by the effect of MGO on decreased GLO1 expression (Hollenbach et al., 2017). MG-AGE levels have been observed to be more significant in the plasma and serum of people with liver illness as well as obese animals in numerous studies. (Spanos et al., 2018). Excess MGO promotes the

synthesis of MG-AGE. In non-diabetic patients, serum MG-AGEs and sRAGE are linked to non-alcoholic fatty liver disease (Palma-Duran et al., 2018)

Furthermore, steatosis and inflammation of the liver resulted in increased levels of circulating MG-AGEs. The MG-AGE/RAGE axis was activated, which resulted in higher levels of apoptosis, TGF- $\beta$ , TNF- $\alpha$ , IL-8, and IFN- $\gamma$  (Kim et al., 2012; Serban et al., 2016). More research is needed to characterise the interplay between the pro- and anti-inflammatory cytokines produced as a result of the AGE/RAGE axis in liver disease in order to understand their role in hepatic dysfunction. After the delivery of a siRNA targeting RAGE in primary rat hepatic stellate cells, the elevation of these cytokines seemed to be abated, and the overt disease progression was stopped (Xia et al., 2015). Subsequent in vivo injection of RAGE siRNA into rats recapitulated these in vitro results and prevented the activation of NF- $\kappa$ B, which in turn prevented the development of liver fibrosis (Cai et al., 2014). It's interesting to note that deletion of the RAGE gene, *Ager*, did not stop the development of hepatic steatosis, suggesting a different, RAGE-independent mechanism of MG-AGE-mediated liver dysfunction (Bijnen et al., 2018; K et al., 2021).

#### **1.5.4.3 The Role of MGO and MGO-AGES in cancer**

According to Leone et al., there is an inverse relationship between MGO concentration and the development and spread of cancer (Leone et al., 2021). Cancers employ glycolysis more frequently, have improved glucose absorption, and secrete more MGO (Hosoda et al., 2015; Hu et al., 2014; Tamori et al., 2018). To combat this, tumours overexpress GLO1, which could result in excess of the substance's availability, which would then cause MGO buildup and toxicity. However, according to recent research, MGO has a hormetic effect on cancer, acting as a pro-tumorigenic agent in some circumstances and an antitumorigenic agent in

others. The result of a hormetic effect by MGO at low concentrations promotes cancer growth but can have adverse effects at high concentrations (Nokin et al., 2017).

In 2000, Weinberg and Hanahan wrote about how complicated the scientific literature on cancer was. They predicted that instead of adding more information in a random way, research in the next 25 years would move towards a more logical way to understand this complexity "in terms of a small number of underlying principles."

The original "Hallmarks of Cancer" review was the authors' effort and contribution to this shift. It led to the list of six core "rules" that guide the many steps of normal cells turning into cancerous cells (Hanahan & Weinberg, 2000): 1) Self-sufficiency in growth signals, 2) Insensitivity to growth suppressive signals, 3) Ability to evade programmed cell death, 4) Enabling replicative immortality, 5) Sustained angiogenesis, 6) Tissue invasion and metastasis. In 2011, Weinberg and Hanahan put out an update in which they talked about how our knowledge of the six original hallmarks had changed over the past ten years. They also added two features that were becoming popular (Hanahan & Weinberg, 2011): Reprogramming energy metabolism and Evading immune destruction.

Ten years later, Hanahan goes back to the hallmarks again. He acknowledges the fantastic progress in the investigation of cancer via big data and reconfirms the relevance of the hallmarks in making sense of the new discoveries and "helping to distil this sophistication into a growingly rational science." In the most recent article, the two hallmarks that were added as "emerging" in 2011 were officially added as "core" hallmarks. This is because research over the past 10 years has shown that metabolic reprogramming and keeping the immune system from being destroyed are very important in cancer. Hanahan also suggested another sign that was becoming clear: Phenotypic plasticity and disrupted differentiation (Hanahan, 2022).

Studies have shown that RAGE stimulation by its ligands is related to the development and survival of cancers, such as metastasis and a poor prognosis (Figure 1.4). This receptor-ligand axis is the molecular link between things like hypoxia, hyperglycemia, glycation, inflammation, oxidative stress, and the start of cancers (Palanissami & Paul, 2018). RAGE and cancer stem cells are stimulated by chronic inflammatory, hyperglycemia, and glycoxidative stress, which is prevalent in diabetes and obesity and is accompanied by the production of RAGE ligands. This oncogenic transformation of normal and premalignant tissues results in the development of neoplasms. Palanissami & Paul, 2018, reviewed about possibilities of future RAGE-ligand driven, new combinational, and targeted oncotherapies that may leverage AGEs, soluble RAGE, and RAGE gene polymorphisms as prognostic and diagnostic biological indicators for the early diagnosis of malignancies. (Palanissami & Paul, 2018).



**Figure 1.4:** RAGE and its ligands' molecular interactions control the following cellular events that lead to the manifestation of cancer's hallmarks. P C: (Palanissami & Paul, 2018).

#### 1.5.4.4 The Role of MGO and MGO-AGES in cardiovascular diseases

When compared to non-failing controls or patients with heart failure who are not diabetic, patients with heart failure associated with diabetes had higher levels of MG-AGES on actin and myosin in the heart muscle (Papadaki et al., 2018). These alterations impair calcium sensitivity and interfere with protein-muscle interactions, both of which are essential for healthy cardiac function (Papadaki et al., 2018). A positive correlation between MGO in the heart and plasma and an increased risk for heart failure was found in a study of comorbidity with HIV infection (Dash et al., 2021). Furthermore, in people with type 1 diabetes (T1D), higher plasma MGO levels were consistently linked to fatal cardiovascular events (Dash et al., 2021). Interest in its potential as a predictive biomarker for cardiovascular disease was sparked by a similar finding in people with type 2 diabetes (T2D), where greater plasma MGO was linked to an elevated risk for atherosclerosis and blood pressure (Ogawa et al., 2010).

When myocardial infarction occurs in mice, MG-AGES in the heart are linked to worse outcomes, notably unfavourable cardiac remodelling and cardiac dysfunction (Blackburn et al., 2017). Increased aortic and plasma concentrations of MGO and MG-AGES were linked to ROS generation, endothelial dysfunction, hypertension, and altered vasculature in hypertensive rats (X. Wang et al., 2005). Increased blood pressure, microvascular issues, signs of atherosclerosis and coronary heart disease, as well as elevated plasma and serum MG-AGES, have all been associated with these conditions. Recently, these results were confirmed in diabetic patients. (Aso et al., 2000; Kilhovd et al., 2005; Miura et al., 2003).

The interaction between AGE formation, binding to RAGE, and RAGE stimulation is known as the AGE/RAGE axis, and it has been linked to coronary artery disease brought on by hyperglycemia brought on by insulin resistance from T2D (Fishman et al., 2018). It is hypothesised that AGEs cause blood vessel lining to stiffen by crosslinking low-density

lipoproteins and extracellular matrix proteins like collagen and elastin, which results in cardiac dysfunction (Fishman et al., 2018). Blocking the AGE/RAGE axis by administering sRAGE to mice caused the development of indicators for atherosclerosis to decline in a dose-dependent manner (Park et al., 1998). All of these shows that MG-AGEs may act as a warning sign before atherosclerosis and diminished cardiac function emerge.

## 1.6 Aim and Objectives

Patients with hyperglycemia experience elevated MGO concentrations and are consequently prone to developing diabetic complications. MG-AGEs formation is expected to induce various complications based on various alterations caused by MGO in different signaling pathways essential for the everyday survival of cells. The analysis of these alterations connects MGO to cancer development prevalence in diabetic patients. However, details of various proteins involved in this process are not fully elucidated. Our understanding of the complex toxicity of MGO stress in the biological system will be mutually improved by the identification of novel protein targets under these circumstances. In order to improve the prognosis for diabetes and cancer, it will be critical to recognise the impacts of MGO and how MGO-AGEs differ in their roles. Hence, our major aim of the work is to understand the basic biology involved in the effect of methylglyoxal in the progression of cancer in HepG2 cells and the consequences of methylglyoxal exposure on H9c2 cells depicting the role in CVD development. Therefore, the primary objectives of this work were to investigate the effect of MGO on HepG2 cells in the induction of oxidative stress and AGEs production and the alteration of various metabolic and molecular pathways. The second objective of the study was to understand the effect of MGO on the cardiomyocytes, H9c2 cells.

## 1.7 References

1. Abdrakhmanov, A., Gogvadze, V., & Zhivotovsky, B. (2020). To Eat or to Die: Deciphering Selective Forms of Autophagy. In *Trends in Biochemical Sciences* (Vol. 45, Issue 4, pp. 347–364). <https://doi.org/10.1016/j.tibs.2019.11.006>
2. Abordo, E. A., Minhas, H. S., & Thornalley, P. J. (1999). Accumulation of  $\alpha$ -oxoaldehydes during oxidative stress: a role in cytotoxicity. *Biochemical Pharmacology*, 58(4), 641–648. [https://doi.org/10.1016/S0006-2952\(99\)00132-X](https://doi.org/10.1016/S0006-2952(99)00132-X)
3. Ahmed, N., Babaei-Jadidi, R., Howell, S. K., Beisswenger, P. J., & Thornalley, P. J. (2005). Degradation products of proteins damaged by glycation, oxidation and nitration in clinical type 1 diabetes. *Diabetologia*, 48(8), 1590–1603. <https://doi.org/10.1007/S00125-005-1810-7>
4. Ahmed, N., Thornalley, P. J., Dawczynski, J., Franke, S., Strobel, J., Stein, G., & Haik, G. M. (2003). Methylglyoxal-Derived Hydroimidazolone Advanced Glycation Endproducts of Human Lens Proteins. *Investigative Ophthalmology & Visual Science*, 44(12), 5287–5292. <https://doi.org/10.1167/IOVS.03-0573>
5. Aragonès, G., Rowan, S., Francisco, S. G., Yang, W., Weinberg, J., Taylor, A., & Bejarano, E. (2020). Glyoxalase System as a Therapeutic Target against Diabetic Retinopathy. *Antioxidants*, 9(11), 1–25. <https://doi.org/10.3390/ANTIOX9111062>
6. Asadipooya, K., & Uy, E. M. (2019). Advanced Glycation End Products (AGEs), Receptor for AGEs, Diabetes, and Bone: Review of the Literature. In *Journal of the Endocrine Society* (Vol. 3, Issue 10, pp. 1799–1818). <https://doi.org/10.1210/js.2019-00160>
7. Aso, Y., Inukai, T., Tayama, K., & Takemura, Y. (2000). Serum concentrations of advanced glycation endproducts are associated with the development of atherosclerosis

- as well as diabetic microangiopathy in patients with type 2 diabetes. *Acta Diabetologica*, 37(2), 87–92. <https://doi.org/10.1007/S005920070025>
8. Bijnen, M., Beelen, N., Wetzels, S., Gaar, J. van de, Vroomen, M., Wijnands, E., Scheijen, J. L., van de Waarenburg, M. P. H., Gijbels, M. J., Cleutjens, J. P., Biessen, E. A. L., Stehouwer, C. D. A., Schalkwijk, C. G., & Wouters, K. (2018). RAGE deficiency does not affect non-alcoholic steatohepatitis and atherosclerosis in Western type diet-fed Ldlr<sup>-/-</sup> mice. *Scientific Reports*, 8(1). <https://doi.org/10.1038/S41598-018-33661-Y>
  9. Blackburn, N. J. R., Vulesevic, B., McNeill, B., Cimenci, C. E., Ahmadi, A., Gonzalez-Gomez, M., Ostojic, A., Zhong, Z., Brownlee, M., Beisswenger, P. J., Milne, R. W., & Suuronen, E. J. (2017). Methylglyoxal-derived advanced glycation end products contribute to negative cardiac remodeling and dysfunction post-myocardial infarction. *Basic Research in Cardiology*, 112(5). <https://doi.org/10.1007/S00395-017-0646-X>
  10. Bongarzone, S., Savickas, V., Luzi, F., & Gee, A. D. (2017). Targeting the Receptor for Advanced Glycation Endproducts (RAGE): A Medicinal Chemistry Perspective. *Journal of Medicinal Chemistry*, 60(17), 7213–7232. [https://doi.org/10.1021/ACS.JMEDCHEM.7B00058/ASSET/IMAGES/LARGE/JM-2017-00058M\\_0007.JPEG](https://doi.org/10.1021/ACS.JMEDCHEM.7B00058/ASSET/IMAGES/LARGE/JM-2017-00058M_0007.JPEG)
  11. Brett, J., Marie Schmidt, A., Du Yan, S., Shan Zou, Y., Weidman, E., Pinsky, D., Nowygrad, R., Neper, M., Przysiecki, C., Shaw, A., Migheli, A., & Stern, D. (1993). Survey of the Distribution of a Newly Characterised Receptor for Advanced Glycation End Products in Tissues. In *American Journal of Pathology* (Vol. 143, Issue 6). <https://www.ncbi.nlm.nih.gov/pmc/articles/pmc1887265/>

12. Cade, W. T. (2008). Diabetes-Related Microvascular and Macrovascular Diseases in the Physical Therapy Setting. *Physical Therapy*, 88(11), 1322. <https://doi.org/10.2522/PTJ.20080008>
13. Cai, X. G., Xia, J. R., Li, W. D., Lu, F. L., Liu, J., Lu, Q., & Zhi, H. (2014). Anti-fibrotic effects of specific-siRNA targeting of the receptor for advanced glycation end products in a rat model of experimental hepatic fibrosis. *Molecular Medicine Reports*, 10(1), 306–314. <https://doi.org/10.3892/MMR.2014.2207>
14. Cameron, A. D., Ridderström, M., Olin, B., & Mannervik, B. (1999). Crystal structure of human glyoxalase II and its complex with a glutathione thiolester substrate analogue. *Structure*, 7(9), 1067–1078. [https://doi.org/10.1016/S0969-2126\(99\)80174-9](https://doi.org/10.1016/S0969-2126(99)80174-9)
15. Cerami, C., Founds, H., Nicholl, I., Mitsuhashi, T., Giordano, D., Vanpatten, S., Lee, A., Al-Abed, Y., Vlassara, H., Bucala, R., & Cerami, A. (1997). Tobacco smoke is a source of toxic reactive glycation products. *Proceedings of the National Academy of Sciences of the United States of America*, 94(25), 13915–13920. <https://doi.org/10.1073/pnas.94.25.13915>
16. Chakraborty, S., Karmakar, K., & Chakravorty, D. (2014). Cells producing their own nemesis: Understanding methylglyoxal metabolism. *IUBMB Life*, 66(10), 667–678. <https://doi.org/10.1002/IUB.1324>
17. Chaudhuri, J., Bains, Y., Guha, S., Kahn, A., Hall, D., Bose, N., Gugliucci, A., & Kapahi, P. (2018). The Role of Advanced Glycation End Products in Aging and Metabolic Diseases: Bridging Association and Causality. In *Cell Metabolism* (Vol. 28, Issue 3, pp. 337–352). <https://doi.org/10.1016/j.cmet.2018.08.014>
18. Clausen, T. D., Mathiesen, E. R., Hansen, T., Pedersen, O., Jensen, D. M., Lauenborg, J., & Damm, P. (2008). High Prevalence of Type 2 Diabetes and Pre-Diabetes in Adult Offspring of Women With Gestational Diabetes Mellitus or Type 1 DiabetesThe role

- of intrauterine hyperglycemia. *Diabetes Care*, 31(2), 340–346.  
<https://doi.org/10.2337/DC07-1596>
19. Connolly, D. T. (1991). Vascular permeability factor: A unique regulator of blood vessel function. *Journal of Cellular Biochemistry*, 47(3), 219–223.  
<https://doi.org/10.1002/jcb.240470306>
20. Dash, P. K., Alomar, F. A., Cox, J. L., McMillan, J., Hackfort, B. T., Makarov, E., Morsey, B., Fox, H. S., Gendelman, H. E., Gorantla, S., & Bidasee, K. R. (2021). A Link Between Methylglyoxal and Heart Failure During HIV-1 Infection. *Frontiers in Cardiovascular Medicine*, 8. <https://doi.org/10.3389/FCVM.2021.792180>
21. Deshpande, A. D., Harris-Hayes, M., & Schootman, M. (2008). Epidemiology of Diabetes and Diabetes-Related Complications. *Physical Therapy*, 88(11), 1254.  
<https://doi.org/10.2522/PTJ.20080020>
22. Fishman, S. L., Sonmez, H., Basman, C., Singh, V., & Poretzky, L. (2018). The role of advanced glycation end-products in the development of coronary artery disease in patients with and without diabetes mellitus: a review. *Molecular Medicine (Cambridge, Mass.)*, 24(1). <https://doi.org/10.1186/S10020-018-0060-3>
23. Fleming, T. H., Humpert, P. M., Nawroth, P. P., & Bierhaus, A. (2011). Reactive metabolites and AGE/RAGE-mediated cellular dysfunction affect the aging process - A mini-review. *Gerontology*, 57(5), 435–443. <https://doi.org/10.1159/000322087>
24. Fritz, G. (2011). RAGE: A single receptor fits multiple ligands. In *Trends in Biochemical Sciences* (Vol. 36, Issue 12, pp. 625–632).  
<https://doi.org/10.1016/j.tibs.2011.08.008>
25. Galicia-Garcia, U., Benito-Vicente, A., Jebari, S., Larrea-Sebal, A., Siddiqi, H., Uribe, K. B., Ostolaza, H., & Martín, C. (2020). Pathophysiology of Type 2 Diabetes Mellitus.

- International Journal of Molecular Sciences*, 21(17), 1–34.  
<https://doi.org/10.3390/IJMS21176275>
26. Genuth, S. M., Palmer, J. P., & Nathan, D. M. (2018). Classification and Diagnosis of Diabetes. *Diabetes in America, 3rd Edition*, 2(4), 1–39.  
<https://www.ncbi.nlm.nih.gov/books/NBK568014/>
27. Gerrard, J. (2005). The Maillard Reaction: Chemistry, Biochemistry and Implications by Harry Nursten. *Australian Journal of Chemistry*, 58(10), 756.  
[https://doi.org/10.1071/ch0505\\_br](https://doi.org/10.1071/ch0505_br)
28. Hanahan, D. (2022). Hallmarks of Cancer: New Dimensions. *Cancer Discovery*, 12(1), 31–46. <https://doi.org/10.1158/2159-8290.CD-21-1059>
29. Hanahan, D., & Weinberg, R. A. (2000). The Hallmarks of Cancer Review evolve progressively from normalcy via a series of pre. *Cell*, 100, 57–70.
30. Hanahan, D., & Weinberg, R. A. (2011). Hallmarks of cancer: The next generation. *Cell*, 144(5), 646–674. <https://doi.org/10.1016/J.CELL.2011.02.013/ATTACHMENT/3F528E16-8B3C-4D8D-8DE5-43E0C98D8475/MMC1.PDF>
31. Han, Y., Randell, A. E., Sudesh, A. E., Ae, V., Gill, V., Gadag, A. V., Leigh, A. E., Newhook, A., Marie, A. E., Ae, G., & Hagerty, D. (2007). Plasma methylglyoxal and glyoxal are elevated and related to early membrane alteration in young, complication-free patients with Type 1 diabetes. *Springer*, 305(1–2), 123–131.  
<https://doi.org/10.1007/s11010-007-9535-1>
32. HODGE, & E., J. (1953). Chemistry of browning reactions in model systems. *J. Agric. Food Chem.*, 46, 2599–2600. <https://ci.nii.ac.jp/naid/10008765425>
33. Hollenbach, M., Thonig, A., Pohl, S., Ripoll, C., Michel, M., & Zipprich, A. (2017). Expression of glyoxalase-I is reduced in cirrhotic livers: A possible mechanism in the development of cirrhosis. *PLoS ONE*, 12(2). <https://doi.org/10.1371/JOURNAL.PONE.0171260>

34. Hosoda, F., Arai, Y., Okada, N., Shimizu, H., Miyamoto, M., Kitagawa, N., Katai, H., Taniguchi, H., Yanagihara, K., Imoto, I., Inazawa, J., Ohki, M., & Shibata, T. (2015). Integrated genomic and functional analyses reveal glyoxalase I as a novel metabolic oncogene in human gastric cancer. *Oncogene*, *34*(9), 1196–1206. <https://doi.org/10.1038/ONC.2014.57>
35. Hsu, L. C., Tani, K., Fujiyoshi, T., Kurachi, K., & Yoshida, A. (1985). Cloning of cDNAs for human aldehyde dehydrogenases 1 and 2. *Proceedings of the National Academy of Sciences of the United States of America*, *82*(11), 3771–3775. <https://doi.org/10.1073/PNAS.82.11.3771>
36. Hu, X., Yang, X., He, Q., Chen, Q., & Yu, L. (2014). Glyoxalase 1 is up-regulated in hepatocellular carcinoma and is essential for HCC cell proliferation. *Biotechnology Letters*, *36*(2), 257–263. <https://doi.org/10.1007/s10529-013-1372-6>
37. Izaguirre, G., Kikonyogo, A., & Pietruszko, R. (1998). Methylglyoxal as substrate and inhibitor of human aldehyde dehydrogenase: comparison of kinetic properties among the three isozymes. *Comparative Biochemistry and Physiology. Part B, Biochemistry & Molecular Biology*, *119*(4), 747–754. [https://doi.org/10.1016/S0305-0491\(98\)00051-0](https://doi.org/10.1016/S0305-0491(98)00051-0)
38. Jules, J., Maignel, D., & Hudson, B. I. (2013). Alternative splicing of the RAGE cytoplasmic domain regulates cell signaling and function. *PLoS ONE*, *8*(11). <https://doi.org/10.1371/journal.pone.0078267>
39. Jung, H. S., Chung, K. W., Won Kim, J., Kim, J., Komatsu, M., Tanaka, K., Nguyen, Y. H., Kang, T. M., Yoon, K. H., Kim, J. W., Jeong, Y. T., Han, M. S., Lee, M. K., Kim, K. W., Shin, J., & Lee, M. S. (2008). Loss of Autophagy Diminishes Pancreatic  $\beta$  Cell Mass and Function with Resultant Hyperglycemia. *Cell Metabolism*, *8*(4), 318–324. <https://doi.org/10.1016/j.cmet.2008.08.013>

40. Kador, P. F., & Kinoshita, J. H. (1985). Role of aldose reductase in the development of diabetes-associated complications. *The American Journal of Medicine*, 79(5A), 8–12. [https://doi.org/10.1016/0002-9343\(85\)90504-2](https://doi.org/10.1016/0002-9343(85)90504-2)
41. Kay, A. M., Simpson, C. L., & Stewart, J. A. (2016). The Role of AGE/RAGE Signaling in Diabetes-Mediated Vascular Calcification. In *Journal of Diabetes Research* (Vol. 2016). <https://doi.org/10.1155/2016/6809703>
42. Kilhovd, B. K., Juutilainen, A., Lehto, S., Rönnemaa, T., Torjesen, P. A., Birkeland, K. I., Berg, T. J., Hanssen, K. F., & Laakso, M. (2005). High serum levels of advanced glycation end products predict increased coronary heart disease mortality in non-diabetic women but not in non-diabetic men: a population-based 18-year follow-up study. *Arteriosclerosis, Thrombosis, and Vascular Biology*, 25(4), 815–820. <https://doi.org/10.1161/01.ATV.0000158380.44231.FE>
43. Kim, J., Kim, O. S., Kim, C. S., Sohn, E., Jo, K., & Kim, J. S. (2012). Accumulation of argpyrimidine, a methylglyoxal-derived advanced glycation end product, increases apoptosis of lens epithelial cells both in vitro and in vivo. *Experimental & Molecular Medicine*, 44(2), 167. <https://doi.org/10.3858/EMM.2012.44.2.012>
44. Klöpfer, A., Spanneberg, R., & Glomb, M. A. (2010). Formation of Arginine Modifications in a Model System of Na-tert-Butoxycarbonyl (Boc)-Arginine with Methylglyoxal. *Journal of Agricultural and Food Chemistry*, 59(1), 394–401. <https://doi.org/10.1021/JF103116C>
45. Kong, X., Ma, M. zhe, Huang, K., Qin, L., Zhang, H. mei, Yang, Z., Li, X. yong, & Su, Q. (2014). Increased plasma levels of the methylglyoxal in patients with newly diagnosed type 2 diabetes. *Journal of Diabetes*, 6(6), 535–540. <https://doi.org/10.1111/1753-0407.12160>

46. Kurys, G., Ambroziak, W., & Pietruszkos, R. (1989). *THE JOURNAL OF BIOLOGICAL CHEMISTRY Human Aldehyde Dehydrogenase PURIFICATION AND CHARACTERISATION OF A THIRD ISOZYME WITH LOW K<sub>m</sub> FOR  $\gamma$ -AMINO BUTYRALDEHYDE\**. 264(8), 4715–4721. [https://doi.org/10.1016/S0021-9258\(18\)83802-9](https://doi.org/10.1016/S0021-9258(18)83802-9)
47. K, W., AS, C., KH, G., M, T., JLJM, S., F, B., F, C., D, C., M, A., G, G., M, C., CG, S., & R, M. (2021). Deletion of RAGE fails to prevent hepatosteatosis in obese mice due to impairment of other AGEs receptors and detoxifying systems. *Scientific Reports*, 11(1). <https://doi.org/10.1038/S41598-021-96859-7>
48. Lai, S. W. T., Lopez Gonzalez, E. D. J., Zoukari, T., Ki, P., & Shuck, S. C. (2022a). Methylglyoxal and Its Adducts: Induction, Repair, and Association with Disease. *Chemical Research in Toxicology*, 35(10), 1720. <https://doi.org/10.1021/ACS.CHEMRESTOX.2C00160>
49. Lapolla, A., Traldi, P., & Fedele, D. (2005). Importance of measuring products of nonenzymatic glycation of proteins. *Clinical Biochemistry*, 38(2), 103–115. <https://doi.org/10.1016/j.clinbiochem.2004.09.007>
50. Leone, A., Nigro, C., Nicolò, A., Prevezano, I., Formisano, P., Beguinot, F., & Miele, C. (2021a). The Dual-Role of Methylglyoxal in Tumor Progression – Novel Therapeutic Approaches. *Frontiers in Oncology*, 11. <https://doi.org/10.3389/FONC.2021.645686>
51. Lorenzi, M. (2007). The polyol pathway as a mechanism for diabetic retinopathy: Attractive, elusive, and resilient. In *Experimental Diabetes Research* (Vol. 2007). <https://doi.org/10.1155/2007/61038>
52. Lo, T. W. C., Westwood, M. E., McLellan, A. C., Selwood, T., & Thornalley, P. J. (1994). Binding and modification of proteins by methylglyoxal under physiological conditions. A kinetic and mechanistic study with N alpha-acetylarginine, N alpha-acetylcysteine, and N alpha-acetyllysine, and bovine serum albumin. *Journal of*

- Biological Chemistry*, 269(51), 32299–32305. [https://doi.org/10.1016/S0021-9258\(18\)31635-1](https://doi.org/10.1016/S0021-9258(18)31635-1)
53. MAILLARD, & L.C. (1912). Action of amino acids on sugars. Formation of melanoidins in a methodical way. *Compte-Rendu de l'Academie Des Sciences*, 154, 66–68. <https://ci.nii.ac.jp/naid/20000509994>
54. McEwen, J. M., Fraser, S., Guir, A. L. S., Dave, J., & Scheck, R. A. (2021). Synergistic sequence contributions bias glycation outcomes. *Nature Communications* 2021 12:1, 12(1), 1–10. <https://doi.org/10.1038/s41467-021-23625-8>
55. Michel, M., Hess, C., Kaps, L., Kremer, W. M., Hilscher, M., Galle, P. R., Moehler, M., Schattenberg, J. M., Wörns, M. A., Labenz, C., & Nagel, M. (2021). Elevated serum levels of methylglyoxal are associated with impaired liver function in patients with liver cirrhosis. *Scientific Reports* 2021 11:1, 11(1), 1–11. <https://doi.org/10.1038/s41598-021-00119-7>
56. Miura, J., Yamagishi, S. I., Uchigata, Y., Takeuchi, M., Yamamoto, H., Makita, Z., & Iwamoto, Y. (2003). Serum levels of non-carboxymethyllysine advanced glycation endproducts are correlated to severity of microvascular complications in patients with Type 1 diabetes. *Journal of Diabetes and Its Complications*, 17(1), 16–21. [https://doi.org/10.1016/S1056-8727\(02\)00183-6](https://doi.org/10.1016/S1056-8727(02)00183-6)
57. Mumtaz, M. (2000). Gestational Diabetes Mellitus. *The Malaysian Journal of Medical Sciences : MJMS*, 7(1), 4. [/pmc/articles/PMC3406210/](https://pubmed.ncbi.nlm.nih.gov/11811810/)
58. Narumi, K., Miyakawa, R., Ueda, R., Hashimoto, H., Yamamoto, Y., Yoshida, T., & Aoki, K. (2015). Proinflammatory Proteins S100A8/S100A9 Activate N.K. Cells via Interaction with RAGE. *The Journal of Immunology*, 194(11), 5539–5548. <https://doi.org/10.4049/jimmunol.1402301>

59. Neeper, M., Marie Schmidt, A., Brett, J., Du YanQ, S., Wangll, F., Pan, Y.-C. E., Elliston, K., Stern, D., & ShawS, A. (1992). THE JOURNAL OF BIOLOGICAL CHEMISTRY Cloning and Expression of a Cell Surface Receptor for Advanced Glycosylation End Products of Proteins\*. In *ASBMB* (Vol. 267, Issue 21). <https://www.jbc.org/content/267/21/14998.short>
60. Negre-Salvayre, A., Salvayre, R., Augé, N., Pamplona, R., & Portero-Otín, M. (2009). Hyperglycemia and glycation in diabetic complications. In *Antioxidants and Redox Signaling* (Vol. 11, Issue 12, pp. 3071–3109). <https://doi.org/10.1089/ars.2009.2484>
61. Nemet, I., Varga-Defterdarović, L., & Turk, Z. (2006). Methylglyoxal in food and living organisms. *Molecular Nutrition & Food Research*, 50(12), 1105–1117. <https://doi.org/10.1002/MNFR.200600065>
62. Nokin, M. J., Durieux, F., Bellier, J., Peulen, O., Uchida, K., Spiegel, D. A., Cochrane, J. R., Hutton, C. A., Castronovo, V., & Bellahcène, A. (2017). Hormetic potential of methylglyoxal, a side-product of glycolysis, in switching tumours from growth to death. *Scientific Reports*, 7(1). <https://doi.org/10.1038/S41598-017-12119-7>
63. Ogawa, S., Nakayama, K., Nakayama, M., Mori, T., Matsushima, M., Okamura, M., Senda, M., Nako, K., Miyata, T., & Ito, S. (2010). Methylglyoxal is a predictor in type 2 diabetic patients of intima-media thickening and elevation of blood pressure. *Hypertension (Dallas, Tex. : 1979)*, 56(3), 471–476. <https://doi.org/10.1161/HYPERTENSIONAHA.110.156786>
64. Oliveira, M. I. A., De Souza, E. M., Pedrosa, F. D. O., Réa, R. R., Alves, A. D. S. C., Geraldo Picheth, & Fabiane Gomes de Moraes Rego. (2013). Rage receptor and its soluble isoforms in diabetes mellitus complications : O receptor rage e suas isoformas solúveis nas complicações do diabetes mellitus. *Jornal Brasileiro de Patologia e*

- Medicina Laboratorial*, 49(2), 97–108. <https://doi.org/10.1590/S1676-24442013000200004>
65. Palanissami, G., & Paul, S. F. D. (n.d.). *RAGE and Its Ligands: Molecular Interplay Between Glycation, Inflammation, and Hallmarks of Cancer-a Review*. <https://doi.org/10.1007/s12672-018-0342-9>
66. Palanissami, G., & Paul, S. F. D. (2018). *RAGE and Its Ligands: Molecular Interplay Between Glycation, Inflammation, and Hallmarks of Cancer-a Review*. <https://doi.org/10.1007/s12672-018-0342-9>
67. Palma-Duran, S. A., Kontogianni, M. D., Vlassopoulos, A., Zhao, S., Margariti, A., Georgoulis, M., Papatheodoridis, G., & Combet, E. (2018). Serum levels of advanced glycation endproducts (AGEs) and the decoy soluble receptor for AGEs (sRAGE) can identify non-alcoholic fatty liver disease in age-, sex- and BMI-matched normoglycemic adults. *Metabolism: Clinical and Experimental*, 83, 120–127. <https://doi.org/10.1016/J.METABOL.2018.01.023>
68. Papadaki, M., Holewinski, R. J., Previs, S. B., Martin, T. G., Stachowski, M. J., Li, A., Blair, C. A., Moravec, C. S., Van Eyk, J. E., Campbell, K. S., Warshaw, D. M., & Kirk, J. A. (2018). Diabetes with heart failure increases methylglyoxal modifications in the sarcomere, which inhibit function. *JCI Insight*, 3(20). <https://doi.org/10.1172/JCI.INSIGHT.121264>
69. Park, L., Raman, K. G., Lee, K. J., Lu, Y., Ferran, L. J., Choe, W. S., Stern, D., & Schmidt, A. M. (1998). Suppression of accelerated diabetic atherosclerosis by the soluble receptor for advanced glycation endproducts. *Nature Medicine*, 4(9), 1025–1031. <https://doi.org/10.1038/2012>
70. Ramasamy, R., Yan, S. F., & Schmidt, A. M. (2011). Receptor for AGE (RAGE): Signaling mechanisms in the pathogenesis of diabetes and its complications. *Annals of*

*the New York Academy of Sciences*, 1243(1), 88–102. <https://doi.org/10.1111/j.1749-6632.2011.06320.x>

71. Rasheed, Z., & Haqqi, T. M. (2012). Endoplasmic reticulum stress induces the expression of COX-2 through activation of eIF2 $\alpha$ , p38-MAPK and NF- $\kappa$ B in advanced glycation end products stimulated human chondrocytes. *Biochimica et Biophysica Acta - Molecular Cell Research*, 1823(12), 2179–2189. <https://doi.org/10.1016/j.bbamcr.2012.08.021>
72. Raucci, A., Cugusi, S., Antonelli, A., Barabino, S. M., Monti, L., Bierhaus, A., Reiss, K., Saftig, P., & Bianchi, M. E. (2008). A soluble form of the receptor for advanced glycation endproducts (RAGE) is produced by proteolytic cleavage of the membrane-bound form by the sheddase a disintegrin and metalloprotease 10 (ADAM10). *The FASEB Journal*, 22(10), 3716–3727. <https://doi.org/10.1096/fj.08-109033>
73. Reichard, G. A., Skutches, C. L., Hoeldtke, R. D., & Owen, O. E. (1986). Acetone metabolism in humans during diabetic ketoacidosis. *Diabetes*, 35(6), 668–674. <https://doi.org/10.2337/DIAB.35.6.668>
74. Riboulet-Chavey, A., Pierron, A., Durand, I., Murdaca, J., Giudicelli, J., & Obberghen, E. Van. (2006). Methylglyoxal impairs the insulin signaling pathways independently of the formation of intracellular reactive oxygen species. *Am Diabetes Assoc*. <https://doi.org/10.2337/db05-0857>
75. Sapra, A., & Bhandari, P. (2022). Diabetes Mellitus. *StatPearls*. <https://www.ncbi.nlm.nih.gov/books/NBK551501/>
76. Schmidt, A. M. (2017). RAGE and Implications for the Pathogenesis and Treatment of Cardiometabolic Disorders – Spotlight on the Macrophage. *Arteriosclerosis, Thrombosis, and Vascular Biology*, 37(4), 613. <https://doi.org/10.1161/ATVBAHA.117.307263>

77. Seo, K., Ki, S., research, S. S.-T., & 2014, undefined. (2014). Methylglyoxal induces mitochondrial dysfunction and cell death in liver. *Springer*, *30*(3), 193–198. <https://doi.org/10.5487/TR.2014.30.3.193>
78. Serban, A. I., Stanca, L., Geicu, O. I., Munteanu, M. C., & Dinischiotu, A. (2016). RAGE and TGF- $\beta$ 1 Cross-Talk Regulate Extracellular Matrix Turnover and Cytokine Synthesis in AGEs Exposed Fibroblast Cells. *PLOS ONE*, *11*(3), e0152376. <https://doi.org/10.1371/JOURNAL.PONE.0152376>
79. Sorci, G., Riuzzi, F., Giambanco, I., & Donato, R. (2013). RAGE in tissue homeostasis, repair and regeneration. *Biochimica et Biophysica Acta - Molecular Cell Research*, *1833*(1), 101–109. <https://doi.org/10.1016/j.bbamcr.2012.10.021>
80. Spanos, C., Maldonado, E. M., Fisher, C. P., Leenutaphong, P., Oviedo-Orta, E., Windridge, D., Salguero, F. J., Bermúdez-Fajardo, A., Weeks, M. E., Evans, C., Corfe, B. M., Rabbani, N., Thornalley, P. J., Miller, M. H., Wang, H., Dillon, J. F., Quaglia, A., Dhawan, A., Fitzpatrick, E., & Bernadette Moore, J. (2018). Proteomic identification and characterisation of hepatic glyoxalase 1 dysregulation in non-alcoholic fatty liver disease. *Proteome Science*, *16*(1). <https://doi.org/10.1186/S12953-018-0131-Y>
81. Sparvero, L. J., Asafu-Adjei, D., Kang, R., Tang, D., Amin, N., Im, J., Rutledge, R., Lin, B., Amoscato, A. A., Zeh, H. J., & Lotze, M. T. (2009). RAGE (Receptor for advanced glycation endproducts), RAGE ligands, and their role in cancer and inflammation. *Journal of Translational Medicine*, *7*, 1–21. <https://doi.org/10.1186/1479-5876-7-17>
82. Sruthi, C. R., & Raghu, K. G. (2021). Advanced glycation end products and their adverse effects: The role of autophagy. *Journal of Biochemical and Molecular Toxicology*, *35*(4), e22710. <https://doi.org/10.1002/JBT.22710>

83. Takahashi, K. (1968). The Reaction of Phenylglyoxal with Arginine Residues in Proteins\*. *Journal of Biological Chemistry*, 243, 6171–6179. [https://doi.org/10.1016/S0021-9258\(18\)94475-3](https://doi.org/10.1016/S0021-9258(18)94475-3)
84. Tamori, S., Nozaki, Y., Motomura, H., Nakane, H., Katayama, R., Onaga, C., Kikuchi, E., Shimada, N., Suzuki, Y., Noike, M., Hara, Y., Sato, K., Sato, T., Yamamoto, K., Hanawa, T., Imai, M., Abe, R., Yoshimori, A., Takasawa, R., ... Akimoto, K. (2018). Glyoxalase 1 gene is highly expressed in basal-like human breast cancers and contributes to survival of ALDH1-positive breast cancer stem cells. *Oncotarget*, 9(92), 36515–36529. <https://doi.org/10.18632/ONCOTARGET.26369>
85. Teissier, T., & Boulanger, É. (2019). The receptor for advanced glycation endproducts (RAGE) is an important pattern recognition receptor (PRR) for inflammaging. In *Biogerontology* (Vol. 20, Issue 3, pp. 279–301). Springer Netherlands. <https://doi.org/10.1007/s10522-019-09808-3>
86. Thornalley, P. J., Yurek-George, A., & Argirov, O. K. (2000). Kinetics and mechanism of the reaction of aminoguanidine with the  $\alpha$ -oxoaldehydes glyoxal, methylglyoxal, and 3-deoxyglucosone under physiological conditions. *Biochemical Pharmacology*, 60(1), 55–65. [https://doi.org/10.1016/S0006-2952\(00\)00287-2](https://doi.org/10.1016/S0006-2952(00)00287-2)
87. Tomic, D., Shaw, J. E., & Magliano, D. J. (2022). The burden and risks of emerging complications of diabetes mellitus. In *Nature Reviews Endocrinology* (Vol. 18, Issue 9, pp. 525–539). Nature Research. <https://doi.org/10.1038/s41574-022-00690-7>
88. Toren, E., Burnette, K. L. S., Banerjee, R. R., Hunter, C. S., & Tse, H. M. (2021). Partners in Crime: Beta-Cells and Autoimmune Responses Complicit in Type 1 Diabetes Pathogenesis. *Frontiers in Immunology*, 12. <https://doi.org/10.3389/FIMMU.2021.756548>
89. Ulrich, P., & Cerami, A. (2001). *Protein Glycation, Diabetes, and Aging*.

90. Uribarri, J., Woodruff, S., Goodman, S., Cai, W., Chen, X., Pyzik, R., Yong, A., Striker, G. E., & Vlassara, H. (2010). Advanced Glycation End Products in Foods and a Practical Guide to Their Reduction in the Diet. *Journal of the American Dietetic Association*, *110*(6), 911. <https://doi.org/10.1016/j.jada.2010.03.018>
91. Vander Jagt, D. L., Hassebrook, R. K., Hunsaker, L. A., Brown, W. M., & Royer, R. E. (2001). Metabolism of the 2-oxoaldehyde methylglyoxal by aldose reductase and by glyoxalase-I: Roles for glutathione in both enzymes and implications for diabetic complications. *Chemico-Biological Interactions*, *130–132*(1–3), 549–562. [https://doi.org/10.1016/S0009-2797\(00\)00298-2](https://doi.org/10.1016/S0009-2797(00)00298-2)
92. Vistoli, G., De, D., Cipak, A., Zarkovic, N., Carini, M., & Aldini, G. (2013). Advanced glycoxidation and lipoxidation end products (AGEs and ALEs): an overview of their mechanisms of formation. *Taylor & Francis*, *47*(S1), 3–27. <https://doi.org/10.3109/10715762.2013.815348>
93. Wang, W. C., Chou, C. K., Chuang, M. C., Li, Y. C., & Lee, J. A. (2018). Elevated levels of liver methylglyoxal and d-lactate in early-stage hepatitis in rats. *Biomedical Chromatography*, *32*(2). <https://doi.org/10.1002/BMC.4039>
94. Wang, X., Desai, K., Chang, T., & Wu, L. (2005). Vascular methylglyoxal metabolism and the development of hypertension. *Journal of Hypertension*, *23*(8), 1565–1573. <https://doi.org/10.1097/01.HJH.0000173778.85233.1B>
95. Willett, T. L., Kandel, R., De Croos, J. N. A., Avery, N. C., & Grynpas, M. D. (2012). Enhanced levels of nonenzymatic glycation and pentosidine crosslinking in spontaneous osteoarthritis progression. *Osteoarthritis and Cartilage*, *20*(7), 736–744. <https://doi.org/10.1016/j.joca.2012.03.012>

96. Wondmkun, Y. T. (2020). <p>Obesity, Insulin Resistance, and Type 2 Diabetes: Associations and Therapeutic Implications</p>. *Diabetes, Metabolic Syndrome and Obesity*, *13*, 3611–3616. <https://doi.org/10.2147/DMSO.S275898>
97. Xia, J. R., Chen, T. T., Li, W. D., Lu, F. L., Liu, J., Cai, X. G., Lu, Q., & Yang, C. P. (2015). Inhibitory effect of receptor for advanced glycation end product-specific small interfering RNAs on the development of hepatic fibrosis in primary rat hepatic stellate cells. *Molecular Medicine Reports*, *12*(1), 569–574. <https://doi.org/10.3892/MMR.2015.3342>
98. Xie, J., Méndez, J. D., Méndez-Valenzuela, V., & Aguilar-Hernández, M. M. (2013). Cellular signalling of the receptor for advanced glycation end products (RAGE). In *Cellular Signalling* (Vol. 25, Issue 11, pp. 2185–2197). <https://doi.org/10.1016/j.cellsig.2013.06.013>
99. Yan, S. F., Ramasamy, R., & Schmidt, A. M. (2010). The RAGE axis a fundamental mechanism signaling danger to the vulnerable vasculature. *Circulation Research*, *106*(5), 842–853. <https://doi.org/10.1161/CIRCRESAHA.109.212217>
100. Yatime, L., & Andersen, G. R. (2013). Structural insights into the oligomerisation mode of the human receptor for advanced glycation endproducts. *FEBS Journal*, *280*(24), 6556–6568. <https://doi.org/10.1111/febs.12556>
101. Yu, Y., Wang, L., Delguste, F., Durand, A., Guilbaud, A., Rousselin, C., Schmidt, A. M., Tessier, F., Boulanger, E., & Neviere, R. (2017). Advanced glycation end products receptor RAGE controls myocardial dysfunction and oxidative stress in high-fat fed mice by sustaining mitochondrial dynamics and autophagy-lysosome pathway. *Free Radical Biology and Medicine*, *112*, 397–410. <https://doi.org/10.1016/j.freeradbiomed.2017.08.012>

## Chapter 2

# Alterations on glyoxalase pathway and redox status by methylglyoxal in HepG2 cells

---

---

## 2.1 Introduction

Methylglyoxal is the most potent precursor for advanced glycation end product formation. It is a highly reactive dicarbonyl glycolytic metabolite that is produced during hyperglycaemia (Rabbani & Thornalley, 2015). Diabetic patients are seen to have high levels of MGO in their plasma due to uncontrolled blood glucose levels for extended durations (Kilhovd et al., 2003, Reyaz et al., 2020). The increased level of MGO in diabetic patients is believed to be associated with various secondary diabetic complications. It can react with various proteins, lipids and nucleic acid, hampering these macromolecules' structural and functional behaviour. In proteins, MGO can react with lysine, arginine and cysteine residues to form chemically stable MG-AGEs leading to cross-linking and denaturation (Liu et al., 2012; Zhou et al., 2019). The involvement of MG-AGEs, like hydroimidazolones (MG-Hs) and argpyrimidines, in various diseases has caught the attention of scientists worldwide. Immense research has recorded the involvement of MGO in the pathophysiology of several diseases like diabetes, cancer, Alzheimer's disease, Parkinson's disease and CVD (Schalkwijk & Stehouwer, 2020). The research is yet lacking in exploring the exact molecular mechanisms through which MGO can exert or stimulate the pathology of these diseases.

Considering the harmful effects of MGO due to its highly reactive nature, cells have their own defence systems. One of the central defence systems is the glyoxalase pathway,

consisting of two main enzymes, Glyoxalase I and Glyoxalase II (Yang et al., 2022). The disturbance in the balance between the formation and the detoxification of MGO during pathological conditions like diabetes can accumulate the MGO in the cells leading to various complications like AGEs formation, RAGE stimulation leading to oxidative stress, apoptosis, inflammation, autophagy etc. (Lee et al., 2020).

The receptor for advanced glycation end products or RAGE is a multiligand receptor which can bind several ligands, including AGEs or MG-AGEs and activate or stimulate various pathophysiological signalling cascades (Yue et al., 2022). RAGE stimulation is also implicated in the increase of its own expression, thus worsening conditions (Bongarzone et al., 2017).

Oxidative stress is one of the major culprits in the generation of various diseases and their complications. When it comes to AGEs formation and RAGE stimulation, the first and foremost response to this disturbance in the cell is indicated as oxidative stress or ROS generation. ROS generation and AGEs formation play a vicious cycle leading to several cellular damages, including mitochondrial dysfunction, inflammation, ER stress and even cell death (Sruthi & Raghu, 2021). Various antioxidants in the cell prevent the damage caused by oxidative stress. The master transcription regulator involved in the expression of antioxidant genes is Nrf2 (Vomund et al., 2017).

This study mainly focuses on the pathway of how MGO induces AGE formation and RAGE activation by hampering the glyoxalase pathway, which is mainly involved in the detoxification of MGO in the endogenous environment. AGE formation and ROS generation run a vicious cycle, impairing the antioxidant network. In this chapter, we focus on ROS generation and the effect of MGO in the oxidation of proteins for protein carbonyl formation. We also focus on the effect of MGO on the innate antioxidant system in the HepG2 cells. This chapter gives you preliminary information or the base of the MGO action in the cells, i.e., how

MGO impairs the glyoxalase system and increases MGO-AGEs formation and the effect of MGO various receptors like RAGE-1 and AGE-R1. It could lead to ROS generation along with the depletion of the innate antioxidant network.

## 2.2 Materials and methods

### 2.2.1 Reagents

MGO (Cat no. M0252) was obtained from Sigma Aldrich, USA. Minimal essential media Eagles (MEME) with Earle's salt (Cat no. AL047S), Phosphate buffered saline (PBS; Cat no. TL1099), and aminoguanidine bicarbonate (Cat no. RM1573) were purchased from Himedia, India. Fetal bovine serum (FBS; Cat no. 16000044), penicillin-streptomycin antibiotics (Cat no. 15070063), 0.5% trypsin-ethylene diamine tetra acetic acid (trypsin-EDTA; Cat no. R001100), and Hanks balanced saline solution or HBSS (Cat no. 1835981) were from Gibco-BRL Life Technologies (Waltham, MA, USA). Methyl thiazolyl blue tetrazolium bromide (MTT; Cat no. 33611) was purchased from Sisco Research Laboratories Pvt. Ltd. Dimethyl sulfoxide (DMSO; Cat no. D8418), 2, 7-dichlorodihydrofluorescein diacetate (DCFH-DA; Cat no. D6883) and radioimmunoprecipitation assay (RIPA) buffer (Cat no. R0278) were from Sigma Aldrich, USA. Primary antibodies against Glyoxalase 1 (GLO1; Cat no. ab96032) and Advanced glycation end products-receptor 1 (AGE-R1; Cat no. ab204314) were purchased from Abcam, Cambridge, UK. MG-Hs (Cat no. STA-011) was obtained from Cell Biolabs, San Diego, USA. RAGE 1 (Cat no. MA5-30062) was purchased from ThermoFisher Scientific, USA. Glyoxalase 2 (GLO2; Cat no. sc-365233), Nuclear factor E2-related factor 2 (Nrf2; Cat no. sc-365949), Heme oxygenase 1 (HO-1; Cat no. sc-10789) Superoxide dismutase 1 (SOD1; Cat no. 2770S) and Superoxide dismutase 2 (SOD2; Cat no. sc-137254) were obtained from Santa Cruz Biotechnology, Dallas, USA.

### 2.2.2 Cell culture and treatment

The human hepatocellular carcinoma cell line (HepG2) was purchased from the National Centre for Cell Sciences (NCCS, Pune) and grown in MEME medium supplemented with 10% FBS, 100 U/ml penicillin, and 100 µg/ml streptomycin. The cells were maintained in a humidified atmosphere with 5% (v/v) CO<sub>2</sub> at 37°C.

The following are details of the experimental groups:

- **Control** – Normal cells,
- **MGO** – cells were exposed to 50 µM MGO for 24 h,
- **MGO + A** – the cells were simultaneously exposed to 50 µM MGO and 200 µM aminoguanidine.

### 2.2.3 Cell viability analysis

The cell viability was checked with the methyl thiazolyl blue tetrazolium bromide (MTT) assay, following the protocol of Anupama et al., 2018. Briefly, HepG2 cells were seeded at a  $5 \times 10^3$ /well density in 96-well plates. Cells were then exposed to different concentrations of MGO (10, 50, 100, 500, and 1000 µM) for 24 h at 37°C. After incubation, the culture media was replaced with 100 µl of MTT solution (5 mg/ml) in each well, and the plate was incubated for 4 h in 5% CO<sub>2</sub> at 37°C. Then MTT solution was aspirated off, and 100 µl of dimethyl sulfoxide (DMSO) was added to each well and placed on a shaker for 20 min to dissolve the formazan crystals formed. The absorbance was measured at 570 nm using a spectrophotometer (BioTek, Synergy 4, BioTek Instruments Corp., Winooski, VT, USA).

### 2.2.4 ROS generation analysis

After respective treatments, 20 µM of 2',7'-dichlorofluorescein diacetate (DCFH-DA), a fluorescent dye (Mohan et al., 2021), was added to the cell for the estimation of the reactive oxygen species (ROS) formation. The cells were then incubated at 37°C for 20 min, then

washed 3 times with HBSS. DCF fluorescence was analysed under a fluorescent microscope (Olympus IX 83), and fluorescence intensity was measured at excitation/ emission: 488/525 nm).

### 2.2.5 Protein carbonyl assay

Following the corresponding treatments, cells were pelleted and homogenised with a cold buffer (50 mM phosphate, pH 6.7, with 1 mM EDTA). The cells were then centrifuged at 10,000 x g at 4°C for 15 min. The supernatant was collected in a fresh tube and placed on ice. 200 µl of the sample was transferred to two separate 2ml tubes. Tubes were labelled as a sample and the other as a control for each sample. 800 µl of DNPH and 800 µl of 2.5 M HCl were added to the sample and control tubes, respectively. Both tubes underwent a one-hour incubation period in the dark while being vortexed every 15 min.

Following incubation, 20 % TCA was added to all the tubes, vortexed, and placed on ice for 5 min. After 5 min of incubation, the tubes were subjected to centrifugation at 10,000 x g for 10 min at 4°C. The pellet was redissolved in 1 ml 10% TCA and incubated on ice for 5 min, and centrifuged again at 10,000 x g for 10 min at 4°C.

The supernatant was discarded, and the pellet was mixed in 1 ml of 1:1 ethanol/ethyl acetate mixture and vortexed to dissolve thoroughly. The tubes were again centrifuged at 10,000 x g for 10 min at 4°C. The wash was repeated 2 times. Then, the protein pellets were redissolved in guanidine hydrochloride and vortexed. The tubes were again centrifuged at 10,000 x g for 10 min at 4°C. The supernatant was collected and transferred to 96 well plates, and absorbance was taken at 360 nm. The following formula was used to determine the protein carbonyl content:

$$\text{Protein carbonyl (nmol/ml)} = [(CA) / (0.011 \mu\text{M}^{-1}) (500 \mu\text{l} / 200 \mu\text{l})]$$

Where CA = corrected absorbance

### 2.2.6 Western blotting analysis

After respective treatments, cells were lysed with RIPA buffer supplemented with a protease inhibitor (Sigma Aldrich, USA). Protein concentrations were determined by a bicinchoninic acid protein assay kit (BCA kit, Merck, USA). Equalised protein samples were resolved on 10% SDS PAGE and electrophoretically transferred to PVDF membranes (Millipore, Merck, USA) using Mini Trans-Blot Cell (Bio-Rad Laboratories, USA). The membranes were blocked with 5% BSA and incubated with primary antibodies at 4°C overnight. The membranes were then washed and incubated with the HRP-conjugated secondary antibodies at room temperature for 2 h and visualised with western blot hyper HRP substrate (Cat no. T7103A, Takara-Bio).  $\beta$  actin (Cat no. 4970) or GAPDH (Cat no. 5174S) was the loading control. The immunoblot images were analysed with the help of the ChemiDOC XRS system using Image Lab software.

### 2.2.7 Statistics

Results are shown as mean  $\pm$  SEM for the control and experimental groups after sextuplicate samples from each group were used in all analyses. Using ANOVA, the results were examined. All the data were analysed using SPSS for Windows, standard version 26 (SPSS), and a p-value  $\leq$  0.05 was considered significant.

## 2.3 Results

### 2.3.1 Effects of MGO on the viability of HepG2 cells

Our results revealed that MGO had no significant toxicity on the cell up to 500  $\mu$ M, but 1000  $\mu$ M significantly decreased the cell viability (70%;  $p \leq 0.05$ ; Figure 2.1). In our study, 50  $\mu$ M of MGO with 24 h of incubation was found to induce pathological changes, which were visible by molecular and biochemical assays. Due to the hermetic or dual properties of MGO,

sub-toxic doses are recommended for cancer-related studies (Nokin et al., 2019). Based on these 50  $\mu\text{M}$  of MGO was taken for further research.

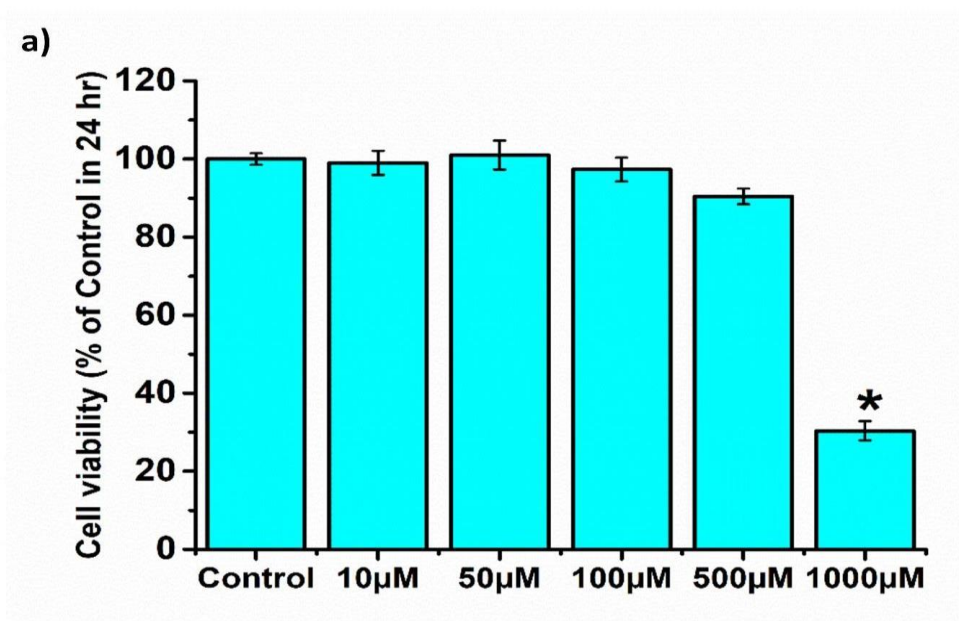


**Figure.2.1: a) Effect of various concentrations of MGO on cell viability in HepG2 cells.** Concentrations ranging from 10  $\mu\text{M}$  to 1 mM were tested. All data are represented as mean  $\pm$  SEM (n = 6). \*denotes that the mean value significantly differed from control cells ( $p \leq 0.05$ ).

### 2.3.2 MGO impairs the glyoxalase system

MGO downregulated the expression of both GLO 1 (27%) and GLO 2 (11%; Figure. 2.2) significantly ( $p \leq 0.05$ ) compared to the control. At the same time, aminoguanidine treatment maintained the expressions of both enzymes at a more or less control level.

### 2.3.3 MGO-induced accumulation of MGO-adducts

MGO-adduct formation during MGO treatment was evaluated by western blot. MGO-induced adduct formation was visible as multiple bands in the MGO (Figure 2.2.a) compared to less prominent bands in control. In contrast, adduct formation was found to be prevented in the MGO + A group (Figure 2).

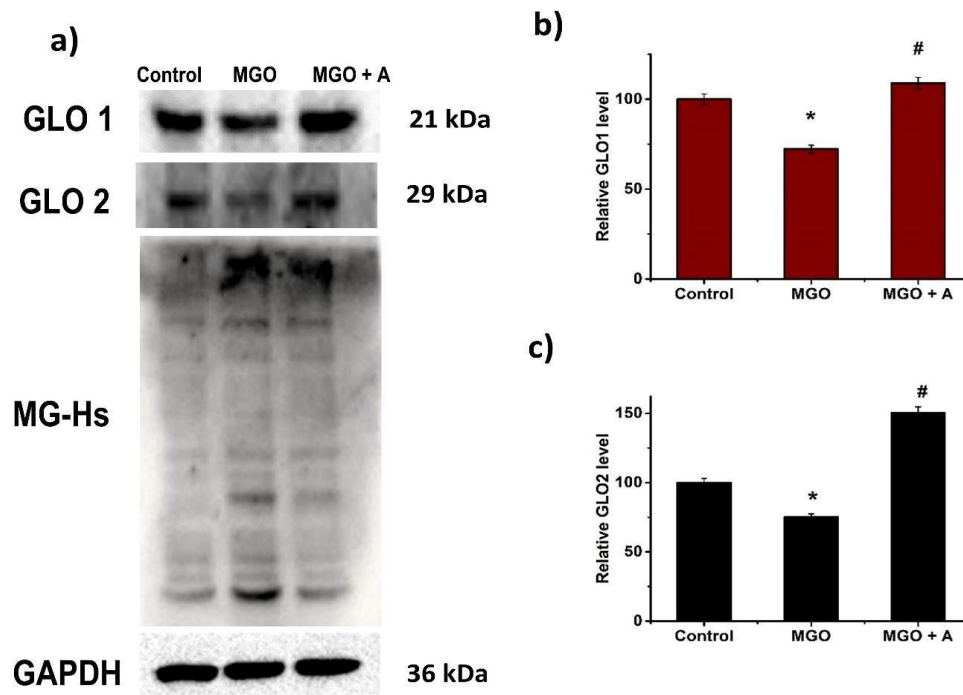


**Figure. 2.2. Effect of MGO on glyoxalase system and intracellular adduct formation.** a) Immunoblot analysis of Glyoxalase 1(GLO 1), Glyoxalase 2 (GLO 2) and MG-Hs in HepG2 cells b) & c) Densitometric analysis of GLO 1 and GLO 2, respectively, with respect to  $\beta$ -actin. Control (Control), Methylglyoxal (MGO, 50  $\mu$ M), MGO + Aminoguanidine (A, 200  $\mu$ M). Data are present mean values  $\pm$  SEM (n = 6). \* denotes  $p \leq 0.05$  with a significant difference from control cells. # denotes  $p \leq 0.05$  with a significant difference from MGO cells.

### 2.3.4 MGO stimulated the expression RAGE and AGE-R1

MGO caused significant overexpression of RAGE ( $p \leq 0.05$ ). A 95% increase in expression was observed in the MGO compared to the control, and aminoguanidine prevented the RAGE overexpression by 47% compared to the MGO (Figure 2.3.a & b). We also wanted to explore the role of MGO in AGE-R1 involved in AGE processing, and the results strongly indicated the negative impact of MGO on the same significantly ( $p \leq 0.05$ ) by decreasing (16%; Figure 2.3.a & c) the expression. And aminoguanidine reversed the effect of MGO by increasing AGE-R1 expression (15%) compared to the MGO.

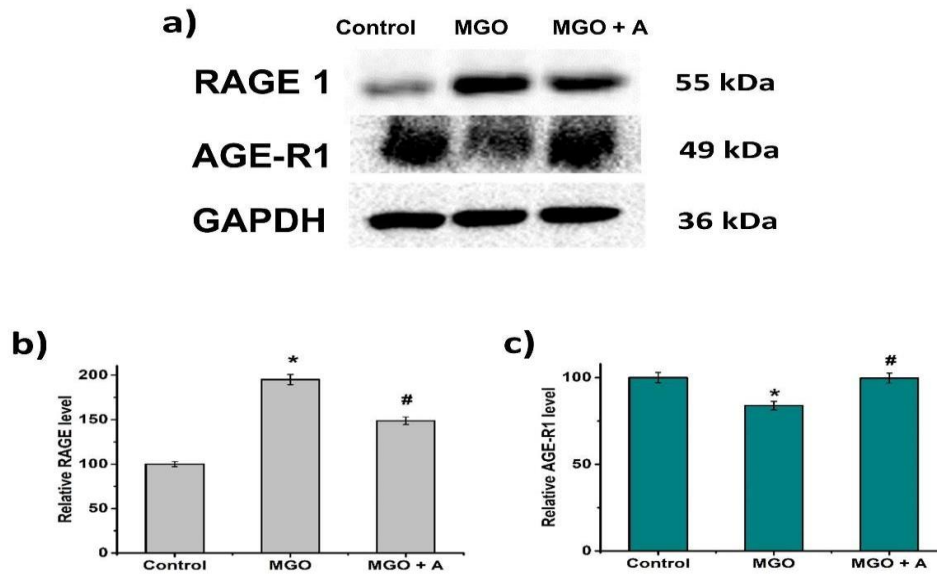


**Figure. 2.3: Effect of MGO receptors for AGEs.** a) Immunoblot analysis of RAGE 1 and AGE-R1 in HepG2 cells b) & c) Densitometric analysis of RAGE 1 and AGE-R1, respectively, with respect to  $\beta$ -actin. Control (Control), Methylglyoxal (MGO, 50  $\mu$ M), MGO + Aminoguanidine (A, 200  $\mu$ M). Data are present mean values  $\pm$  SEM (n = 6). \* denotes  $p \leq 0.05$  with a significant difference from control cells. # denotes  $p \leq 0.05$  with a significant difference from MGO cells.

### 2.3.5 MGO stimulates ROS generation and protein carbonyl formation

There was a significant increase (24%;  $p \leq 0.05$ ; Figures 2.4.a & b) in the intracellular ROS level in the MGO compared to the control. On the other hand, aminoguanidine significantly prevented ROS generation by 20.3% compared to the MGO.

We also analysed the level of oxidised proteins in the form of protein carbonyl formation and observed that protein carbonyl concentration was significantly increased in the MGO group (74.7273 nmol/ml;  $p \leq 0.05$ , Figure 2.4.c) compared to the control (1.2955 nmol/ml;  $p \leq 0.05$ ) and aminoguanidine could reverse (64.3182 nmol/ml;  $p \leq 0.05$ ) the effect up to a certain level but not fully.

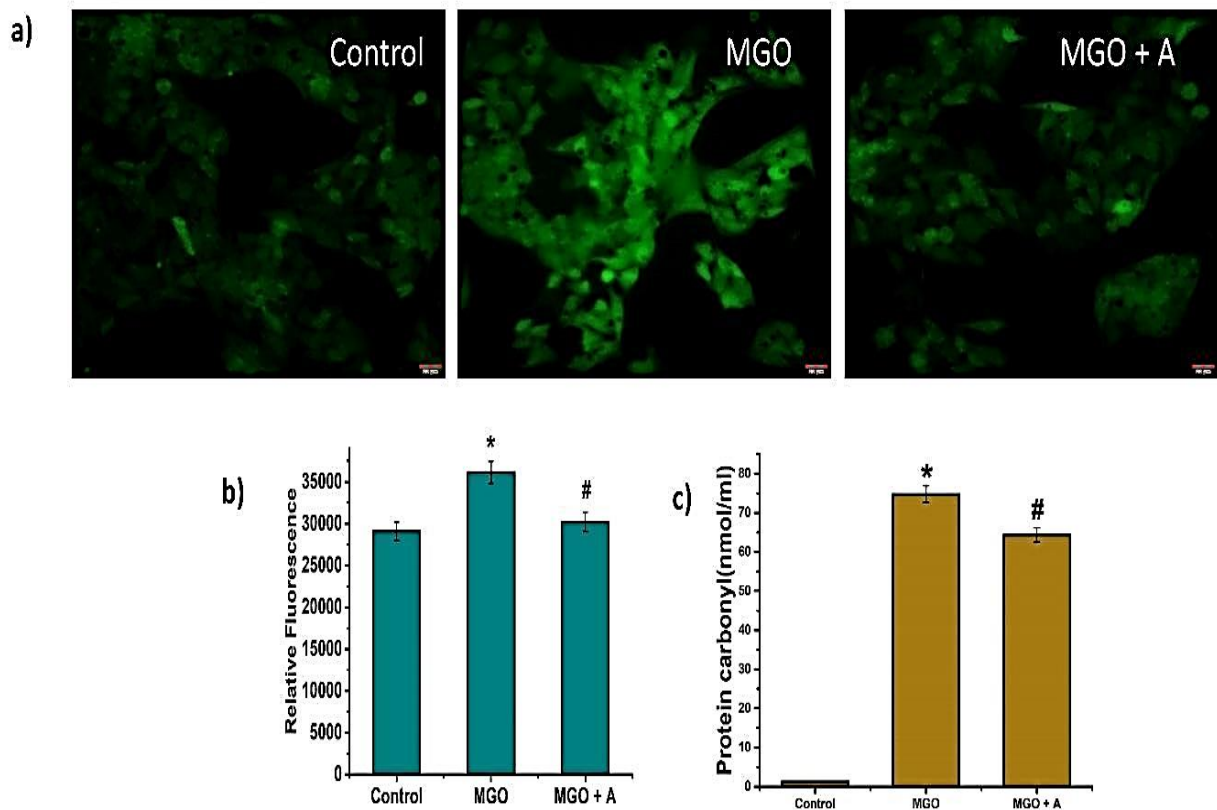


**Figure. 2.4: Genesis of oxidative stress with MGO in HepG2 cells.** a) Intracellular ROS production, b) fluorescent intensity and c) protein carbonyl formation analysis in HepG2 cells. Original magnification 20X. The scale bar corresponds to 20  $\mu$ M. Control (Control), Methylglyoxal (MGO, 50  $\mu$ M), MGO + Aminoguanidine (A, 200  $\mu$ M). Data are present mean values  $\pm$  SEM (n = 6). \* denotes  $p \leq 0.05$  with a significant difference from control cells. # denotes  $p \leq 0.05$  with a significant difference from MGO cells.

### 2.3.6 MGO alters innate antioxidants protein expression

MGO exposure significantly increased the expression of Nrf2 (12.6 %;  $p \leq 0.05$ ; Figure 2.5. a & b) compared to the control group and the aminoguanidine could reduce the effect by reducing the expression levels to the normal in HepG2 cells. MGO also significantly upregulated the expression of HO-1 by 23% ( $p \leq 0.05$ ) (Figure 2.5. a & c) compared to the control cells, and aminoguanidine treated groups reversed the effect significantly by reducing 15% ( $p \leq 0.05$ ) of the MGO treatment effect. MGO negatively affected the SOD1 expression

by 42 % ( $p \leq 0.05$ ; Figure 2.5. a & d) compared to the control cells, while aminoguanidine increased the expression by 15 % ( $p \leq 0.05$ ) compared to the MGO groups. Similarly, SOD2 was also significantly downregulated by 17 % ( $p \leq 0.05$ ; Figure 2.5. a & e) in the MGO group compared to the control groups, while aminoguanidine could not reverse the effect significantly.

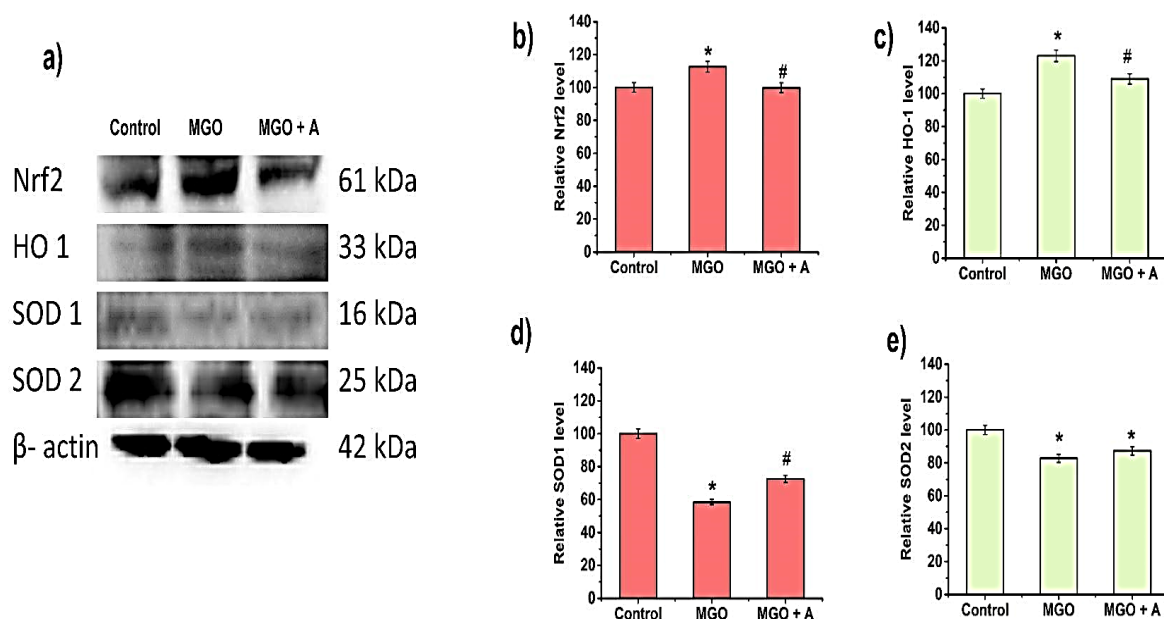


**Figure. 2.5: Antioxidant status MGO treated HepG2 cells.** a) Immunoblot analysis of Nrf2, HO-1, SOD1 and SOD2 b), c), d) & e) Densitometric analysis of Nrf2, HO-1, SOD1 and SOD2, respectively, with respect to  $\beta$ -actin. Control (Control), Methylglyoxal (MGO, 50  $\mu$ M), MGO + Aminoguanidine (A, 200  $\mu$ M). Data are present mean values  $\pm$  SEM ( $n = 6$ ). \* denotes  $p \leq 0.05$  with a significant difference from control cells. # denotes  $p \leq 0.05$  with a significant difference from MGO cells.

## 2.4 Discussion

MGO highly reactive alpha-oxoaldehyde can be generated in cells by a number of distinct mechanisms. In glycolysis, it is mainly produced as a by-product by the spontaneous breakdown of triose phosphate intermediates, glyceraldehyde-3-phosphate (G3P), and

dihydroxyacetone phosphate (DHAP) (Rabbani et al., 2016) MGO can also emerge from oxidation breakdown of glycated proteins, catabolism of threonine, and acetone metabolism (Lai et al., 2022). Considering MGO has a detrimental effect on biological systems, all mammalian cells have established an enzyme system that is specifically designed to detoxify MGO. Key enzymes in the anti-glycation defence, glyoxalase 1 (GLO1) and glyoxalase 2 (GLO2), catalyse the processing of MGO to D-lactate through the intermediate product S-D-lactoylglutathione (Farrera & Galligan, 2022). The imbalance in MGO generation, buildup, and clearance is referred to as MGO dicarbonyl stress (Nigro et al., 2019).

In the present study, we have seen a decreased expression and activity of GLO1 along with the decreased expression of GLO2 in the MGO treated group. MGO is thought to be the most powerful glycating agent because it is up to 20,000–50,000 times more reactive than glucose (Annibal et al., 2016). MGO causes proteins, lipids, and nucleotides to modify chemically rapidly. The synthesis of argpyrimidines, hydroimidazolones (MG-H1, MG-H2, and MG-H3), and tetrahydropyrimidines might result from irreversible reactions between MGO and the side chain amino group arginine residues in proteins (Schalkwijk & Stehouwer, 2020). Moreover, it produces small MG-derived lysine adducts such N-carboxyethyl-lysine when it interacts with lysine residues (CEL) (Schalkwijk & Stehouwer, 2020). Methylglyoxal, a potent inducer of AGEs, connects diabetes and cancer (Bellier et al., 2019)

Arginine is the principal amino acid that is affected by methylglyoxal glycation, which causes a loss of positive charge through the generation of hydroimidazolones. The hydroimidazolones generated from methylglyoxal (MG-Hs) have three structural isomers that are physiological ligands for RAGE: N $\delta$ -(5-hydro-5-methyl-4-imidazol-2-yl)ornithine (MG-H1), 5-(2-amino-5-hydro-5-methyl-4-imidazol-1-yl)norvaline (MG-H2) and 5-(2-amino-4-hydro-4-methyl-5-imidazol-1-yl)norvaline (MG-H3) (Xue et al., 2014). Here also we noticed that MGO treated HepG2 cells depicted an increased expression of MG-Hs, the

methylglyoxal adducts that act as ligands for receptors for advanced glycation end products (RAGE). The pathogenicity of AGEs is believed to be caused mainly by RAGE stimulation (Hofmann et al., 1999). Although AGE-RAGE biology has been researched for more than 20 years, relatively little is known about the biology of the AGE-RAGE axis. Since lysine and arginine residues are particularly susceptible to glycation, glycation events are not primarily dependent on sequence specificity (Xue et al., 2014). This explains, in large part, why AGEs produced by glycation reactions have a wide variety. Therefore, RAGE expression in the MGO treated cells was analysed, and we noticed a considerable increase in the expression of RAGE in the MGO treated HepG2 cells.

Extracellular proteolysis and intracellular absorption and degradation within cells mediated by AGEs-receptor 1 (AGE-R1) are the two most significant processes involved in the degradation of endogenous AGEs (Stirban et al., 2014). This made us look for the expression of AGE-R1 in the MGO treated cells, and as expected, the expression of AGE-R1 was negatively affected by MGO in HepG2 cells.

ROS generation is a natural outcome of metabolism. Oxidative stress can be produced by an imbalance of MGO formation, which promotes ROS production (de Bari et al., 2021). In this study, we noticed an increased ROS production in the MGO group compared to the control groups. Free radical species, which are highly reactive in nature, can attack proteins, lipids and nucleic acids to oxidise them. Significant quantities of protein carbonyl or oxidised proteins have been linked to diseases like Alzheimer's disease (AD), rheumatoid arthritis, diabetes, chronic renal failure, and respiratory distress syndrome. Protein carbonyls are also known as the most common biomarkers for ROS production (Dalle-Donne et al., 2003). Glycation also promotes protein carbonyl production. Considering these facts, we also checked the protein carbonyl levels in MGO treated HepG2 cells and found an enormously elevated level of protein carbonyl in the MGO group compared to the control group.

Excessive ROS generation can lead to cellular damage and eventually lead to cell death. Therefore, our innate system has developed an extensive network of various endogenous antioxidants, which maintains a balance between generating and scavenging ROS. Nrf2 is a transcriptional signal that controls the expression of various antioxidant genes in the cells (He et al., n.d.). Exposure to tolerable oxidative stress activates Nrf 2, while unrestricted and persistent ROS can reduce Nrf 2 signalling in the liver (Mahmoud et al., 2017). Here in this study, we have noticed an increase in the expression of Nrf 2 in the MGO group compared to the control group. HO-1 is one of the major antioxidants, which is activated by Nrf2, and we have noticed that the increased Nrf2 expression by MGO could also increase the expression of HO-1 in HepG2 cells. At the same time, MGO decreased the expression of SOD1 and SOD2 in HepG2 cells. This indicates a clear disbalance in the antioxidant system by MGO in HepG2 cells.

## 2.5 Summary and Conclusion

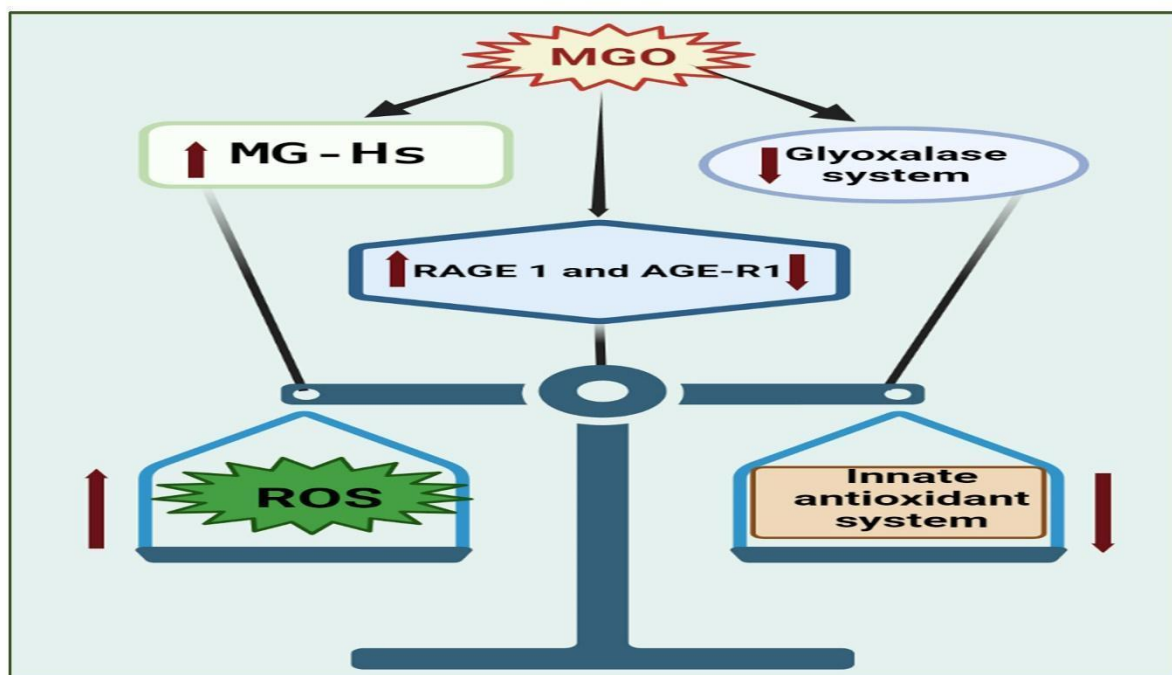


Figure. 2.6: Schematic representation of altered glyoxalase pathway and redox status by MGO

Upon MGO exposure, the HepG2 cells were unable to detoxify the MGO as the function of the Glyoxalase system was hampered, and this increased the formation of MG-Hs in cells. RAGE-1 upregulation was also noticed in the MGO group, while the expression of AGE detoxifying receptor AGE-R1 was found to be downregulated by MGO. MGO-AGE or MG-Hs formation increases ROS generation in the cells, negatively affecting the balance between oxidative stress and antioxidant activation.

## 2.6 References

1. Annibal, A., Riemer, T., Jovanovic, O., Westphal, D., Griesser, E., Pohl, E. E., Schiller, J., Hoffmann, R., & Fedorova, M. (2016). Structural, biological and biophysical properties of glycated and glycoxidized phosphatidylethanolamines. *Free Radical Biology and Medicine*, 95, 293–307. <https://doi.org/10.1016/j.freeradbiomed.2016.03.011>
2. Anupama, N., Preetha Rani, M. R., Shyni, G. L., & Raghu, K. G. (2018). Glucotoxicity results in apoptosis in H9c2 cells via alteration in redox homeostasis linked mitochondrial dynamics and polyol pathway and possible reversal with cinnamic acid. *Toxicology in Vitro*, 53, 178–192. <https://doi.org/10.1016/J.TIV.2018.08.010>
3. Bellier, J., Nokin, M. J., Lardé, E., Karoyan, P., Peulen, O., Castronovo, V., & Bellahcène, A. (2019). Methylglyoxal, a potent inducer of AGEs, connects diabetes and cancer. *Diabetes Research and Clinical Practice*, 148, 200–211. <https://doi.org/10.1016/J.DIABRES.2019.01.002>
4. Bongarzone, S., Savickas, V., Luzi, F., & Gee, A. D. (2017). Targeting the Receptor for Advanced Glycation Endproducts (RAGE): A Medicinal Chemistry Perspective. *Journal of Medicinal Chemistry*, 60(17), 7213–7232.

[https://doi.org/10.1021/ACS.JMEDCHEM.7B00058/ASSET/IMAGES/LARGE/JM-2017-00058M\\_0007.JPEG](https://doi.org/10.1021/ACS.JMEDCHEM.7B00058/ASSET/IMAGES/LARGE/JM-2017-00058M_0007.JPEG)

5. Dalle-Donne, I., Rossi, R., Giustarini, D., Milzani, A., & Colombo, R. (2003). Protein carbonyl groups as biomarkers of oxidative stress. *Clinica Chimica Acta*, 329(1–2), 23–38. [https://doi.org/10.1016/S0009-8981\(03\)00003-2](https://doi.org/10.1016/S0009-8981(03)00003-2)
6. de Bari, L., Scirè, A., Minnelli, C., Cianfruglia, L., Kalapos, M. P., & Armeni, T. (2021). Interplay among Oxidative Stress, Methylglyoxal Pathway and S-Glutathionylation. *Antioxidants*, 10(1), 1–17. <https://doi.org/10.3390/ANTIOX10010019>
7. Farrera, D. O., & Galligan, J. J. (2022). The Human Glyoxalase Gene Family in Health and Disease. *Chemical Research in Toxicology*, 35(10), 1766–1776. [https://doi.org/10.1021/ACS.CHEMRESTOX.2C00182/ASSET/IMAGES/LARGE/TX2C00182\\_0006.JPEG](https://doi.org/10.1021/ACS.CHEMRESTOX.2C00182/ASSET/IMAGES/LARGE/TX2C00182_0006.JPEG)
8. He, F., Ru, X., & Wen, T. (n.d.). *Molecular Sciences NRF2, a Transcription Factor for Stress Response and Beyond*. <https://doi.org/10.3390/ijms21134777>
9. Hofmann, M. A., Drury, S., Fu, C., Qu, W., Taguchi, A., Lu, Y., Avila, C., Kambham, N., Bierhaus, A., Nawroth, P., Neurath, M. F., Slattery, T., Beach, D., McClary, J., Nagashima, M., Morser, J., Stern, D., & Schmidt, A. M. (1999). RAGE mediates a novel proinflammatory axis: A central cell surface receptor for S100/calgranulin polypeptides. *Cell*, 97(7), 889–901. [https://doi.org/10.1016/S0092-8674\(00\)80801-6](https://doi.org/10.1016/S0092-8674(00)80801-6)
10. Kilhovd, B. K., Giardino, I., Torjesen, P. A., Birkeland, K. I., Berg, T. J., Thornalley, P. J., Brownlee, M., & Hanssen, K. F. (2003). Increased serum levels of the specific AGE-compound methylglyoxal-derived hydroimidazolone in patients with type 2 diabetes. *Metabolism: Clinical and Experimental*, 52(2). <https://doi.org/10.1053/meta.2003.50035>

11. Lai, S. W. T., Lopez Gonzalez, E. D. J., Zoukari, T., Ki, P., & Shuck, S. C. (2022). Methylglyoxal and Its Adducts: Induction, Repair, and Association with Disease. *Chemical Research in Toxicology*, 35(10), 1720–1746. [https://doi.org/10.1021/ACS.CHEMRESTOX.2C00160/ASSET/IMAGES/LARGE/TX2C00160\\_0007.JPEG](https://doi.org/10.1021/ACS.CHEMRESTOX.2C00160/ASSET/IMAGES/LARGE/TX2C00160_0007.JPEG)
12. Lee, J. H., Parveen, A., Do, M. H., Kang, M. C., Yumnam, S., & Kim, S. Y. (2020). Molecular mechanisms of methylglyoxal-induced aortic endothelial dysfunction in human vascular endothelial cells. *Cell Death & Disease*, 11(5), 403. <https://doi.org/10.1038/s41419-020-2602-1>
13. Liu, J., Mak, T. C. P., Banigesh, A., Desai, K., Wang, R., & Wu, L. (2012). Aldolase B knockdown prevents high glucose-induced methylglyoxal overproduction and cellular dysfunction in endothelial cells. *PLoS ONE*, 7(7). <https://doi.org/10.1371/journal.pone.0041495>
14. Mahmoud, A. M., Hozayen, W. G., & Ramadan, S. M. (2017). Berberine ameliorates methotrexate-induced liver injury by activating Nrf2/HO-1 pathway and PPAR $\gamma$ , and suppressing oxidative stress and apoptosis in rats. *Biomedicine & Pharmacotherapy*, 94, 280–291. <https://doi.org/10.1016/J.BIOPHA.2017.07.101>
15. Mohan, S., George, G., & Raghu, K. G. (2021). Vanillic acid retains redox status in HepG2 cells during hyperinsulinemic shock using the mitochondrial pathway. *Food Bioscience*, 41, 101016. <https://doi.org/10.1016/J.FBIO.2021.101016>
16. Nigro, C., Leone, A., Fiory, F., Prevezano, I., Nicolò, A., Mirra, P., Beguinot, F., & Miele, C. (2019). *cells Dicarbonyl Stress at the Crossroads of Healthy and Unhealthy Aging*. <https://doi.org/10.3390/cells8070749>
17. Nokin, M. J., Bellier, J., Durieux, F., Peulen, O., Rademaker, G., Gabriel, M., Monseur, C., Charlotiaux, B., Verbeke, L., van Laere, S., Roncarati, P., Herfs, M., Lambert, C.,

- Scheijen, J., Schalkwijk, C., Colige, A., Caers, J., Delvenne, P., Turtoi, A., ... Bellahcène, A. (2019). Methylglyoxal, a glycolysis metabolite, triggers metastasis through MEK/ERK/SMAD1 pathway activation in breast cancer. *Breast Cancer Research, 21*(1). <https://doi.org/10.1186/S13058-018-1095-7>
18. Rabbani, N., & Thornalley, P. J. (2015). Dicarbonyl stress in cell and tissue dysfunction contributing to ageing and disease. In *Biochemical and Biophysical Research Communications* (Vol. 458, Issue 2). <https://doi.org/10.1016/j.bbrc.2015.01.140>
19. Rabbani, N., Xue, M., & Thornalley, P. J. (2016). Methylglyoxal-induced dicarbonyl stress in aging and disease: first steps towards glyoxalase 1-based treatments. *Clinical Science, 130*(19), 1677–1696. <https://doi.org/10.1042/CS20160025>
20. Reyaz, A., Alam, S., Chandra, K., Kohli, S., & Agarwal, S. (2020). *Methylglyoxal and soluble RAGE in type 2 diabetes mellitus: Association with oxidative stress.* <https://doi.org/10.1007/s40200-020-00543-y>
21. Schalkwijk, C. G., & Stehouwer, C. D. A. (2020). Methylglyoxal, a highly reactive dicarbonyl compound, in diabetes, its vascular complications, and other age-related diseases. *Physiological Reviews, 100*(1), 407–461. <https://doi.org/10.1152/PHYSREV.00001.2019/ASSET/IMAGES/LARGE/Z9J0012029260011.JPEG>
22. Sruthi, C. R., & Raghu, K. G. (2021). Advanced glycation end products and their adverse effects: The role of autophagy. *Journal of Biochemical and Molecular Toxicology, 35*(4), e22710. <https://doi.org/10.1002/JBT.22710>
23. Stirban, A., Gawlowski, T., & Roden, M. (2014). Vascular effects of advanced glycation endproducts: Clinical effects and molecular mechanisms. *Molecular Metabolism, 3*(2), 94–108. <https://doi.org/10.1016/J.MOLMET.2013.11.006>

24. Vomund, S., Schäfer, A., Parnham, M. J., Brüne, B., & von Knethen, A. (2017). Molecular Sciences Nrf2, the Master Regulator of Anti-Oxidative Responses. *J. Mol. Sci*, 18. <https://doi.org/10.3390/ijms18122772>
25. Xue, J., Ray, R., Singer, D., Böhme, D., Burz, D. S., Rai, V., Hoffmann, R., & Shekhtman, A. (2014). The Receptor for Advanced Glycation End Products (RAGE) Specifically Recognises Methylglyoxal-Derived AGEs. *Biochemistry*, 53(20), 3327. <https://doi.org/10.1021/BI500046T>
26. Yang, Z., Zhang, W., Lu, H., & Cai, S. (2022). Methylglyoxal in the Brain: From Glycolytic Metabolite to Signalling Molecule. In *Molecules* (Vol. 27, Issue 22). MDPI. <https://doi.org/10.3390/molecules27227905>
27. Yue, Q., Song, Y., Liu, Z., Zhang, L., Yang, L., & Li, J. (2022). Receptor for Advanced Glycation End Products (RAGE): A Pivotal Hub in Immune Diseases. *Molecules* 2022, Vol. 27, Page 4922, 27(15), 4922. <https://doi.org/10.3390/MOLECULES27154922>
28. Zhou, Q., Gong, J., & Wang, M. (2019). Phloretin and its methylglyoxal adduct: Implications against advanced glycation end products-induced inflammation in endothelial cells. *Food and Chemical Toxicology*, 129, 291–300. <https://doi.org/10.1016/J.FCT.2019.05.004>

## Chapter 3

# **The alterations in glucose metabolism and genesis of the Warburg effect in HepG2 cells by methylglyoxal**

---

---

### **3.1 Introduction**

A crucial part of metabolism is glucose. It serves as a fuel source and a substrate for the synthesis of cell components (Towle, 2005). The primary cause of diabetic morbidity and mortality, as well as the main consequence of the development of diabetes, is the metabolic dysregulation of glucose homeostasis (Jiang et al., 2020).

The liver, which produces glucose during fasting and stores it postprandially, is essential for maintaining appropriate glucose homeostasis. However, type 1 and type 2 diabetes mellitus both have dysregulation of these liver functions, and this imbalance makes fasting and postprandial hyperglycemia more likely. The total glucose fluxes from several pathways, including gluconeogenesis, glycogenolysis, glycogen synthesis, and glycolysis, which is known as net hepatic glucose production (Petersen et al., 2017).

The liver produces about 90% of endogenous glucose (Ekberg et al., 1999), vital for maintaining systemic glucose homeostasis (Moore et al., 2012). Net hepatic glucose production (HGP) is the total fluxes from many pathways, including gluconeogenesis, glycogenolysis, glycogen synthesis, and glycolysis. During fasting, the liver produces glucose to provide euglycemia and supply energy to tissues that must consume glucose, including neurons, red blood cells, and renal medullary cells (Rizza, 2010). Following a meal, the liver helps to maintain appropriate glucose tolerance (Moore et al., 2017). As a result, the liver is a crucial

target organ that controls glucose homeostasis and can be targeted by the administration of particular diabetes medications (Rines et al., 2016)

In comparison to people without diabetes, people with diabetes are thought to have an average two times higher chance of developing liver cancer and a roughly 50% higher risk of dying from this illness. It has also been suggested that diabetes may be responsible for 15% of liver cancer cases globally (Wang et al., 2012).

Carbonyl stress is a frequent aspect of the metabolic disorders linked to diabetes and cancer at the molecular level. Most frequently detected in the context of diabetes, MGO-related AGEs have been found to be raised two- to fivefold. For instance, voltage-gated sodium channel Nav1.8 (Bierhaus et al., 2012) and type IV collagen of the vascular basement membrane (Dobler et al., 2006) have both been linked to secondary diabetic complications. Carbonyl stress and cancer are poorly understood, despite the well-established link between oxidative stress, cancer formation, progression, and therapeutic response. It has never been thought to be possibly related. MGO-derived AGEs were detected in malignant tumours (Leone et al., 2021). Indeed, over the past few years, mounting data has emphasised the significance of MGO-mediated stress, particularly when it comes to the development of cancer (Bellahcène et al., 2018); (Bellier et al., 2019).

One of the primary metabolic alterations in cancer cells is the propensity for anaerobic glycolysis to create ATP, regardless of the presence or absence of oxygen (DeBerardinis & Chandel, 2020). Otto Warburg first identified this phenomenon as the "Warburg effect" in the 1920s when he demonstrated that cultivated tumour tissues have a high glucose uptake rate, lactate production, and oxygen availability (DeBerardinis & Chandel, 2020). Even in oxygen-rich environments and with functioning mitochondria, cancer cells prefer the fermentation of

glucose to lactate because it happens 10-100 times faster than the complete oxidation of glucose in mitochondria (Liberti & Locasale, 2016).

We were curious about the effect of MGO mediated dicarbonyl stress on HepG2 cells and whether MGO could induce metabolic reprogramming of the non-tumorigenic cells to promote cancer.

## **3.2 Materials and methods**

### **2.2.1 Reagents**

MGO (Cat no. M0252) was obtained from Sigma Aldrich, USA. Minimal essential media Eagles (MEME) with Earle's salt (Cat no. AL047S), Phosphate buffered saline (PBS; Cat no. TL1099), and aminoguanidine bicarbonate (Cat no. RM1573) were purchased from Himedia, India. Fetal bovine serum (FBS; Cat no. 16000044), penicillin–streptomycin antibiotics (Cat no. 15070063), 0.5% trypsin-ethylene diamine tetra acetic acid (trypsin-EDTA; Cat no. R001100), and Hanks balanced saline solution or HBSS (Cat no. 1835981) were from Gibco-BRL Life Technologies (Waltham, MA, USA). Methyl thiazolyl blue tetrazolium bromide (MTT) was purchased from Sisco Research Laboratories Pvt. Ltd. Dimethyl sulfoxide (DMSO; Cat no. D8418) and radioimmunoprecipitation assay (RIPA; Cat no. R0278) buffer were from Sigma Aldrich, USA. Hypoxia-inducible factor (HIF-1 $\alpha$ ; Cat no. ITT01009), Lactate dehydrogenase-A (LDH-A; Cat no. ITT06280), c-Myc (Cat no. ITT00358), Yes Associated Protein (YAP, Cat no. ITT03182), and phosphorylated YAP (p-YAP, Cat no. ITT03382) were purchased from G-Biosciences, St. Louis, USA. Glucose transporter 1 (GLUT1; Cat no. sc-1603), Glucose transporter 2 (GLUT2; Cat no. sc-518022), Hexokinase II (HK II; Cat no. 2867S), Phosphofructokinase 1 (PFK1; Cat no. sc-377346), Enolase 1 (Cat no. sc-15343), Pyruvate dehydrogenase lipoamide kinase isozyme 1 (PDK1; Cat no. sc-515944)

were obtained from Santa Cruz Biotechnology (Dallas, USA). Hexokinase II (HK II; Cat no. 2867S) was purchased from Cell signaling Technology, Danvers, MA, USA.

### **3.2.2 Cell culture and treatment**

A human hepatocellular carcinoma cell line (HepG2) was procured from the National Centre for Cell Sciences (NCCS; Pune) and maintained in Minimal essential media eagle's (MEME) supplemented with 10% foetal bovine serum, 100 U/ml penicillin, and 100 µg/ml streptomycin. The cells were grown at 37°C in a humidified atmosphere containing 5% (v/v) CO<sub>2</sub>.

### **3.2.3 Glucose uptake analysis**

#### **3.2.3.1 Analysis of glucose uptake by flow cytometry**

After receiving the treatment plans for 24 h, the cell culture medium was replaced with new media containing 100 µM 2-[N-(7-nitrobenz-2-oxa-1,3-diazol-4-yl) amino]-2-deoxy-D-glucose (2-NBDG), which was then incubated for 30 min. The fluorescent probe 2-NBDG is a D-glucose derivative. Negative controls were cells that lacked 2 NBDG. After two washes, the cells were trypsinised by adding 100 µl of 10X trypsin-EDTA and centrifuged at 20,000 x g for 15 min at 4 °C (Kubota Laboratory Centrifuges Co. in Tokyo, Japan). The pellets were dissolved in PBS and centrifuged at 20,000 x g for 15 min at 4 °C. After being redissolved in PBS, the pellet was filtered using a cell strainer. Using a flow cytometer, the FACS Aria TM II (BD Biosciences), the cells were then examined for fluorescence intensity.

#### **3.2.3.2 Analysis of glucose uptake**

The manufacturer's recommendations were followed while measuring 2DG6P uptake using a cell-based glucose uptake colorimetric assay kit (Abcam, Cambridge, UK) (Sun et al., 2021) for the purpose of quantifying glucose uptake in HepG2 cells. Briefly, the cells were incubated for 5 min at room temperature (RT, 22 to 28 °C) in a solution of HEPES buffer

containing 10  $\mu$ M 2-deoxy-D-glucose (2-DG). After incubation, cells were washed twice and trypsinised with 100  $\mu$ L of 10X trypsin-EDTA followed by centrifugation at 20,000 x g for 15 min. at 4 °C using a high-speed refrigerated centrifuge (Kubota Laboratory Centrifuges Co., Tokyo, Japan). The pellets were dissolved in 10  $\mu$ l of a neutralising buffer and again centrifuged at 20,000 x g at 4 °C for 15 min. The supernatant was transferred to a fresh tube. 50  $\mu$ l of the supernatant was combined with 10  $\mu$ l of the reaction mix A, and the mixture was incubated at RT for 1 hour. 90  $\mu$ l of extraction buffer was added and heated for 40 min at 90 °C. 38  $\mu$ l of reaction mix B and 12  $\mu$ l of neutralising buffer were then added. Next, absorbance was measured at 412 nm every 2 min (BioTek Synergy 4, BioTek Instruments Corp., Winooski, VT, USA).

### **3.2.4 Western blotting analysis**

Cells were grown in T25 flasks containing 5 ml of culture medium. Cells were then subjected to treatments for 24 h; After 24 h, cells were collected and lysed in an ice-cold RIPA buffer containing a protease inhibitor cocktail (Sigma-Aldrich). The homogenate was centrifuged at 12,000 rpm for 20 min at 4 °C. The supernatants were collected, and protein concentrations were determined by a bicinchoninic acid protein assay kit (BCA kit, Merck) in accordance with the manufacturer's instructions. Equalised total protein from each sample was resolved by 10% SDS PAGE and electrophoretically transferred to PVDF membranes (Millipore) using the Trans-Blot® Turbo™ Transfer system (Bio-Rad, USA). After blocking the membranes with 5 percent skimmed milk in TBST (tris buffered saline-Tween 20) for 1 h, the primary antibodies were incubated with the membranes at 4°C overnight with gentle agitation. The membranes were then washed three times with TBST for 10 min and then incubated with the HRP conjugated secondary antibodies at room temperature for 2 h after incubation; membranes were again washed 3 times with TBST and developed with western blot hyper HRP substrate (Takara-Bio, USA).  $\beta$  actin or GAPDH was the loading control. The

immunoblot images were analysed, and bands' relative intensity were quantified using the ChemiDOC XRS system and Image Lab software (BioRad Quantity One version 4.5 software).

### **3.2.5 Measurement of hexokinase activity (HK)**

Hexokinase activity was evaluated by using a kit (Biovision, Waltham, MA, USA) (Mack et al., 2015). Cells were homogenised with a cold HK assay buffer. Samples were then centrifuged at 12000 RPM for 5 min at 4°C. Supernatants were collected for HK activity analysis. Samples were incubated with a reaction mixture for 1 hr at RT. NADH interference in the samples was avoided by using sample background controls. After incubation, absorbance was measured at 450 nm by using a microplate reader (Infinite® M200 PRO, Tecan).

### **3.2.6 Analysis of lactate production**

The lactate concentration in the culture media was calculated using a Biovision test kit (Lee et al., 2019). The kit's protocol was followed when performing the assay. Culture mediums from each group were used as samples for the study. The samples were added to a reaction mixture composed of lactate enzyme mixture and lactate probe and incubated at room temperature in the dark for 30 min. After incubation, the absorbance (OD 570 nm) was read using a microplate reader (Infinite® M200 PRO, Tecan).

### **3.2.7 Oxygen consumption rate assay**

Using an assay kit from Cayman, the oxygen consumption rate (OCR) in the cells was calculated (Swapna Sasi et al., 2020). This test is designed to evaluate the mitochondria's functioning state. The kit measures mitochondrial-associated OCR in live cells using a phosphorescent oxygen probe that is sensitive to oxygen concentrations between 0% and 20%. After treatments, the spent medium was discarded, and fresh medium was added to all the wells. 10 µl of phosphorescence of mitoxpress-xtra was added to all the wells except blank wells. Afterwards, each well received 100 µl of HS mineral oil (supplied with the kit). The

phosphorescence of mitoxpress-xtra was quenched by oxygen in the media; thus, the signal was inversely proportional to the amount of oxygen present. At an excitation/emission rate of 380/650 nm, the change in the mitoxpress probe signal was monitored for 120 min.

### **3.2.8 Statistics**

Results are shown as mean  $\pm$  SEM for the control and experimental groups after sextuplicate samples from each group were used in all analyses. Using ANOVA, the results were examined. All the data were analysed using SPSS for Windows, standard version 26 (SPSS), and a p-value  $\leq 0.05$  was considered significant.

## **3.3 Results**

### **3.3.1 MGO enhanced glucose uptake in HepG2 cells**

To examine the impact of MGO on glucose uptake, cytometry analysis was carried out by observing the fluorescence of 2NBDG. The findings showed MGO significantly increased HepG2 cells' basal glucose uptake. In comparison to the control, it was learned that glucose absorption had risen by 15.1% (Figure 3.1. a).

A colorimetric glucose uptake experiment to evaluate the uptake of glucose quantitatively. The same pattern was also noticed here. When compared to the control, the MGO group significantly increased glucose uptake (6 pmol/l,  $p \leq 0.05$ ; Figure. 3.1.b). In contrast, aminoguanidine considerably mitigated this impact by lowering 6 pmol/l compared to the MGO.

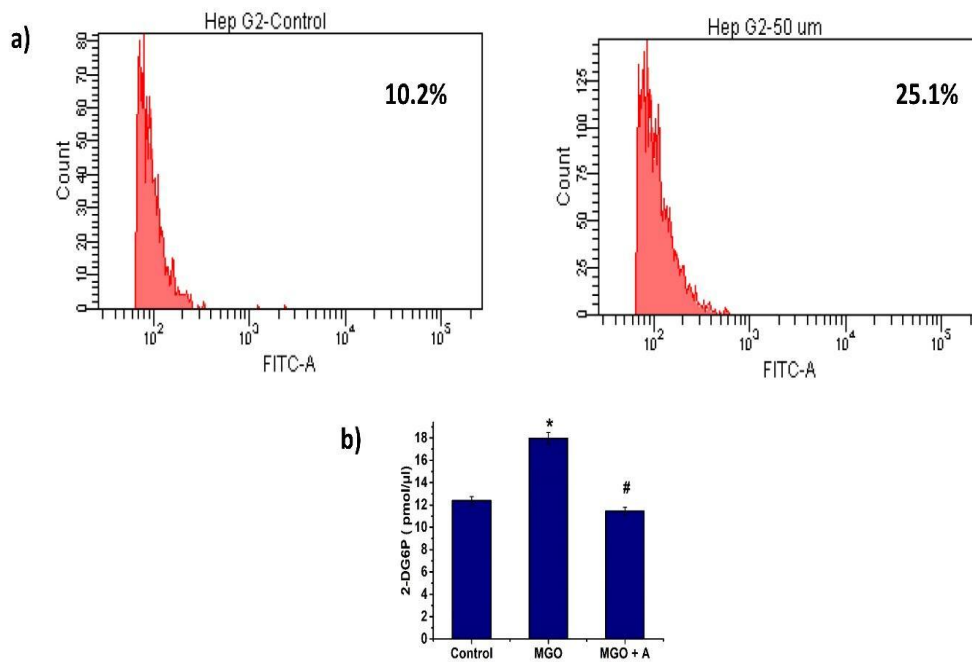


**Figure. 3.1: Determination of glucose uptake in HepG2 cells.** a) Glucose using flow cytometry and b) Glucose uptake (colorimetric). Control (Control), Methylglyoxal (MGO, 50  $\mu$ M), MGO + Aminoguanidine (A, 200  $\mu$ M). Data are present mean values  $\pm$  SEM (n = 6). \* denotes  $p \leq 0.05$  with a significant difference from control cells. # denotes  $p \leq 0.05$  with a significant difference from MGO cells.

### 3.3.2 Effect of MGO on glucose transporters (GLUT 1 and GLUT 2)

The expression of GLUT 1 was examined using western blot analysis, and we discovered that this was significantly increased in the MGO (35%; Figure.3.2). When compared to cells from the MGO group, the MGO + A group's GLUT1 expression was shown to be 28% lower.

The expression of GLUT 2 was also examined using western blot analysis; we discovered that the MGO had considerably higher levels (21%;  $p \leq 0.05$ ) of GLUT 2 expression than the control samples. The MGO+A group's cells showed a 30% reduction in GLUT 2 expression when compared to the MGO group's cells.

So, here we observed an increased expression of GLUT1 and GLUT 2 in HepG2 cells upon MGO exposure (Figure.3.2).

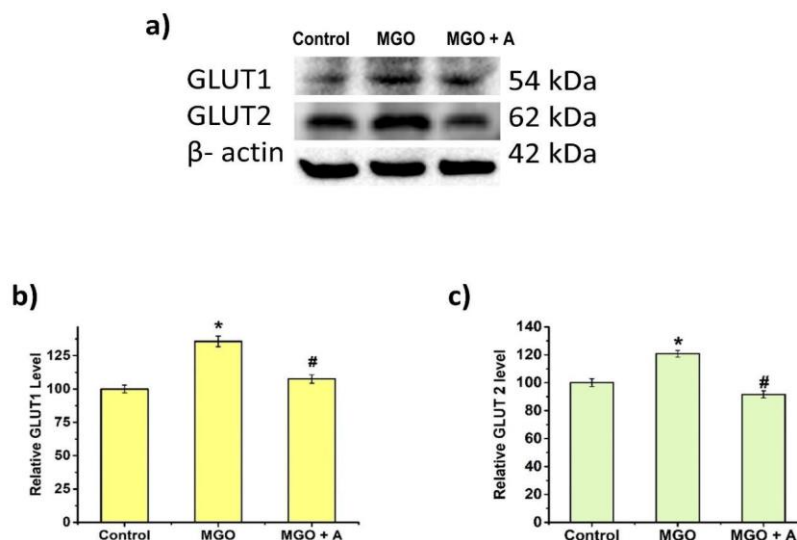


**Figure. 3.2: Effect of MGO on GLUTs expression.** a) Immunoblot analysis of GLUT1 and GLUT2 b) & c) Densitometric analysis of GLUT1 and GLUT2, respectively, with respect to  $\beta$ -actin. Control (Control), Methylglyoxal (MGO, 50  $\mu$ M), MGO + Aminoguanidine (A, 200  $\mu$ M). Data are present mean values  $\pm$  SEM (n = 6). \* denotes  $p \leq 0.05$  with a significant difference from control cells. # denotes  $p \leq 0.05$  with a significant difference from MGO cells.

### 3.3.3 Effect of MGO on glycolytic enzymes

The effect of the elevated glucose absorption by MGO on glycolysis (Figure.3.3) was analysed. It was investigated how it might affect the major glycolysis enzymes. Comparing the MGO to the control, we saw a significant (42%;  $p \leq 0.05$ ) rise in HK II activity. As compared to the control, it was also seen that the expression of the glycolytic enzymes HK II, PFK1, and enolase1 increased significantly ( $p \leq 0.05$ ). In addition, aminoguanidine dramatically reduced the expression of HK II, PFK1, and enolase 1 compared to MGO by 40%, 41%, and 25%, respectively.

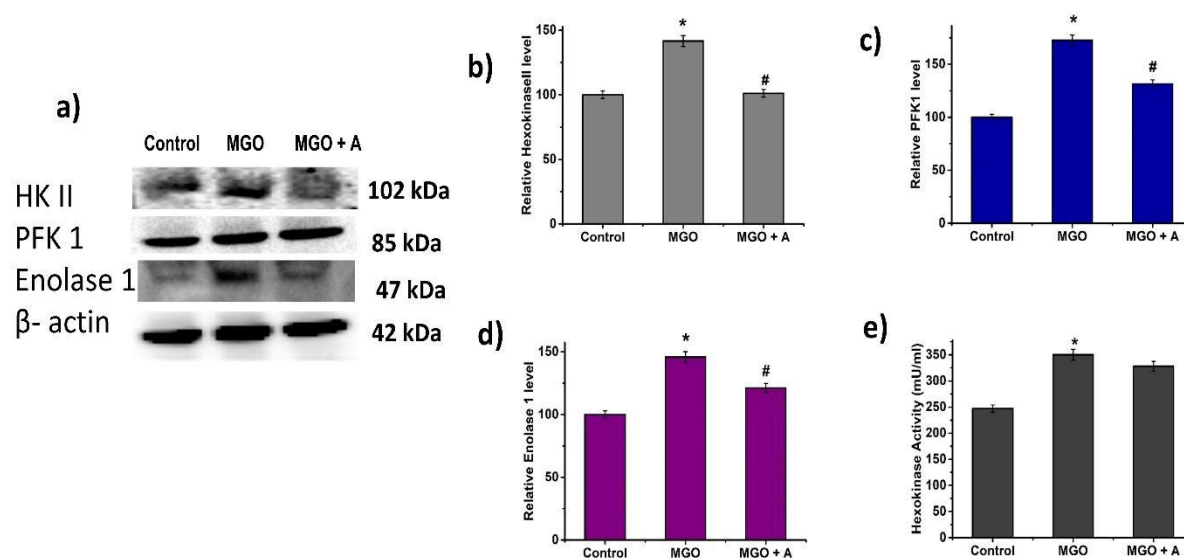


**Figure. 3.3: Effect of MGO on glycolytic enzymes.** a) Immunoblot analysis of Hexokinase II (HKII), phosphofructokinase 1 (PFK 1), and Enolase 1 in HepG2 cells. b), c) & d) Densitometric analysis of hexokinase II (HKII), phosphofructokinase 1 (PFK 1), and Enolase 1, respectively, with respect to  $\beta$ -actin. e) Determination of hexokinase activity. Control (Control), Methylglyoxal (MGO, 50  $\mu$ M), MGO + Aminoguanidine (A, 200  $\mu$ M). Data are present mean values  $\pm$  SEM (n = 6). \* denotes  $p \leq 0.05$  with a significant difference from control cells. # denotes  $p \leq 0.05$  with a significant difference from MGO cells.

### 3.3.4 MGO facilitates metabolic flux toward aerobic glycolysis in HepG2 cells

A closer look was taken at what happened to the pyruvate generated by the increased glycolysis. When compared to the control, we witnessed a significant ( $p \leq 0.05$ ) rise in the expression of PDK1 (34%). (Figure 3.4). By drastically reducing (by 48%) the PDK1 expression compared to MGO, aminoguanidine kept the enzyme at its normal level. After that, we investigated LDHA expression and lactate generation. Both the production of lactate (20%) and LDHA expression were observed to be significantly ( $p \leq 0.05$ ) higher in the MGO when compared to the control (Figure 5G). When compared to the MGO, aminoguanidine

considerably reduced lactate generation (13%;  $p \leq 0.05$ ) and LDHA expression (25%; Figure 3.4). The results demonstrated that the MGO enhances the metabolic flux away from the TCA cycle and toward aerobic glycolysis.

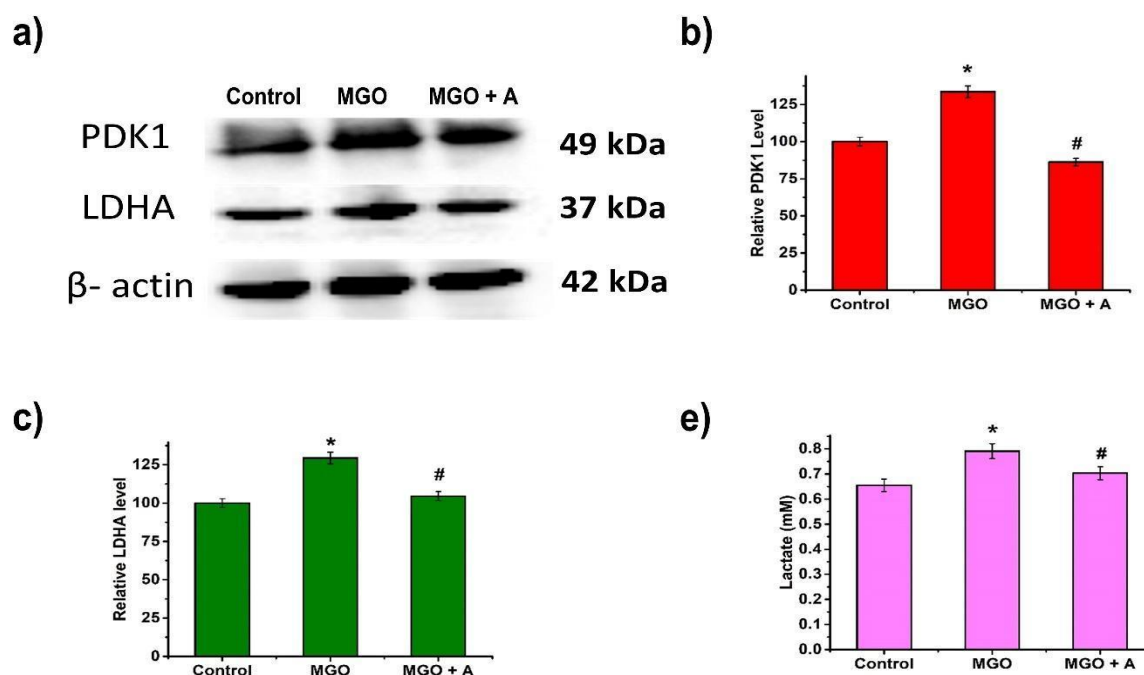


**Figure. 3.4: Effect of MGO on aerobic glycolysis.** a) Immunoblot analysis of pyruvate dehydrogenase kinase 1 (PDK1) and lactate dehydrogenase A (LDHA) in HepG2 cells. b) & c) Densitometric analysis of pyruvate dehydrogenase Kinase 1 (PDK1) and lactate dehydrogenase A (LDHA), respectively, with respect to  $\beta$ -actin. e) Determination of lactate production. Control (Control), Methylglyoxal (MGO, 50  $\mu$ M), MGO + Aminoguanidine (A, 200  $\mu$ M). Data are present mean values  $\pm$  SEM ( $n = 6$ ). \* denotes  $p \leq 0.05$  with a significant difference from control cells. # denotes  $p \leq 0.05$  with a significant difference from MGO cells.

### 3.3.5 Effect of MGO on oxygen consumption rate (OCR)

The OCR in the cells was then examined. OCR was observed to be significantly lower (40%;  $p \leq 0.05$ ; Figure 3.5) in the MGO than in control. When compared to MGO, aminoguanidine increased OCR by 62% and maintained a normal OCR.

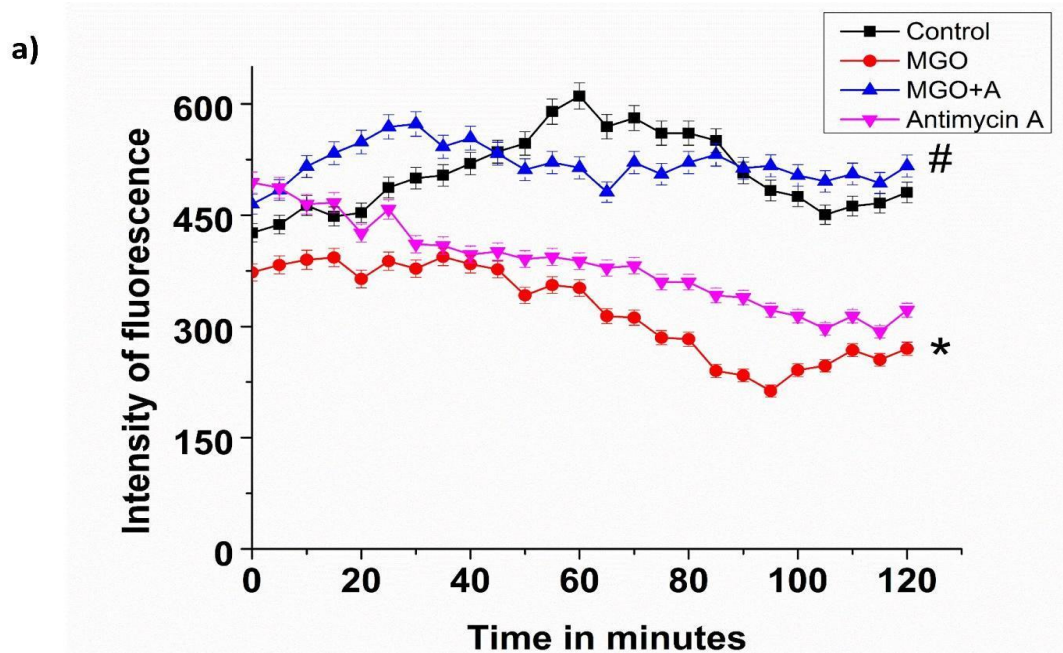


**Figure. 3.5: a) Determination of oxygen consumption rate.** Control (Control), Methylglyoxal (MGO, 50  $\mu$ M), MGO + Aminoguanidine (A, 200  $\mu$ M). Data are present mean values  $\pm$  SEM (n = 6). \* denotes  $p \leq 0.05$  with a significant difference from control cells. # denotes  $p \leq 0.05$  with a significant difference from MGO cells.

### 3.3.6 MGO mediated induction of HIF-1 $\alpha$ expression

HIF1 is one of the main regulators of aerobic glycolysis in cancer cells. Therefore, we also sought to determine if MGO had any impact on HIF1 expression and found that the expression of HIF1 was significantly ( $p \leq 0.05$ ) upregulated in MGO by 35% compared to the control. In contrast to MGO, aminoguanidine dramatically reduced HIF-1 expression by 13% (Figure.3.6). The outcomes once more support the involvement of MGO as a pro-oncogenic metabolite in HepG2 cells by promoting aerobic glycolysis.

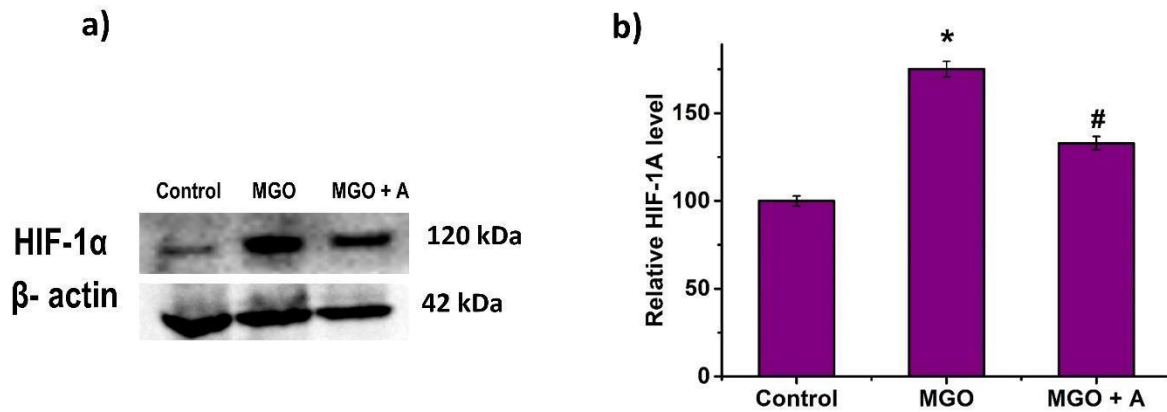


**Figure. 3.6: Effect of MGO on HIF-1 $\alpha$  expression.** a) Immunoblot analysis of HIF-1 $\alpha$  b) Densitometric analysis of HIF-1 $\alpha$  expression with respect to  $\beta$ -actin. Control (Control), Methylglyoxal (MGO, 50  $\mu$ M), MGO + Aminoguanidine (A, 200  $\mu$ M). Data are present mean values  $\pm$  SEM (n = 6). \* denotes  $p \leq 0.05$  with a significant difference from control cells. # denotes  $p \leq 0.05$  with a significant difference from MGO cells.

### 3.3.7 Effect of MGO on Hippo pathway

The major transcriptional coactivator of the Hippo pathway, the Yes-associated protein (YAP), is involved in regulating cellular nutrition and energy status and is thus implicated in the poor prognosis of several cancers. pYAP is the inhibited form of YAP protein. MGO significantly decreases pYAP expression (50 %) to the YAP expression in HepG2 cells. In contrast, aminoguanidine could increase the pYAP expression to the YAP expression by 30% (Figure.3.7) in HepG2 cells.

### 3.3.8 MGO induced c-Myc expression

c-Myc is one of the master regulators of the Warburg effect and also promotes cancer growth. MGO induced increased expression of c-Myc (43 %; (Figure.3.7)), which is an active regulator of glycolysis in cancer cells. While aminoguanidine reversed the effect of MGO by downregulating the c-Myc expression by 51 % in HepG2 cells.

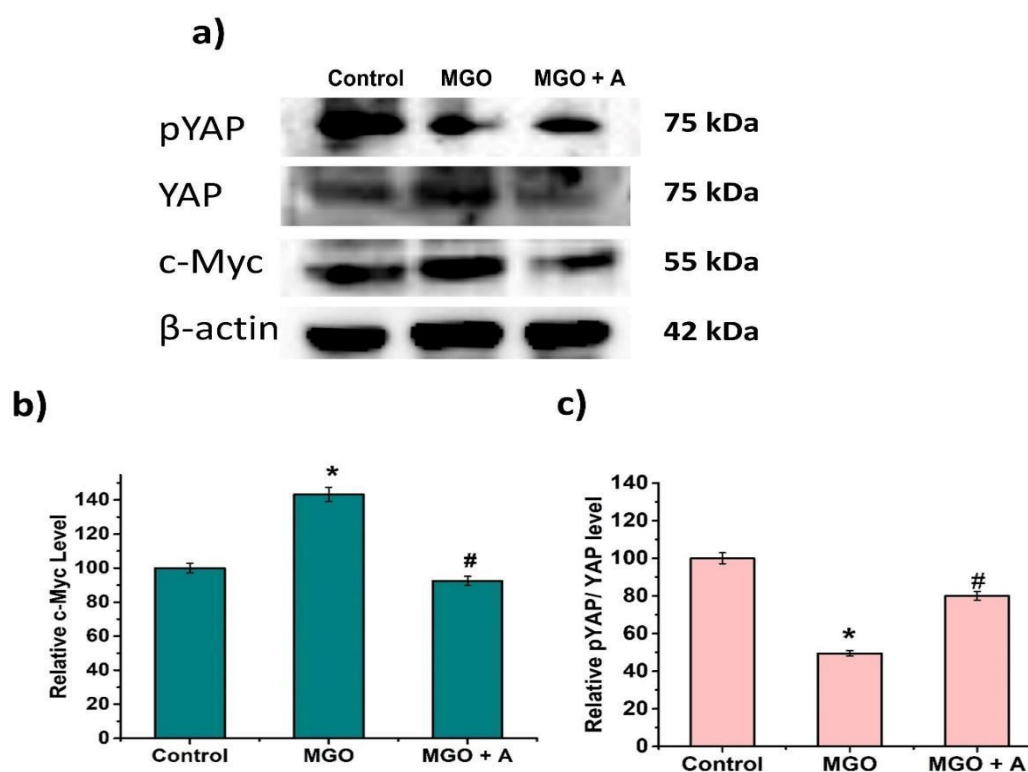


**Figure. 3.7: Effect of MGO on the expression of pYAP/YAP and c-Myc.** a) Immunoblot analysis of pYAP/YAP and c-Myc b) & c) Densitometric analysis of pYAP/YAP and c-Myc expression with respect to  $\beta$ -actin. Control (Control), Methylglyoxal (MGO, 50  $\mu$ M), MGO + Aminoguanidine (A, 200  $\mu$ M). Data are present mean values  $\pm$  SEM (n = 6). \* denotes  $p \leq 0.05$  with a significant difference from control cells. # denotes  $p \leq 0.05$  with a significant difference from MGO cells.

### 3.4 Discussion

Beginning from glucose metabolism, cancer cells rely primarily on glycolysis, even in the presence of oxygen, while normal cells need oxidative phosphorylation and glycolysis to produce energy. Normal cells adopt this type of abnormal behaviour only in anaerobic settings, where there is a lack of oxygen and cells do not wish to carry out oxygen-consuming mitochondrial metabolism (Li et al., 2016). The "Warburg effect", or aerobic glycolysis, is a term that refers to the aberrant behaviour that Otto Warburg originally noticed in cancer cells (Warburg & Minami, 1923). Methylglyoxal has been shown to promote the development of

several malignancies, including lung, breast, colorectal, and anaplastic thyroid cancer. However, the precise chemical pathways behind this occurrence still need to be explored. In hyperglycemia, glucose breakdown is abnormally enhanced, which has a number of adverse effects on the liver. By producing advanced glycation end products, MGO causes protein modification and hampers the structure and function of the proteins. MGO is present in free and reversibly or irreversibly bound forms under physiological settings, and variations in sample treatment methodology lead to a highly inconsistent assessment of MGO levels in samples (Chaplen et al., 1998). The intracellular MGO concentration is substantially greater than the plasma MGO levels (Jang et al., 2017). In Chinese hamster ovary cells, 310  $\mu\text{M}$  of MGO was found (Chaplen et al., 1998).

In order to determine if MGO increases aerobic glycolysis on HepG2 cells to promote cancer, we looked closely at the effect of MGO in HepG2 cells concerning glucose metabolism, transport, and associated metabolic changes. For this, we checked the impact of MGO on glucose uptake. Here, we were surprised by an unexpectedly increased glucose uptake by MGO in HepG2 cells.

The metabolism of glucose is frequently accelerated in cancer cells. We, therefore, wanted to understand the route used by glucose uptake. Our study discovered that exposure to MGO had raised GLUT 1 and GLUT 2 expressions. Once glucose reaches the cells, it is subsequently metabolised to pyruvate by the glycolytic pathway. To analyse whether this increased glucose uptake is concurrent with glycolysis, we checked the expression of three glycolytic enzymes, HK II, PFK 1 and enolase 1. The first committed step of the metabolism of glucose, which transforms glucose into glucose-6-phosphate in the presence of ATP, is catalysed by HK II. Its high expression in cancer cells has been documented (W. C. Li et al., 2020). It is a stimulator for developing tumours and maintaining malignant situations (Patra et al., 2013). Increased GLUT1 and HK II activity have also been linked to the emergence of

insulin resistance (Ebeling et al., 1998) and the encouragement of cancer in the biological system (Wu et al., 2020). As one of the rate-limiting stages in glycolysis by converting fructose-6-phosphate to fructose 1, 6-bisphosphate, PFK1 is known as the "gatekeeper of glycolysis" (Cho et al., 2020). An important glycolysis enzyme called enolase 1 has been linked to the carcinogenesis of different cancer cells (Didiasova et al., 2019). Enolase 1 has been proposed as a promising biomarker for hepatocellular carcinoma patients in terms of both diagnosis and prognosis (Zhu, Li et al., 2018). And as expected, we got an upregulated glycolytic pathway with higher expression of all these three enzymes. The results were again confirmed by checking the hexokinase activity, which was again found to be increased, pointing towards the upregulation of glycolysis in MGO exposed HepG2 cells.

At this point, we anticipated the role of MGO in the Warburg effect or aerobic glycolysis. Warburg effect is the increase in the rate of glucose uptake and preferential production of lactate, even in the presence of oxygen. Moreover, cancer cells can rewire their metabolism to promote growth, survival, proliferation and long-term maintenance. And the Warburg effect is one such rewiring of glucose metabolism seen in cancer cells, where the end product of glycolysis, the pyruvate, is redirected towards lactate rather than the entry into the TCA cycle. LDH-A catalyses pyruvate to L-lactate conversion. LDH-A is claimed to be involved in tumour growth and proliferation and is reported to be elevated in a number of malignancies (Zhu, Ma et al., 2018). In the metabolic reprogramming of cancer, lactate has been recognised as an oncometabolite (San-Millán et al., 2020).

Now we wanted to confirm our prediction about the Warburg effect in MGO exposed HepG2 cells. PDK1 is an inhibitor of pyruvate dehydrogenase which converts pyruvate to acetyl Co-A. We first analysed if MGO had any impact on PDK 1 expression, and as expected, its expression was significantly raised in the MGO exposed groups compared to the control group indicating that MGO induced inhibition of pyruvate entry to the TCA cycle. The next

step was to confirm if the pyruvate was converted to lactate by LDH-A or not. And this was positive; we found an increased expression of LDH-A along with increased lactate production. So, these results confirmed that MGO induces aerobic glycolysis or the Warburg effect in HepG2 cells.

The Warburg effect is linked with decreased oxygen consumption rate (OCR) in cancer cells. So, we checked the impact of MGO on the OCR in HepG2 cells and found that MGO significantly reduced the OCR in HepG2 cells.

In cancer cells, increased expression of oncogenes, inactivation of tumour suppressor genes and hypoxia conditions can upregulate HIF-1 $\alpha$  and this reprogramming of metabolism with higher glycolysis than OXPHOS contributes to the tumour growth and proliferation. A characteristic of cancer is an increase in aerobic glycolysis, and the Warburg effect has allowed researchers to clearly identify HIF-1 $\alpha$ 's role in the upregulation of glycolysis in diverse cancer types (Infantino et al., 2021). And MGO has increased the HIF-1 $\alpha$  expression in the HepG2 cells compared to the control and positive control groups.

Two more proteins associated with glycolysis and carcinogenesis are Yes-associated protein (YAP) and c-Myc. YAP, the downstream effector of the Hippo signalling pathway as well as c-Myc, has been linked to hepatocarcinogenesis (Xiao et al., 2013a). YAP is a tumour accelerant, while p-YAP is the inhibited form of YAP (Zhao et al., 2007).

The upregulation of c-Myc protects and enhances YAP expression. An accumulation of YAP, in turn, promotes the transcription of c-Myc. Interaction between YAP and c-Myc is found to promote liver cancer growth (Xiao et al., 2013b). Furthermore, when we exposed HepG2 cells with MGO, it increased the expression of both c-Myc and YAP while decreasing p-YAP expression.

Our findings demonstrate that MGO-treated HepG2 cells have abnormal glucose metabolism, supporting malignancy. Additionally, the MGO scavenger aminoguanidine partially protected cells from the harmful effects of MGO. This research is preliminary; more thorough in vitro and in vivo experiments are needed.

### 3.5 Summary and Conclusion

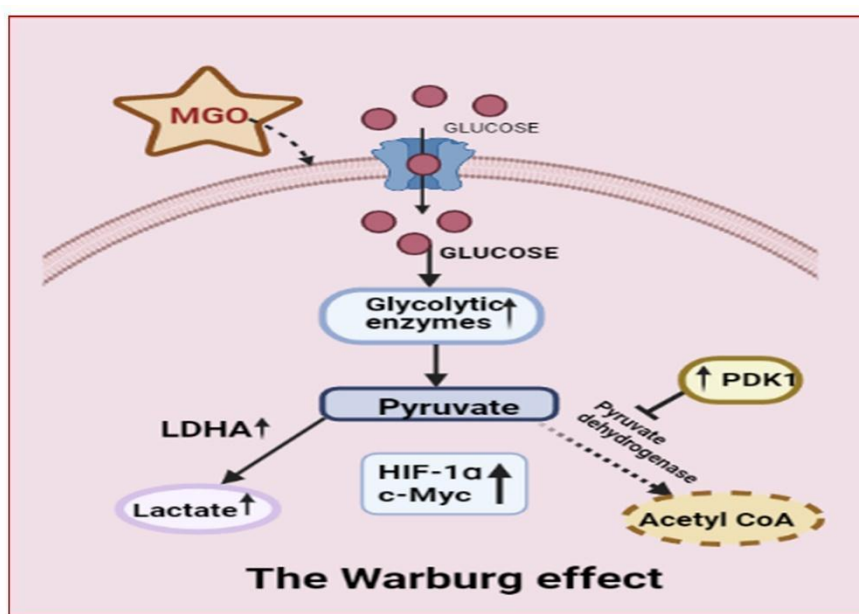


**Figure. 3.8: Schematic representation of MGO-induced Warburg effect**

MGO impacts glucose metabolism, enhancing aerobic glycolysis in HepG2 cells. MGO also led to the overexpression of cancer-promoting enzymes, including HKII, PFK1, LDHA, and PDK1. HIF1 overexpression is also brought on by it. All these modifications aid in the propagation of cancer by inducing the Warburg effect and glycation in HepG2 cells by MGO.

## 3.6 References

1. Bellahcène, A., Nokin, M. J., Castronovo, V., & Schalkwijk, C. (2018). Methylglyoxal-derived stress: An emerging biological factor involved in the onset and progression of cancer. *Seminars in Cancer Biology*, *49*, 64–74. <https://doi.org/10.1016/J.SEMCANCER.2017.05.010>
2. Bellier, J., Nokin, M. J., Lardé, E., Karoyan, P., Peulen, O., Castronovo, V., & Bellahcène, A. (2019). Methylglyoxal, a potent inducer of AGEs, connects between diabetes and cancer. *Diabetes Research and Clinical Practice*, *148*, 200–211. <https://doi.org/10.1016/J.DIABRES.2019.01.002>
3. Bierhaus, A., Fleming, T., Stoyanov, S., Leffler, A., Babes, A., Neacsu, C., Sauer, S. K., Eberhardt, M., Schnölzer, M., Lasischka, F., Neuhuber, W. L., Kichko, T. I., Konrade, I., Elvert, R., Mier, W., Pirags, V., Lukic, I. K., Morcos, M., Dehmer, T., ... Nawroth, P. P. (2012). Methylglyoxal modification of Nav1.8 facilitates nociceptive neuron firing and causes hyperalgesia in diabetic neuropathy. *Nature Medicine* *2012* *18*:6, *18*(6), 926–933. <https://doi.org/10.1038/nm.2750>
4. Chaplen, F. W. R., Fahl, W. E., & Cameron, D. C. (1998). Evidence of high levels of methylglyoxal in cultured Chinese hamster ovary cells. *Proceedings of the National Academy of Sciences*, *95*(10), 5533–5538. <https://doi.org/10.1073/PNAS.95.10.5533>
5. Cho, E. S., Kim, N. H., Yun, J. S., Cho, S. B., Kim, H. S., & Yook, J. I. (2020). Breast Cancer Subtypes Underlying EMT-Mediated Catabolic Metabolism. *Cells*, *9*(9). <https://doi.org/10.3390/CELLS9092064>
6. DeBerardinis, R. J., & Chandel, N. S. (2020). We need to talk about the Warburg effect. *Nature Metabolism* *2020* *2*:2, *2*(2), 127–129. <https://doi.org/10.1038/s42255-020-0172-2>

7. Didiasova, M., Schaefer, L., & Wygrecka, M. (2019). When place matters: Shuttling of enolase-1 across cellular compartments. In *Frontiers in Cell and Developmental Biology* (Vol. 7, Issue APR, p. 61). Frontiers Media S.A. <https://doi.org/10.3389/fcell.2019.00061>
8. Dobler, D., Ahmed, N., Song, L., Eboigbodin, K. E., & Thornalley, P. J. (2006). Increased Dicarbonyl Metabolism in Endothelial Cells in Hyperglycemia Induces Anoikis and Impairs Angiogenesis by RGD and GFOGER Motif Modification. *Diabetes*, 55(7), 1961–1969. <https://doi.org/10.2337/DB05-1634>
9. Ebeling, P., Koistinen, H. A., & Koivisto, V. A. (1998). Insulin-independent glucose transport regulates insulin sensitivity. *FEBS Letters*, 436(3), 301–303. [https://doi.org/10.1016/S0014-5793\(98\)01149-1](https://doi.org/10.1016/S0014-5793(98)01149-1)
10. Ekberg, K., Landau, B. R., Wajngot, A., Chandramouli, V., Efendic, S., Brunengraber, H., & Wahren, J. (1999). Contributions by kidney and liver to glucose production in the postabsorptive state and after 60 h of fasting. *Diabetes*, 48(2), 292–298. <https://doi.org/10.2337/DIABETES.48.2.292>
11. Infantino, V., Santarsiero, A., Convertini, P., Todisco, S., & Iacobazzi, V. (2021). Cancer cell metabolism in hypoxia: Role of HIF-1 as key regulator and therapeutic target. In *International Journal of Molecular Sciences* (Vol. 22, Issue 11). MDPI. <https://doi.org/10.3390/ijms22115703>
12. Jiang, S., Young, J. L., Wang, K., Qian, Y., & Cai, L. (2020). Diabetic-induced alterations in hepatic glucose and lipid metabolism: The role of type 1 and type 2 diabetes mellitus (Review). In *Molecular Medicine Reports* (Vol. 22, Issue 2, pp. 603–611). Spandidos Publications. <https://doi.org/10.3892/mmr.2020.11175>
13. Lee, H. J., Jung, Y. H., Choi, G. E., Kim, J. S., Chae, C. W., Lim, J. R., Kim, S. Y., Lee, J. E., Park, M. C., Yoon, J. H., Choi, M. J., Kim, K. S., & Han, H. J. (2019). O-

- cyclic phytosphingosine-1-phosphate stimulates HIF1 $\alpha$ -dependent glycolytic reprogramming to enhance the therapeutic potential of mesenchymal stem cells. *Cell Death & Disease* 2019 10:8, 10(8), 1–21. <https://doi.org/10.1038/s41419-019-1823-7>
14. Leone, A., Nigro, C., Nicolò, A., Prevezano, I., Formisano, P., Beguinot, F., & Miele, C. (2021). The Dual-Role of Methylglyoxal in Tumor Progression – Novel Therapeutic Approaches. *Frontiers in Oncology*, 11. <https://doi.org/10.3389/FONC.2021.645686>
15. Li, C., Zhang, G., Zhao, L., Ma, Z., & Chen, H. (2016). Metabolic reprogramming in cancer cells: Glycolysis, glutaminolysis, and Bcl-2 proteins as novel therapeutic targets for cancer. *World Journal of Surgical Oncology*, 14(1). <https://doi.org/10.1186/S12957-016-0769-9>
16. Li, W. C., Huang, C. H., Hsieh, Y. T., Chen, T. Y., Cheng, L. H., Chen, C. Y., Liu, C. J., Chen, H. M., Huang, C. L., Lo, J. F., & Chang, K. W. (2020). Regulatory Role of Hexokinase 2 in Modulating Head and Neck Tumorigenesis. *Frontiers in Oncology*, 10. <https://doi.org/10.3389/FONC.2020.00176>
17. Liberti, M. v., & Locasale, J. W. (2016). The Warburg Effect: How Does it Benefit Cancer Cells? HHS Public Access. *Trends Biochem Sci*, 41(3), 211–218. <https://doi.org/10.1016/j.tibs.2015.12.001>
18. Mack, S. C., Agnihotri, S., Bertrand, K. C., Wang, X., Shih, D. J., Witt, H., Hill, N., Zayne, K., Barszczyk, M., Ramaswamy, V., Remke, M., Thompson, Y., Ryzhova, M., Massimi, L., Grajkowska, W., Lach, B., Gupta, N., Weiss, W. A., Guha, A., ... Taylor, M. D. (2015). Spinal Myxopapillary Ependymomas Demonstrate a Warburg Phenotype. *Clinical Cancer Research*, 21(16), 3750–3758. <https://doi.org/10.1158/1078-0432.CCR-14-2650>

19. Moore, M. C., Coate, K. C., Winnick, J. J., An, Z., & Cherrington, A. D. (2012). Regulation of Hepatic Glucose Uptake and Storage In Vivo. *Advances in Nutrition*, 3(3), 286. <https://doi.org/10.3945/AN.112.002089>
20. Moore, M. C., Smith, M. S., Farmer, B., Kraft, G., Shiota, M., Williams, P. E., & Cherrington, A. D. (2017). Priming Effect of a Morning Meal on Hepatic Glucose Disposition Later in the Day. *Diabetes*, 66, 1136–1145. <https://doi.org/10.2337/db16-1308>
21. Patra, K. C., Wang, Q., Bhaskar, P. T., Miller, L., Wang, Z., Wheaton, W., Chandel, N., Laakso, M., Muller, W. J., Allen, E. L., Jha, A. K., Smolen, G. A., Clasquin, M. F., Robey, R. B., & Hay, N. (2013). Hexokinase 2 is required for tumor initiation and maintenance and its systemic deletion is therapeutic in mouse models of cancer. *Cancer Cell*, 24(2), 213–228. <https://doi.org/10.1016/J.CCR.2013.06.014>
22. Petersen, M. C., Vatner, D. F., & Shulman, G. I. (2017). Regulation of hepatic glucose metabolism in health and disease. *Nature Reviews. Endocrinology*, 13(10), 572. <https://doi.org/10.1038/NREND0.2017.80>
23. Rines, A. K., Sharabi, K., Tavares, C. D. J., & Puigserver, P. (2016). Targeting hepatic glucose output in the treatment of type 2 diabetes. *Nature Reviews. Drug Discovery*, 15(11), 786. <https://doi.org/10.1038/NRD.2016.151>
24. Rizza, R. A. (2010). Pathogenesis of Fasting and Postprandial Hyperglycemia in Type 2 Diabetes: Implications for Therapy. *Diabetes*, 59(11), 2697. <https://doi.org/10.2337/DB10-1032>
25. San-Millán, I., Julian, C. G., Matarazzo, C., Martinez, J., & Brooks, G. A. (2020). Is Lactate an Oncometabolite? Evidence Supporting a Role for Lactate in the Regulation of Transcriptional Activity of Cancer-Related Genes in MCF7 Breast Cancer Cells. *Frontiers in Oncology*, 9. <https://doi.org/10.3389/FONC.2019.01536>

26. Sun, Z., Tan, Z., Peng, C., & Yi, W. (2021). HK2 is associated with the Warburg effect and proliferation in liver cancer: Targets for effective therapy with glycyrrhizin. *Molecular Medicine Reports*, 23(5), 1–8. <https://doi.org/10.3892/MMR.2021.11982/HTML>
27. Swapna Sasi, U. S., Sindhu, G., & Raghu, K. G. (2020). Fructose-palmitate based high calorie induce steatosis in HepG2 cells via mitochondrial dysfunction: An in vitro approach. *Toxicology in Vitro*, 68, 104952. <https://doi.org/10.1016/J.TIV.2020.104952>
28. Towle, H. C. (2005). Glucose as a regulator of eukaryotic gene transcription. *Trends in Endocrinology & Metabolism*, 16(10), 489–494. <https://doi.org/10.1016/J.TEM.2005.10.003>
29. Wang, C., Wang, X., Gong, G., Ben, Q., Qiu, W., Chen, Y., Li, G., & Wang, L. (2012). Increased risk of hepatocellular carcinoma in patients with diabetes mellitus: A systematic review and meta-analysis of cohort studies. *International Journal of Cancer*, 130(7), 1639–1648. <https://doi.org/10.1002/IJC.26165>
30. Warburg, O., & Minami, S. (1923). Versuche an Überlebendem Carcinom-gewebe. *Klinische Wochenschrift*, 2(17), 776–777. <https://doi.org/10.1007/BF01712130>
31. Wu, Z., Han, X., Tan, G., Zhu, Q., Chen, H., Xia, Y., Gong, J., Wang, Z., Wang, Y., & Yan, J. (2020). Dioscin inhibited glycolysis and induced cell apoptosis in colorectal cancer via promoting c-myc ubiquitination and subsequent hexokinase-2 suppression. *OncoTargets and Therapy*, 13, 31–44. <https://doi.org/10.2147/OTT.S224062>
32. Xiao, W., Wang, J., Ou, C., Zhang, Y., Ma, L., Weng, W., Pan, Q., & Sun, F. (2013a). Mutual interaction between YAP and c-Myc is critical for carcinogenesis in liver cancer. *Biochemical and Biophysical Research Communications*, 439(2), 167–172. <https://doi.org/10.1016/J.BBRC.2013.08.071>

33. Xiao, W., Wang, J., Ou, C., Zhang, Y., Ma, L., Weng, W., Pan, Q., & Sun, F. (2013b). Mutual interaction between YAP and c-Myc is critical for carcinogenesis in liver cancer. *Biochemical and Biophysical Research Communications*, 439(2), 167–172. <https://doi.org/10.1016/J.BBRC.2013.08.071>
34. Zhao, B., Wei, X., Li, W., Udan, R. S., Yang, Q., Kim, J., Xie, J., Ikenoue, T., Yu, J., Li, L., Zheng, P., Ye, K., Chinnaiyan, A., Halder, G., Lai, Z.-C., & Guan, K.-L. (2007). *Inactivation of YAP oncoprotein by the Hippo pathway is involved in cell contact inhibition and tissue growth control*. <https://doi.org/10.1101/gad.1602907>
35. Zhu, W., Li, H., Yu, Y., Chen, J., Chen, X., Ren, F., Ren, Z., & Cui, G. (2018). Enolase-1 serves as a biomarker of diagnosis and prognosis in hepatocellular carcinoma patients. *Cancer Management and Research*, 10, 5735–5745. <https://doi.org/10.2147/CMAR.S182183>
36. Zhu, W., Ma, L., Qian, J., Xu, J., Xu, T., Pang, L., Zhou, H., Shu, Y., & Zhou, J. (2018). The molecular mechanism and clinical significance of LDHA in HER2-mediated progression of gastric cancer. *American Journal of Translational Research*, 10(7), 2055–2067. [/pmc/articles/PMC6079134/](https://pubmed.ncbi.nlm.nih.gov/3079134/)

## Chapter 4

# Alterations in fatty acid metabolism by methylglyoxal via the amendment of autophagy, mitochondrial dynamics and endoplasmic reticulum stress in HepG2 cells

---

---

## 4.1 Introduction

Cancer is the result of unchecked cell growth and division. Cancerous cells cease to function normally and frequently do not respond to signals which might usually stop uncontrolled proliferation.

In 2000, Hanahan and Weinberg suggested that cancer cells develop six characteristics, or hallmarks, that ultimately aid in developing tumours and metastases, these include a) self-sufficient growth signalling, b) growth suppressor insensitivity, c) cell death evasion, d) sustained angiogenesis, e) unlimited replication potential, and f) invasion and metastasis. Reprogramming of the metabolic activities and evasion of immunological destruction were added to these markers in 2011 (Fouad Y A & Aanei C, 2017). Ultimately, genomic instability was added to essential characteristics of malignant cells (Fouad Y A & Aanei C, 2017).

In the previous chapters, we have seen MGO increase the MGO-AGEs, downregulate the glyoxalase system, increase RAGE 1 expression and ultimately lead to oxidative stress in the HepG2 cells. We have also seen that MGO could upregulate the glycolysis or the Warburg effect in HepG2 cells. The results indicated metabolic reprogramming by MGO.

AGEs have been shown to cause mutations (Tamae et al., 2011; Wei et al., 2009), protein misfolding and destruction of protein functions (Ansari et al., 2011; Baraka-Vidot et

al., 2012). They also cause cancer cells to grow and migrate (Bao et al., 2015; Matou-Nasri et al., 2017; Yaser et al., 2012). When its ligands activate RAGE, people who are diabetic or obese are more likely to get cancer. This receptor-ligand axis is the molecular link between pre-existing conditions like hypoxia, high blood sugar, glycation, inflammatory responses, oxidative stress, and the onset of cancer. The RAGE-ligand signalling network is crucial for every aspect of cancer, from its genesis to its progression (Palanissami & Paul, 2018). Research has suggested that RAGE and RAGE ligands are exciting areas to focus on when treating hepatocellular carcinoma (Yaser et al., 2012).

RAGE and its associated systems (AGEs, soluble RAGE, and RAGE gene polymorphisms) could be used to diagnose and quickly predict the outcome of cancers (Palanissami & Paul, 2018). During this study, we have already observed the involvement of MGO in the activation of RAGE in the previous chapter. The interaction between RAGE and its ligands at the molecular level guides a cascade of events towards the operation of hallmarks of cancer (Palanissami & Paul, 2018).

Moreover, in this chapter, we explore the various proteins or pathways from the hallmark of cancer. Here, we are trying to understand the involvement of MGO in the promotion of cancer with respect to lipid metabolism, autophagy, AKT pathway, ERK pathway, ER stress and mitochondrial dynamics and biogenesis.

## **4.2 Materials and Methods**

### **4.2.1 Reagents**

MGO (Cat no. M0252) was obtained from Sigma Aldrich, USA. Minimal Essential Media Eagles (MEME) with Earle's salt (Cat no. AL047S), Phosphate Buffered Saline (PBS; Cat no. TL1099), and aminoguanidine bicarbonate (Cat no. RM1573) were purchased from Himedia, India. Fetal bovine serum (FBS; Cat no. 16000044), penicillin–streptomycin

antibiotics (Cat no. 15070063), 0.5% trypsin-ethylene diamine tetra acetic acid (trypsin-EDTA; Cat no. R001100), and Hanks balanced saline solution or HBSS (Cat no. 1835981) were from Gibco-BRL Life Technologies (Waltham, MA, USA). Methyl thiazolyl blue tetrazolium bromide (MTT) was purchased from Sisco Research Laboratories Pvt. Ltd. Dimethyl sulfoxide (DMSO; Cat no. D8418) and radioimmunoprecipitation assay (RIPA; Cat no. R0278) buffer were from Sigma Aldrich, USA.

Primary antibodies for Fatty acid synthase (FASN; Cat no. 3189), phosphorylated Acetyl CoA carboxylase (pACC; Cat no.11818), Stearoyl-CoA desaturase 1 (SCD1; Cat no. 2794), , CD-36 (Cat no. 28109), AMP-activated protein kinase (AMPK; Cat no. 2532), phosphorylated AMP-activated protein kinase (pAMPK; Cat no. 2535), mammalian target of rapamycin (mTOR; Cat no.2983) and all the secondary antibodies were purchased from Cell Signaling Technology (Beverly, MA, USA).

Primary antibodies for Phosphatase and tensin homolog (PTEN; Cat no. sc-7974), protein kinase B or AKT (Cat no. sc-55523), p-AKT (Cat no. sc-135650), Vascular endothelial growth factor (VEGF; Cat no. sc-7269), Ras-related C3 botulinum toxin substrate 1 (RAC1; Cat no. sc-514583), proto-oncogene c-RAF (RAF1; Cat no. sc-7267), Extracellular signal-regulated kinase 1/2 (ERK1/2; Cat no.sc-514302), 3-hydroxy-3-methylglutaryl-CoA reductase (HMGCR; Cat no.sc-271595), Peroxisomal acyl-coenzyme A oxidase 1 (ACOX 1; Cat no. sc-517306), p38 mitogen-activated protein kinases (p38; Cat no.sc-81621), phosphorylated p38 (p-p38; Cat no. sc-166182), Dynamin-1-like protein (DRP1; Cat no. sc-271583), Mitochondrial fission 1 (Fis1; Cat no. sc-376447), Optic atrophy-1 (OPA1; Cat no.sc-393296), and Mitofusin-2 (Mfn2 Cat no. sc-515647) antibodies were purchased from Santa Cruz Biotechnology (Dallas, USA).

Primary antibodies for Beclin 1 (Cat no. ITT05128), Microtubule-associated protein 1A/1B-light chain 3 (LC3 A/B Cat no. ITT05402), X-box binding protein 1 (XBP1; Cat no. ITM0653), and Inositol-requiring enzyme type 1 (p-IRE1; Cat no. ITA8134) were purchased from G-Biosciences (St. Louis, USA).

#### **4.2.2 Cell culture and treatment**

A human hepatocellular carcinoma cell line (HepG2) was purchased from the National Centre for Cell Sciences (NCCS, Pune, India) and maintained in MEME medium supplemented with 10% FBS along with 100 U/ml penicillin and 100 µg/ml streptomycin. The cells were grown at 37 °C in a humidified atmosphere containing 5% (v/v) CO<sub>2</sub>.

#### **4.2.3 Oil-red-O staining**

Briefly, after respective treatments, cells were washed with HBSS and fixed with 4% formaldehyde for 15 min at room temperature. The fixing reagent was aspirated off, and the cells were rewashed with HBSS. Then 0.1% triton X-100 was added as a permeabilisation solution and kept for 5 min at RT. The permeabilisation solution was removed after incubation, and the cells were then allowed to dry. Oil red O staining solution was added to the cells and incubated for 15 min at RT. Cells were then washed 3 times with distilled water and observed under a microscope. The absorbed dye was then dissolved in 100 % isopropanol, and the absorbance was measured at 500 nm to quantify the lipid accumulation.

#### **4.2.4 Western Blotting analysis**

After specific treatments for 24 h, cells were lysed in a RIPA buffer supplemented with a protease inhibitor (Sigma-Aldrich). Protein concentrations were determined by a bicinchoninic acid protein assay kit (BCA kit, Merck). Equalised protein samples were resolved by 10% SDS PAGE and electrophoretically transferred to PVDF membranes (Millipore) using Mini Trans-Blot Cell (Bio-Rad Laboratories). The membranes were blocked

with 5% BSA and incubated with primary antibodies at 4°C overnight. The membranes were then washed and incubated with the HRP-conjugated secondary antibodies at room temperature for 2 h and visualised with western blot hyper HRP substrate (Cat no. T7103A, Takara-Bio).  $\beta$ -actin (Cat no. 4970) was the loading control. The immunoblot images were analysed with the help of the ChemiDOC XRS system using Image Lab software.

#### **4.2.5 Detection of autophagy**

Autophagy was detected using a kit from Sigma Aldrich, USA. Briefly, cells were cultured in a 96-well plate and after respective treatment plans of 24 h. After discarding the medium, 100  $\mu$ L of the autophagosome detection reagent was added to each well. Cells were then incubated for 30 min at 37 °C. A fluorescence microscope (Olympus IX 83) was used to evaluate the fluorescence intensity ( $\lambda_{\text{ex}} = 360 \text{ nm} / \lambda_{\text{em}} = 520 \text{ nm}$ ) of the cells after they had been washed three to four times with 100  $\mu$ L of wash buffer.

#### **4.2.6 Determination of the mitochondrial mass**

Alteration in mitochondrial mass was observed using the dye Mitotracker Deep Red FM. Briefly, cells were incubated with 5  $\mu$ M Mitotracker Deep Red dye for 30 min at 37 °C. The cells were then washed 3 times with HBSS and observed under a fluorescent microscope (Olympus IX 83 fluorescence microscope). The fluorescent intensity was noted at an excitation/emission of 644 nm/665 nm, respectively.

#### **4.2.7 Determination of the mitochondrial transmembrane potential ( $\Delta\Psi$ M)**

##### **in HepG2 cells**

Mitochondrial membrane potential was analysed using a kit from G-Biosciences. The kit uses a cationic fluorescent dye, JC-1, which can accumulate in the mitochondrial matrix as aggregates and gives a red fluorescence in normal cells due to the electrochemical potential gradient across the mitochondrial membrane. The accumulation of JC-1 aggregates is

prevented by the dissipation of mitochondrial membrane potential, thus resulting in the presence of JC-1 monomers in the cell, which shows a green fluorescence. Briefly, the cells were seeded in 96 black well plates at a density of  $5 \times 10^3$ . After the respective treatments, the cell culture media was replaced with a working solution of JC-1 dye and the cells were incubated at 37 °C for 20 min. The dye was aspirated and washed with HBSS, and the cells were then observed and imaged using a fluorescent microscope (Olympus IX 83 fluorescence microscope).

#### **4.2.8 Statistics**

Results are shown as mean  $\pm$  SEM for the control and experimental groups after sextuplicate samples from each group were used in all analyses. Using ANOVA, the results were examined. All the data were analysed using SPSS for Windows, standard version 26 (SPSS), and a p-value  $\leq 0.05$  was considered significant.

### **4.3 Results**

#### **4.3.1 Effect of MGO on lipid accumulation**

Oil red assay was performed to analyse the oil droplet accumulation in the MGO-treated HepG2 cells. We observed an increased accumulation of oil droplets in the HepG2 cells treated with MGO by microscopic imaging compared to the control and the positive control groups. With the quantification of the absorbed oil red dye, we observed a 55.7 % (Figure. 4.1) increase in the MGO groups than in the control. Aminoguanidine reduced the effect by 50.9 % in the positive control group.

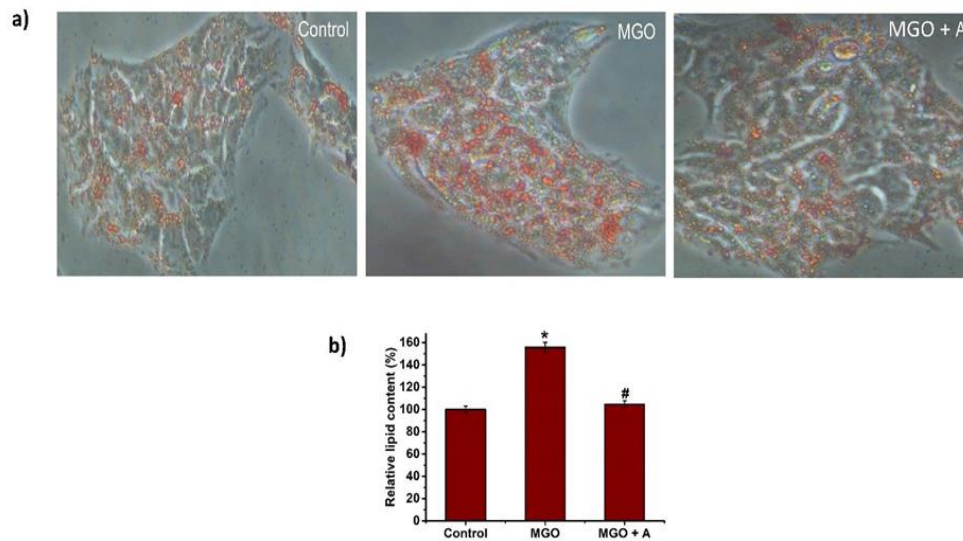


**Figure. 4.1: Analysis of lipid droplet formation using oil red O staining.** a) Lipid droplet generation in various groups. b) Quantification of lipid by oil red O staining. Control - Control, MGO - Methylglyoxal (50  $\mu$ M), MGO + A - Aminoguanidine (200  $\mu$ M). Data are present mean values  $\pm$  SEM (n = 6). \* denotes  $p \leq 0.05$  with a significant difference from control cells. # denotes  $p \leq 0.05$  with a significant difference from MGO cells.

### 4.3.2 Effect of MGO on lipid metabolism

FASN is the fatty acid synthase protein which initiates the fatty acid synthesis, and here we have observed (Figure. 4.2) that MGO could upregulate the FASN expression significantly by 43.36%, and aminoguanidine was not much effective but reduced the effect of MGO by 3.45 % only. We also observed a significant decrease in the expression pACC (42.15 %,  $p \leq 0.05$ ) which indicated the lipogenesis in the MGO group, whereas aminoguanidine increased the expression by 64.2 % compared to the control. SCD1 is the protein involved in fatty acid desaturation, and here we have seen a decrease in the Stearoyl-CoA desaturase-1 (SCD1) expression (10 %;  $p \leq 0.05$ ) while positive control groups increased the expression by 16 %. HMGCR protein expression was also seen to be negatively affected by the MGO by a significant decrease in the expression by 16.35 %, and aminoguanidine treatment further decreased the expression by 26.86 %. A decrease was observed in the expression of ACOX 1

significantly (55.98 %;  $p \leq 0.05$ ) by MGO compared to the control, and positive control groups could increase the expression (39.58 %;  $p \leq 0.05$ ). CD36 is a fatty acid receptor which mediates the fatty acid uptake in cells, here, there was a significant decrease in the expression of CD36 in the MGO (25.54 %;  $p \leq 0.05$ ) exposed HepG2 cells compared to control and positive control aminoguanidine could bring back expression to a normal level.

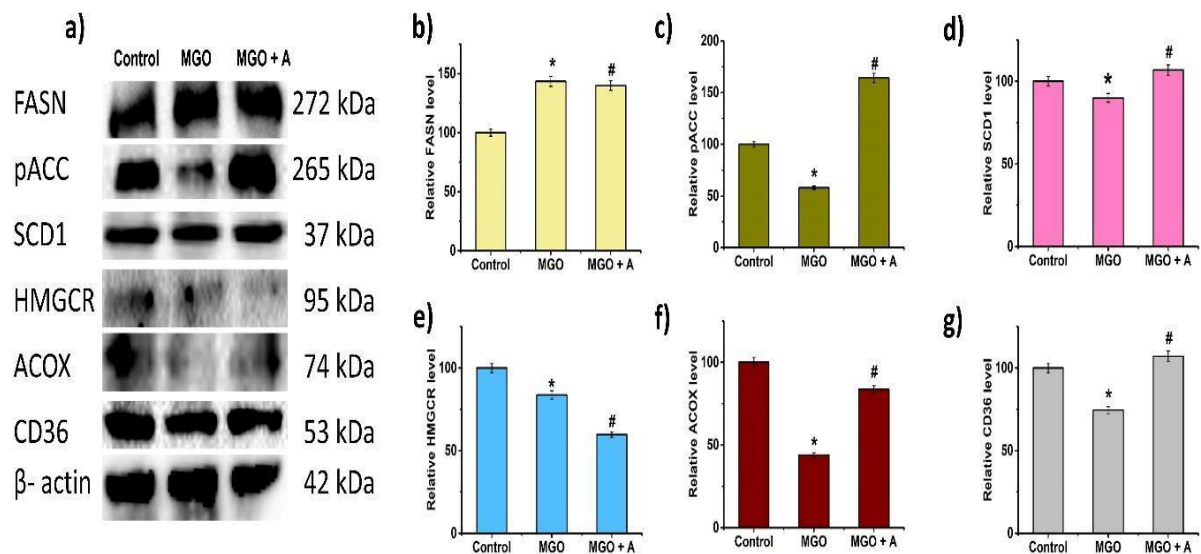


**Figure.4.2: MGO induces aberrant lipid metabolism in HepG2 cells.** a) Immunoblot analysis of FASN, pACC, SCD1, HMGCR, ACOX and CD36 during MGO exposure. b), c), d), e), f) & g) Densitometric analysis of FASN, pACC, SCD1, HMGCR, ACOX and CD36 expression with respect to  $\beta$ -actin. Control (Control), Methylglyoxal (MGO, 50  $\mu$ M), MGO + Aminoguanidine (A, 200  $\mu$ M). Data are present mean values  $\pm$  SEM (n = 6). \* denotes  $p \leq 0.05$  with a significant difference from control cells. # denotes  $p \leq 0.05$  with a significant difference from MGO cells.

### 4.3.3 MGO activated autophagy by activating AMPK and inhibiting mTOR

Here we have observed (Figure. 4.3) that MGO could significantly increase the expression of pAMPK/AMPK by 28.02 % compared to the control and positive control, aminoguanidine reduced the effect by 52.98 % ( $p \leq 0.05$ ) groups, and MGO also downregulated mTOR by 24.72 % while aminoguanidine could not restore the expression. Activation of

AMPK could positively regulate the activation of the autophagy pathway. In this study, we noticed that there was enhanced autophagy by MGO via upregulating autophagosome formation, as seen in the microscopic images (Figure 4.3. a). We also observed a significant increase in the expression of LCA3-II/I (41.388 %;  $p \leq 0.05$ ) and Beclin 1 (75.23%;  $p \leq 0.05$ ) proteins in the MGO exposed groups in HepG2 cells compared to the control and positive control groups showed decreased the expression of both the proteins to a normal level.

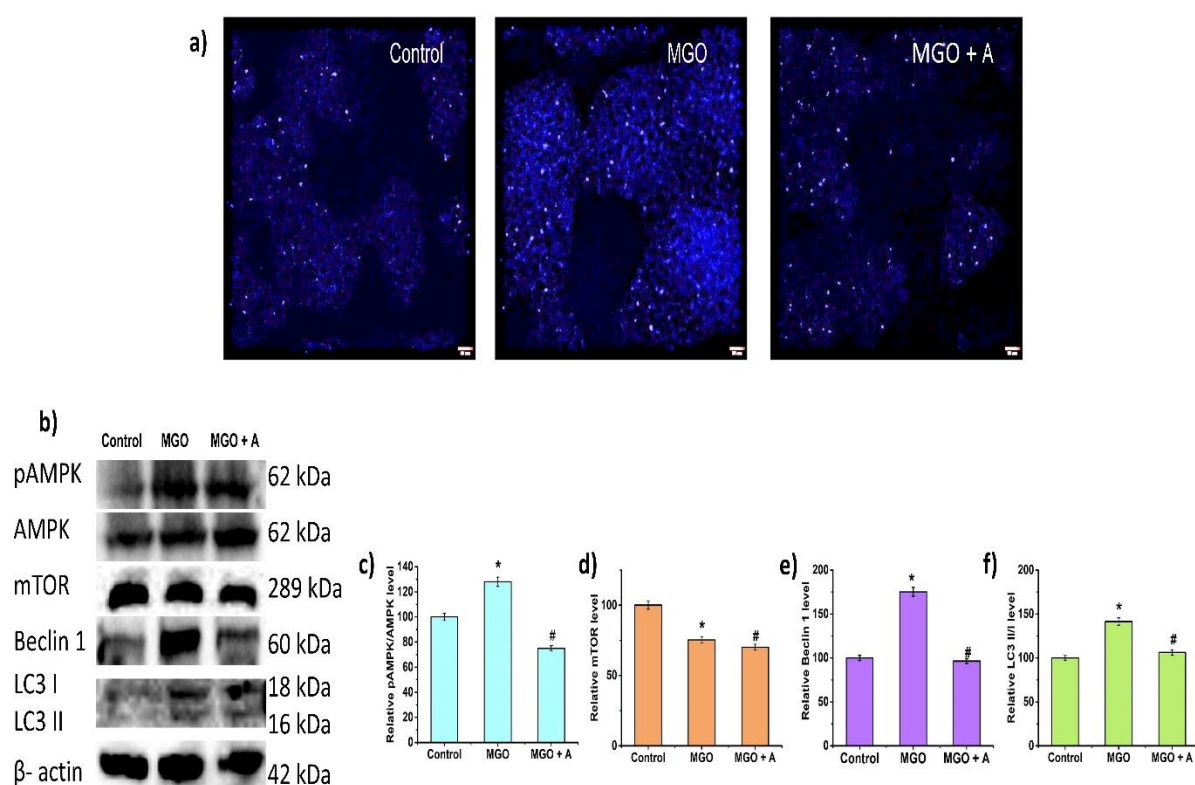


**Figure.4.3: MGO induces AMPK activation for the initiation of autophagy.** a) Fluorescence microscopy image of autophagosome formation b) Immunoblot analysis of pAMPK, AMPK, mTOR, Beclin1 and LC3 II/I during MGO exposure. c), d), e), & f) Densitometric analysis of pAMPK/AMPK, mTOR, Beclin1 and LC3 II/I expression with respect to  $\beta$ -actin. Control (Control), Methylglyoxal (MGO, 50  $\mu$ M), MGO + Aminoguanidine (A, 200  $\mu$ M). Data are present mean values  $\pm$  SEM (n = 6). \* denotes  $p \leq 0.05$  with a significant difference from control cells. # denotes  $p \leq 0.05$  with a significant difference from MGO cells.

#### 4.3.4 MGO regulates PTEN/ Akt pathway

MGO could downregulate PTEN (10 %) while aminoguanidine decreased the expression by 24 % (Figure 4.4). PTEN downregulation can regulate the activation of AKT in MGO exposed group in HepG2 cells; this led us to check the expression of pAKT/AKT and observed a significant increase by 61.24 % in the MGO group compared to the control group and positive control aminoguanidine reduced the expression by 27.74 % (Figure 4.4).

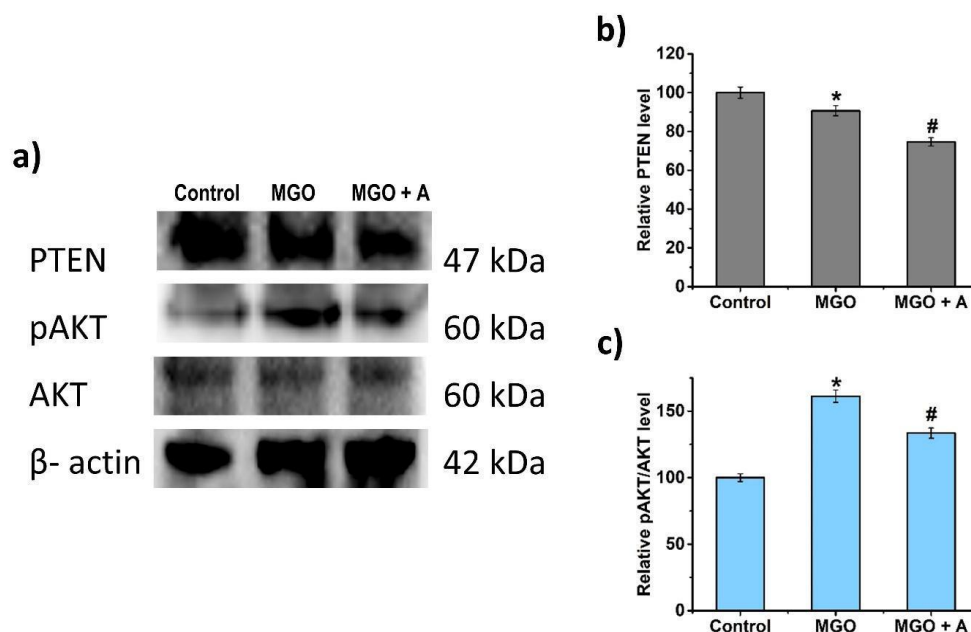


**Figure.4.4: MGO induces AKT activation via PTEN inhibition.** a) Immunoblot analysis of PTEN, pAKT and AKT during MGO exposure. b) & c) Densitometric analysis of PTEN & pAKT/AKT expression with respect to  $\beta$ -actin. Control (Control), Methylglyoxal (MGO, 50  $\mu$ M), MGO + Aminoguanidine (A, 200  $\mu$ M). Data are present mean values  $\pm$  SEM (n = 6). \* denotes  $p \leq 0.05$  with a significant difference from control cells. # denotes  $p \leq 0.05$  with a significant difference from MGO cells.

#### 4.3.5 MGO regulated ERK pathway

We observed (Figure 4.5) an increased expression of VEGF (65.7 %) in MGO groups, which can stimulate the RTK receptors and activate Raf. We also observed a significant

increase in the Raf expression in MGO treated groups (145.5 %;  $p \leq 0.05$ ), and aminoguanidine treatment reduced the effect by 141.83%. Raf can stimulate the expression of ERK1/2, and we noticed a significant increase in the MGO (36.19 %;  $p \leq 0.05$ ) compared to the control and aminoguanidine treated groups could reduce the effect by 24.29 %. RAC1 is another protein involved in the activation of Akt as well as ERK for cell growth and stimulations. And in this study, there was an upregulation of RAC 1 by 278 % ( $p \leq 0.05$ ) in the MGO group compared to control groups. In the aminoguanidine treated groups, downregulated expression of RAC1 (294.207 %) (Figure 4.5) was observed, indicating the involvement of MGO in the sustained proliferation of hallmark.

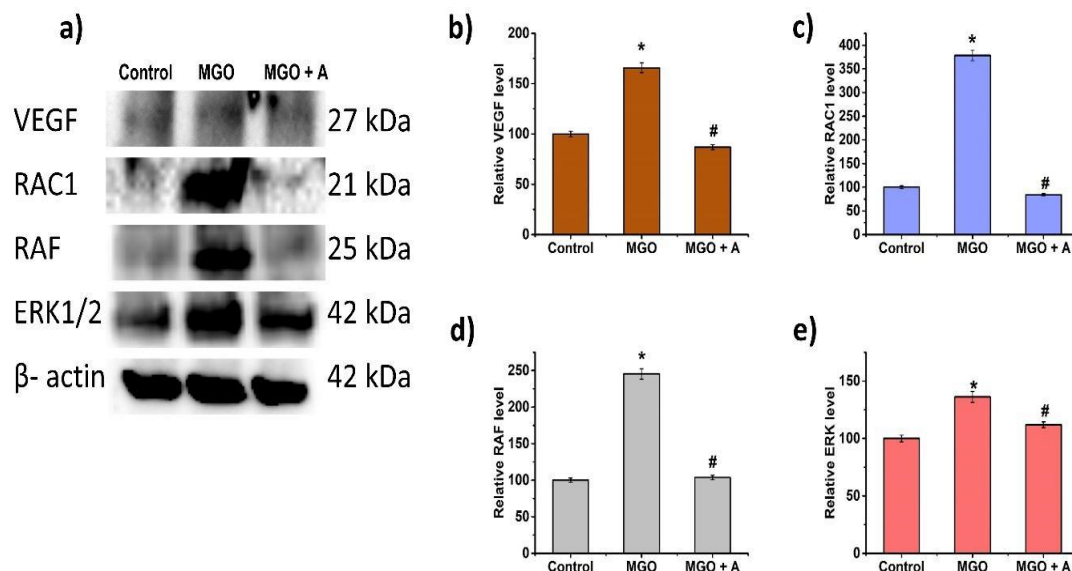


**Figure.4.5: MGO induces RAF/ERK pathway.** a) Immunoblot analysis of VEGF, RAC1, RAF and ERK1/2 during MGO exposure. b), c), d) & e) Densitometric analysis of VEGF, RAC1, & pAKT/AKT expression with respect to  $\beta$ -actin. Control (Control), Methylglyoxal (MGO, 50  $\mu$ M), MGO + Aminoguanidine (A, 200  $\mu$ M). Data are present mean values  $\pm$  SEM (n = 6). \* denotes  $p \leq 0.05$  with a significant difference from control cells. # denotes  $p \leq 0.05$  with a significant difference from MGO cells.

### 4.3.6 Effect of MGO on the p38 pathway

MGO downregulated (51.41 %;  $p \leq 0.05$ ) the expression of p-p38/p38 in HepG2 cells significantly compared to the control groups, and aminoguanidine could increase the expression by 10.36 % than the MGO alone groups in HepG2 cells (Figure 4.6).

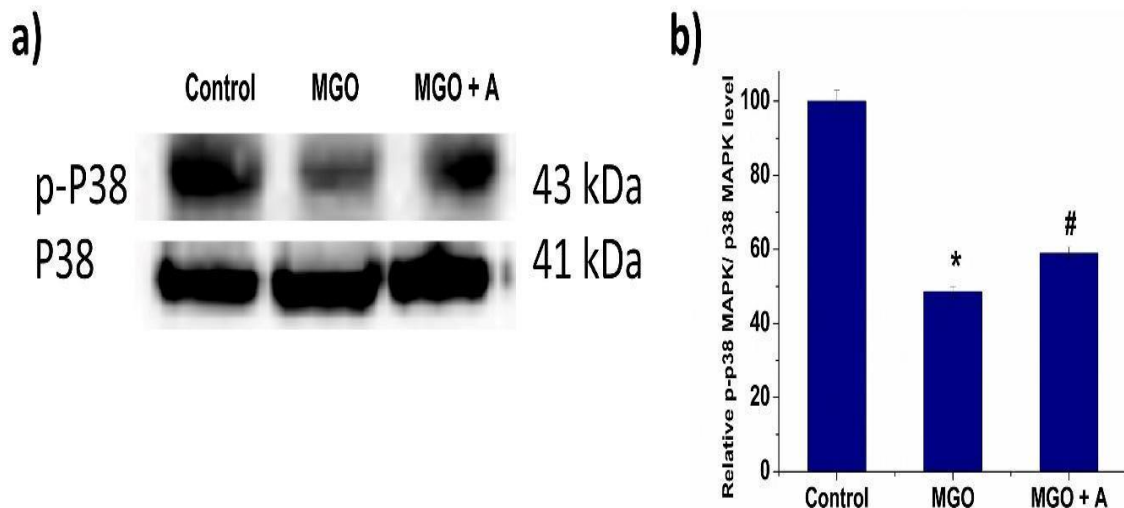


**Figure.4.6: Effect of MGO on p38 expression.** a) Immunoblot analysis of p-p38 & p-38 during MGO exposure. b) Densitometric analysis of p-p38/p-38 expression. Control (Control), Methylglyoxal (MGO, 50  $\mu$ M), MGO + Aminoguanidine (A, 200  $\mu$ M). Data are presents mean values  $\pm$  SEM (n = 6). \* denotes  $p \leq 0.05$  with significant difference from control cells. # denotes  $p \leq 0.05$  with significant difference from MGO cells.

### 4.3.7 MGO induced ER stress in HepG2 cells

In this study, it was noticed that there was a significant ( $p \leq 0.05$ ) upregulation of p-IRE- $\alpha$  by 237.411% and XBP1 by 33 % in the MGO exposed HepG2 cells compared to the control group. The positive control, aminoguanidine could reduce the effect by downregulation of the expression of p-IRE by 112.74 % and XBP1 by 50.87 %, indicating ER stress-mediated cell survival (Figure 4.7).

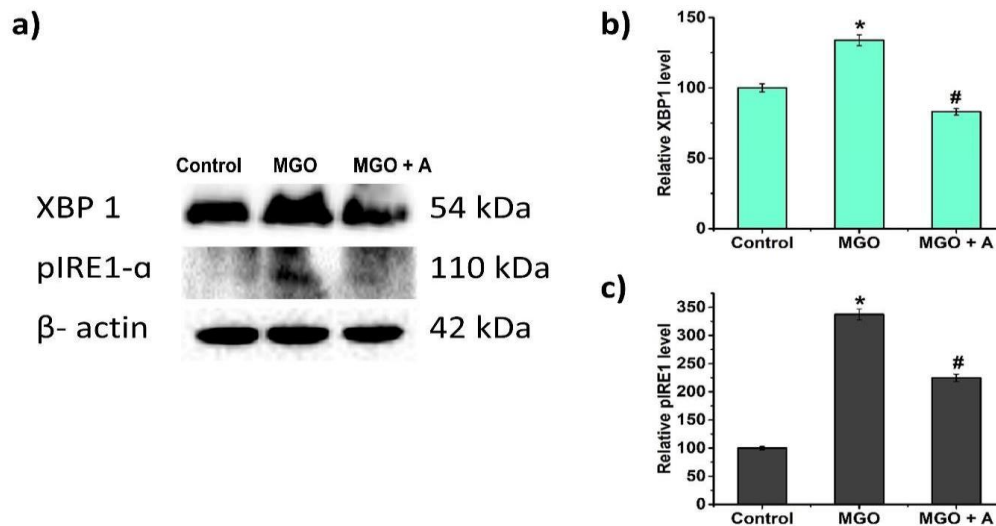


**Figure.4.7: MGO induces initiation of ER stress.** a) Immunoblot analysis of XBP1 and pIRE1- $\alpha$  during MGO exposure. b) & c) Densitometric analysis of XBP1 and pIRE1- $\alpha$  expression with respect to  $\beta$ -actin. Control (Control), Methylglyoxal (MGO, 50  $\mu$ M), MGO + Aminoguanidine (A, 200  $\mu$ M). Data are present mean values  $\pm$  SEM (n = 6). \* denotes  $p \leq 0.05$  with a significant difference from control cells. # denotes  $p \leq 0.05$  with a significant difference from MGO cells.

#### 4.3.7 Effect of MGO on mitochondrial mass

Mitochondrial mass was analysed with a dye, mitotracker. Here, a reduced mitochondrial mass was observed in the MGO group, which is evident from the microscopic images and the fluorescent intensity (35.49 %). At the same time, aminoguanidine reduced the effect by 13.27 % compared to the MGO group (Figure 4.8).

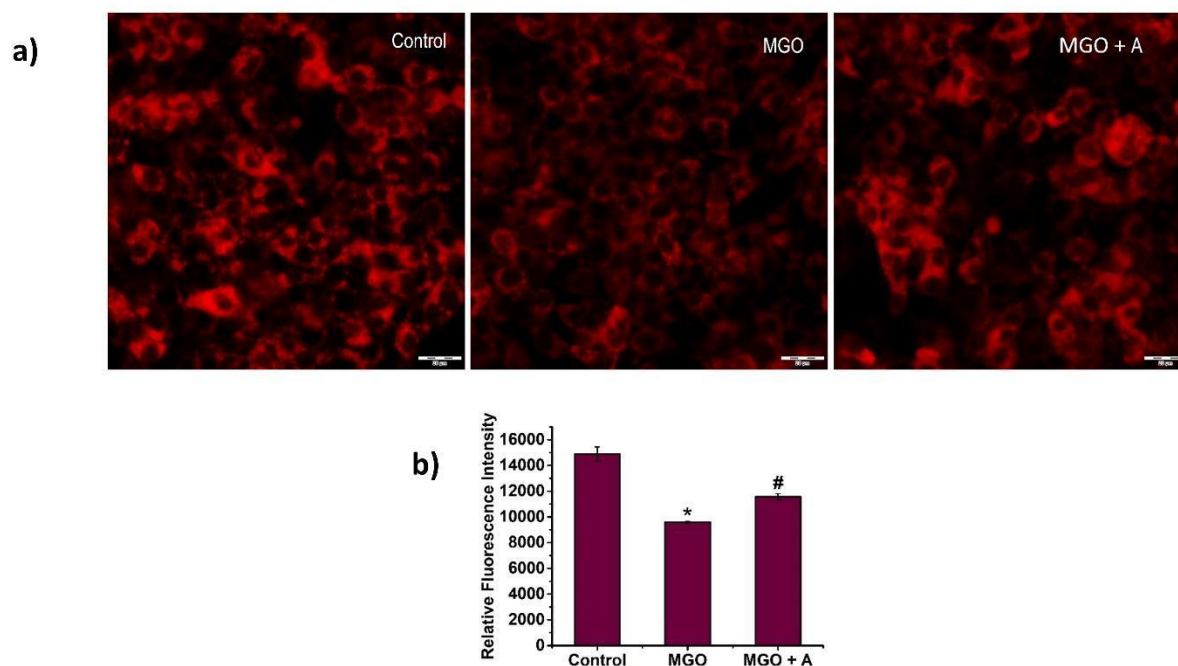


**Figure.4.8: Effect of MGO on mitochondrial mass.** a) The fluorescent microscopic images of HepG2 cells. b) The graphical representation of fluorescence intensity (Excitation: 644 nm, Emission: 665 nm. Original magnification 20X. The scale bar corresponds to 50  $\mu$ M. Control (Control), Methylglyoxal (MGO, 50  $\mu$ M), MGO + Aminoguanidine (A, 200  $\mu$ M). Data are present mean values  $\pm$  SEM (n = 6). \* denotes  $p \leq 0.05$  with a significant difference from control cells. # denotes  $p \leq 0.05$  with a significant difference from MGO cells.

#### 4.3.8 MGO causes the dissipation of $\Delta\Psi$ M.

Mitochondrial transmembrane potential ( $\Delta\Psi$ M), which aids in ATP production, anion transport, and cation transport, is a vital sign of healthy mitochondria. Disturbances in this area can seriously impair the operation of mitochondria. When compared to the control, analysis of the  $\Delta\Psi$ M of mitochondria during MGO exposure revealed a substantial  $\Delta\Psi$ M distortion (Figure.:4.9). The JC-1 dye aggregates within the mitochondrial matrix of control cells and, as a result of the potential gradient, emits red fluorescence. A change in  $\Delta\Psi$ M prevented the passage of JC-1 into the mitochondria and produced green fluorescence (JC-1 monomers).

As demonstrated in Figure 4.9.a, MGO exposed cells displayed depolarised  $\Delta\Psi_M$ , which had less red-to-green fluorescence ratio (23.24 %;  $p \leq 0.05$ ) than control cells. Red to green fluorescence ratio increased significantly ( $p \leq 0.05$ ) for the aminoguanidine group by 29.08%. Valinomycin served as the negative control, and when compared to the control, it reduced the red to green fluorescence ratio by 87.87 %.

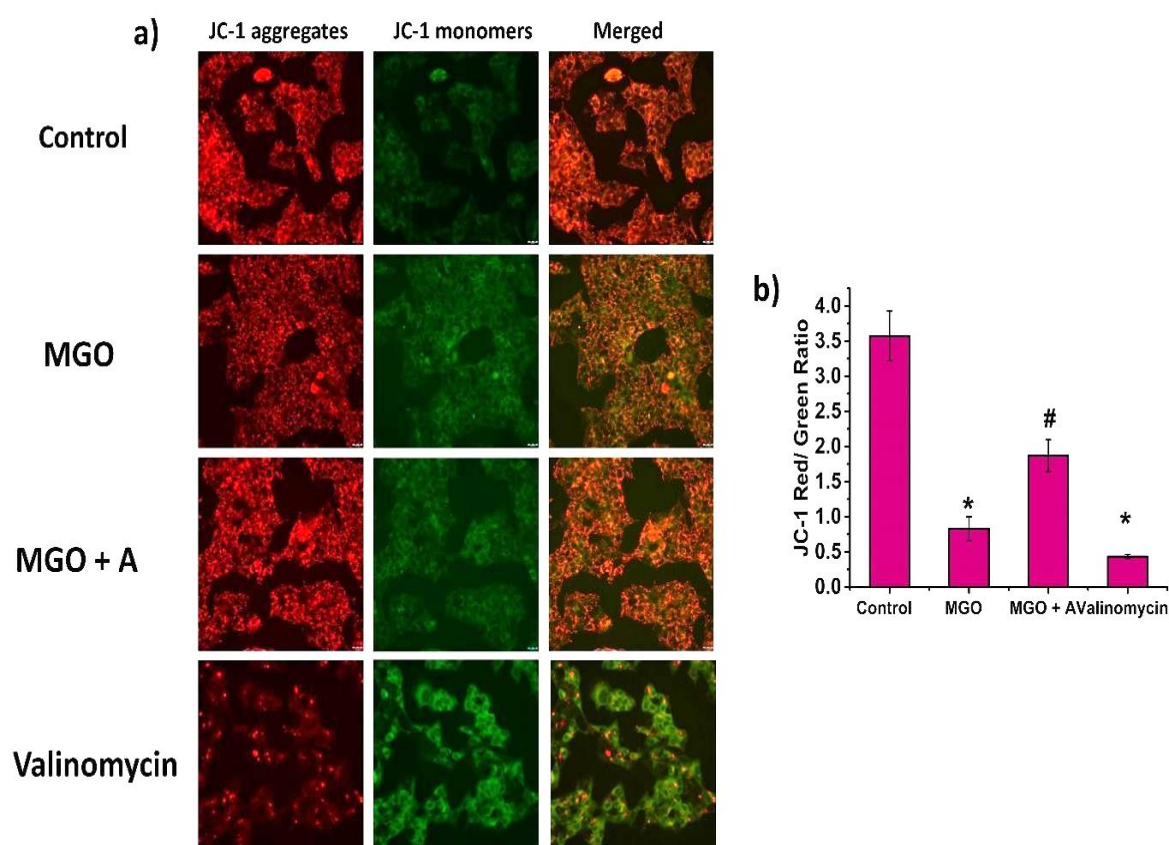


**Figure.4.9: MGO causes dissipation of  $\Delta\Psi_M$ .** a) The fluorescent microscopic images of HepG2 cells. b) The graphical representation of JC-1 aggregates to JC-1 monomers (ratio of 590:530 nm emission intensity). Original magnification 20X. The scale bar corresponds to 50  $\mu\text{M}$ . Control (Control), Methylglyoxal (MGO, 50  $\mu\text{M}$ ), MGO + Aminoguanidine (A, 200  $\mu\text{M}$ ). Data are present mean values  $\pm$  SEM (n = 6). \* denotes  $p \leq 0.05$  with a significant difference from control cells. # denotes  $p \leq 0.05$  with a significant difference from MGO cells.

### 4.3.9 Effect of MGO on mitochondrial dynamics

Here we have seen a significant upregulation of both DRP 1 (112.79 %;  $p \leq 0.05$ ) and Fis 1 (158.44 %;  $p \leq 0.05$ ) in MGO compared to the control cells. In contrast, aminoguanidine could somewhat reduce the effect by reducing the expressions of DRP-1 (63.5 %) and Fis 1 (61 %). On the other hand, expression of Mfn1/2 and OPA1 was not affected by MGO in HepG2 cells, with no significant difference among all three groups (Figure 4.10).

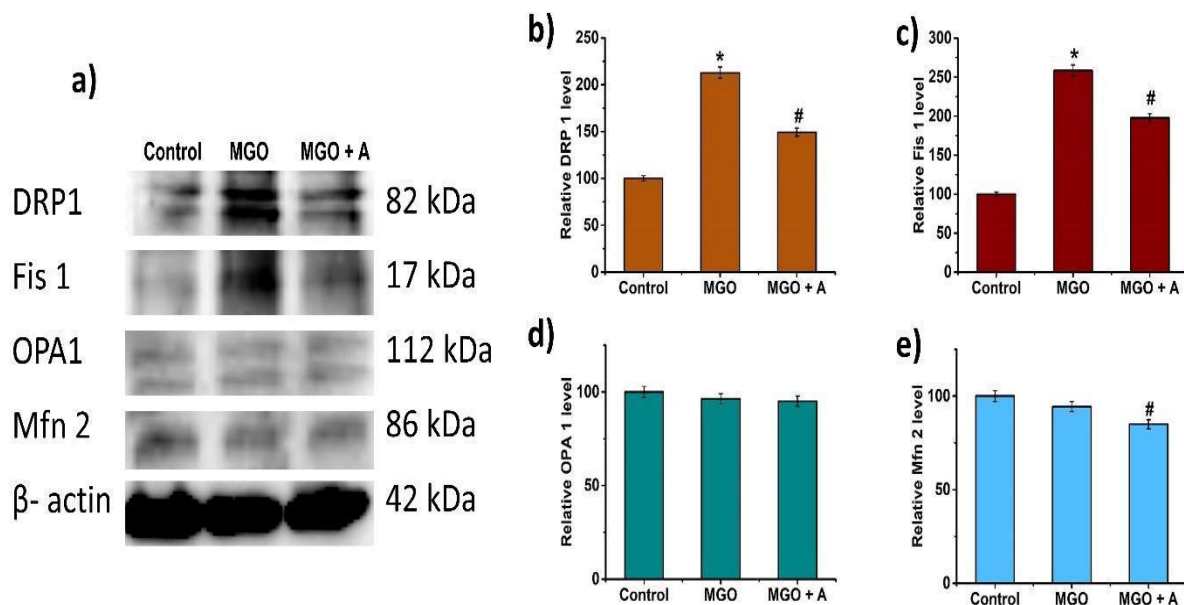


**Figure.4.10: Effect of MGO on mitochondrial dynamics.** a) Immunoblot analysis of DRP1, Fis1, OPA1 and MFN2 during MGO exposure. b), c), d) & e) Densitometric analysis of DRP1, Fis1, OPA1 and MFN2 expression with respect to  $\beta$ -actin. Control (Control), Methylglyoxal (MGO, 50  $\mu$ M), MGO + Aminoguanidine (A, 200  $\mu$ M). Data are present mean values  $\pm$  SEM (n = 6). \* denotes  $p \leq 0.05$  with a significant difference from control cells. # denotes  $p \leq 0.05$  with a significant difference from MGO cells.

## 4.4 Discussion

As we reported earlier, the MGO is augmenting the growth of HepG2 (Sruthi & Raghu, 2022). Here we are exploring the altered molecular mechanisms that are supporting the growth

of cancer cells stimulated by MGO. The liver serves as the principal organ for the metabolism of fats (Alves-Bezerra & Cohen, 2017; Dhamija et al., 2019; Raza et al., 2019). Moreover, it is widely appreciated that fatty acids are essential for cancer cells because they sustain membrane biosynthesis during high proliferation and provide energy during conditions of metabolic stress (Broadfield et al., 2021).

We already explored the reprogramming of glucose metabolism in MGO; now, we want to know the status of fat metabolism. Starting with the oil red assay, we observed an increased lipid droplet formation in the HepG2 cells by MGO. Major pathways in fat metabolism include fatty acid synthesis, desaturation, cholesterol synthesis and beta-oxidation. FASN is the fatty acid synthase protein that initiates fatty acid synthesis. Here we have observed that MGO could upregulate the FASN expression along with decreased pACC, which indicated lipogenesis in the MGO group. SCD1 is the protein involved in fatty acid desaturation, and here we have seen a decrease in the SCD1 expression. HMGCR protein, involved in cholesterol biosynthesis, and ACOX 1, involved in peroxisomal beta-oxidation, also downregulated. CD36 is a fatty acid receptor which mediates the fatty acid uptake in cells, here, we have observed a decrease in the expression of CD36 in the MGO-exposed HepG2 cells. So, this shows how MGO has affected fatty acid metabolism through the abnormal expressions of these proteins.

Cancer cells are under extremely demanding circumstances, such as hypoxia and nutritional deprivation. In this scenario, cells can adapt to the challenges with the aid of autophagy. The cancer cells could depend highly on autophagy to compensate for the heavy metabolic demands and stress (Li et al., 2020). Recycling of intracellular constituents to provide metabolic substrates, autophagy supports the high metabolic and energy demands of growing malignancies. So, the activation of autophagy in cancer cells may lead to several tumour growth-promoting pathways (Li et al., 2020). We are well aware that hypoxia and AMPK are inducers of autophagy via inhibiting mTORC1, which negatively regulates

autophagy (Chun & Kim, 2021). Autophagy is triggered in the centre of solid tumours, where cells are exposed to hypoxia. We have already reported that MGO could augment a hypoxic condition in HepG2 cells. Here we have seen that MGO could activate AMPK and downregulate mTOR. In this study, we noticed enhanced autophagy by MGO by upregulating autophagosome formation. This was again confirmed by the expression of biomarker proteins for autophagy, i.e., LCA3-II and Beclin 1; we found an increased expression of both these proteins MGO exposed groups in HepG2 cells, indicating that MGO could induce autophagy.

Hallmarks of cancer are a set of functional capabilities acquired by human cells as they progress from normalcy to neoplastic growth, specifically speaking about the capabilities crucial for their ability to grow as a tumour. As of now, 14 hallmarks have been proposed as important in tumour growth (Hanahan, 2022). There are many reports of RAGE ligand interactions triggering various signalling events involved in the hallmarks of cancer like self-sufficient growth signalling, growth suppressor insensitivity, cell death evasion, sustained angiogenesis, unlimited replication potential, and invasion and metastasis, reprogramming of the metabolic activities, evasion of immunological destruction and genomic instability are the list of crucial traits that make up cancerous cells (Palanissami & Paul, 2018).

We have seen in earlier chapters that MGO could regulate the associated signalling pathways. We also observed aerobic glycolysis in dysregulated cellular metabolism, autophagy, ROS generation, MG-Hs formation and upregulation of RAGE. So, now we wanted to explore some of the other proteins and pathways involved in cancer hallmarks. To start with, the activation of the Akt pathway, which is involved in sustained proliferative signalling and drug resistance, contributes to the resistance to apoptosis in cancer cells (Liu et al., 2020; Xu et al., 2010). PTEN, on the other hand, is a tumour suppressor and inhibits AKT activation. Here, we have seen that MGO could downregulate PTEN for the activation of AKT in the MGO-exposed group in HepG2 cells.

Another pathway involved in the hallmark of sustained proliferative signalling is the ERK pathway (Luongo et al., 2019). ERK pathway is activated via growth factors stimulation on the RTK receptors through Raf activation. ERK1/2 can stimulate cell proliferation and survival in tumour cells. RAC1 is another protein involved in the action of AKT as well as ERK for cell growth and stimulations. The RAC1 signalling pathway is overactive in human cancers, which helps tumours initiate, grow, and spread to other parts of the body (Olson, 2018). And in our study, we have seen upregulation of all these proteins in the MGO group compared to control groups and the aminoguanidine-treated groups, indicating the involvement of MGO in the sustained proliferation of hallmark.

Among the three MAPK pathways, ERK plays a role in cell proliferation and survival, while the other two, i.e., p38 and JNK, play a role in stress response and apoptosis (Kim et al., 2020). Upregulation of the p38 pathway typically results in a response that inhibits cancer cell proliferation. This fact made us curious about the effects of MGO on the p38 activation in HepG2 cells. As expected, we observed a downregulation of p38 activation by MGO in HepG2 cells, indicating the resistance of apoptosis, another hallmark of cancer.

Imbalanced proteostasis appears as a hallmark of cancer development and metastasis. Beyond the adverse environmental conditions generated by tumours, genetic alterations in the cancer cells can fuel ER stress and activation of UPR pathways (Oakes, 2020). As the most conserved branch among the three unfolded protein response (UPR) pathways, Inositol-requiring enzyme 1 $\alpha$  (IRE1 $\alpha$ )-X-box-binding protein 1 (XBP1) signalling has been implicated in cancer development and progression (Shi et al., 2019). In this study, we observed an upregulation of p-IRE1  $\alpha$  and XBP1 in the MGO-exposed HepG2 cells indicating ER stress-mediated cell survival.

Mitochondria play a vital role in energy metabolism. Cancer cells experience mitochondrial stress as they undergo unchecked cellular proliferation and generate ROS, which can damage mitochondrial function (O'Malley et al., 2020). Mitochondrial transmembrane potential ( $\Delta\Psi$ M) is a crucial indicator of healthy mitochondria, which helps in ATP synthesis, and anion and cation transport, and disturbances here can severely hamper the function of mitochondria. This made us analyse the effect of MGO on mitochondrial health (Zorova et al., 2018). Here we observed that MGO exposed cells displayed depolarised  $\Delta\Psi$ M, indicating that MGO is hampering the mitochondrial function in HepG2 cells.

As is well known, the term "mitochondrial dynamics" describes the fluctuating balance of mitochondrial fusion and fission to preserve the homeostasis and quality of the mitochondria (Wang et al., 2020). Depending on the type of cell, a mammalian cell may contain a few to thousands of mitochondria (Boguszewska et al., 2020). In metabolically active cells like hepatocytes and cardiomyocytes, the mitochondria make up about 20–30% of the cell volume (Chen & Chan, 2017). Under the influence of environmental stimuli, mitochondria constantly engage in fusion and fission dynamics to adapt to varied cellular demands (Chen & Chan, 2017). The two essential proteins for mammalian mitochondrial fission are Drp1 and Fis1, and fission is impaired in the absence of either protein. Mitofusin 1 (Mfn1), Mitofusin 2 (Mfn2), and optic atrophy 1 (OPA1) are three crucial dynamin-related proteins that regulate mitochondrial fusion in animals (Yu et al., 2020).

As said mitochondrial fission is mediated by DRP1 and Fis 1, which are known to increase the energetic yield of glycolysis and reduce ROS generation, so easing the process of metastasis in cancer cells. Here we have seen upregulation of both DRP 1 and Fis 1 in MGO indicating the role of MGO in mitochondrial fission in HepG2 cells. On the other hand, mitochondrial fusion is mediated by Mfn1/2 and OPA1 which also promotes OXPHOS and

inhibits migration and metastasis in cancer. In this study, we didn't find any significant difference in the fusion protein in all three groups.

## 4.5 Summary and Conclusion

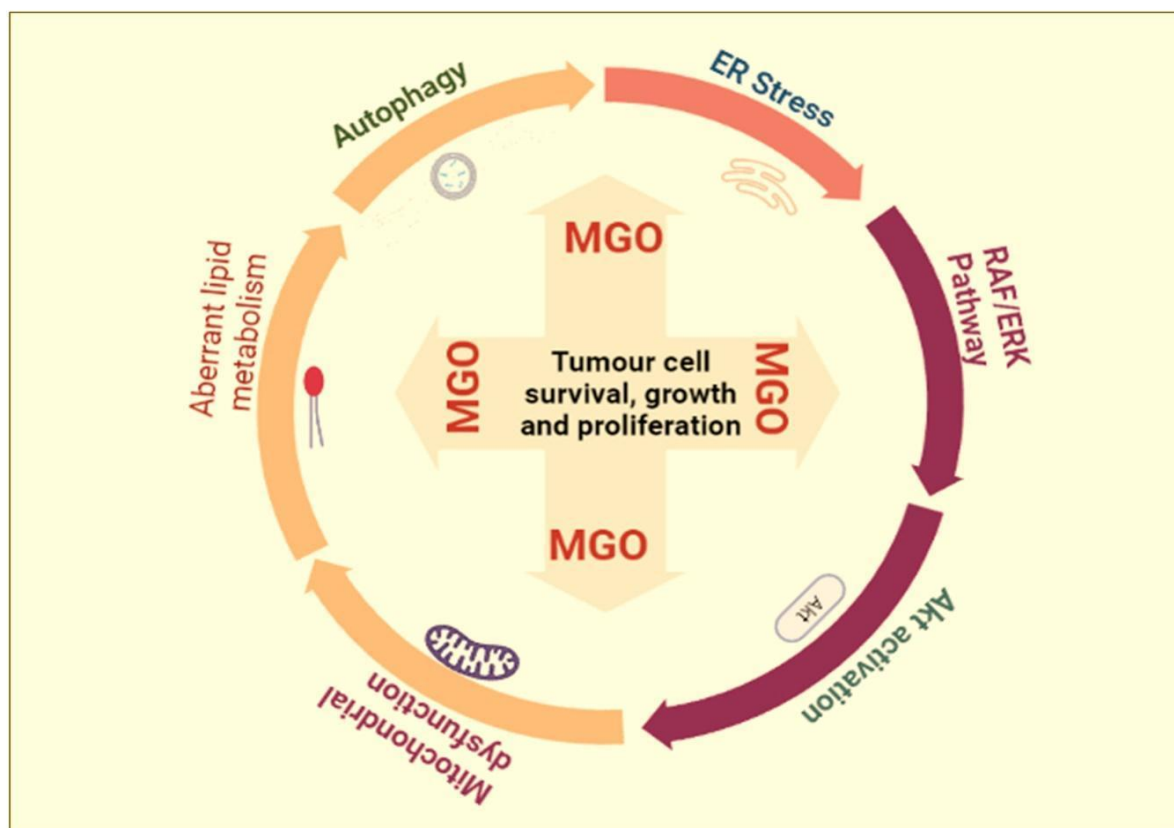


**Figure. 4.11: Schematic representation of MGO-induced tumour cell survival, growth and proliferation.**

MGO can favour tumour cell survival, growth and proliferation in HepG2 cells by altering the various signalling pathways like aberrant lipid metabolism, ER stress, mitochondrial dysfunction, RAF/ERK pathway and AKT activation etc which are considered as hallmarks of cancer.

## 4.6 References

1. Alves-Bezerra, M., & Cohen, D. E. (2017). Triglyceride metabolism in the liver. *Comprehensive Physiology*, 8(1), 1. <https://doi.org/10.1002/CPHY.C170012>
2. Ansari, N. A., Moinuddin, & Ali, R. (2011). Physicochemical analysis of poly-L-lysine: An insight into the changes induced in lysine residues of proteins on modification with glucose. *IUBMB Life*, 63(1), 26–29. <https://doi.org/10.1002/IUB.410>
3. Bao, J. M., He, M. Y., Liu, Y. W., Lu, Y. J., Hong, Y. Q., Luo, H. H., Ren, Z. L., Zhao, S. C., & Jiang, Y. (2015). AGE/RAGE/Akt pathway contributes to prostate cancer cell proliferation by promoting Rb phosphorylation and degradation. *American Journal of Cancer Research*, 5(5), 1741. <https://doi.org/10.21037/tau.2016.s044>
4. Baraka-Vidot, J., Guerin-Dubourg, A., Bourdon, E., & Rondeau, P. (2012). Impaired drug-binding capacities of in vitro and in vivo glycated albumin. *Biochimie*, 94(9), 1960–1967. <https://doi.org/10.1016/J.BIOCHI.2012.05.017>
5. Boguszewska, K., Szewczuk, M., Kazmierczak-Baranska, J., & Karwowski, B. T. (2020). The Similarities between Human Mitochondria and Bacteria in the Context of Structure, Genome, and Base Excision Repair System. *Molecules* 2020, Vol. 25, Page 2857, 25(12), 2857. <https://doi.org/10.3390/MOLECULES25122857>
6. Broadfield, L. A., Pane, A. A., Talebi, A., Swinnen, J. v., & Fendt, S. M. (2021). Lipid metabolism in cancer: New perspectives and emerging mechanisms. *Developmental Cell*, 56(10), 1363–1393. <https://doi.org/10.1016/J.DEVCEL.2021.04.013>
7. Chen, H., & Chan, D. C. (2017). *Mitochondrial dynamics in regulating the unique phenotypes of cancer and stem cells*. <https://doi.org/10.1016/j.cmet.2017.05.016>
8. Chun, Y., & Kim, J. (2021). AMPK–mTOR Signaling and Cellular Adaptations in Hypoxia. *International Journal of Molecular Sciences* 2021, Vol. 22, Page 9765, 22(18), 9765. <https://doi.org/10.3390/IJMS22189765>

9. Dhamija, E., Paul, S., & Kedia, S. (2019). Non-alcoholic fatty liver disease associated with hepatocellular carcinoma: An increasing concern. *The Indian Journal of Medical Research*, 149(1), 9. [https://doi.org/10.4103/IJMR.IJMR\\_1456\\_17](https://doi.org/10.4103/IJMR.IJMR_1456_17)
10. Fouad Y A, & Aanei C. (2017). *Revisiting the hallmarks of cancer*. *Am J Cancer Res*. <https://www.ncbi.nlm.nih.gov/pmc/articles/PMC5446472/pdf/ajcr0007-1016.pdf>
11. Hanahan, D. (2022). Hallmarks of Cancer: New Dimensions. In *Cancer Discovery* (Vol. 12, Issue 1, pp. 31–46). American Association for Cancer Research Inc. <https://doi.org/10.1158/2159-8290.CD-21-1059>
12. Kim, D., Park, M., Haleem, I., Lee, Y., Koo, J., Na, Y. C., Song, G., & Lee, J. (2020). Natural Product Ginsenoside 20(S)-25-Methoxyl-Dammarane-3 $\beta$ , 12 $\beta$ , 20-Triol in Cancer Treatment: A Review of the Pharmacological Mechanisms and Pharmacokinetics. *Frontiers in Pharmacology*, 11. <https://doi.org/10.3389/FPHAR.2020.00521>
13. Li, X., He, S., & Ma, B. (2020). Autophagy and autophagy-related proteins in cancer. *Molecular Cancer* 2020 19:1, 19(1), 1–16. <https://doi.org/10.1186/S12943-020-1138-4>
14. Liu, R., Chen, Y., Liu, G., Li, C., Song, Y., Cao, Z., Li, W., Hu, J., Lu, C., & Liu, Y. (2020). PI3K/AKT pathway as a key link modulates the multidrug resistance of cancers. *Cell Death & Disease*, 11(9). <https://doi.org/10.1038/S41419-020-02998-6>
15. Luongo, F., Colonna, F., Calapà, F., Vitale, S., Fiori, M. E., & de Maria, R. (2019). *PTEN Tumor-Suppressor: The Dam of Stemness in Cancer*. <https://doi.org/10.3390/cancers11081076>
16. Matou-Nasri, S., Sharaf, H., Wang, Q., Almobadel, N., Rabhan, Z., Al-Eidi, H., Yahya, W. bin, Trivilegio, T., Ali, R., Al-Shanti, N., & Ahmed, N. (2017). Biological impact of advanced glycation endproducts on estrogen receptor-positive MCF-7 breast cancer

- cells. *Biochimica et Biophysica Acta (BBA) - Molecular Basis of Disease*, 1863(11), 2808–2820. <https://doi.org/10.1016/J.BBADIS.2017.07.011>
17. Oakes, S. A. (2020). *ASIP OUTSTANDING INVESTIGATOR AWARD LECTURE Endoplasmic Reticulum Stress Signaling in Cancer Cells*. <https://doi.org/10.1016/j.ajpath.2020.01.010>
18. Olson, M. F. (2018). *Rho GTPases, their post-translational modifications, disease-associated mutations and pharmacological inhibitors*. <https://doi.org/10.1080/21541248.2016.1218407>
19. O'malley, J., Kumar, R., Inigo, J., Yadava, N., & Chandra, D. (2020). *Trends Cancer*. 6(8), 688–701. <https://doi.org/10.1016/j.trecan.2020.04.009>
20. Palanissami, G., & Paul, S. F. D. (2018). *RAGE and Its Ligands: Molecular Interplay Between Glycation, Inflammation, and Hallmarks of Cancer-a Review*. <https://doi.org/10.1007/s12672-018-0342-9>
21. Raza, S., Rajak, S., Anjum, B., & Sinha, R. A. (2019). Molecular links between non-alcoholic fatty liver disease and hepatocellular carcinoma. *Hepatoma Research*, 5, 42. <https://doi.org/10.20517/2394-5079.2019.014>
22. Shi, W., Chen, Z., Li, L., Liu, H., Zhang, R., Cheng, Q., Xu, D., & Wu, L. (2019). Unravel the molecular mechanism of XBP1 in regulating the biology of cancer cells. *Journal of Cancer*, 10. <https://doi.org/10.7150/jca.29421>
23. Sruthi, C. R., & Raghu, K. G. (2022). Methylglyoxal induces ambience for cancer promotion in HepG2 cells via Warburg effect and promotes glycation. *Journal of Cellular Biochemistry*, 123(10), 1532–1543. <https://doi.org/10.1002/jcb.30215>
24. Tamae, D., Lim, P., Wuenschell, G. E., & Termini, J. (2011). Mutagenesis and repair induced by the DNA advanced glycation end product N 2-1-(carboxyethyl)-2'-

- deoxyguanosine in human cells. *Biochemistry*, 50(12), 2321–2329.  
[https://doi.org/10.1021/BI101933P/SUPPL\\_FILE/BI101933P\\_SI\\_001.PDF](https://doi.org/10.1021/BI101933P/SUPPL_FILE/BI101933P_SI_001.PDF)
25. Wang, Y., Liu, H. H., Cao, Y. T., Zhang, L. L., Huang, F., & Yi, C. (2020). The Role of Mitochondrial Dynamics and Mitophagy in Carcinogenesis, Metastasis and Therapy. *Frontiers in Cell and Developmental Biology*, 8, 413.  
<https://doi.org/10.3389/FCELL.2020.00413/BIBTEX>
26. Wei, Y., Chen, L., Chen, J., Ge, L., & He, R. Q. (2009). Rapid glycation with D-ribose induces globular amyloid-like aggregations of BSA with high cytotoxicity to SH-SY5Y cells. *BMC Cell Biology*, 10(1), 1–15. <https://doi.org/10.1186/1471-2121-10-10/FIGURES/13>
27. Xu, J., Zhou, J. Y., Wei, W. Z., & Wu, G. S. (2010). Activation of the Akt Survival Pathway Contributes to TRAIL Resistance in Cancer Cells. *PLOS ONE*, 5(4), e10226.  
<https://doi.org/10.1371/JOURNAL.PONE.0010226>
28. Yaser, A. M., Huang, Y., Zhou, R. R., Hu, G. S., Xiao, M. F., Huang, Z. B., Duan, C. J., Tian, W., Tang, D. L., & Fan, X. G. (2012). The Role of Receptor for Advanced Glycation End Products (RAGE) in the Proliferation of Hepatocellular Carcinoma. *International Journal of Molecular Sciences* 2012, Vol. 13, Pages 5982-5997, 13(5), 5982–5997. <https://doi.org/10.3390/IJMS13055982>
29. Yu, R., Lendahl, U., Nistér, M., & Zhao, J. (2020). Regulation of Mammalian Mitochondrial Dynamics: Opportunities and Challenges. *Frontiers in Endocrinology*, 11, 374. <https://doi.org/10.3389/FENDO.2020.00374/BIBTEX>
30. Zorova, L. D., Popkov, V. A., Plotnikov, E. Y., Silachev, D. N., Pevzner, I. B., Jankauskas, S. S., Babenko, V. A., Zorov, S. D., Balakireva, A. V., Juhaszova, M., Sollott, S. J., & Zorov, D. B. (2018). Mitochondrial membrane potential. *Analytical Biochemistry*, 552, 50–59. <https://doi.org/10.1016/J.AB.2017.07.009>

## Chapter 5

# Variation in redox status via modification in glyoxalase pathway by methylglyoxal in H9c2 cells

---

---

## 5.1 Introduction

In modern societies, DM is the most prevalent metabolic condition and, if not appropriately treated in the clinical environment, can have fatal systemic effects. Numerous experimental and clinical studies have shown a strong correlation between severe cardiovascular morbidity and death and diabetes. A precursor of advanced glycation end products, which are intimately linked to vascular complications in diabetes, is MGO. But more research is still needed to understand how MGO directly affects cardiac myocytes.

In people with diabetes, long-term exposure to high blood sugar levels (hyperglycemia) can promote the production of ROS and hazardous byproducts of glycolysis, including MGO, which causes the overexpression of AGEs (Giacco & Brownlee, 2010). By disrupting MMP and suppressing oxidative phosphorylation (OXPHOS) at the respiratory chain complexes, MGO was found to cause mitochondrial injury (de Arriba et al., 2007; Shangari & O'Brien, 2004). This resulted in a decrease in ATP production and an increase in ROS levels in the mitochondrial matrix. Elevated and accumulated MGO has been linked to cell damage in a variety of tissues, including the heart (Dhar et al., 2016; Vulesevic et al., 2016).

Papadaki et al. (2018) found that patients with heart failure caused by diabetes had higher levels of MG-AGEs on actin and myosin in the heart muscle than patients with heart failure who did not have diabetes (Papadaki et al., 2018). These changes make the heart less

sensitive to calcium and get in the way of protein-muscle interactions, both of which are important for the heart to work well (Papadaki et al., 2018). In a study of people with HIV and other diseases, there was a link between MGO in the heart and plasma and a higher risk of heart failure (Dash et al., 2021). Also, higher levels of MGO in the blood of people with type 1 diabetes (T1D) were always linked to fatal heart events (Dash et al., 2021). People with type 2 diabetes (T2D), where higher plasma MGO was linked to a higher risk for atherosclerosis and blood pressure, sparked interest in its potential as a biomarker for cardiovascular disease (Ogawa et al., 2010).

Therefore, the objectives of the current study were to 1) ascertain whether MGO incubation can enhance the injury of cultured H9c2 cardiomyocytes and, if so, 2) to identify the signalling mechanism(s) and 3) to find out if administering the glycation inhibitor aminoguanidine could be a therapeutic intervention to reverse the observed phenomena connected to cardiomyocyte exposure to MGO. Therefore, we aimed to explore the basic biological mechanisms underlying the toxicity of MGO-induced glycation, oxidative stress and mitochondrial dysfunction and NF- $\kappa$ B in H9c2 cells.

## **5.2 Materials and Methods**

### **5.2.1 Reagents**

MGO was obtained from Sigma Aldrich, USA. Minimal essential media Eagles (MEME) with Earle's salt, phosphate-buffered saline (PBS), aminoguanidine bicarbonate, and radioimmunoprecipitation assay (RIPA) buffer were purchased from Himedia, India. Fetal bovine serum, penicillin–streptomycin antibiotics, 0.5% trypsin-ethylene diamine tetra acetic acid, and Hanks balanced saline solution (HBSS) were from Gibco-BRL Life Technologies (Waltham, MA, USA). Methyl thiazolyl blue tetrazolium bromide (MTT) was purchased from Sisco Research Laboratories Pvt. Ltd (SRL; India) Dimethyl sulfoxide (DMSO), 2, 7-

dichlorodihydrofluorescein diacetate (DCFH-DA) were from Sigma Aldrich, USA. Primary antibodies of NF- $\kappa$ B and Heat shock proteins (Hsp60 and Hsp70) were obtained from Santa Cruz Biotechnology, Dallas, USA.

### **5.2.2 Cell culture and treatment**

Rat cardiac myocyte cell line (H9c2) was obtained from National Center for Cell Science, Pune, India and cultured in Dulbecco's Modified Eagle's Medium (DMEM) containing 10% fetal bovine serum (FBS), 100 U/ml penicillin, and 100  $\mu$ g/ml streptomycin at 37 °C in a humidified atmosphere of 95% air and 5% CO<sub>2</sub>.

### **5.2.3 Cell viability analysis**

The cell viability analysis was carried out according to the protocol of Anupama et al., 2018. H9c2 were seeded in 96-well plates at a density of  $5 \times 10^3$  per well. Cell viability with MGO was checked by methyl thiazolyl blue tetrazolium bromide (MTT) assay. Cells were incubated with different concentrations of MGO (10, 50, 100, 500, and 1000  $\mu$ M) for 24 h. About 100  $\mu$ l of MTT solution (5 mg/ml) was added to each well, and the plate was incubated for 4 h in 5% CO<sub>2</sub> at 37°C. Then MTT solution was removed, and DMSO was added to each well and placed on a shaker for 20 min. The absorbance was measured at 570 nm using a spectrophotometer (BioTek, Synergy 4, BioTek Instruments Corp., Winooski, VT, USA).

### **5.2.4 ROS generation analysis**

The formation of ROS was estimated using DCFH-DA fluorescent dye. Briefly, DCFH-DA was added (20  $\mu$ M) to the cells, and incubated for 20 min at 37°C, then washed three times with HBSS and fluorescence intensity was measured using a microplate reader (Infinite® M200 PRO, Tecan Group Ltd; excitation/ emission: 488/525 nm), then images were taken (Olympus IX 83).

### 5.2.5 Western blotting analysis

After respective treatments for 24 h, cells were lysed in RIPA buffer supplemented with a protease inhibitor (Sigma Aldrich, USA). Protein concentrations were determined by a bicinchoninic acid protein assay kit (BCA kit, Merck, USA). Equalised protein samples were resolved by 10% SDS PAGE and electrophoretically transferred to PVDF membranes (Millipore, Merck, USA) using Mini Trans-Blot Cell (Bio-Rad Laboratories). The membranes were blocked with 5% BSA and incubated with primary antibodies at 4°C overnight. The membranes were then washed and incubated with the HRP-conjugated secondary antibodies at room temperature for 2 h and visualised with western blot hyper HRP substrate (Cat no. T7103A, Takara-Bio).  $\beta$  actin (Cat no. 4970) or GAPDH (Cat no. 5174S) was the loading control. The immunoblot images were analysed with the help of the ChemiDOC XRS system using Image Lab software.

### 5.2.6 Glucose uptake analysis

Following the respective treatments, cell culture media was replaced with fresh media containing 100  $\mu$ M 2-NBDG (Cat no. ab146200) and incubated for 30 min. Cells with a medium lacking 2-NBDG were considered as a negative control; after incubation, cells were trypsinised and washed three times with cold PBS before fluorescence intensity detection using a FACS Aria II flow cytometer (BD Bioscience).

### 5.2.7 Determination of the mitochondrial transmembrane potential ( $\Delta\Psi$ M) in H9c2 cells

Mitochondrial membrane potential was analysed using a kit from G-Biosciences, St. Louis, USA. The kit uses a cationic fluorescent dye, JC-1, which can accumulate in the mitochondrial matrix as aggregates and gives a red fluorescence in normal cells due to the electrochemical potential gradient across the mitochondrial membrane. The accumulation of

JC-1 aggregates is prevented by the dissipation of mitochondrial membrane potential, thus resulting in the presence of JC-1 monomers in the cell, which shows a green fluorescence. Briefly, the cells were seeded in 96 black well plates at a density of  $5 \times 10^3$ . After the respective treatments, the cell culture media was replaced with a working solution of JC-1 dye, and the cells were incubated at 37 °C for 20 min. The dye was aspirated off and washed with HBSS, and the cells were then observed and imaged using a fluorescent microscope (Olympus IX 83 fluorescence microscope).

### **5.2.8 Determination of the mitochondrial Superoxide production in H9c2**

#### **cells**

Mitochondrial superoxide production was analysed using MitoSOX<sup>TM</sup> red. Briefly, the cells were seeded in 96 black well plates at a density of  $5 \times 10^3$  and subjected to respective treatments. After 24 h, cell culture media was replaced with a working solution of MitoSOX<sup>TM</sup> red (5  $\mu$ M in HBSS) and incubated for 15 min at 37 °C. After incubation, the dye was washed off with HBSS and the cells were then subjected to imaging at an excitation and emission of 514 nm and 580 nm, respectively.

### **5.2.9 Immunofluorescence**

Cells were seeded, and the following days, cells were treated. Prior to permeabilisation in 0.25 % Triton X-100 in PBS for 15 min at room temperature with gentle agitation, cells were fixed with 1 mL of 4 % paraformaldehyde in PBS for 20 min. Cells were blocked for 1 h with 10% natural goat serum, followed by incubation with primary antibodies (4 °C, overnight) and secondary antibodies (1 h, at room temperature). Primary antibodies were detected with fluorescently labelled anti-rabbit Alexa 555 (Cell Signaling Technology, USA). Nuclei were counterstained with DAPI (1 mg/mL in PBS) and visualised with a fluorescence microscope (Olympus IX 83).

### 5.2.10 Statistics

Results are shown as mean  $\pm$  SEM for the control and experimental groups after sextuplicate samples from each group were used in all analyses. Using ANOVA, the results were examined. All the data were analysed using SPSS for Windows, standard version 26 (SPSS), and a p-value  $\leq 0.05$  was considered significant.

## 5.3 Results

### 5.3.1 Effects of MGO on the viability of H9c2 cells

Our results revealed that MGO had no significant toxicity on the cell up to 100  $\mu$ M, but 500  $\mu$ M and 1000  $\mu$ M significantly decreased the cell viability (70 % and 77.3 % decrease, respectively;  $p \leq 0.05$ ; Figure 5.1.a). In this study, 50  $\mu$ M of MGO with 24 h of incubation was taken for further experiments, which is the same as used in the previous experiments with HepG2 cells.

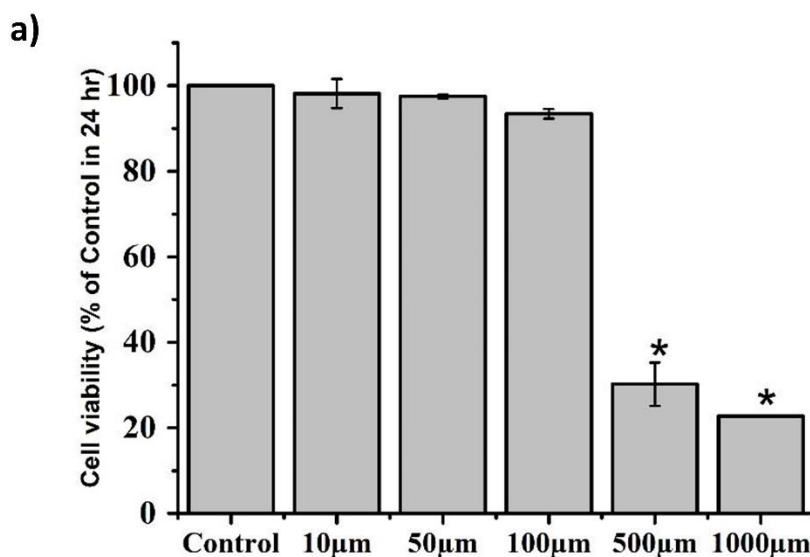


**Figure.5.1: a) Effect of various concentrations of MGO in H9c2 cells.** Concentrations ranging from 10  $\mu$ M to 1 mM were tested. All data are represented as mean  $\pm$  SEM (n = 6). \*denotes that the mean value was significantly different from control cells ( $p \leq 0.05$ ).

### 5.3.2 MGO impairs the glyoxalase system

MGO downregulated the expression of both GLO 1 (34 %; Figure.5.2. b) and GLO 2 (53 %; Figure.5.2.c) significantly ( $p \leq 0.05$ ) compared to the control. At the same time, aminoguanidine treatment could not alleviate the effect of MGO on H9c2 cells.

### 5.3.3 MGO-induced accumulation of MG-adducts

MG-adduct formation during MGO treatment was evaluated by western blot. MGO-induced adduct formation was visible as multiple bands in the MGO (Figure 5.2. a.) compared to less prominent bands in control. While adduct formation was found to be prevented in the MGO+A group.

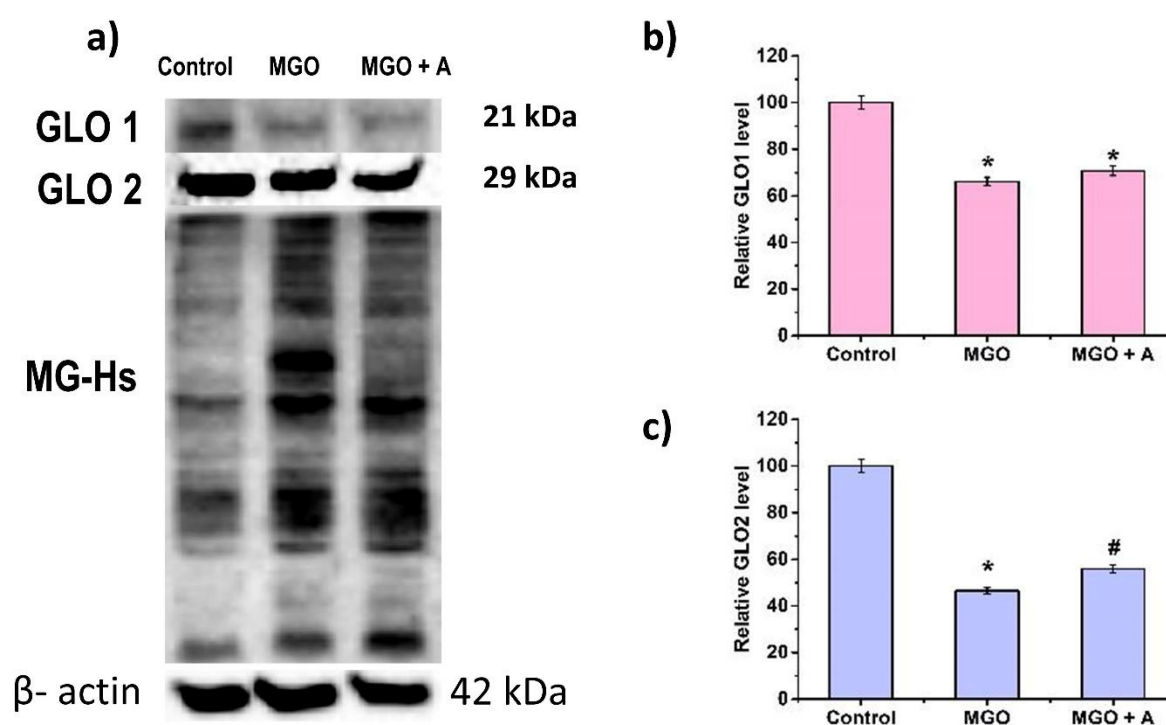


**Figure.5.2: Effect of MGO on glyoxalase system and intracellular adducts formation.** a) Immunoblot analysis of glyoxalase 1 (GLO 1), glyoxalase 2 (GLO 2) and MG-Hs in H9c2 cells b) & c) Densitometric analysis of GLO 1 and GLO 2, respectively, with respect to  $\beta$ -actin. Control (Control), Methylglyoxal (MGO, 50  $\mu$ M), MGO + Aminoguanidine (A, 200  $\mu$ M). Data are present mean values  $\pm$

SEM (n = 6). \* denotes  $p \leq 0.05$  with a significant difference from control cells. # denotes  $p \leq 0.05$  with a significant difference from MGO cells.

### 5.3.4 MGO stimulated the expression RAGE and AGE-R1

MGO caused significant overexpression of RAGE ( $p \leq 0.05$ ). A 22 % increase in expression was observed in the MGO compared to the control, and aminoguanidine prevented the RAGE overexpression by 23% compared to the MGO (Figure 5.3.b).

We also wanted to explore the role of MGO in AGE-R1 involved in AGE processing, and the results strongly indicated the upregulation of the same significantly ( $p \leq 0.05$ ) by increasing (37%; Figure 5.3.c) the expression. And aminoguanidine also increased AGE-R1 expression (75%) compared to the control. The increased expression of AGE-R1 could be an adaptive measure against MGO toxicity.

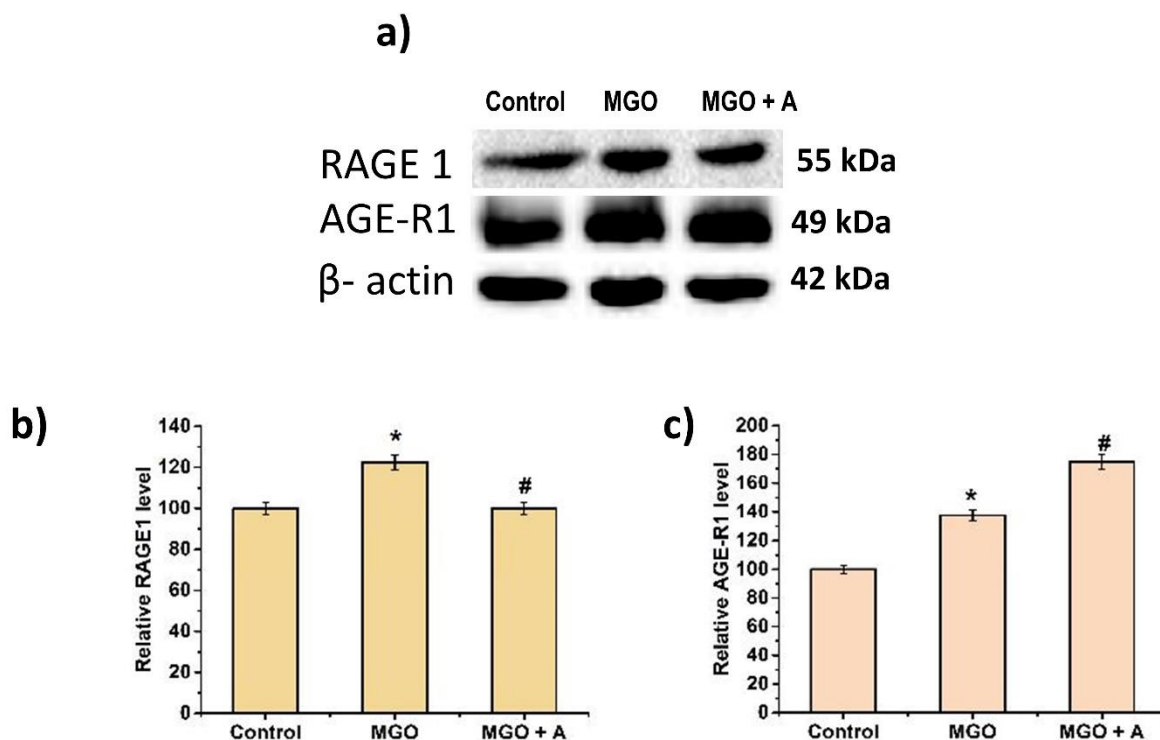


**Figure.5.3: Effect of MGO AGEs stimulated receptors.** a) Immunoblot analysis of RAGE 1 and AGE-R1 in H9c2 cells. b) & c) Densitometric analysis of RAGE 1 and AGE-R1, respectively, with

respect to  $\beta$ -actin. Control (Control), Methylglyoxal (MGO, 50  $\mu$ M), MGO + Aminoguanidine (A, 200  $\mu$ M). Data are present mean values  $\pm$  SEM (n = 6). \* denotes  $p \leq 0.05$  with a significant difference from control cells. # denotes  $p \leq 0.05$  with a significant difference from MGO cells.

### 5.3.5 Effect of MGO in ROS generation in H9c2 cells

There was a significant increase (77%;  $p \leq 0.05$ ; Figure. 5.4) in the intracellular ROS level in the MGO compared to the control. On the other hand, aminoguanidine significantly prevented ROS generation by 41% compared to the MGO.

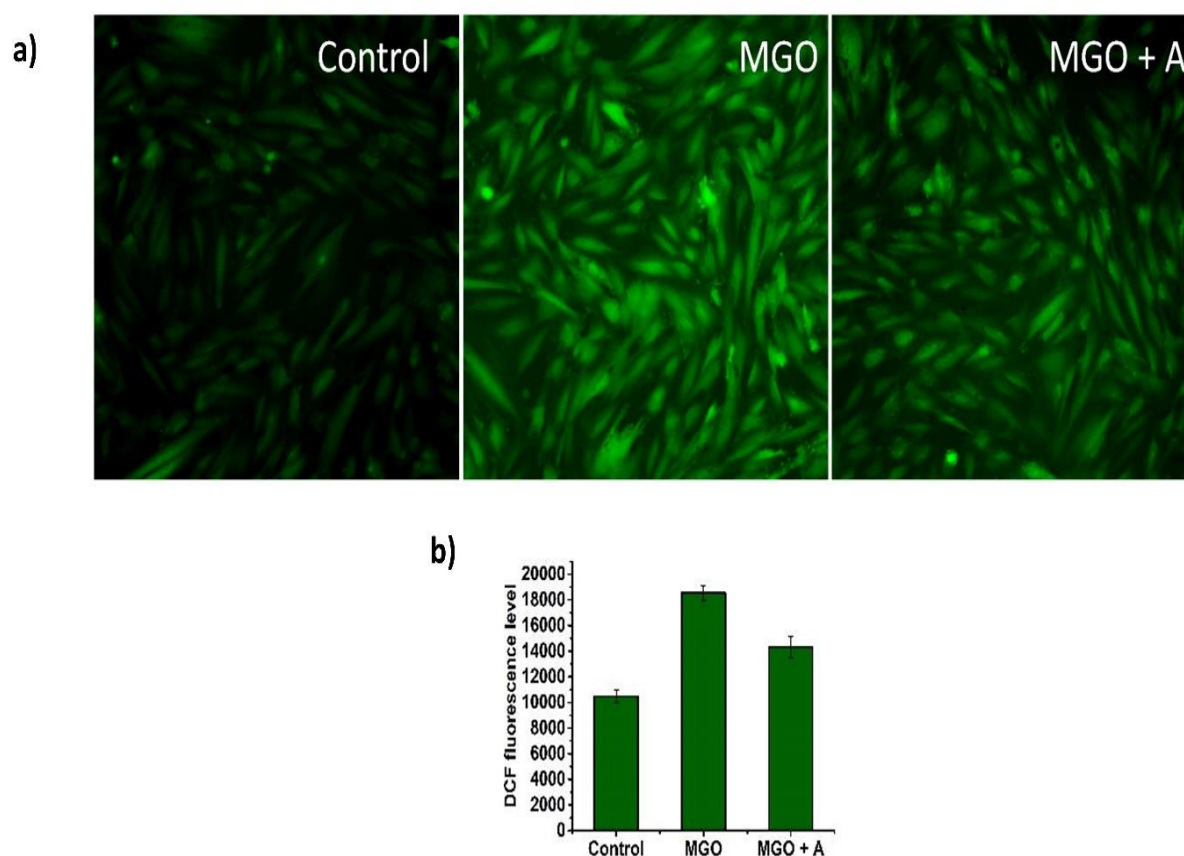


**Figure.5.4: Effect of MGO in induction of oxidative stress.** a) Intracellular ROS production, b) fluorescent intensity. Control (Control), Methylglyoxal (MGO, 50  $\mu$ M), MGO + Aminoguanidine (A, 200  $\mu$ M). Data are present mean values  $\pm$  SEM (n = 6). \* denotes  $p \leq 0.05$  with a significant difference from control cells. # denotes  $p \leq 0.05$  with a significant difference from MGO cells.

### 5.3.6 Effect of MGO on glucose uptake in H9c2 cells

As in the previous chapters, we observed an increase in the glucose uptake in the HepG2 cells; we were curious about the effect of MGO on the glucose uptake in the H9c2 cells. This made us determine the glucose uptake in H9c2 cells. Here, we observed a completely opposite result with a 7% decrease in glucose uptake in MGO exposed groups, while aminoguanidine increased the glucose uptake by 12.7 % (Figure.5.5).

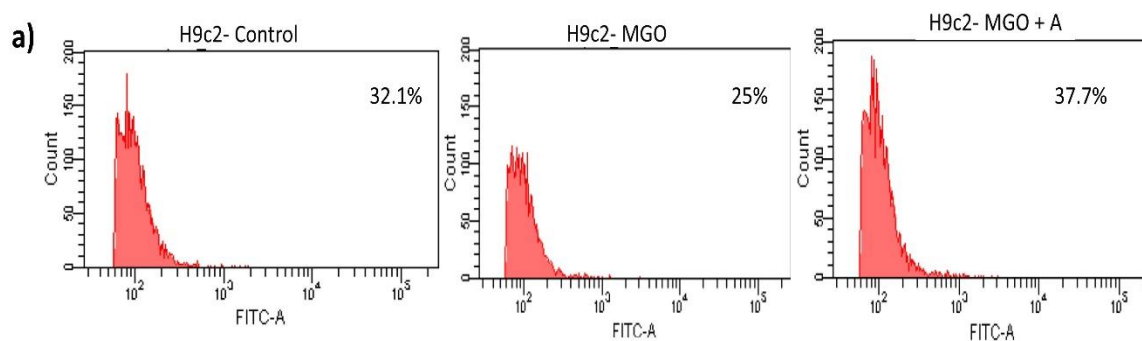


**Figure.5.5: Determination of glucose uptake in H9c2 cells.** a) Flowcytometric analysis (2-NBDG uptake). Control (Control), Methylglyoxal (MGO, 50  $\mu$ M), MGO + Aminoguanidine (A, 200  $\mu$ M). Data are present mean values  $\pm$  SEM (n = 6). \* denotes  $p \leq 0.05$  with a significant difference from control cells. # denotes  $p \leq 0.05$  with a significant difference from MGO cells.

### 5.3.7 MGO causes alteration of mitochondrial transmembrane potential

#### ( $\Delta\Psi$ M)

Mitochondrial transmembrane potential ( $\Delta\Psi$ M), which aids in ATP production, anion transport, and cation transport, is a vital sign of healthy mitochondria. Disturbances in this area can seriously impair the operation of mitochondria. A decreased mitochondrial membrane potential is evident from the fluorescent images where more green intensity means disturbance in the mitochondrial membrane potential and red means healthy mitochondria, and it could be noticed that there was a shift towards the increased green fluorescence and decrease in red

fluorescence (66.77 %;  $p \leq 0.05$ ; Figure. 5.6) in the MGO group compared to the control groups and aminoguanidine could restore the effect by 35.57 % in HepG2 cells.

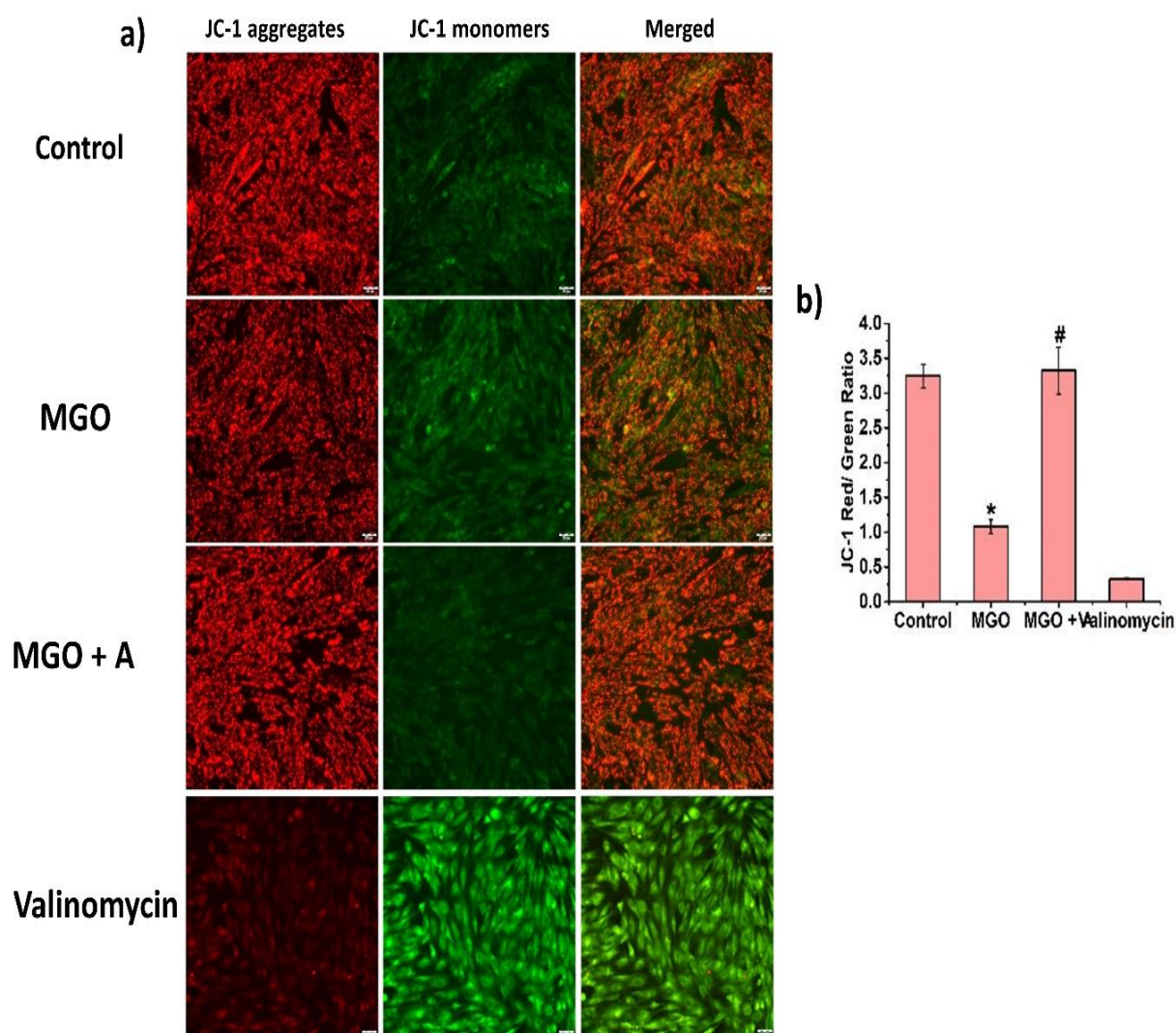


**Figure.5.6: MGO causes dissipation of  $\Delta\Psi$  in H9c2 cells.** a) The fluorescent microscopic images of H9c2 cells, b) The graphical representation of JC-1 aggregates to JC-1 monomers (ratio of 590:530 nm emission intensity). Original magnification 40X. Control (Control), Methylglyoxal (MGO, 50  $\mu$ M), MGO + Aminoguanidine (A, 200  $\mu$ M). Data are present mean values  $\pm$  SEM (n = 6). \* denotes  $p \leq 0.05$  with a significant difference from control cells. # denotes  $p \leq 0.05$  with a significant difference from MGO cells.

### 5.3.8 MGO induced mitochondrial superoxide production in H9c2 cells

Mitochondrial superoxide generation was detected with MitoSOX<sup>TM</sup> red. MGO significantly increased (435.42 %; Figure. 5.7) the generation of superoxides, while aminoguanidine prevented superoxide generation significantly ( $p \leq 0.05$ ) by 245.18 %.

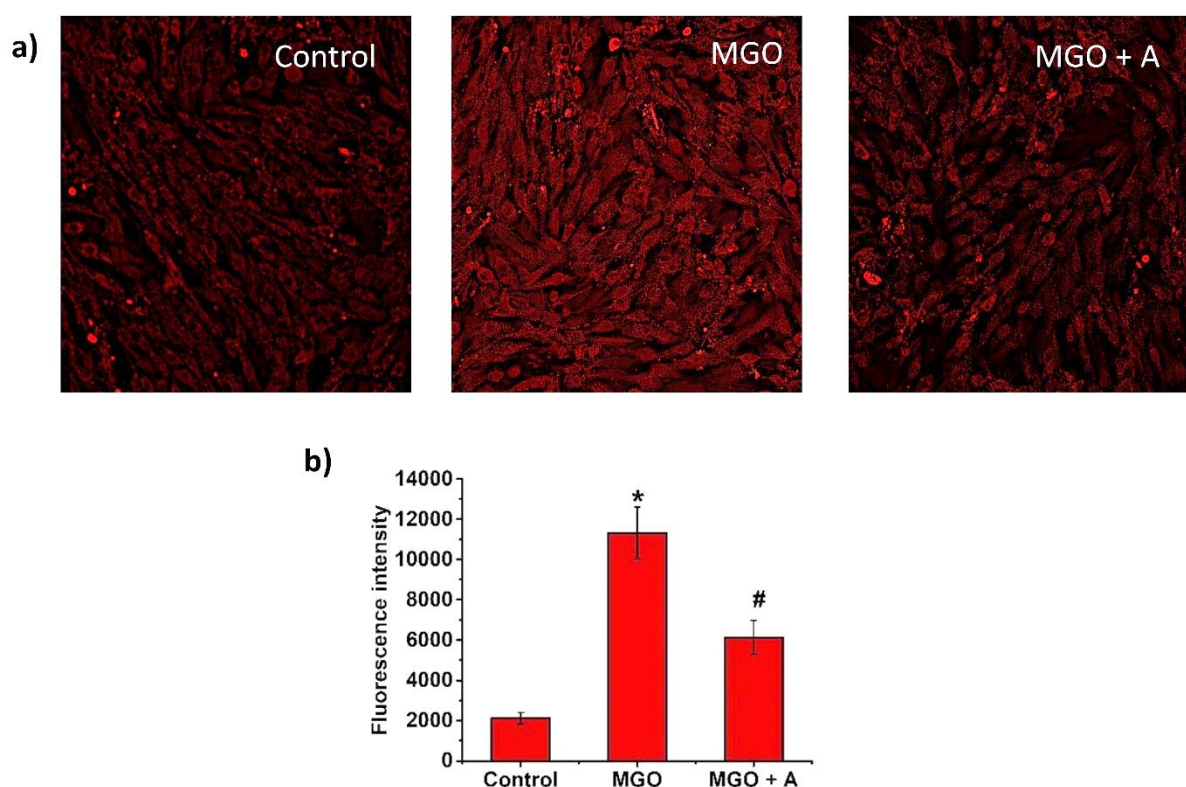


**Figure.5.7: Mitochondrial superoxide generation in H9c2 cells.** a) The fluorescent microscopic images of cells stained with MitoSOX<sup>TM</sup> Red indicator, b) Fluorescence intensity emitted by MitoSOX<sup>TM</sup> in control and treated cells. Original magnification 40X. Control (Control), Methylglyoxal (MGO, 50  $\mu$ M), MGO + Aminoguanidine (A, 200  $\mu$ M). Data are present mean values  $\pm$  SEM (n = 6). \* denotes  $p \leq 0.05$  with a significant difference from control cells. # denotes  $p \leq 0.05$  with a significant difference from MGO cells.

### 5.3.9 Effect of MGO on Hsp60 and Hsp70

MGO increased the expression of both Hsp60 (94.6 %) and Hsp70 (21.67 %; Figure.5.8) significantly ( $p \leq 0.05$ ) compared to the control. Aminoguanidine treatment significantly downregulated the expression of Hsp60 by 72.91 % compared to the MGO group, while it did not alleviate the effect of MGO on Hsp70 in H9c2 cells.

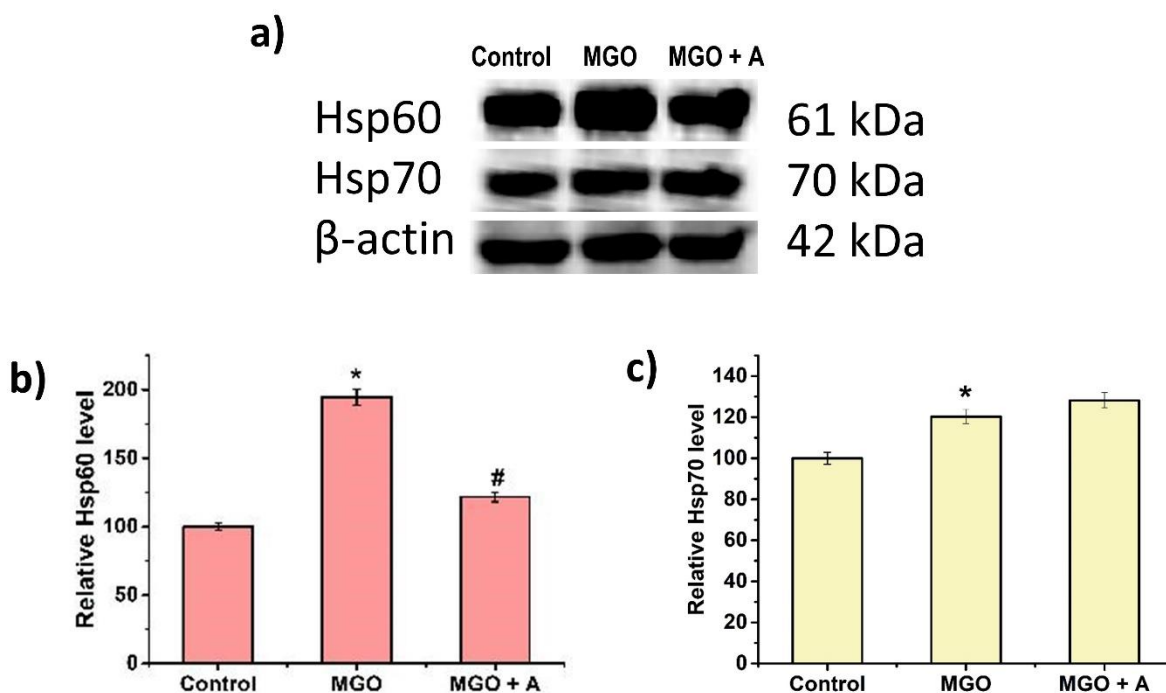


**Figure.5.8: Alteration in expression of heat shock proteins.** a) Immunoblot analysis of Heat shock proteins (Hsp60 and Hsp70) in H9c2 cells. b) & c) Densitometric analysis of Hsp60 and Hsp70, respectively, with respect to  $\beta$ -actin. Control (Control), Methylglyoxal (MGO, 50  $\mu$ M), MGO + Aminoguanidine (A, 200  $\mu$ M). Data are present mean values  $\pm$  SEM (n = 6). \* denotes  $p \leq 0.05$  with a significant difference from control cells. # denotes  $p \leq 0.05$  with a significant difference from MGO cells.

### 5.3.10 NF- $\kappa$ B translocation during MGO exposure

NF- $\kappa$ B translocation indicates the induction of inflammation. In this study, we noticed a significant nuclear translocation of NF- $\kappa$ B in the MGO-treated H9c2 cells, and treatment with

aminoguanidine ameliorated the translocation of NF- $\kappa$ B compared to the MGO group (Figure. 5.9 a)). We also analysed the expression of NF- $\kappa$ B in the MGO treated H9c2 cell and saw a slight but significant increase of 17.17 % (Figure. 5.9 b) & c)) was observed, while aminoguanidine decreased the effect of MGO by 20.92 %.

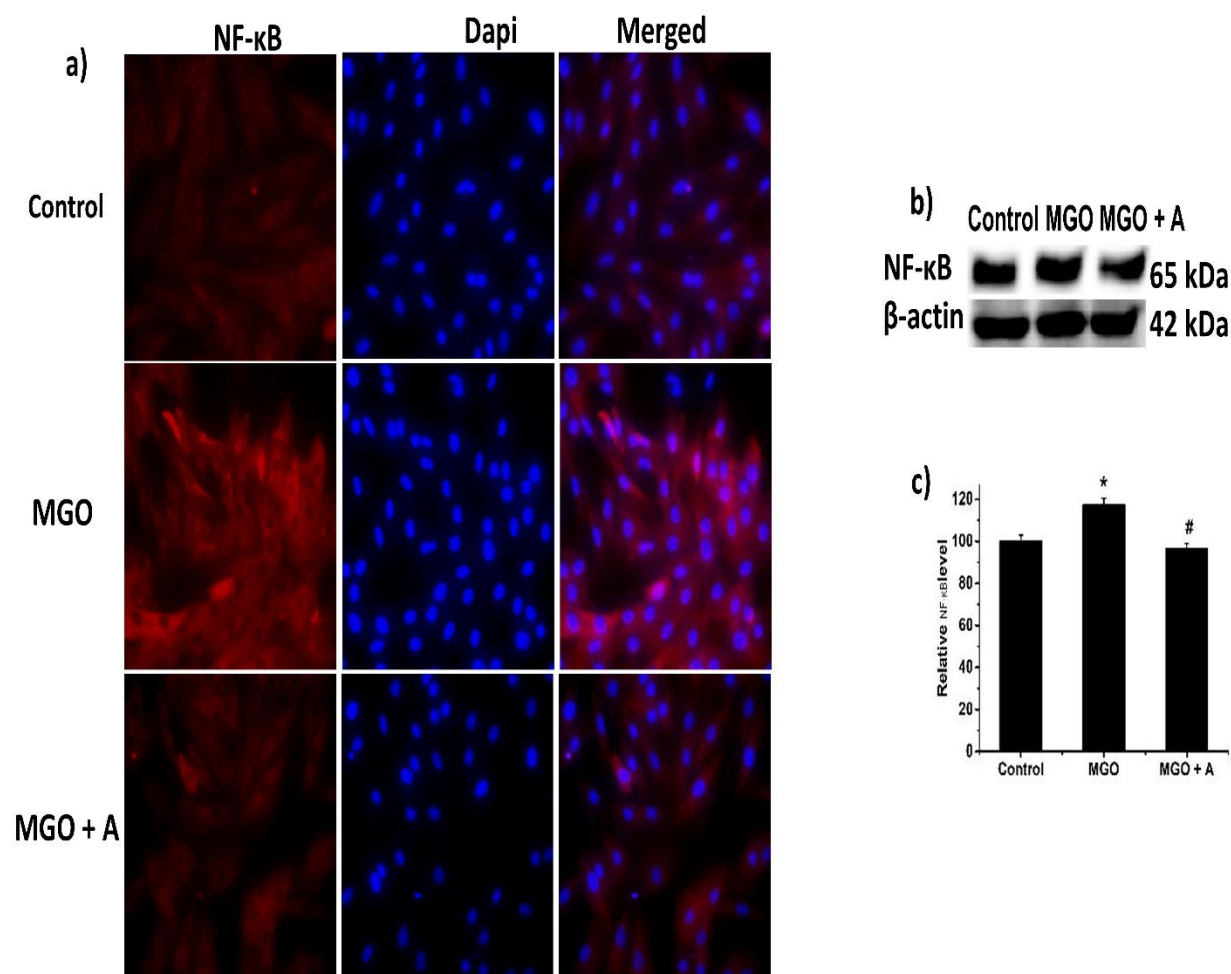


**Figure.5.9: Alteration of NF- $\kappa$ B signalling pathway in H9c2 cells.** a) Immunofluorescence staining of NF- $\kappa$ B, Original magnification 40X. b) Immunoblot analysis of NF- $\kappa$ B. c) Densitometric analysis of NF- $\kappa$ B with respect to  $\beta$ -actin. Control (Control), Methylglyoxal (MGO, 50  $\mu$ M), MGO +Aminoguanidine (A, 200  $\mu$ M). Data are present mean values  $\pm$  SEM (n = 6). \* denotes  $p \leq 0.05$  with a significant difference from control cells. # denotes  $p \leq 0.05$  with a significant difference from MGO cells.

## 5.4 Discussion

Cardiovascular morbidity and mortality are interconnected with DM. This relation has caught the eyes of researchers worldwide; however, the exact molecular mechanisms relating these two remain to be uncovered. MGO and its relation with cardiovascular diseases are unclear. Here, with this study, we are exploring the toxicity of MGO in cardiomyocytes.

As we have seen earlier, MGO increased the expression of MG-Hs or MGO-AGEs in HepG2 cells. The same results were seen here in the case of H9c2 cells also. Prominent bands of MG-Hs were seen in the MGO group compared to the control and positive control groups. We also noticed that MGO downregulated the expression of both GLO 1 and GLO 2 proteins, indicating the hampering the functioning of the glyoxalase system that detoxifies MGO.

MGO-mediated deleterious cellular effects are also the results of the formation of MGO-AGEs. AGEs activate the receptor for advanced glycation end products (RAGE). RAGE is the major culprit in inducing cellular toxicity by AGEs (Sruthi & Raghu, 2021). Now, we were curious about the effect of MGO on the RAGE 1, i.e., the receptor for the advanced glycation end products. MGO significantly increased the expression of RAGE 1 in H9c2 cells compared to the control and positive control groups.

Interaction of AGEs with RAGE initiates several transcription factors, including nuclear factor-kappaB (NF- $\kappa$ B), activator protein-1 (AP-1), cAMP response element-binding protein (CREB), signal transducer and activator of transcription 3 (STAT3), or p21<sup>ras</sup>, which in turn causes inflammation, oxidative stress, or impairs tissue remodelling (Ramasamy et al., 2012; Sorci et al., 2013). In this study, we noticed an increased ROS production along with increased expression of Hsp60 and Hsp70, indicating the severity of oxidative stress resulting in the oxidation of proteins which in turn results in the expression of heat shock proteins. Moreover, Hsp60 is also believed to be involved in the regulation of the commencement and

succession of atherosclerosis and heart failure. More importantly, serum HSP60 (sHSP60) may act as a biomarker for heart failure. During heart failure, cardiomyocytes release HSP60; several studies have correlated the increased serum HSP60 to the seriousness of the disease. In fact, high levels of sHSP60 are related to the higher mortality rate in patients with acute heart failure (AHF) (Bonanad et al., 2013). In heart failure, NF- $\kappa$ B is activated and results in the increased expression of Hsp60 in the cardiomyocytes (Wang et al., 2010; Wong et al., 1998). There are reports stating the involvement of Hsp70 in the translocation of NF- $\kappa$ B.

As we have already seen that MGO could increase the expression of Hsp60 and Hsp70, now we wanted to know the status of NF- $\kappa$ B in MGO-exposed H9c2 cells. And as expected, NF- $\kappa$ B translocation was very evident upon MGO exposure to the H9c2 cells. NF- $\kappa$ B translocation could regulate the expression of hundreds of genes that regulate processes, including cell survival, apoptosis, and inflammation (Chen & Greene, 2004; Hayden & Ghosh, 2012; Rubio et al., 2013). The repercussion of NF- $\kappa$ B activation varies with cell type, magnitude, and duration of exposure (Dhingra et al., 2010; Van Der Heiden et al., 2010). The importance of NF- $\kappa$ B in cardiac health and disease has been well-explored, particularly during acute ischemia/reperfusion injury (Gordon et al., 2011; Van Der Heiden et al., 2010).

Cardiomyocytes rely heavily on aerobic oxidation for their energy needs. Up to 20–30% of their total cell volume is made up of mitochondria, which power the heart muscle with more than 90% of its energy (Lesnefsky et al., 2016; Martín-Fernández & Gredilla, 2016). More research has revealed a strong link between mitochondrial dysfunction and CVD. The major mechanisms are abnormalities of oxidative stress, abnormalities of calcium, a decrease in mitochondrial biosynthesis, a change in mitochondrial permeability, and an accumulation of mutations in the mitochondrial DNA (Zhu et al., 2020).

In the current study, we have also noticed a disturbance in mitochondrial transmembrane potential in the MGO-exposed H9c2 cells compared to the control and aminoguanidine-treated groups. An increased mitochondrial ROS production is also noticed in the MGO-exposed groups compared to the control and the aminoguanidine-treated groups.

## 5.5 Summary and Conclusion

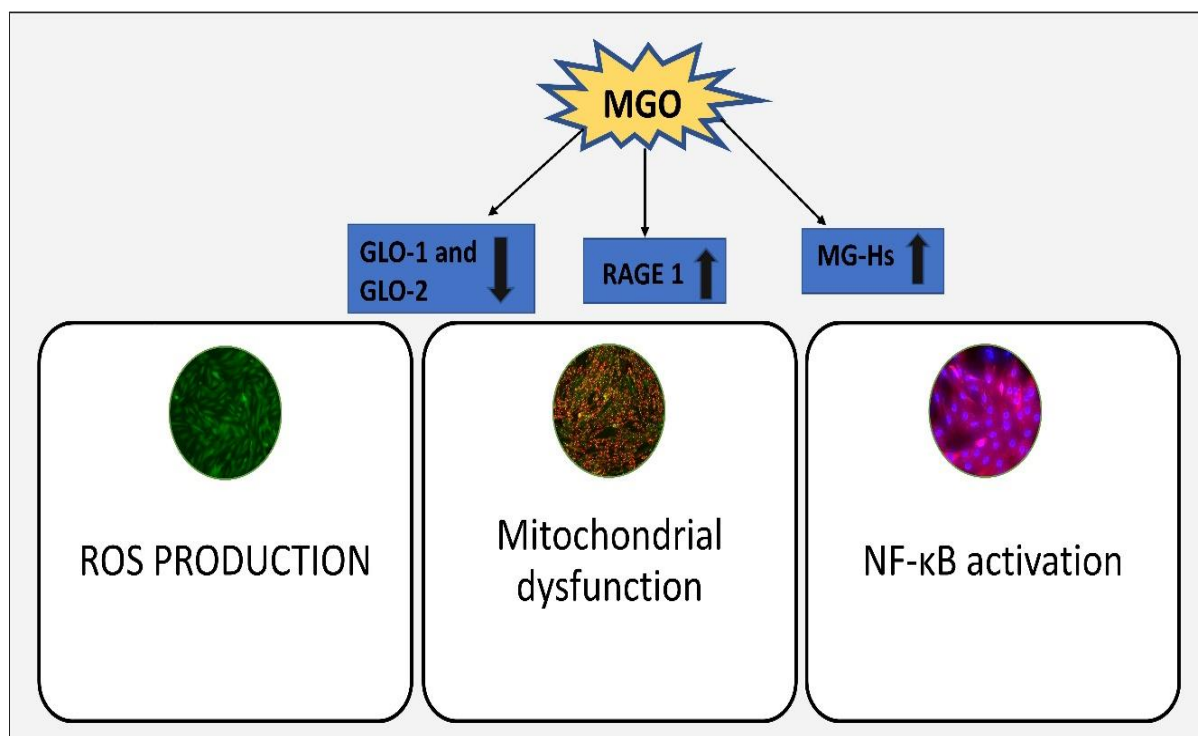


**Figure. 5.10: Schematic representation of MGO induced cellular dysfunction in H9c2**

In conclusion, our results showed that methylglyoxal induces mitochondrial dysfunction by RAGE activation via the production of ROS and NF- $\kappa$ B. These findings would provide insights into understanding the mechanism underlying methylglyoxal-mediated toxicity in the H9c2 cells.

## 5.6 References

1. Anupama, N., Preetha Rani, M. R., Shyni, G. L., & Raghu, K. G. (2018). Glucotoxicity results in apoptosis in H9c2 cells via alteration in redox homeostasis linked

- mitochondrial dynamics and polyol pathway and possible reversal with cinnamic acid. *Toxicology in Vitro*, 53, 178–192. <https://doi.org/10.1016/J.TIV.2018.08.010>
2. Bonanad, C., Núñez, J., Sanchis, J., Bodi, V., Chaustre, F., Chillet, M., Miñana, G., Forteza, M. J., Palau, P., Núñez, E., Navarro, D., Llàcer, A., & Chorro, F. J. (2013). Serum heat shock protein 60 in acute heart failure: a new biomarker? *Congestive Heart Failure (Greenwich, Conn.)*, 19(1), 6–10. <https://doi.org/10.1111/J.1751-7133.2012.00299.X>
  3. Chen, L. F., & Greene, W. C. (2004). Shaping the nuclear action of NF-κB. *Nature Reviews Molecular Cell Biology* 2004 5:5, 5(5), 392–401. <https://doi.org/10.1038/nrm1368>
  4. Dash, P. K., Alomar, F. A., Cox, J. L., McMillan, J., Hackfort, B. T., Makarov, E., Morsey, B., Fox, H. S., Gendelman, H. E., Gorantla, S., & Bidasee, K. R. (2021). A Link Between Methylglyoxal and Heart Failure During HIV-1 Infection. *Frontiers in Cardiovascular Medicine*, 8. <https://doi.org/10.3389/FCVM.2021.792180>
  5. de Arriba, S. G., Stuchbury, G., Yarin, J., Burnell, J., Loske, C., & Münch, G. (2007). Methylglyoxal impairs glucose metabolism and leads to energy depletion in neuronal cells—protection by carbonyl scavengers. *Neurobiology of Aging*, 28(7), 1044–1050. <https://doi.org/10.1016/J.NEUROBIOLAGING.2006.05.007>
  6. Dhar, A., Dhar, I., Bhat, A., & Desai, K. M. (2016). Alagebrium attenuates methylglyoxal induced oxidative stress and AGE formation in H9C2 cardiac myocytes. *Life Sciences*, 146, 8–14. <https://doi.org/10.1016/J.LFS.2016.01.006>
  7. Dhingra, R., Shaw, J. A., Aviv, Y., & Kirshenbaum, L. A. (2010). Dichotomous actions of NF-κB signaling pathways in heart. *Journal of Cardiovascular Translational Research*, 3(4), 344–354. <https://doi.org/10.1007/S12265-010-9195-5/METRICS>

8. Giacco, F., & Brownlee, M. (2010). Oxidative stress and diabetic complications. *Circulation Research*, 107(9), 1058. <https://doi.org/10.1161/CIRCRESAHA.110.223545>
9. Gordon, J. W., Shaw, J. A., & Kirshenbaum, L. A. (2011). Multiple Facets of NF- $\kappa$ B in the Heart. *Circulation Research*, 108(9), 1122–1132. <https://doi.org/10.1161/CIRCRESAHA.110.226928>
10. Hayden, M. S., & Ghosh, S. (2012). NF- $\kappa$ B, the first quarter-century: remarkable progress and outstanding questions. *Genes & Development*, 26(3), 203–234. <https://doi.org/10.1101/GAD.183434.111>
11. Lesnefsky, E. J., Chen, Q., & Hoppel, C. L. (2016). Mitochondrial Metabolism in Aging Heart. *Circulation Research*, 118(10), 1593–1611. <https://doi.org/10.1161/CIRCRESAHA.116.307505>
12. Martín-Fernández, B., & Gredilla, R. (2016). Mitochondria and oxidative stress in heart aging. *Age*, 38(4), 225. <https://doi.org/10.1007/S11357-016-9933-Y>
13. Ogawa, S., Nakayama, K., Nakayama, M., Mori, T., Matsushima, M., Okamura, M., Senda, M., Nako, K., Miyata, T., & Ito, S. (2010). Methylglyoxal is a predictor in type 2 diabetic patients of intima-media thickening and elevation of blood pressure. *Hypertension (Dallas, Tex. : 1979)*, 56(3), 471–476. <https://doi.org/10.1161/HYPERTENSIONAHA.110.156786>
14. Papadaki, M., Holewinski, R. J., Previs, S. B., Martin, T. G., Stachowski, M. J., Li, A., Blair, C. A., Moravec, C. S., Van Eyk, J. E., Campbell, K. S., Warshaw, D. M., & Kirk, J. A. (2018). Diabetes with heart failure increases methylglyoxal modifications in the sarcomere, which inhibit function. *JCI Insight*, 3(20). <https://doi.org/10.1172/JCI.INSIGHT.121264>
15. Ramasamy, R., Yan, S. F., & Schmidt, A. M. (2012). The diverse ligand repertoire of the receptor for advanced glycation endproducts and pathways to the complications of diabetes. *Vascular Pharmacology*, 57(5–6), 160–167. <https://doi.org/10.1016/J.VPH.2012.06.004>
16. Rubio, D., Xu, R. H., Remakus, S., Krouse, T. E., Truckenmiller, M. E., Thapa, R. J., Balachandran, S., Alcamí, A., Norbury, C. C., & Sigal, L. J. (2013). Crosstalk between the Type 1 Interferon and Nuclear Factor Kappa B Pathways Confers Resistance to a

- Lethal Virus Infection. *Cell Host & Microbe*, 13(6), 701–710.  
<https://doi.org/10.1016/J.CHOM.2013.04.015>
17. Shangari, N., & O'Brien, P. J. (2004). The cytotoxic mechanism of glyoxal involves oxidative stress. *Biochemical Pharmacology*, 68(7), 1433–1442.  
<https://doi.org/10.1016/J.BCP.2004.06.013>
18. Sorci, G., Riuzzi, F., Giambanco, I., & Donato, R. (2013). RAGE in tissue homeostasis, repair and regeneration. *Biochimica et Biophysica Acta - Molecular Cell Research*, 1833(1), 101–109. <https://doi.org/10.1016/j.bbamcr.2012.10.021>
19. Sruthi, C. R., & Raghu, K. G. (2021). Advanced glycation end products and their adverse effects: The role of autophagy. *Journal of Biochemical and Molecular Toxicology*, 35(4), e22710. <https://doi.org/10.1002/JBT.22710>
20. Van Der Heiden, K., Cuhlmann, S., Luong, L. A., Zakkar, M., & Evans, P. C. (2010). Role of nuclear factor  $\kappa$ B in cardiovascular health and disease. *Clinical Science*, 118(10), 593–605. <https://doi.org/10.1042/CS20090557>
21. Vulesevic, B., McNeill, B., Giacco, F., Maeda, K., Blackburn, N. J. R., Brownlee, M., Milne, R. W., & Suuronen, E. J. (2016). Methylglyoxal-Induced Endothelial Cell Loss and Inflammation Contribute to the Development of Diabetic Cardiomyopathy. *Diabetes*, 65(6), 1699–1713. <https://doi.org/10.2337/DB15-0568>
22. Wang, Y., Chen, L., Hagiwara, N., & Knowlton, A. A. (2010). Regulation of heat shock protein 60 and 72 expression in the failing heart. *Journal of Molecular and Cellular Cardiology*, 48(2), 360–366. <https://doi.org/10.1016/J.YJMCC.2009.11.009>
23. Wong, S. C. Y., Fukuchi, M., Melnyk, P., Rodger, I., & Giaid, A. (1998). Induction of cyclooxygenase-2 and activation of nuclear factor- $\kappa$ B in myocardium of patients with congestive heart failure. *Circulation*, 98(2), 100–103.  
<https://doi.org/10.1161/01.CIR.98.2.100>

24. Zhu, L., Chen, Z., Han, K., Zhao, Y., Li, Y., Li, D., Wang, X., Li, X., Sun, S., Lin, F., & Zhao, G. (2020). Correlation between Mitochondrial Dysfunction, Cardiovascular Diseases, and Traditional Chinese Medicine. *Evidence-Based Complementary and Alternative Medicine : ECAM*, 2020. <https://doi.org/10.1155/2020/2902136>

## Chapter 6

### Summary and conclusion

---

---

Methylglyoxal (MGO) is an alpha-oxoaldehyde that is very reactive and is made in cells in many different ways. It is thought to be the most potent glycating agent because it is 20,000 to 50,000 times more reactive than glucose and quickly changes the chemical structure of proteins, lipids, and nucleotides. Glyoxalases (GLO1 and GLO2), which are important parts of the anti-glycation defence, speed up the conversion of MGO to D-lactate via the intermediate product S-D-lactoylglutathione. In this study, I saw that both the expression and activity of GLO1 and GLO2 went down in the group that was exposed to MGO. This imbalance between making MGO, letting it build up, and getting rid of it is called MGO dicarbonyl stress. Dicarbonyl stress causes MG-AGEs or MG-Hs to build up in the cells, and we've seen the same thing in MGO-treated HepG2 and H9c2 cells.

Glycation doesn't depend on the sequence of amino acids, and proteins are full of lysine and arginine residues, which are especially susceptible to glycation. Endogenous AGEs are broken down in two main ways: extracellular proteolysis and intracellular absorption and breakdown within cells, which are controlled by AGEs-receptor 1 (AGE-R1). In the present study, MGO decreased the expression of AGE-R1 HepG2 cells. The expression of RAGE 1 in HepG2 cells treated with MGO was analysed, and it was found that MGO had a increased RAGE 1 expression. ROS production is a natural result of metabolism, and oxidative stress can be caused by an imbalance in MGO formation, which enhances ROS production. Significant amounts of protein carbonyl or oxidised proteins have been linked to Alzheimer's disease, rheumatoid arthritis, diabetes, chronic renal failure, and respiratory distress syndrome.

Too much ROS production can damage and kill cells, so our innate system has made a large network of antioxidants from within to balance ROS production and removal. In this study, it was found that MGO increased the production of ROS and the buildup of protein carbonyl. It also increased the expression of Nrf2 and HO-1 and decreased the expression of SOD1 and SOD2 in HepG2 cells, which shows that MGO upsets the balance of the antioxidant system.

Methylglyoxal (MGO) has been shown to promote the development of several malignancies, including lung, breast, colorectal, and anaplastic thyroid cancer. To find out if MGO makes HepG2 cells do more aerobic glycolysis to help cancer grow, we looked closely at how MGO affected glucose metabolism, transport, and other metabolic changes. In our study, we found that MGO increased the uptake of glucose and the expression of GLUT 1 and GLUT 2, and the glycolytic pathway metabolised that glucose. Hexokinase activity was found to be increased in MGO-exposed HepG2 cells, indicating an upregulated glycolytic pathway with higher expression of HK II, GLUT1, and PFK1. Enolase 1 has been proposed as a promising biomarker for hepatocellular carcinoma patients.

The Warburg effect is the increase in the rate of glucose uptake and preferential production of lactate in cancer cells, where the end product of glycolysis, pyruvate, is redirected toward lactate rather than the entry into the TCA cycle. The access of pyruvate to the TCA cycle is regulated by PDK 1, and the LDHA enzyme converts the pyruvate to lactate. Here, in this study, MGO has been found to increase the expression of LDHA and lactate production along with the PDK 1 expression and decrease the oxygen consumption rate (OCR) in HepG2 cells. This suggests that MGO is reprogramming metabolism by redirecting pyruvate towards lactate production rather than entering the TCA cycle to promote growth, survival, proliferation and long-term maintenance. This phenomenon is well explained by the Warburg effect.

The MGO augments the growth of HepG2 cells, and this study explored the altered molecular mechanisms that support the growth of cancer cells stimulated by MGO. The liver is the central organ for fatty acid metabolism, and fatty acids are essential for cancer cells because they sustain membrane biosynthesis during high proliferation and provide energy during conditions of metabolic stress. FASN is the fatty acid synthase protein which initiates the fatty acid synthesis, and MGO could upregulate the FASN expression along with decreased pACC. SCD1 is the protein involved in fatty acid desaturation, HMGCR protein is involved in cholesterol biosynthesis, and ACOX 1, engaged in peroxisomal beta-oxidation also downregulated. This shows how MGO has affected fatty acid metabolism through the abnormal expressions of these proteins.

Autophagy supports the high metabolic and energy demands of growing malignancies, and activation of autophagy in cancer cells may lead to several tumour growth-promoting pathways. MGO has been found to upregulate autophagy by upregulating autophagosome formation in HepG2 cells. This was confirmed by the expression of biomarker proteins for autophagy, LCA3-II and Beclin 1.

Hallmarks of cancer include self-sufficient growth signalling, growth suppressor insensitivity, cell death evasion, sustained angiogenesis, unlimited replication potential, and invasion and metastasis. MGO could also downregulate PTEN for the activation of Akt and ERK pathways for cell growth and stimulation. MGO downregulates p38 activation in HepG2 cells, indicating resistance to apoptosis, and upregulates p-IRE1  $\alpha$  and XBP1 signalling, indicating ER stress-mediated cell survival.

Mitochondria play a vital role in energy metabolism. MTP is an important indicator of healthy mitochondria, and MGO is seen to be involved in the dissipation of mitochondrial transmembrane potential in HepG2 cells. Mitochondria make up 20-30% of the cell volume in

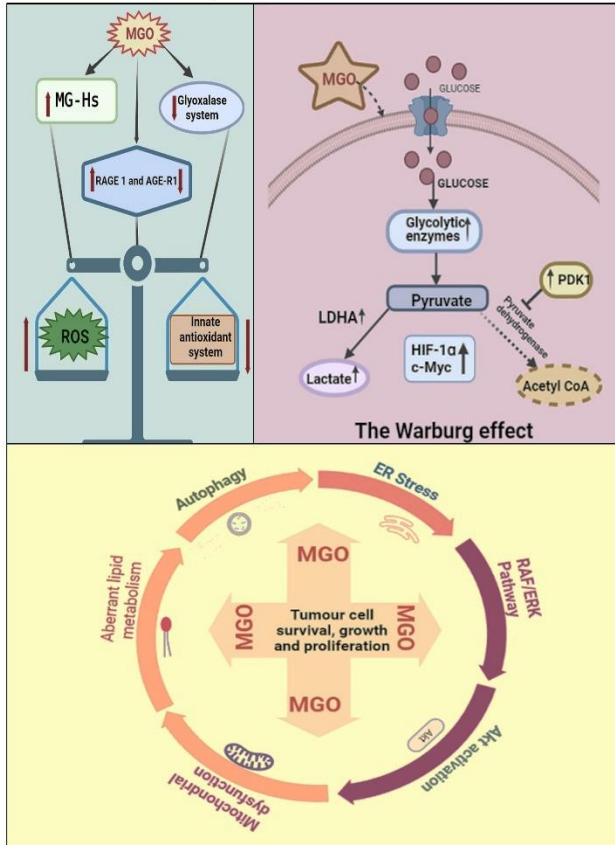
metabolically active cells and undergo fusion and fission dynamics to maintain homeostasis and quality. Mitofusin 1 (Mfn1), mitofusin 2 (Mfn2), and optic atrophy 1 (OPA1) are three essential dynamin-related proteins that control mitochondrial fusion in mammals. This study found upregulation of both DRP 1 and Fis 1 in MGO, indicating the role of MGO in mitochondrial fission in HepG2 cells.

This study also explored the toxicity of MGO in cardiomyocytes or H9c2 cells, showing that it increased the expression of MG-Hs or MGO-AGEs in H9c2 cells, as seen in the HepG2 cells. It also downregulated the expression of GLO 1 and GLO 2 proteins, indicating the hampering of the glyoxalase system that detoxifies MGO. MGO-mediated deleterious cellular effects are also caused by AGEs activating the receptor for advanced glycation end products (RAGE). Interaction of AGEs with RAGE initiates several transcription factors, including nuclear factor-kappaB (NF- $\kappa$ B), activator protein-1 (AP-1), cAMP response element-binding protein (CREB), signal transducer and activator of transcription 3 (STAT3), or p21ras, which can cause inflammation, oxidative stress, or impairs tissue remodelling. As we noticed the induction of the Warburg effect in HepG2 cells, we were curious about the effect of MGO in H9c2, and analysed the glucose uptake in the same. We observed an entirely contrasting results here; MGO downregulates the glucose uptake in H9c2 cells. This study found an increased ROS production along with increased expression of Hsp60 and Hsp70, indicating the severity of oxidative stress.

Hsp60 is also believed to be involved in the regulation of the commencement and succession of atherosclerosis and heart failure and may act as a biomarker for heart failure. NF- $\kappa$ B translocation could regulate the expression of hundreds of genes that regulate processes, including cell survival, apoptosis, and inflammation. Its repercussion varies with cell type, magnitude, and duration of exposure. And this study, we have noticed an increased translocation of NF- $\kappa$ B by MGO, which indicates the toxic outcomes of MGO exposure to the

H9c2 cells. MGO also hampered the mitochondrial transmembrane potential and increased mitochondrial ROS generation in the H9c2 cells.

MGO induces Warburg effect and promotes cancer in HepG2 cells.



MGO alters redox status, causes mitochondrial stress and activates NF-κB in H9c2 cells.

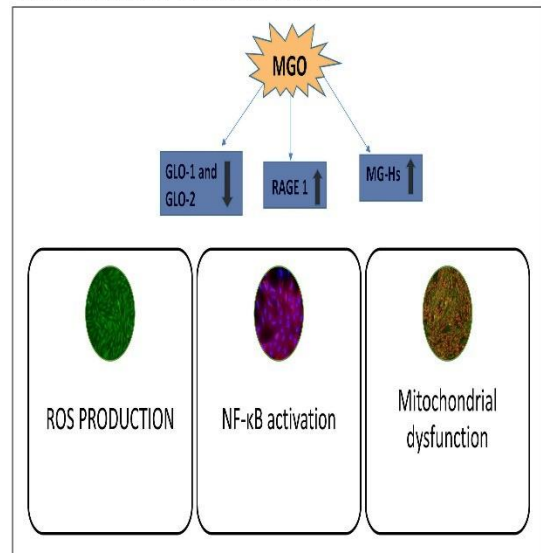


Figure. 6.1: Schematic representation of MGO-induced toxicity in HepG2 and H9c2 cells.

## ABSTRACT

---

Name of the Student: **Sruthi C R**

Registration No.: **10BB17J39012**

Faculty of Study: **Biological Sciences**

Year of Submission: **April 2023**

AcSIR academic centre/CSIR Lab: **CSIR NIIST**

Name of the Supervisor(s): **Dr. K G Raghu**

Title of the thesis: **Cytotoxicity evaluation of Methylglyoxal in HepG2 and H9c2 cells with emphasis on oxidative stress, cancer promotion and general metabolism**

---

Our main aim of the work was to understand the basic biology involved in the effect of methylglyoxal (MGO) in the progression of cancer in HepG2 cells and the consequences of MGO exposure on H9c2 cells depicting the role in CVD development. Therefore, the primary objectives of this work were to investigate the effect of MGO on HepG2 cells in the induction of oxidative stress and AGEs production and the alteration of various metabolic and molecular pathways. The second objective of the study was to understand the effect of MGO on the cardiomyocytes, H9c2 cells. Our research starts with the induction of glycation in HepG2 cells with MGO incubation. Upon MGO exposure the HepG2 cells were unable to detoxify the MGO as the function of the Glyoxalase system was hampered, and this increased the formation of MG-Hs in cells. RAGE-1 upregulation was also noticed in the MGO group, while the expression of AGE detoxifying receptor AGE-R1 was found to be downregulated by MGO. MGO-AGE or MG-Hs formation increases ROS generation in the cells, negatively affecting the balance between oxidative stress and antioxidant activation. MGO impacts glucose metabolism, enhancing aerobic glycolysis in HepG2 cells. MGO also led to a rise in the number of cancer-promoting enzymes, including HKII, PFK1, LDHA, and PDK1. HIF1 and c-Myc overexpression was also observed in MGO group. All these modifications aid in the propagation of cancer by inducing the Warburg effect and glycation in HepG2 cells by MGO. MGO can favour tumour cell survival, growth and proliferation in HepG2 cells by altering the various signalling pathways like aberrant lipid metabolism, ER stress, mitochondrial dysfunction, RAF/ERK pathway and AKT activation etc which are considered as hallmarks of cancer. In H9c2 cells, methylglyoxal induced mitochondrial dysfunction by RAGE activation via the production of ROS and NF- $\kappa$ B translocation. These findings would provide insights into understanding the mechanism underlying methylglyoxal-mediated toxicity in the H9c2 cells.

## PUBLICATIONS

### ➤ EMANATING FROM THE THESIS WORK

1. **Sruthi, C. R.**, & Raghu, K. G. (2022). Methylglyoxal induces ambience for cancer promotion in HepG2 cells via Warburg effect and promotes glycation. *Journal of cellular biochemistry*, 123(10), 1532–1543. <https://doi.org/10.1002/jcb.30215>
2. **Sruthi, C. R.**, & Raghu, K. G. (2021). Advanced glycation end products and their adverse effects: The role of autophagy. *Journal of biochemical and molecular toxicology*, 35(4), e22710. <https://doi.org/10.1002/jbt.22710> (Review article)

### ➤ OTHER PUBLICATIONS

1. Poornima, M.S., Sindhu, G., Billu, A., **Sruthi, C.R.**, Nisha, P., Gogoi, P., Baishya, G. and Raghu, K.G., 2022. Pretreatment of hydroethanolic extract of *Dillenia indica* L. attenuates oleic acid induced NAFLD in HepG2 cells via modulating SIRT-1/p-LKB-1/AMPK, HMGCR & PPAR- $\alpha$  signaling pathways. *Journal of Ethnopharmacology*, 292, p.115237.
2. Narayanan SV, Kumar M, Gnanaraj VR, **Rajan SC**, Selvaraj V, Ananthakumar S. 2-Hydroxy-1,4-naphthoquinone [Lawsone] integrated rare-earth hybrid materials as biocompatible UV/IR filter agents. *MedComm— Biomater Appl.* 2022;e29. doi:10.1002/mba2.29
3. Anto, E.M., **Sruthi, C.R.**, Krishnan, L., Raghu, K.G. and Purushothaman, J., 2023. Tangeretin alleviates Tunicamycin-induced endoplasmic reticulum stress and associated complications in skeletal muscle cells. *Cell Stress Chaperones*, pp.1-15.
4. Ravi lankalapalli, Abdul Jesmina, Dehannath Induja, Thankappan Drissya, **C. R. Sruthi**, K. G. Raghu, Shijulal Nelson-Sathi, and B. Kumar, In vitro antibacterial effects of combination of ciprofloxacin with compounds isolated from *Streptomyces luteireticuli* NIIST-D75" *J Antibiotics*.

## Conference Presentations

1. International Conference on Diabetes and Phytotherapy (ICDP), on 18-20 August, 2017 at Dept. of Biochemistry & Biotechnology, Annamalai University. (**Poster presentation**)
2. International Conference on Advances in Degenerative Diseases and Molecular Interventions (ADDMI), on 23-24<sup>th</sup> November 2017 at Hycinth, Trivandrum. (**Poster presentation**).
3. 8<sup>th</sup> Annual conference of Indian Academy of Biomedical Sciences, on 25<sup>th</sup>-27<sup>th</sup> February 2019 at CSIR-NIIST, Trivandrum.
4. 9<sup>th</sup> Annual conference of Indian Academy of Biomedical Sciences held at Department of Biochemistry, D. Y. Patil Medical College, Kolhapur, from 27<sup>th</sup> - 29<sup>th</sup> February 2020. (**Best Poster Award**)
5. International Congress on Obesity and Metabolic Syndrome hosted by Korean Society for the study of Obesity held at Conard Hotel, Seoul, Korea, on 2<sup>nd</sup> – 4<sup>th</sup> September 2021. (**Online Oral presentation**)
6. 10<sup>th</sup> Annual conference of Indian Academy of Biomedical Sciences Department of Biochemistry, King George's Medical University, Lucknow & Department of Biotechnology, Era University, Lucknow (**Oral presentation**)

# Methylglyoxal induces ambience for cancer promotion in HepG2 cells via Warburg effect and promotes glycation

C R Sruthi<sup>1,2</sup>  | K. G. Raghu<sup>1,2</sup> 

<sup>1</sup>Biochemistry and Molecular Mechanism Laboratory, Agro-Processing and Technology Division, CSIR-National Institute for Interdisciplinary Science and Technology (NIIST), Thiruvananthapuram, Kerala, India

<sup>2</sup>Academy of Scientific and Innovative Research (AcSIR), Ghaziabad, 201002, India

## Correspondence

K. G. Raghu, Agro-Processing and Technology Division, Council of Scientific and Industrial Research (CSIR) – National Institute for Interdisciplinary Science and Technology (NIIST), Thiruvananthapuram 695019, Kerala, India.  
Email: [raghukgopal@niist.res.in](mailto:raghukgopal@niist.res.in)

## Abstract

Methylglyoxal (MGO) is a toxic, highly reactive metabolite derived mainly from glucose and amino acids degradation. MGO is also one of the prime precursors for advanced glycation end products formation. The present research was performed to check whether MGO has any role in the promotion of cancer in HepG2 cells. For this, cells were incubated with MGO (50  $\mu$ M) for 24 h and subjected to various analyses. Aminoguanidine (200  $\mu$ M) was positive control. The various biochemical and protein expression studies, relevant to the MGO detoxification system, oxidative stress, and glycolysis were performed. MGO caused the reduction of expression of GLO 1 (27%) and GLO 2 (11%) causing weakening of the innate detoxification system. This is followed by an increase of RAGE (95%), AGEs or methylglyoxal adducts. We also observed hypoxia via estimation of oxygen consumption rate and surplus reactive oxygen species (ROS) (24%). To investigate the off-target effect of MGO we checked its effect on glucose transport, and its associated proteins. Glucose uptake was found to increase (15%) significantly with overexpression of GLUT 1 (35%). We also found a significant increase of glycolytic enzymes such as hexokinase II, phosphofructokinase 1, and lactate dehydrogenase along with lactate production. Observation of surplus ROS and enhanced glycolysis led us to check the expression of HIF 1 $\alpha$  which is their downstream signaling pathway. Interestingly HIF 1 $\alpha$  was found to increase significantly (35%). It is known that enhanced glycolysis and oxidative stress are catalysts for the overexpression of HIF 1 $\alpha$  which in turn creates an ambience for the promotion of cancer. Aminoguanidine was able to prevent the adverse effect of MGO partially. This is the first study to show the potential of MGO for the promotion of cancer in the non-tumorigenic HepG2 cells via the Warburg effect and glycation.

## KEYWORDS

aerobic glycolysis, GLUT1, HepG2, HIF 1 $\alpha$ , methylglyoxal

## 1 | INTRODUCTION

Diabetes is one of the most prevalent metabolic disorders in the world, which has reached pandemic proportions.<sup>1</sup> The hyperglycemia in diabetic patients triggers major secondary complications like diabetic nephropathy, neuropathy, retinopathy, atherosclerosis, and cancer.<sup>2</sup> Researchers nowadays have pointed out advanced glycation end products (AGEs) as one of the major players in diabetes and associated complications.<sup>3</sup> Prolonged hyperglycemia during diabetes is responsible for the nonenzymatic covalent adducts formation in the form of AGEs between reducing sugars and macromolecules like proteins, lipids, or nucleic acids.<sup>4</sup> One of the prime precursors for AGEs formation is methylglyoxal (MGO).<sup>5</sup> MGO is a highly reactive dicarbonyl metabolite, which can react with the lysine and arginine residues of proteins to form AGEs mostly hydroimidazolones adducts and argpyrimidines.<sup>6</sup> These can link with receptors of advanced glycation end products (RAGE) to stimulate several pathological signaling pathways.<sup>4,7</sup> The gradual accumulation of MGO has been linked with several age-related diseases,<sup>8</sup> cardiovascular diseases (CVDs), Alzheimer's disease, and liver complications.<sup>2,9</sup> It is also implicated as an emerging biological factor in cancer development and progression.<sup>10</sup>

Pathophysiological complications implicated in MGO stress can be minimized by reducing the MGO accumulation by strategies like prevention or reduction of MGO formation, scavenging of MGO, or by using inducers for glyoxalase system.<sup>11</sup>

MGO, a metabolite, is produced mainly by the glycolytic pathway. The balance between the formation and detoxification of this harmful metabolite is carried out in sequential reactions by a glyoxalase system consisting of two enzymes glyoxalase I (GLO 1) and glyoxalase II (GLO2).<sup>9</sup> Pathophysiological conditions like hyperglycemia disrupt this balance with excessive formation of MGO. Excessive intake of processed food also speeds up the formation and accumulation of MGO and AGEs in our system.<sup>12</sup> The liver is one of the major sites for glucose metabolism thus it is the prime site for MGO and AGEs formation.

There are highly contradictory reports in the literature supporting the protumorigenic as well as anticancer nature of MGO.<sup>5</sup> However, the majority report the hormetic role of MGO in cancer progression, where the presence of endurable MGO benefits in the cancer growth, while the concentrations exceeding the threshold result in cytotoxicity in the cancer cells<sup>13</sup> including normal cells. Since MGO is reported toxic to

both normal and cancerous cells, the importance of MGO as an anticancer agent has not gained much support.<sup>14</sup> Cancer progression via MGO mediated stress has been reported by various researchers<sup>1,2,13,14</sup> but not on the liver. The connection between the AGEs and diabetic complications has widely been established and their involvement in cancer development, progression, and drug resistance in diabetic patients is an evolving concept.<sup>2</sup> In line with these diabetic patients are more prone to cancer development along with a higher risk of mortality than cancer patients without diabetes.<sup>15</sup>

However, some studies have shown the involvement of MGO in liver diseases.<sup>16–18</sup> We were curious to know whether MGO creates an ambience for cancer in the liver cells. So, we put forth a hypothesis that MGO could trigger metabolic reprogramming to induce cancer development in the HepG2 cells through its multifaceted pathologies like the Warburg effect and glycation. For this, the present study is investigating the action of MGO in the glucose metabolism and AGE – oxidative stress axis in non-tumorigenic HepG2 cells which is one of the most used human liver-based *in vitro* models for the study of hepatocyte function and specific protein expression. Investigation in the present study on glucose metabolism and associated pathways is due to the dependence of glycolytic pathway by cancer cells for their energy needs.

## 2 | MATERIALS AND METHODS

### 2.1 | Reagents

MGO (Cat no. M0252) was obtained from Sigma-Aldrich. Minimal essential media Eagles (MEME) with Earle's salt (Cat no. AL047S), phosphate-buffered saline (PBS, Cat no. TL1099), and aminoguanidine bicarbonate (Cat no. RM1573) were purchased from Himedia, India. Fetal bovine serum (Cat no. 16000044), penicillin–streptomycin antibiotics (Cat no. 15070063), 0.5% trypsin-ethylene diamine tetra acetic acid (trypsin-EDTA; Cat no. R001100), and Hanks balanced saline solution or HBSS (Cat no. 1835981) were from Gibco-BRL Life Technologies. Methyl thiazolyl blue tetrazolium bromide (MTT; Cat no. 33611) was purchased from Sisco Research Laboratories Pvt. Ltd. Dimethyl sulfoxide (Cat no. D8418; DMSO), 2, 7-dichlorodihydrofluorescein diacetate (DCFH-DA; Cat no. D6883) and radio-immunoprecipitation assay (RIPA) buffer (Cat no. R0278) were from Sigma-Aldrich.

## 2.2 | Cell culture and treatment

A human hepatocellular carcinoma cell line (HepG2) was obtained from the National Centre for Cell Sciences (NCCS) and maintained in MEME medium supplemented with 10% FBS, 100 U/ml penicillin, and 100 µg/ml streptomycin. The cells were grown at 37°C in a humidified atmosphere containing 5% (v/v) CO<sub>2</sub>.

*The following are details of experimental groups:*

**Control** – control, **MGO** – the cells were incubated with 50 µM of MGO for 24 h, **MGO+A** – the cells were incubated simultaneously with 50 µM of MGO and 200 µM of aminoguanidine.

## 2.3 | Cell viability assay

The cell viability analysis was carried out according to the protocol of Anupama et al.<sup>19</sup> HepG2 were seeded in 96-well plates at a density of 5\*10<sup>3</sup> per well. Cell viability with MGO was checked by methyl thiazolyl blue tetrazolium bromide (MTT) assay. Cells were incubated with different concentrations of MGO (10, 50, 100, 500, and 1000 µM) for 24 h. About 100 µl of MTT solution (5 mg/ml) was added to each well and the plate was incubated for 4 h in 5% CO<sub>2</sub> at 37°C. Then MTT solution was removed and dimethyl sulfoxide (DMSO) was added to each well and placed on a shaker for 20 min. The absorbance was measured at 570 nm using a spectrophotometer (BioTek, Synergy 4).

## 2.4 | Oxygen consumption rate assay

The oxygen consumption rate (OCR) in the cells was determined using an assay kit from Cayman (Cat no. 600800). This assay is meant to assess the functional status of mitochondria.<sup>20,21</sup> The kit utilizes a phosphorescent oxygen probe (sensitive to 0%–20% oxygen concentration) to measure mitochondrial-associated OCR in the live cells. The phosphorescence of mitoxpress-xtra was quenched by oxygen in the media, thus, the signal was inversely proportional to the amount of oxygen present. The change in mitoxpress probe signal was measured at an excitation/emission rate of 380/650 nm, for 120 min.

## 2.5 | Evaluation of reactive oxygen species production

The reactive oxygen species (ROS) formation was estimated using DCFH-DA fluorescent dye.<sup>22</sup> Briefly, DCFH-DA was added (20 µM) to the cells, and incubated for

20 min at 37°C, then washed three times with HBSS and fluorescence intensity was measured using a microplate reader (Infinite® M200 PRO, Tecan Group Ltd; excitation/emission: 488/525 nm), then images were taken (Olympus IX 83).

## 2.6 | Glucose uptake assay

Following the respective treatments for 24 h, cell culture media was replaced with fresh media containing 100 µM 2-NBDG (Cat no. ab146200) and incubated for 30 min. Cells with medium lacking 2-NBDG were considered as a negative control. After incubation cells were trypsinized and washed three times with cold PBS before fluorescence intensity detection using a FACS Aria II flow cytometer (BD Bioscience).

For quantitative determination of glucose uptake in HepG2 cells, 2-DG6P uptake was measured using a cell-based glucose uptake colorimetric assay kit (Cat no. ab136955, Abcam) following the manufacturer's instructions.<sup>23</sup>

## 2.7 | Measurement of hexokinase II activity

Hexokinase II (HK II) activity was evaluated by using an assay kit (Cat no. K789) from Biovision.<sup>24</sup> Briefly, cells were homogenized in the HK II assay buffer for 10 min on ice and then centrifuged at 12 000 RPM at 4°C for 5 min. Supernatants were collected for further experiments. All the samples were analyzed for HK II activity by mixing with the reaction mixture and incubating for 60 min at room temperature. A parallel sample background controls were also analyzed to avoid interference due to NADH in the sample. After 60 min, absorbance was read (Infinite® M200 PRO, Tecan) to calculate the HK II activity of the sample.

## 2.8 | Lactate colorimetric assay

The lactate concentration was estimated in the culture media using an assay kit (Cat no. K607) of Biovision.<sup>25</sup> The assay was performed following the manufacturer's protocol.

## 2.9 | Western blot analysis

After specific treatments for 24 h, cells were lysed in RIPA buffer supplemented with protease inhibitor

(Sigma-Aldrich). Protein concentrations were determined by a bicinchoninic acid protein assay kit (BCA kit, Merck). Equalized protein samples were resolved by 10% SDS PAGE and electrophoretically transferred to PVDF membranes (Millipore) using Mini Trans-Blot Cell (Bio-Rad Laboratories). The membranes were blocked with 5% BSA and incubated with primary antibodies of GLO1 (Cat no. ab96032), GLO2 (Cat no. sc-365233), MG-Hs (Cat no. STA-011), RAGE (Cat no. MA5-30062), Advanced glycation end products-receptor 1 (AGE-R1; Cat no. ab204314), Hypoxia-Inducible Factor (HIF-1 $\alpha$ ; Cat no. ITT01009), Glucose transporter 1 (GLUT1; Cat no. sc-1603), HK II (Cat no. 2867S), Phosphofructokinase 1 (PFK1; Cat no. sc-377346), Enolase 1 (Cat no. sc-15343), Lactate dehydrogenase-A (LDH-A; Cat no. ITT06280), and Pyruvate dehydrogenase lipoamide kinase isozyme 1 (PDK1; Cat no. sc-515944) at 4°C overnight. The membranes were then washed and incubated with the HRP conjugated secondary antibodies at room temperature for 2 h and visualized with western blot hyper HRP substrate (Cat no. T7103A, Takara-Bio).  $\beta$  actin (Cat no. 4970) or GAPDH (Cat no. 5174S) was the loading control. The immunoblot images were analyzed with the help of the ChemIDOC XRS system using Image Lab software.

## 2.10 | Statistical analysis

Data were expressed as means  $\pm$  standard deviation. Results were subjected to one-way ANOVA analyzed for significant differences among means by Duncan's multiple range tests. All the data were analyzed using SPSS for Windows, standard version 26 (SPSS), and a  $p$ -value  $\leq 0.05$  was considered significant.

## 3 | RESULTS

### 3.1 | Effects of MGO on the viability of HepG2 cells

Our results revealed that MGO had no significant toxicity on the cell up to 500  $\mu$ M but 1000  $\mu$ M significantly decreased the cell viability (70%;  $p \leq 0.05$ ; Figure 1). In our study 50  $\mu$ M of MGO with 24 h of incubation was found to induce pathological changes which were visible by molecular and biochemical assays. Due to the hormetic or dual properties of MGO, sub-toxic doses are recommended for cancer-related studies.<sup>26</sup> Based on these 50  $\mu$ M of MGO was taken for further study.

### 3.2 | MGO impairs the glyoxalase system

MGO downregulated the expression of both GLO 1 (27%) and GLO2 (11%; Figure 2A,B) significantly ( $p \leq 0.05$ ) compared to control. While aminoguanidine treatment maintained the expressions of both the enzymes at a more or less control level.

### 3.3 | MGO stimulated the expression RAGE and AGE-R1

MGO caused significant overexpression of RAGE ( $p \leq 0.05$ ). A 95% increase in expression was observed in the MGO compared to the control and aminoguanidine prevented the RAGE overexpression by 47% compared to the MGO (Figure 2C). We also wanted to explore the role of MGO in AGE-R1 involved in AGE processing and the results strongly indicated the negative impact of MGO on the same significantly ( $p \leq 0.05$ ) by decreasing (16%; Figure 2D) the expression. And aminoguanidine reversed the effect of MGO by increasing AGE-R1 expression (15%) compared to the MGO.

### 3.4 | MGO induced accumulation of MG-adducts

MG-adduct formation during MGO treatment was evaluated by western blot. MGO induced adduct formation was visible as multiple bands in the MGO (Figure 2) compared to less prominent bands in the control. While

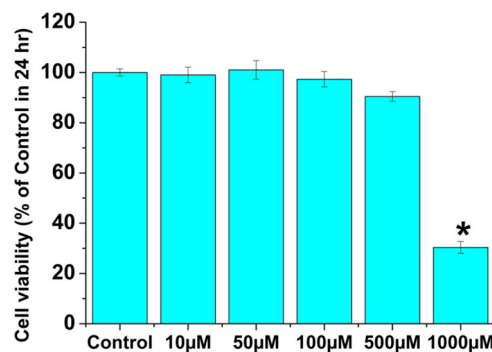


**FIGURE 1** MTT assay of HepG2 cells treated with different concentrations of methylglyoxal (MGO) for 24 h. Concentrations ranging from 10  $\mu$ M to 1 mM were tested. All data are represented as mean  $\pm$  SEM ( $n = 6$ ). \* indicates the mean value was significantly different from control cells ( $p \leq 0.05$ )

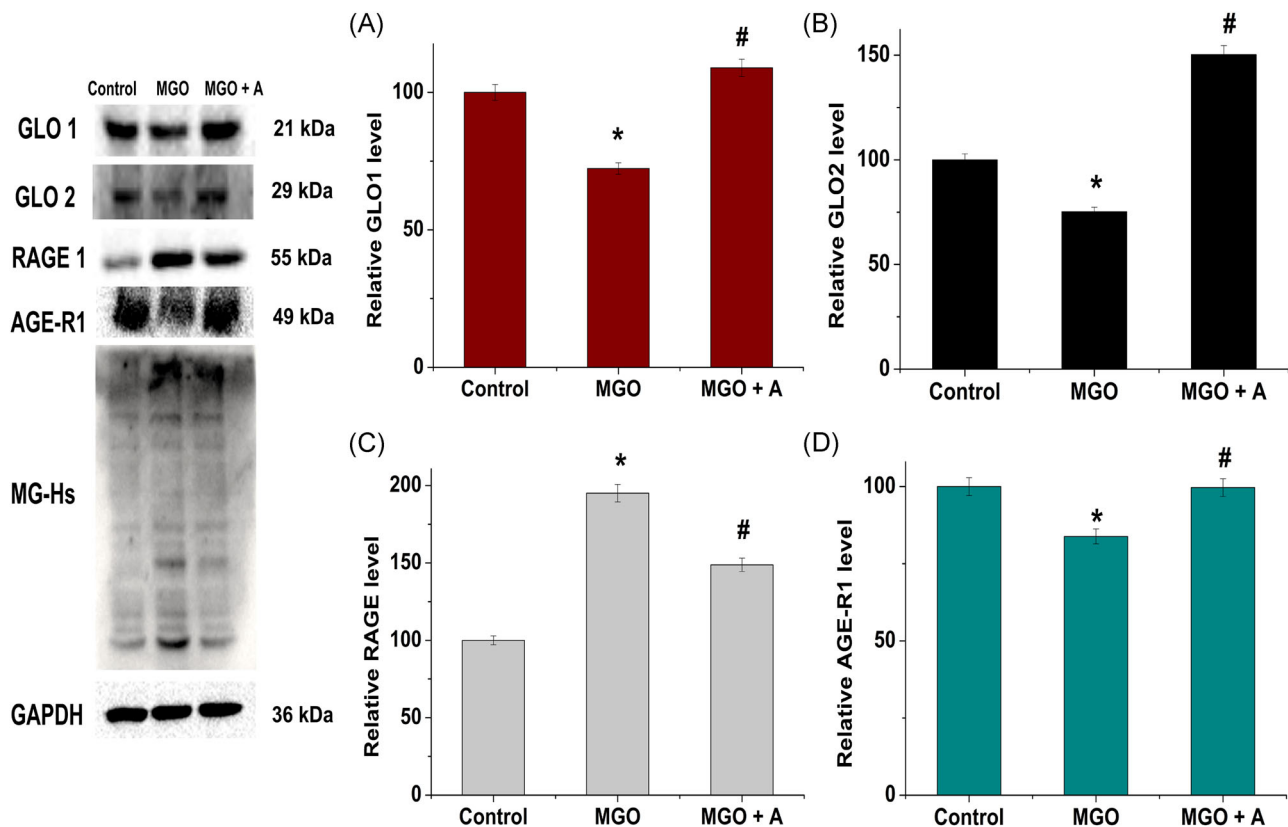


**FIGURE 2** Western blot analysis of Glyoxalase system (A) Glyoxalase1 (GLO1) and (B) Glyoxalase2 (GLO2), receptors (C) Receptor for Advanced Glycation Endproducts RAGE1 and (D) Advanced glycation endproducts receptor-1 (AGE-R1) and Methylglyoxal-hydroimidazolone (MG-Hs) in HepG2 cells. Control, MGO - Methylglyoxal (50  $\mu$ M), MGO+A -Methylglyoxal (50  $\mu$ M) + Aminoguanidine (200  $\mu$ M). Values are expressed as mean  $\pm$  SEM where  $n = 3$ . \* indicates the mean value was significantly different from control cells ( $p \leq 0.05$ ). # indicates the mean value was significantly different from MGO treated cells ( $p \leq 0.05$ )

adducts formation was found prevented in MGO+A group (Figure 2).

### 3.5 | Effect of MGO on oxygen consumption rate

Next, we analyzed the OCR in the cells. OCR was found to decrease significantly (40%;  $p \leq 0.05$ ; Figure 3A) in the MGO compared to control. While aminoguanidine maintained a normal OCR by increasing (62%) OCR compared to MGO.

### 3.6 | MGO induces surplus ROS production

There was a significant increase (24%;  $p \leq 0.05$ ; Figure 3A,B) in the intracellular ROS level in the MGO compared to the control. On the other hand, aminoguanidine significantly prevented ROS generation by 20.3% compared to the MGO.

### 3.7 | Effects of MGO on glucose uptake in HepG2 cells

Cytometry analysis was performed by detecting the fluorescence of 2-NBDG to analyze the effect of MGO on glucose uptake. The results indicated that MGO significantly increased basal glucose uptake in HepG2 cells. Glucose uptake was found to be increased by 15.1% (Figure 4A) compared to the control. For quantitative measurement of glucose uptake, we also performed colorimetric glucose uptake assay. The same trend was observed here also. The MGO group exhibited significantly high glucose uptake ( $p \leq 0.05$ , 6 pmol/ $\mu$ l compared to the control; Figure 4B). Whereas, aminoguanidine reversed this effect significantly by decreasing 6 pmol/ $\mu$ l compared to the MGO. We also performed Western blot analysis to check the expression of GLUT 1 and found that the expression was significantly increased in the MGO (35%; Figure 5A). GLUT1 expression was found to decrease by 28% in the MGO+A group compared to cells from the MGO.

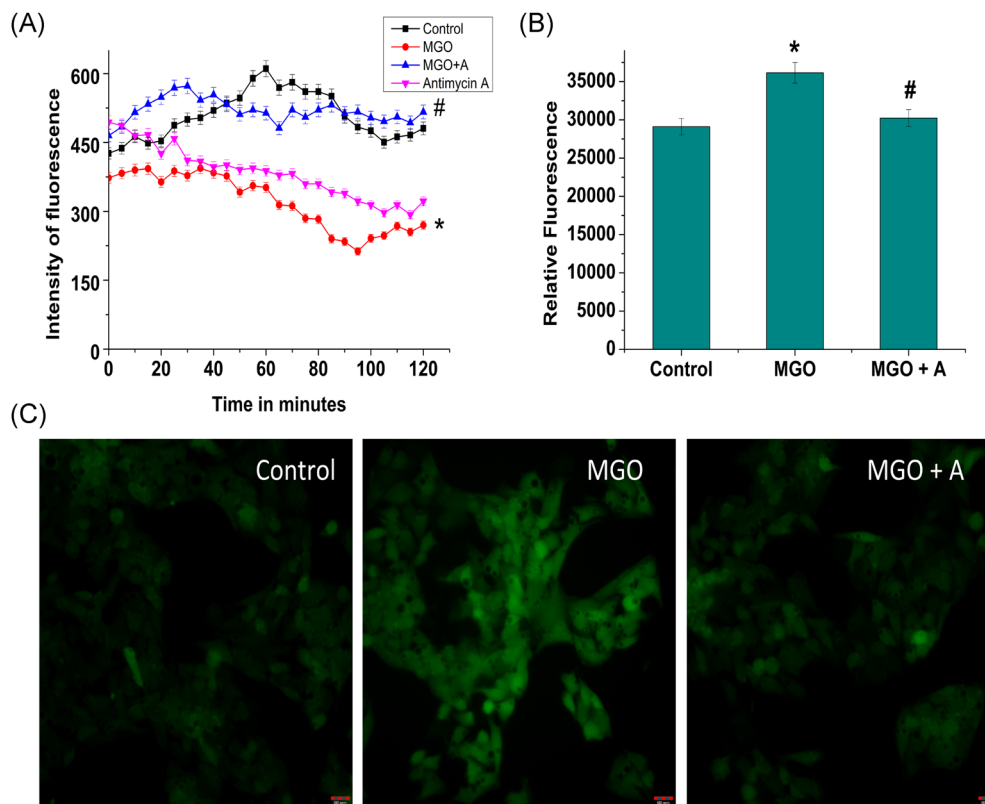


**FIGURE 3** Effect of MGO on oxygen consumption rate (OCR) and reactive oxygen species (ROS) production. (A) OCR, (B) fluorescent intensity of ROS analysis in HepG2 cells, and (C) intracellular ROS production images. Control, MGO – Methylglyoxal (50  $\mu$ M), MGO+A -Methylglyoxal (50  $\mu$ M) + Aminoguanidine (200  $\mu$ M). Values are expressed as mean  $\pm$  SEM where  $n = 6$ . \* indicates the mean value was significantly different from control cells ( $p \leq 0.05$ ). # indicates the mean value was significantly different from MGO treated cells ( $p \leq 0.05$ )

### 3.8 | Effect of MGO on glycolysis

Considering the increased glucose uptake by MGO, we evaluated its impact on glycolysis. The effect on the key enzymes of glycolysis was studied. We observed a significant (42%;  $p \leq 0.05$ ) increase in the activity of HK II in the MGO compared to the control (Figure 5B). The expression of glycolytic enzymes, HK II, PFK1, and enolase1 was also found to increase significantly ( $p \leq 0.05$ ) by 41%, 72%, and 46%, respectively, compared to control (Figure 5C–E, respectively). And aminoguanidine reversed the effects of MGO by significantly decreasing the expression by 40%, 41%, and 25% of HK II, PFK1, and enolase1, respectively, compared to the same in the MGO.

### 3.9 | MGO facilitates metabolic flux toward aerobic glycolysis rather than the TCA cycle in HepG2 cells

We further investigated the fate of pyruvate from the enhanced glycolysis. We observed a significant ( $p \leq 0.05$ )

increase in the expression of PDK1 (34%) in MGO compared to control (Figure 5F). Aminoguanidine was able to maintain the normal level of the enzyme by significantly decreasing (48%) the PDK1 expression compared to MGO. After this, we looked into the expression of LDHA and the production of lactate. Compared to the control expression, LDHA was found to increase significantly ( $p \leq 0.05$ ) by 29% along with the increased production of lactate (20%) in the MGO (Figure 5G). Aminoguanidine reversed the effects significantly by decreasing LDHA expression (25%) and lactate production (13%;  $p \leq 0.05$ ; Figure 6A) compared to the MGO. The results indicated that the MGO facilitates the metabolic flux toward aerobic glycolysis away from the TCA cycle.

### 3.10 | MGO mediated induction of HIF-1 $\alpha$

One of the major regulators of aerobic glycolysis in cancer cells is HIF-1 $\alpha$ . So, we further wanted to know whether MGO had any effect on the expression of

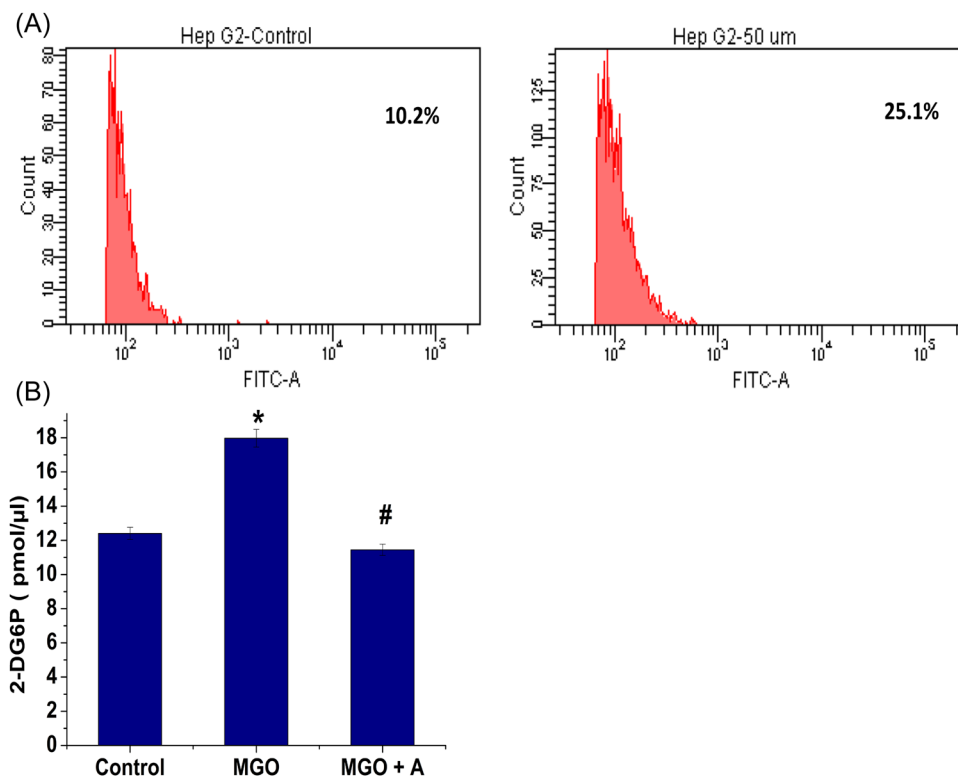


**FIGURE 4** Determination of glucose uptake in HepG2 cells. (A) Flowcytometric analysis (2-NBDG uptake) and (B) 2-DG6P uptake analysis. Control, MGO – Methylglyoxal (50  $\mu$ M), MGO+A -Methylglyoxal (50  $\mu$ M) + Aminoguanidine (200  $\mu$ M). Values are expressed as mean  $\pm$  SEM where  $n = 3$ . \* indicates the mean value was significantly different from control cells ( $p \leq 0.05$ ). # indicates the mean value was significantly different from MGO treated cells ( $p \leq 0.05$ )

HIF-1 $\alpha$ . And detected a significant ( $p \leq 0.05$ ) upregulation in the expression of HIF-1 $\alpha$  (35%) in MGO compared to control. While aminoguanidine decreased the expression of HIF-1 $\alpha$  significantly by 13% (Figure 6B) compared to the MGO. The results again confirm the role of MGO in inducing aerobic glycolysis in HepG2 cells, thus, acting as a pro-oncogenic metabolite.

## 4 | DISCUSSION

Starting with glucose metabolism, where normal cells rely on glycolysis and oxidative phosphorylation for energy production, cancer cells tend to depend only on glycolysis even in the presence of oxygen. This type of aberrant behavior is adapted by normal cells only in anaerobic conditions when there is a shortage of oxygen and cells do not want to perform oxygen consuming mitochondrial metabolism.<sup>27</sup> Otto Warburg was the first to observe the abnormal behavior in cancer cells and the phenomenon is well known as the “Warburg effect” or aerobic glycolysis.<sup>28</sup> Promotion of cancer by methylglyoxal was demonstrated in various cancers such as anaplastic thyroid cancer,<sup>14</sup> breast

cancer,<sup>26</sup> colorectal cancer,<sup>29,30</sup> and lung cancer.<sup>31</sup> But detailed molecular mechanisms responsible for this phenomenon are missing.

Glucose degradation is aberrantly increased in hyperglycemia, which causes various harmful effects on the liver. MGO induces protein modifications via the formation of advanced glycation end-products. Under physiological conditions, MGO is found as free and reversibly or irreversibly bound forms, and differences in the sample treatment methodology result in a highly contradictory estimation of MGO levels in samples.<sup>32</sup> According to Jang et al.,<sup>33</sup> the intracellular MGO concentration is much higher than the plasma MGO levels. Chaplen et al.<sup>32</sup> have reported evidence for 310  $\mu$ M of MGO in Chinese hamster ovary cells.

Based on this basic information, herein, we investigated in detail the effect of MGO in HepG2 cells with respect to glucose metabolism, transport, and associated biochemical changes to check whether it induces aerobic glycolysis in HepG2 cells for promotion of cancer. There are reports indicating the GLO1 as an oncogene,<sup>34</sup> and tumor suppressor gene.<sup>29,35,36</sup> Therefore, it is implicated as a dual mediator in tumorigenesis, as an oncogene and as a tumor suppressor, depending on the cell type.<sup>37</sup>

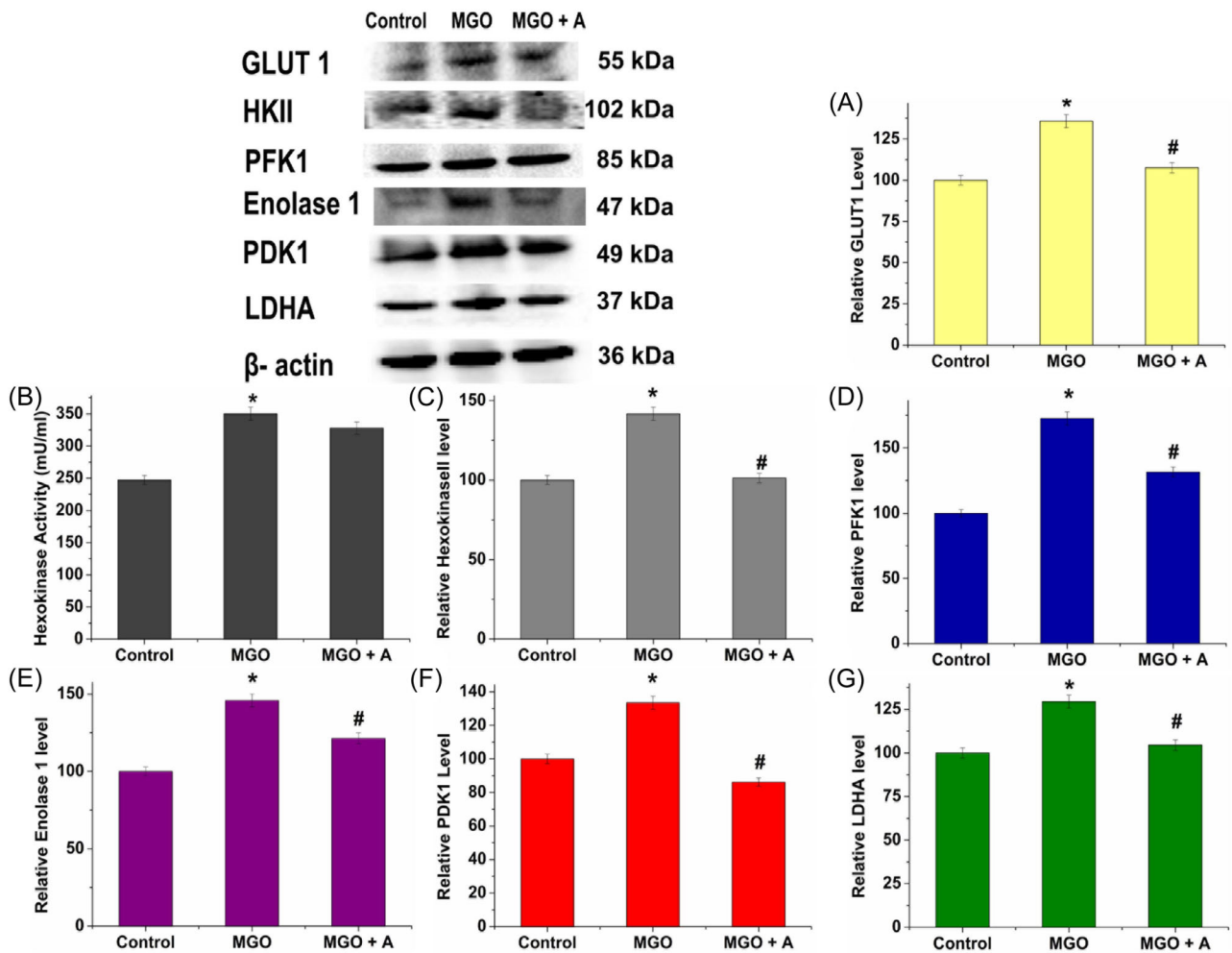


**FIGURE 5** Effect of MGO on the expression of (A) GLUT 1, glycolytic enzymes (Hexokinase II (B) activity and (C) expression), (D) Phosphofructokinase 1, (E) Enolase 1, (F) PDK1, and (G) LDHA in HepG2 cells. Control, MGO – Methylglyoxal (50  $\mu$ M), MGO + A -Methylglyoxal (50  $\mu$ M) + Aminoguanidine (200  $\mu$ M). Values are expressed as mean  $\pm$  SEM where  $n = 3$ . \* indicates the mean value was significantly different from control cells ( $p \leq 0.05$ ). # indicates the mean value was significantly different from MGO treated cells ( $p \leq 0.05$ )

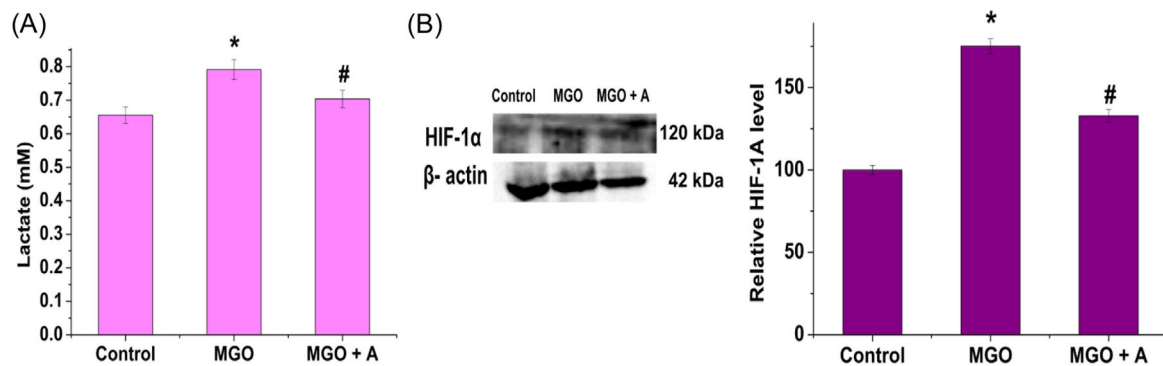


**FIGURE 6** (A) Lactate production, (B) Western blot analysis of HIF-1 $\alpha$ . Control, MGO – Methylglyoxal (50  $\mu$ M), MGO + A -Methylglyoxal (50  $\mu$ M) + Aminoguanidine (200  $\mu$ M). Values are expressed as mean  $\pm$  SEM where  $n = 3$ . \* indicates the mean value was significantly different from control cells ( $p \leq 0.05$ ). # indicates the mean value was significantly different from MGO treated cells ( $p \leq 0.05$ )

We have observed that MGO exposure to HepG2 cells impaired the glyoxalase system by significantly decreasing the expression level of both enzymes.

The activation of receptors for advanced glycation end products (RAGE) has gained interest worldwide because of its downstream regulation of several pathological pathways.<sup>38</sup> AGEs are just one among the many ligands that act upon the RAGE to exert its adverse effects. MGO treatment displayed a significant increase in the expression of RAGE. RAGE plays a crucial role in the pathophysiological signaling cascade.<sup>38</sup> AGE-R1 is yet another receptor for AGEs, which involves the degradation of AGEs via receptor-mediated endocytosis.<sup>39</sup> Here, we observed a significant decrease in the expression of this receptor. With this impairment, we also observed a significant increase in the accumulation of intracellular MGO adducts. Surplus formation of MGO adducts is expected to amplify glycation,<sup>1</sup> which in turn causes oxidative stress. The same phenomenon (oxidative stress) has been observed in the present study too. Interestingly downregulation of GLO1 is also associated with oxidative stress.<sup>40</sup> There are reports to link oxidative stress and cancer via various pathways.<sup>41</sup>

A decrease in mitochondrial-oxygen consumption observed in the present investigation also supports the involvement of MGO in mitochondrial function. Poor mitochondrial-OCR in cells indicates mitochondrial dysfunction<sup>42</sup> and results in disturbances in oxidative phosphorylation.<sup>43</sup> Furthermore, AGE-RAGE interaction activates several signaling pathways that are involved in cancer progression. This information led us to look into the effect of MGO on glycolysis and associated pathways.

Glucose uptake was found to increase significantly with MGO. Accelerated glucose metabolism is a common feature of cancer cells. So, we were curious to know the path of glucose uptake. Our investigation revealed that GLUT 1 expression had increased with MGO exposure. Besides this, the expression of glycolytic enzymes (HK II, phosphofructokinase 1, and Enolase 1), along with hexokinase activity and production of lactate and expression of LDH-A were also found to be increased. HK II catalyzes the first committed step of glucose metabolism, which converts glucose into glucose 6-phosphate in the presence of ATP. Its high expression has been reported in cancer cells.<sup>44</sup> It is a catalyst for tumor initiation and maintenance of cancerous conditions.<sup>45</sup> Enhanced activities of GLUT1 and HK II have also been associated with the development of insulin resistance<sup>46</sup> as well as the promotion of cancer in the biological system.<sup>47</sup> PFK1 is considered as the "gatekeeper of glycolysis," as its catalysis is one of the rate-limiting steps in glycolysis by converting fructose 6-phosphate to fructose 1, 6-bisphosphate.<sup>48</sup> Enolase 1 is a key enzyme in glycolysis

and is connected with tumorigenesis of various cancer cells.<sup>49</sup> Enolase 1 was put forth as a promising diagnostic and prognostic biomarker for hepatocellular carcinoma patients.<sup>50</sup> LDH-A catalyzes the conversion of pyruvate to L-lactate. LDH-A is upregulated in several cancers and it is reported to be involved in tumor growth and proliferation.<sup>51</sup> Lactate is reported as oncometabolite in the metabolic reprogramming of cancer.<sup>52</sup> The surplus lactate observed in the present study supports our claim further on the promotion of cancer by MGO in the HepG2 cells. There are contradictory results on the effect of MGO on insulin signaling pathways and glucose uptake in adipose tissue and adipocytes. Jia & Wu<sup>53</sup> have reported that endogenous MGO had downregulated insulin signaling pathways and inhibited glucose uptake in 3T3 L1 cells. While, recent proteomic study on the effect of MGO on 3T3-L1 cells revealed<sup>54</sup> a similar result as of our study, like an increase in the glucose uptake and aerobic glycolysis. These differences in results among researchers may be due to differences in the experimental setup.

We observed an increase in the expression of PDK1, the inhibitor of pyruvate dehydrogenase, the first enzyme involved in the citric acid cycle or TCA cycle. Pyruvate dehydrogenase catalyzes the conversion of pyruvate to acetyl-CoA and it enters the TCA cycle, whereas LDHA processes pyruvate to lactate. PDK1 inhibits PDH activity by phosphorylation and thus reduces the flux of pyruvate to the TCA cycle. Seo et al.<sup>17</sup> have reported that MGO seriously affects the function of mitochondria in HepG2 cells. Interestingly there was also a significant increase in the expression of HIF-1 $\alpha$  in the MGO treated cells. These results indicate the role of MGO in the induction of aerobic glycolysis in HepG2 cells under normoxia via HIF-1 $\alpha$ .<sup>55</sup> Increased aerobic glycolysis is a hallmark of cancer and the involvement of HIF-1 $\alpha$  in the upregulation of glycolysis is well observed in various cancer types via the Warburg effect.<sup>55</sup> There are reports to link oxidative stress with upregulation of HIF-1 $\alpha$ .<sup>56</sup> So here we observe two pathways through which HIF-1 $\alpha$  is getting upregulated. Our overall results point out an aberrant glucose metabolism and oxidative stress observed in MGO treated HepG2 cells that promote cancer. And aminoguanidine, a MGO scavenger, managed to recover cells from the adverse effects of MGO to a certain extent. This is a preliminary study and detailed in vitro and in vivo studies are required. Moreover, various pathways relevant to carcinogenesis are also required to be investigated in detail. If we are able to get these results translated into human samples there is a chance for utilization of these data for clinical research further. This will pave for MGO scavenger-based anticancer drugs.

## 5 | CONCLUSION

MGO affects glucose metabolism leading to enhanced aerobic glycolysis in HepG2 cells. Various enzymes relevant to cancer promotion like HKII, PFK1, LDHA, and PDK1 were also increased with MGO. It also causes overexpression of HIF-1 $\alpha$ . All these alterations contribute to the promotion of cancer via induction of the Warburg effect and glycation in HepG2 cells with MGO.

### ACKNOWLEDGMENTS

C R Sruthi is thankful to the University Grants Commission (UGC, New Delhi) for the financial support in the form of fellowship. The authors are thankful to the Director, CSIR IIIST, Thiruvananthapuram for providing needful laboratory facilities.

### CONFLICT OF INTERESTS

The authors declare that there are no conflict of interests.

### DATA AVAILABILITY STATEMENT

The data that support the findings of this study are available from the corresponding author upon reasonable request.

### ORCID

C R Sruthi  <http://orcid.org/0000-0002-0355-8769>

K. G. Raghu  <http://orcid.org/0000-0002-1341-5470>

### REFERENCES

- Schalkwijk CG, Stehouwer CDA. Methylglyoxal, a highly reactive dicarbonyl compound, in diabetes, its vascular complications, and other age-related diseases. *Physiol Rev.* 2020; 100(1):407-461. doi:10.1152/PHYSREV.00001.2019
- Bellier J, Nokin MJ, Lardé E, et al. Methylglyoxal, a potent inducer of AGEs, connects between diabetes and cancer. *Diabetes Res Clin Pract.* 2019;148:200-211. doi:10.1016/J.DIABRES.2019.01.002
- Bhat S, Mary S, Giri AP, et al. Advanced glycation end products (AGEs) in diabetic complications. *Mechanisms of Vascular Defects in Diabetes Mellitus.* Vol 17, 2017:423-449. doi:10.1007/978-3-319-60324-7\_19
- Sruthi CR, Raghu KG. Advanced glycation end products and their adverse effects: The role of autophagy. *J Biochem Mol Toxicol.* 2021;35(4):22710. doi:10.1002/JBT.22710
- Leone A, Nigro C, Nicolò A, et al. The dual-role of methylglyoxal in tumor progression – novel therapeutic approaches. *Front Oncol.* 2021;11. doi:10.3389/FONC.2021.645686
- Ahmad S, Khan M, Akhter F, et al. Glycoxidation of biological macromolecules: a critical approach to halt the menace of glycation. *Glycobiology.* 2014;24(11):979-990. <https://academic.oup.com/glycob/article-abstract/24/11/979/2900455>
- Xue J, Ray R, Singer D, et al. The receptor for advanced glycation end products (RAGE) specifically recognizes methylglyoxal-derived AGEs. *Biochemistry.* 2014;53(20):3327-3335. doi:10.1021/BI500046T
- Schröter D, Höhn A. Role of advanced glycation end products in carcinogenesis and their therapeutic implications. *Curr Pharm Des.* 2019;24(44):5245-5251. doi:10.2174/1381612825666190130145549
- Kold-Christensen R, Johannsen M. Methylglyoxal metabolism and aging-related disease: moving from correlation toward causation. *Trends Endocrinol Metabol.* 2020;31(2):81-92. doi:10.1016/J.TEM.2019.10.003
- Bellahcène A, Nokin MJ, Castronovo V, Schalkwijk C. Methylglyoxal-derived stress: an emerging biological factor involved in the onset and progression of cancer. *Sem Cancer Biol.* 2018;49:64-74. doi:10.1016/J.SEMCANCER.2017.05.010
- Patel DM, Bose M, Cooper ME. Glucose and blood pressure-dependent pathways—the progression of diabetic kidney disease. *Int J Mol Sci.* 2020;21(6):2218. doi:10.3390/IJMS21062218
- Zheng J, Guo H, Ou J, et al. Benefits, deleterious effects and mitigation of methylglyoxal in foods: a critical review. *Trends Food Sci Technol.* 2021;107:201-212. doi:10.1016/J.TIFS.2020.10.031
- Nokin MJ, Durieux F, Bellier J, et al. Hormetic potential of methylglyoxal, a side-product of glycolysis, in switching tumours from growth to death. *Sci Rep.* 2017;7(1):1-14. doi:10.1038/s41598-017-12119-7
- Antognelli C, Moretti S, Frosini R, Puxeddu E, Sidoni A, Talesa VN. Methylglyoxal acts as a tumor-promoting factor in anaplastic thyroid cancer. *Cells.* 2019;8(6):547. doi:10.3390/CELLS8060547
- Barone BB, Yeh HC, Snyder CF, et al. Long-term all-cause mortality in cancer patients with preexisting diabetes mellitus: a systematic review and meta-analysis. *JAMA.* 2008;300(23):2754-2764. doi:10.1001/JAMA.2008.824
- Maldonado EM, Rabbani N, Thornalley PJ, et al. Examination of methylglyoxal levels in an in vitro model of steatosis and serum from patients with non-alcoholic fatty liver disease. *Proc Nutr Soc.* 2015;74(OCE1):E1. doi:10.1017/S0029665115000166
- Seo K, Ki SH, Shin SM. Methylglyoxal induces mitochondrial dysfunction and cell death in liver. *Toxicol Res.* 2014;30(3):193-198. doi:10.5487/TR.2014.30.3.193
- Wang WC, Chou CK, Chuang MC, Li YC, Lee JA. Elevated levels of liver methylglyoxal and d-lactate in early-stage hepatitis in rats. *Biomed Chromatogr.* 2018;32(2). doi:10.1002/BMC.4039
- Anupama N, Preetha Rani MR, Shyni GL, Raghu KG. Glucotoxicity results in apoptosis in H9c2 cells via alteration in redox homeostasis linked mitochondrial dynamics and polyol pathway and possible reversal with cinnamic acid. *Toxicol In Vitro.* 2018;53:178-192. doi:10.1016/J.TIV.2018.08.010
- Swapna Sasi US, Sindhu G, Raghu KG. Fructose-palmitate based high calorie induce steatosis in HepG2 cells via mitochondrial dysfunction: an in vitro approach. *Toxicol In Vitro.* 2020;68:104952. doi:10.1016/J.TIV.2020.104952
- Tang R, Kimishima A, Ishida R, Setiawan A, Arai M. Selective cytotoxicity of epidithiodiketopiperazine DC1149B, produced by marine-derived *Trichoderma lixii* on the cancer cells adapted to glucose starvation. *J Nat Med.* 2020;74(1):153-158. doi:10.1007/S11418-019-01357-W/FIGURES/3

22. Mohan S, George G, Raghu KG. Vanillic acid retains redox status in HepG2 cells during hyperinsulinemic shock using the mitochondrial pathway. *Food Biosci.* 2021;41:101016. doi:10.1016/J.FBIO.2021.101016
23. Sun Z, Tan Z, Peng C, Yi W. HK2 is associated with the Warburg effect and proliferation in liver cancer: targets for effective therapy with glycyrrhizin. *Mol Med Rep.* 2021;23(5):1-8. doi:10.3892/MMR.2021.11982/HTML
24. Mack SC, Agnihotri S, Bertrand KC, et al. Spinal myxopapillary ependymomas demonstrate a Warburg phenotype. *Clin Cancer Res.* 2015;21(16):3750-3758. doi:10.1158/1078-0432.CCR-14-2650
25. Lee HJ, Jung YH, Choi GE, et al. O-cyclic phytosphingosine-1-phosphate stimulates HIF1 $\alpha$ -dependent glycolytic reprogramming to enhance the therapeutic potential of mesenchymal stem cells. *Cell Death Dis.* 2019;10(8):1-21. doi:10.1038/s41419-019-1823-7
26. Nokin MJ, Bellier J, Durieux F, et al. Methylglyoxal, a glycolysis metabolite, triggers metastasis through MEK/ERK/SMAD1 pathway activation in breast cancer. *Breast Cancer Res.* 2019;21(1):11. doi:10.1186/S13058-018-1095-7
27. Li C, Zhang G, Zhao L, Ma Z, Chen H. Metabolic reprogramming in cancer cells: glycolysis, glutaminolysis, and Bcl-2 proteins as novel therapeutic targets for cancer. *World J Surg Oncol.* 2016;14(1). doi:10.1186/S12957-016-0769-9
28. Warburg O, Minami S. Versuche an Überlebendem Carcinomgewebe. *Klin Wochenschr.* 1923;2(17):776-777. doi:10.1007/BF01712130
29. Chiavarina B, Nokin MJ, Bellier J, et al. Methylglyoxal-mediated stress correlates with high metabolic activity and promotes tumor growth in colorectal cancer. *Int J Mol Sci.* 2017;18(1):213. doi:10.3390/IJMS18010213
30. Lin JA, Wu CH, Yen GC. Methylglyoxal displays colorectal cancer-promoting properties in the murine models of azoxymethane and CT26 isografts. *Free Radic Biol Med.* 2018;115:436-446. doi:10.1016/J.FREERADBIOMED.2017.12.020
31. Luengo A, Abbott KL, Davidson SM, et al. Reactive metabolite production is a targetable liability of glycolytic metabolism in lung cancer. *Nat Commun.* 2019;10(1):5604. doi:10.1038/S41467-019-13419-4
32. Chaplen FWR, Fahl WE, Cameron DC. Evidence of high levels of methylglyoxal in cultured Chinese hamster ovary cells. *Proc Natl Acad Sci USA.* 1998;95(10):5533-5538. doi:10.1073/PNAS.95.10.5533
33. Jang JH, Kim EA, Park HJ, et al. Methylglyoxal-induced apoptosis is dependent on the suppression of c-FLIPL expression via down-regulation of p65 in endothelial cells. *J Cell Mol Med.* 2017;21(11):2720-2731. doi:10.1111/JCMM.13188
34. Sakamoto H, Mashima T, Sato S, Hashimoto Y, Yamori T, Tsuruo T. Selective activation of apoptosis program by S-p-bromobenzyglutathione cyclopentyl diester in glyoxalase I-overexpressing human lung cancer cells. *Clin Cancer Res.* 2001;7(8):2513-2518.
35. Nokin MJ, Durieux F, Peixoto P, et al. Methylglyoxal, a glycolysis side-product, induces Hsp90 glycation and YAP-mediated tumor growth and metastasis. *eLife.* 2016;5. doi:10.7554/ELIFE.19375
36. Zender L, Xue W, Zuber J, et al. An oncogenomics-based in vivo RNAi screen identifies tumor suppressors in liver cancer. *Cell.* 2008;135(5):852-864. doi:10.1016/J.CELL.2008.09.061
37. Antognelli C, Cecchetti R, Riuzzi F, Peirce MJ, Talesa VN. Glyoxalase 1 sustains the metastatic phenotype of prostate cancer cells via EMT control. *J Cell Mol Med.* 2018;22(5):2865-2883. doi:10.1111/JCMM.13581
38. Jangde N, Ray R, Rai V. RAGE and its ligands: from pathogenesis to therapeutics. *Crit Rev Biochem Mol Biol.* 2020;55(6):555-575. doi:10.1080/10409238.2020.1819194
39. Torreggiani M, Liu H, Wu J, et al. Advanced glycation end product receptor-1 transgenic mice are resistant to inflammation, oxidative stress, and post-injury intimal hyperplasia. *Am J Pathol.* 2009;175(4):1722-1732. doi:10.2353/AJPATH.2009.090138
40. Šilhavý J, Malínská H, Hüttl M, et al. Downregulation of the *glol1* gene is associated with reduced adiposity and ectopic fat accumulation in spontaneously hypertensive rats. *Antioxidants.* 2020;9(12):1-14. doi:10.3390/ANTIOX9121179
41. Sosa V, Moliné T, Somoza R, Paciucci R, Kondoh H, LLeonart ME. Oxidative stress and cancer: an overview. *Ageing Res Rev.* 2013;12(1):376-390. doi:10.1016/J.ARR.2012.10.004
42. Decler M, Jovanovic J, Vakula A, et al. Oxygen consumption rate analysis of mitochondrial dysfunction caused by *Bacillus cereus* cereulide in Caco-2 and hepG2 cells. *Toxins.* 2018;10(7):266. doi:10.3390/TOXINS10070266
43. Wilson DF, Rumsey WL, Green TJ, Vanderkooi JM. The oxygen dependence of mitochondrial oxidative phosphorylation measured by a new optical method for measuring oxygen concentration. *J Biol Chem.* 1988;263(6):2712-2718. doi:10.1016/S0021-9258(18)69126-4
44. Li WC, Huang CH, Hsieh YT, et al. Regulatory role of hexokinase 2 in modulating head and neck tumorigenesis. *Front Oncol.* 2020;10. doi:10.3389/FONC.2020.00176
45. Patra KC, Wang Q, Bhaskar PT, et al. Hexokinase 2 is required for tumor initiation and maintenance and its systemic deletion is therapeutic in mouse models of cancer. *Cancer Cell.* 2013;24(2):213-228. doi:10.1016/J.CCR.2013.06.014
46. Ebeling P, Koistinen HA, Koivisto VA. Insulin-independent glucose transport regulates insulin sensitivity. *FEBS Lett.* 1998;436(3):301-303. doi:10.1016/S0014-5793(98)01149-1
47. Wu Z, Han X, Tan G, et al. Dioscin inhibited glycolysis and induced cell apoptosis in colorectal cancer via promoting c-myc ubiquitination and subsequent hexokinase-2 suppression. *Onco Targets Ther.* 2020;13:31-44. doi:10.2147/OTT.S224062
48. Cho E, Kim N, Yun J, Cho S, Kim H, Yook J. Breast cancer subtypes underlying EMT-mediated catabolic metabolism. *Cells.* 2020;9(9):2064. doi:10.3390/cells9092064
49. Didiasova M, Schaefer L, Wygrecka M. When place matters: shuttling of enolase-1 across cellular compartments. *Front Cell Dev Biol.* 2019;7. doi:10.3389/FCELL.2019.00061
50. Zhu W, Li H, Yu Y, et al. Enolase-1 serves as a biomarker of diagnosis and prognosis in hepatocellular carcinoma patients. *Cancer Manag Res.* 2018;10:5735-5745. doi:10.2147/CMAR.S182183
51. Zhu W, Ma L, Qian J, et al. The molecular mechanism and clinical significance of LDHA in HER2-mediated progression of gastric cancer. *Am J Transl Res.* 2018;10(7):2055-2067.

52. San-Millán I, Julian CG, Matarazzo C, Martinez J, Brooks GA. Is lactate an oncometabolite? Evidence supporting a role for lactate in the regulation of transcriptional activity of cancer-related genes in MCF7 breast cancer cells. *Front Oncol.* 2020;9:1536. doi:10.3389/FONC.2019.01536
53. Jia X, Wu L. Accumulation of endogenous methylglyoxal impaired insulin signaling in adipose tissue of fructose-fed rats. *Mol Cell Biochem.* 2007;306(1):133-139. doi:10.1007/S11010-007-9563-X
54. Komanetsky SM, Hedrick V, Sobreira T, Aryal UK, Kim SQ, Kim H. Proteomic identification of aerobic glycolysis as a potential metabolic target 1 for methylglyoxal in adipocytes. *Nutr Res.* 2020;80:66-77.
55. Feng J, Li J, Wu L, et al. Emerging roles and the regulation of aerobic glycolysis in hepatocellular carcinoma. *J Exp Clin Cancer Res.* 2020;39(1):126. doi:10.1186/S13046-020-01629-4
56. Ryu JM, Lee HJ, Jung YH, et al. Regulation of stem cell fate by ROS-mediated alteration of metabolism. *Int J Stem Cells.* 2015;8(1):24-35. doi:10.15283/ijsc.2015.8.1.24

**How to cite this article:** Sruthi CR, Raghu KG. Methylglyoxal induces ambience for cancer promotion in HepG2 cells via Warburg effect and promotes glycation. *J Cell Biochem.* 2022;1-12. doi:10.1002/jcb.30215

## REVIEW

# Advanced glycation end products and their adverse effects: The role of autophagy

C. R. Sruthi<sup>1,2</sup> | K. G. Raghu<sup>1,2</sup> 

<sup>1</sup>Biochemistry and Molecular Mechanism Laboratory, Agro-processing and Technology Division, CSIR-National Institute for Interdisciplinary Science and Technology (NIIST), Thiruvananthapuram, Kerala, India

<sup>2</sup>Academy of Scientific and Innovative Research (AcSIR), Ghaziabad, India

**Correspondence**

K. G. Raghu, Biochemistry and Molecular Mechanism Laboratory, Agro-processing and Technology Division, Council of Scientific and Industrial Research (CSIR)-National Institute for Interdisciplinary Science and Technology (NIIST), Thiruvananthapuram, Kerala 695019, India.

Email: [raghugopal@niist.res.in](mailto:raghugopal@niist.res.in)

**Funding information**

University Grants Commission, Grant/Award Number: 19/06/2016(i)EU-V (Roll No.320804) (Fellowship)

**Abstract**

The critical roles played by advanced glycation endproducts (AGEs) accumulation in diabetes and diabetic complications have gained intense recognition. AGEs interfere with the normal functioning of almost every organ with multiple actions like apoptosis, inflammation, protein dysfunction, mitochondrial dysfunction, and oxidative stress. However, the development of a potential treatment strategy is yet to be established. Autophagy is an evolutionarily conserved cellular process that maintains cellular homeostasis with the degradation and recycling systems. AGEs can activate autophagy signaling, which could be targeted as a therapeutic strategy against AGEs induced problems. In this review, we have provided an overview of the adverse effects of AGEs, and we put forth the notion that autophagy could be a promising targetable strategy against AGEs.

**KEYWORDS**

advanced glycation end products (AGEs), AGEs-RAGE axis, autophagy, diabetic complications, RAGE

**1 | INTRODUCTION**

Diabetes is a metabolic syndrome characterized by hyperglycemia. Prolonged hyperglycemia because of insulin resistance or insulin deficiency is a key player in the pathogenesis of diabetes. The presence of high glucose for a long period upregulates different metabolic pathways that consequently results in glucotoxicity or hyperglycemic stress. These metabolic pathways include the polyol pathway, the glycolytic pathway, hexosamine pathway, protein kinase C (PKC) activation, and formation of advanced glycation end

products (AGEs).<sup>[1]</sup> For hyperglycemia, nonenzymatic glycation or rate of formation of AGEs increases and causes several diabetic complications such as retinopathy, cataract, neuropathy, nephropathy, and atherosclerosis, and delayed wound healing. The nonenzymatic glycation (Maillard reaction) is the reaction between the carbonyl group of reducing sugars and the free amino group of proteins, lipids, or nucleic acids. Glycation alters protein structure and function, resulting in adverse effects on cellular processes.<sup>[2]</sup> This reaction starts with the formation of a thermodynamically unstable Schiff base, which is highly reversible. These Schiff bases are then

**Abbreviations:** 1-DG, 1-deoxyglucosone; 3-DG, 3-deoxyglucosone; ADA, American Diabetes Association; ADAM 10, a disintegrin and metalloproteinase domain-containing protein 10; AGE, advanced glycation end product; ALE, advanced lipoxidation end product; ATG, autophagy related gene; BBB, blood-brain barrier; BSA, bovine serum albumin; CML, N $\epsilon$ -(carboxymethyl)lysine; COX-2, cyclooxygenase-2; cRAGE, cleaved receptors for advanced glycation end products; CVD, cardiovascular disease; Cys-C, cystatin c; ERK, extracellular signal-regulated kinase; esRAGE, endogenous secretory receptors for advanced glycation end products; GLO, glyoxalase; GO, glyoxal; Hb, hemoglobin; HbA<sub>1c</sub>, hemoglobin A1C; HCC, hepatocellular carcinoma; hIAPP, human islet amyloid polypeptide; ICAM, intercellular adhesion molecules; IL, interleukin; iNOS, inducible nitric oxide synthase; JAK, Janus kinase; LAMP 2A, lysosome-associated membrane protein 2A; LC3, microtubule-associated protein 1A/1B-light chain 3; mAlb, microalbuminuria; MAPK, mitogen-activated protein kinase; MG, methylglyoxal; MMP-9, matrix metalloproteinase 9; MOLD, methylglyoxal-lysine dimer; mTORC1, mechanistic target of rapamycin complex 1; NADPH, reduced nicotinamide adenine dinucleotide phosphate; NAFLD, nonalcoholic fatty liver disease; NF- $\kappa$ B, nuclear factor  $\kappa$ -light-chain-enhancer of activated B cells; ONOO $^-$ , peroxynitrite; PAS, pre-autosomal structure; PE, phosphatidylethanolamine; PEPT1, peptide transporter 1; PI3K, phosphoinositide 3-kinases; PKC, protein kinase C; PRR, pattern recognition receptors; RAGE, receptors for advanced glycation end products; ROS, reactive oxygen species; SIDT2, systemic RNA interference deficient-1; Smad3, mothers against decapentaplegic homolog 3; sRAGE, soluble receptors for advanced glycation end products; STAT, signal transducer and activator of transcription; T2DM, type 2 diabetes mellitus; TGF- $\beta$ 2, transforming growth factor- $\beta$ 2; TNF- $\alpha$ , tumor necrosis factor- $\alpha$ ; ULK, unc-51 like autophagy activating kinase; UPR, unfolded protein response; UVRAG, UV radiation resistance-associated gene; VCAM, vascular cell adhesion molecule; VEGF, vascular endothelial growth factor; WIPI, WD repeat domain phosphoinositide-interacting protein.

converted to Amadori products, which undergo a series of reactions to finally form irreversible AGEs.<sup>[3]</sup> Accumulation of tissue and circulating AGEs results in the development and progression of different pathogenesis like nephropathy, retinopathy, neuropathy, and atherosclerosis.<sup>[2]</sup> Thus, AGEs have received intensive attention from researchers worldwide, and their effects have been extensively studied in search of a suitable target against AGEs and their destructive potential. However, a potential target against AGEs still needs to be established.

Autophagy is an evolutionarily conserved process involved in the degradation or recycling of cellular components, including damaged long-lived proteins and protein aggregates. Autophagy is known to play a protective role against AGEs and their related complications. It could be developed as a potential target against AGEs with proper exploration in the field to know more about the role of autophagy in AGEs induced adverse effects. Thus, in this review, we discuss the impact of AGEs in various systems and the significance of autophagy in the mitigation of AGEs.

## 1.1 | Methodology

For the initial phase of the review, we searched electronic databases like PubMed, Google Scholar, and Web of Science for keywords such as “AGEs AND adverse effects,” and the search generated more than 1 lakh results. In the second phase, we searched the same databases for “Autophagy AND AGEs” and found 182 articles in Pubmed, 491 articles in Web of Science, and 18,000 articles in google scholar. Further selections of articles were based on the analysis of appropriate titles and abstracts. Final data collection was done by analyzing the full text of the selected articles relevant to set down this article.

## 1.2 | Advanced glycation end products

AGEs are chemically modified proteins, lipids, or nucleic acids. AGEs are highly stable and irreversible and accumulate in tissues at a constant and slow rate. Nevertheless, hyperglycemia speeds up the formation of AGEs.<sup>[4]</sup> AGEs can also be originated through the consumption of overheated food<sup>[5]</sup> or even through tobacco.<sup>[6]</sup> These are generated by different mechanisms, including a series of chemical reactions, and results in altering or disabling functions of the macromolecules. Nonenzymatic reactions between nonreducing sugars and free amino groups in these macromolecules lead to the formation of AGEs. The process of AGEs formation accelerates with aging and hyperglycemic conditions. Interaction of AGEs with receptors for advanced glycation end products (RAGE) has been implicated in the development of macrovascular and microvascular complications.<sup>[7]</sup> As AGEs are highly stable, these compounds accumulate in tissues and damage the cellular functions leading to different pathophysiological conditions, mainly diabetic complications, cardiovascular diseases (CVDs), Alzheimer's disease, and cancer.<sup>[8]</sup>

## 2 | FORMATION OF AGES

Formation of AGEs is a complex multistep nonenzymatic process called the Maillard reaction, first described by Louis Camille Maillard in 1912.<sup>[9]</sup> The chemical reactions involved in the Maillard reaction were first described by Hodge in 1953.<sup>[10]</sup> The nonenzymatic process is subdivided into three different stages; early, intermediate, and late stages. The process starts with the reaction between carbonyl groups of reducing sugars and amine residues on proteins, nucleic acid, and lipids. The first product formed here is an unstable compound called a Schiff base. This labile Schiff base then undergoes a rearrangement to form a more stable product known as Amadori products (also known as early glycation products)<sup>[11]</sup> (Figure 1). In the intermediate stage, with a series of reactions, rearrangements, and dehydration, these Amadori products fragment into highly reactive dicarbonyl compounds such as methylglyoxal (MG), glyoxal (GO), or deoxyglucosone (1-deoxyglucosone [1-DG] and 3-deoxyglucosone [3-DG]).<sup>[11]</sup> Accumulation of dicarbonyl compounds results in a condition called “carbonyl stress.”<sup>[12]</sup> The carbonyl compounds can attack lysine, histidine, arginine, or cysteine residues of proteins.<sup>[12]</sup> In the late-stage, these dicarbonyl compounds can further undergo oxidation, dehydration, and cyclization reactions with the cellular components to form highly irreversible brownish compounds called AGEs.<sup>[13]</sup>

### 2.1 | Other pathways involved in AGEs formation

Other pathways involved in AGEs formation include oxidative stress-mediated oxidation of glucose, and peroxidation of lipids leads to the formation of dicarbonyl derivatives, which can result in AGEs formation.<sup>[14]</sup> The polyol pathway is yet another pathway described for AGEs formation. Here, aldose reductase converts glucose to sorbitol, which is then converted to fructose by sorbitol dehydrogenase, and fructose metabolites are derivatives of dicarbonyls contributing to AGEs formation.<sup>[15]</sup>

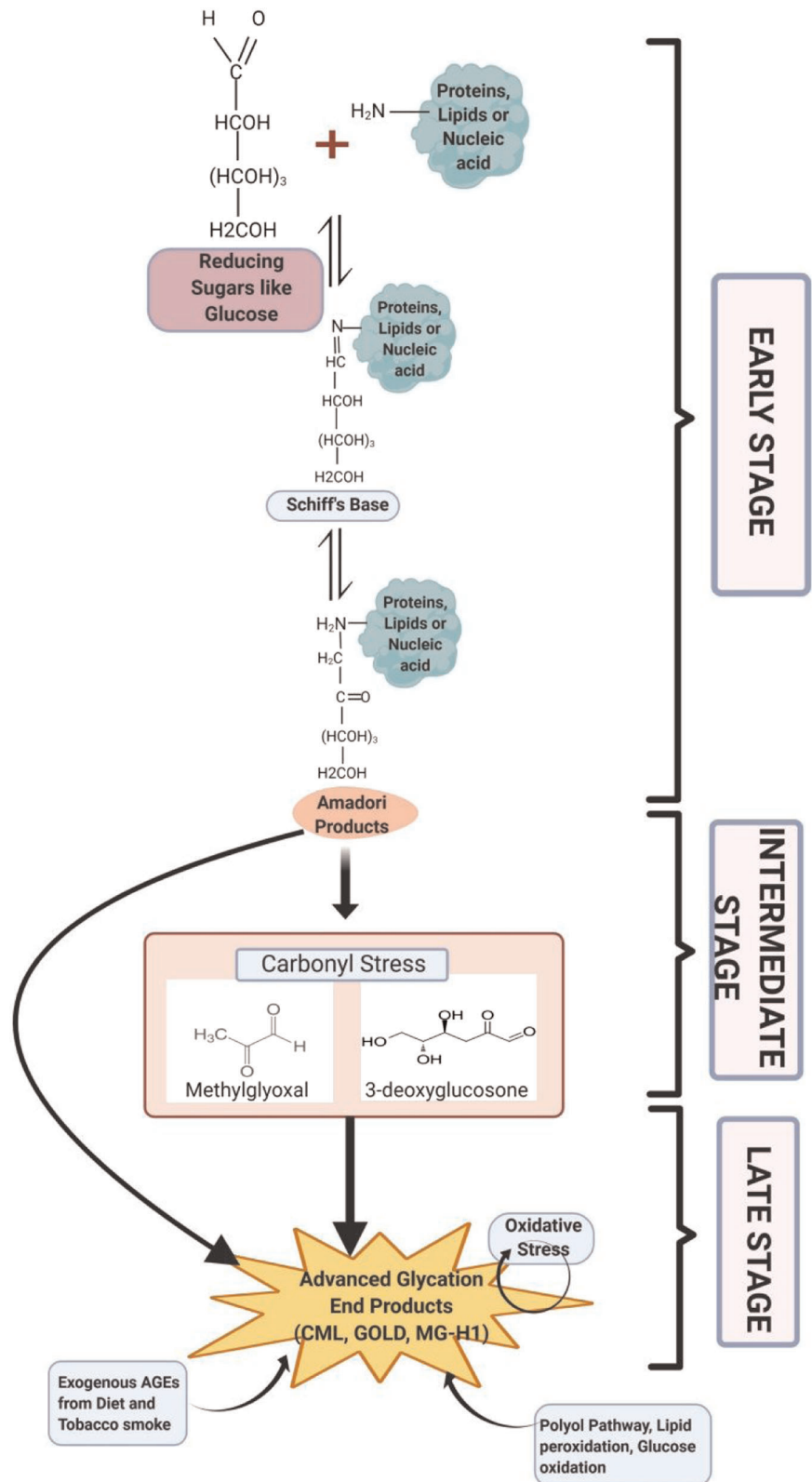
## 3 | EXOGENOUS AGES SOURCES

### 3.1 | Tobacco

Tobacco smokers have higher levels of AGEs and related molecules in the tissues like lenses and blood vessels compared to nonsmokers, irrespective of diabetes.<sup>[16]</sup> Aqueous extracts of tobacco and tobacco smoke are sources of toxic reactive glycation products that rapidly react with proteins and form AGEs.<sup>[6,17]</sup> Cigarette smokers are found to have significantly higher serum-AGEs compared to nonsmokers.<sup>[18]</sup>

There is only a little information regarding the source of AGEs in smokers. Cigarette based toxic reactive glycation products, also known as glycotoxins, reach lung alveoli and then transferred to lung parenchymal cells or bloodstream, where they react with the

**FIGURE 1** AGEs formation. Proteins, lipids, or nucleic acid are glycated by reducing sugars. The process involves three stages, early, intermediate, and late stage. The nonenzymatic reaction starts with the formation of unstable Schiff's base followed by Amadori products and at last the irreversible AGEs. Oxidative stress and AGEs follows a vicious cycle in the formation of AGEs. Even diet, tobacco smoke, and various endogenous pathways like the polyol pathway also contribute to the AGEs pool. AGEs, advanced glycation end products



vascular wall proteins or the proteins in the serum. In the lung parenchymal cells, glycotoxins could also react with the nucleic acid to induce mutation.<sup>[19]</sup> Another study reported that in contrast to AGEs formed from other sources like glucose, which takes

a span of days to weeks to induce AGEs formation, glycotoxins in tobacco take only hours to induce AGEs formation.<sup>[16]</sup> They also indicated the accumulation of AGEs on plasma LDL and the lens proteins of the eye.<sup>[16]</sup>

## 3.2 | Food

The existence of AGEs in food is one of the most focused areas of investigation as it contributes to a noticeable amount of AGEs in the body. Attracting flavors, smell, and texture of processed food are the contributions of AGEs formed in them. Even uncooked animal-derived foods contain a certain amount of AGEs, which increases with further processing like roasting, frying, and grilling.<sup>[20,21]</sup> N $\epsilon$ -carboxymethyl lysine (CML), pentosidine, methylglyoxal-lysine dimers (MOLD), and pyrrolidine are commonly found AGEs in food.<sup>[22]</sup> These are only a few; there are many other AGEs molecules to be identified in our diet. So the need for proper databases to analyze these molecules in food is still a greater field for investigation. The absorption of AGEs to our body can be carried out by simple diffusion or by peptide transporters like PEPT1.<sup>[23–25]</sup> Only about 10% of ingested AGEs are absorbed and distributed to the tissues,<sup>[26,27]</sup> and over 70% of AGEs escape absorption as AGEs crosslinks resist enzymatic or acid hydrolysis.<sup>[28]</sup> About 60% of the absorbed AGEs were found in the liver, kidney, lungs, heart, and spleen showing the global distribution of these compounds.<sup>[27]</sup> One-third of the absorbed AGEs are excreted by the kidneys.<sup>[26]</sup> Cooking conditions with higher heat and lower moisture levels have shown higher levels of AGEs, while food prepared with the addition of acidic solutions like lemon juice or vinegar along with more moisture under low temperature contains comparatively less amount of AGEs.<sup>[5]</sup>

## 3.3 | Pathophysiological effects of AGEs

AGEs may elicit their response through the following pathways:

- Glycating agents can glycate proteins, including enzymes, and alter or dismiss their function.<sup>[29]</sup>
- Glycated proteins can form crosslinks with other proteins resulting in the stiffening of otherwise flexible or elastic tissues.<sup>[30]</sup>
- Glycated proteins can act as ligands and activate specific cell membrane receptors (e.g., RAGE) and eventuate cellular responses.<sup>[31]</sup>

## 3.4 | Major proteins associated with glycation in the living system

### 3.4.1 | Insulin

Insulin is a peptide hormone comprising two polypeptide chains A (21 amino acid residues) and B (30 amino acid residues). Insulin regulates blood glucose concentration by stimulating glucose uptake by muscles and adipose tissue (AT) and inhibits hepatic gluconeogenesis, and stimulates glycogen synthesis in the liver.<sup>[32]</sup> Any disparity in insulin structure or concentrations will lead to its dysfunction. Being a peptide hormone with 51 amino acids, insulin

can also undergo glycation at NH<sub>2</sub>-terminal Phe1 of the B chain.<sup>[33]</sup> Glycated insulin loses its ability to manage blood glucose levels.<sup>[34]</sup> It is reported that lipogenesis and glucose oxidation get impaired as a consequence of glycation of insulin.<sup>[34]</sup> Ultimately, this leads to the development of type 2 diabetes mellitus (T2DM) and associated pathophysiology, including CVDs. It has been demonstrated that there is a significant increase in the concentration of circulating glycated insulin in subjects with poorly controlled diabetes.<sup>[35]</sup> Diglycated insulin was less effective than normal insulin in stimulating glucose uptake and glycogenesis.<sup>[33]</sup> About 10% glycation of insulin is reported to occur in the islets of Langerhans, and unlike other protein glycation, insulin glycation takes place within hours rather than weeks,<sup>[33]</sup> and this glycated insulin is stored and secreted by  $\beta$ -cells.<sup>[36]</sup> These findings also point out the relationship between  $\beta$ -cells dysfunction and glucotoxicity, leading to insulin resistance in T2DM. The evaluation of the pronounced nature of glycated insulin can lead us to a new therapeutic avenue. Glycated insulin is reported as cytotoxic to HUVEC cells and astrocytes. It also induces reactive oxygen species (ROS) production and cell apoptosis and could increase the permeability of the blood–brain barrier models that could cause neurodegenerative diseases.<sup>[37]</sup> During the hyperglycemic condition, insulin glycation could worsen the toxicity of human islet amyloid polypeptide (IAPP) aggregates, which eventually results in  $\beta$  cell death leading to progression in diabetic conditions, thus revealing a vicious cycle in T2DM.<sup>[38]</sup>

### 3.4.2 | Hemoglobin (Hb)

Hb is an iron-containing protein found in red blood cells that gives blood its red color. The primary function of Hb is to carry oxygen to the whole body and to carry carbon dioxide from tissues to the lungs. Hb contains two  $\alpha$  globin chains with 141 amino acid residues each and two  $\beta$  globin chains with 146 residues each. The first endogenous glycated protein discovered was glycated hemoglobin (HbA<sub>1c</sub>) during routine screening of Hb variants.<sup>[39]</sup> The discovery of HbA<sub>1c</sub> was an eye-opening event for the researchers giving a hint on the presence of endogenous Maillard reactions, giving a wide area of scope in the field of research about the endogenous formation of AGEs/advanced lipoxidation end products (ALEs) and their relation to diabetic complications.<sup>[39]</sup> HbA<sub>1c</sub> is glycated with a molecule of glucose attached to the N-terminus valine of the  $\beta$  chain of Hb.<sup>[40]</sup> HbA<sub>1c</sub> later came up as an important biomarker for the long-term control of diabetes.<sup>[41]</sup> The concentration of Hb is correlated with the average blood glucose concentration within the preceding three months. According to the American Diabetes Association, the value for HbA<sub>1c</sub> in diabetics should be below 7%. Studies show that there are about 18% chances of developing myocardial infarction<sup>[42]</sup> with increased HbA<sub>1c</sub> above 7%. Another study revealed that enhanced levels of glycosylated hemoglobin (HbA<sub>1c</sub>), microalbuminuria (24 h microalbuminuria), and serum cystatin C levels in pregnant women with gestational diabetes mellitus could exhibit the chance of high-risk pregnancies.<sup>[43]</sup>

### 3.4.3 | Albumin

Albumin is the most abundant protein in the plasma and known to have multiple functions like regulating blood pH, osmotic pressure, binds free radicals, and transports solutes like hormones and even drugs. It has a molecular weight of 66.7 kDa and comprises 585 amino acids, which include 24 arginines and 59 lysine residues, making the protein a potential target for glycation.<sup>[44]</sup> The predominant sites for glucose attachment are lys-525, lys-439, lys-281, and lys-199.<sup>[45]</sup> Several studies have shown the detrimental effects of glycation on the functions of the protein. For example, the involvement of glycated albumin in different metabolic diseases like nephropathy,<sup>[46,47]</sup> retinopathy,<sup>[48]</sup> and platelet aggregation<sup>[49]</sup> has been recorded. The effect of glycated albumin on glucose metabolism in diabetic complications is also a recent research interest. Glycated albumin interacts with RAGE and affects cellular metabolism through oxidative stress and a series of activation of signaling molecules, including p21ras and mitogen-activated protein (MAP) kinase, resulting in extracellular signal-regulated kinase (ERK) phosphorylation and consequently leads to the pathophysiological effects of glycation.<sup>[50]</sup> Some recent findings suggest glycated albumin better to HbA<sub>1c</sub> as a glycemic indicator in patients undergoing hemodialysis with diabetes.<sup>[51]</sup> It has also been suggested as an early predictor for diabetic nephropathy (DN).<sup>[52,53]</sup> Exploring more about the significance of glycated albumin and its role in pathogenesis would be worth the effort.

### 3.4.4 | Collagen

Collagen is a triple-helical structural protein found in the extracellular matrix. The presence of numerous residues of lysine, arginine, and hydroxylysine in collagen makes it more prone to glycation and crosslink formation.<sup>[54]</sup> AGEs-based crosslink formation in the proteins leads to changes in the physicochemical characteristics of the tissues, and mostly this results in the stiffness of the tissues.<sup>[55]</sup> Myocardial and arterial stiffness is the most worrying problem in the cardiovascular system and is believed to have an important role of AGEs crosslinking or glycation of long-lived proteins like elastin and collagen.<sup>[56]</sup> Adhesion to glycated collagen has been implicated in the activation of the transforming growth factor- $\beta$ 2 (TGF- $\beta$ 2) regulated signaling pathway, which in turn stimulates mothers against decapentaplegic homolog 3 (Smad3) dependent expression of  $\alpha$ 11 integrin, which are involved in fibroblast formation and tumor stiffening.<sup>[57,58]</sup> Soluble AGEs have direct involvement in the crosslinking of collagen.<sup>[59]</sup> The involvement of the crosslinking of collagen fibrils in diabetic complications and CVDs is marked. Collagen is omnipresent, and collagen modification critically affects tissues like the retina, skin, tendons, and ligaments, mostly by losing their elasticity.

### 3.5 | AGEs induced cellular response

AGEs may elicit their response through many intracellular signaling pathways like JAK/STAT, nuclear factor  $\kappa$ -light-chain-enhancer of

activated B cells (NF- $\kappa$ B), PI-3K/Akt, and MAPK/ERK pathways. These signaling pathways trigger the activation of various transcription factors that are responsible for the pathophysiological effects of AGEs. Activation of PI-3K/Akt and MAPK/ERK signaling responses lead to the activation of NF- $\kappa$ B, thereby leading to ROS generation, inflammation, and apoptosis.<sup>[60]</sup> JAK/STAT pathway is implicated in various autoimmune diseases and cell proliferation.<sup>[61]</sup> All these cellular effects are mainly controlled by RAGE activation.

### 3.6 | Receptors for advanced glycation end products

The RAGE is a multiligand receptor belonging to the immunoglobulin superfamily. RAGE can recognize a diverse range of ligands that lack sequence similarity and, thus, is considered as a pattern-recognition receptor.<sup>[62]</sup> RAGE is a protein consisting of 404 amino acid residues with a molecular weight of about 55kDa.<sup>[63]</sup> It is predicted to have one V (variable) and two C (constant) type Ig domains as extracellular domains, followed by a transmembrane spanning domain and a short cytoplasmic domain with <50 amino acid residues.<sup>[64]</sup>

RAGE is widely expressed in all tissues, including lungs, heart, liver, skeletal muscle, and kidney.<sup>[65]</sup> Basal expression of RAGE is low in most of the tissues except in the lungs, where it is expressed more strongly, especially in alveolar epithelial cells.<sup>[66]</sup> It has also been reported to be expressed in innate and adaptive immune cells.<sup>[67,68]</sup>

Many isoforms of RAGE have been widely reported (Figure 2):

#### 1) Full-length RAGE:

Full-length RAGE consists of three extracellular domains (variable domain, C1 domain, and C2 domain) followed by a

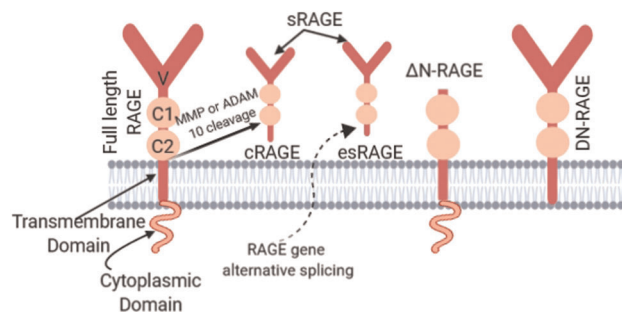


**FIGURE 2** Isoforms of RAGE. The full-length RAGE (with the extracellular domain, transmembrane domain, and cytoplasmic domain) is involved in signal transduction. There are two forms of soluble RAGE: esRAGE (the splice variant of full-length RAGE) and cRAGE (the full-length RAGE cleaved by extracellular proteases). The soluble RAGE only consists of the extracellular domain.  $\Delta$ N RAGE is deficient in the V domain for ligand binding, and DN-RAGE lacks the cytoplasmic domain, both incapable of signal transduction. Created with BioRender.com. cRAGE, cleaved receptors for advanced glycation end products; DN-RAGE, dominant-negative receptors for advanced glycation end products; esRAGE, endogenous secretory receptors for advanced glycation end products; RAGE, receptors for advanced glycation end products

transmembrane and an intracellular or cytoplasmic domain for signal transduction.<sup>[69,70]</sup>

## 2) Soluble forms of RAGE:

Soluble RAGE (sRAGE) are forms of RAGE in circulation, and these serve as a decoy for RAGE ligands. These lack transmembrane and cytoplasmic domains, thus preventing ligand binding and signal transduction that might have led to cellular damage. Two forms of sRAGE are:

- Endogenous secretory RAGE (esRAGE): one of the spliced variants that have been reported. esRAGE is formed from alternative splicing of pre-mRNA,<sup>[71]</sup> and
- Cleaved RAGE (cRAGE): Metalloproteases like matrix metalloproteinase 9 (MMP-9) and a disintegrin and metalloproteinase 10 (ADAM 10) can cleave the extracellular domain of RAGE, which results in cRAGE.<sup>[72]</sup>

## 3) Dominant-negative RAGE (DN-RAGE):

It is another form of RAGE reported that lacks intracellular domain and thus cannot get involved in signal transduction.<sup>[73]</sup>

## 4) $\Delta$ N RAGE:

It lacks the V domain, making it impaired with ligand binding.<sup>[73]</sup>

## 3.7 | Activation of RAGE by AGEs

AGEs are only one ligand among the vast array of ligands that bind RAGE and activate a cascade of cellular signaling. All these ligands bear structural similarities with multiple  $\beta$  sheets that make RAGE identify them.<sup>[74-76]</sup> AGEs-RAGE signaling cascades have been implicated in many diseases. Particularly, diabetes and its associated complications are highly influenced by AGEs-RAGE signaling<sup>[77]</sup> (Figure 3). AGEs-RAGE interaction signals the upregulation of vascular endothelial growth factor (VEGF)<sup>[78]</sup> and tumor necrosis factor- $\alpha$  (TNF- $\alpha$ )<sup>[79]</sup> are known to decline vascular barrier properties and increase permeability in DN.<sup>[80]</sup>

The activated cascade of signals has a direct impact on cellular function and metabolism. The main course of damage is caused by inflammation and oxidative stress. The cell signaling pathway

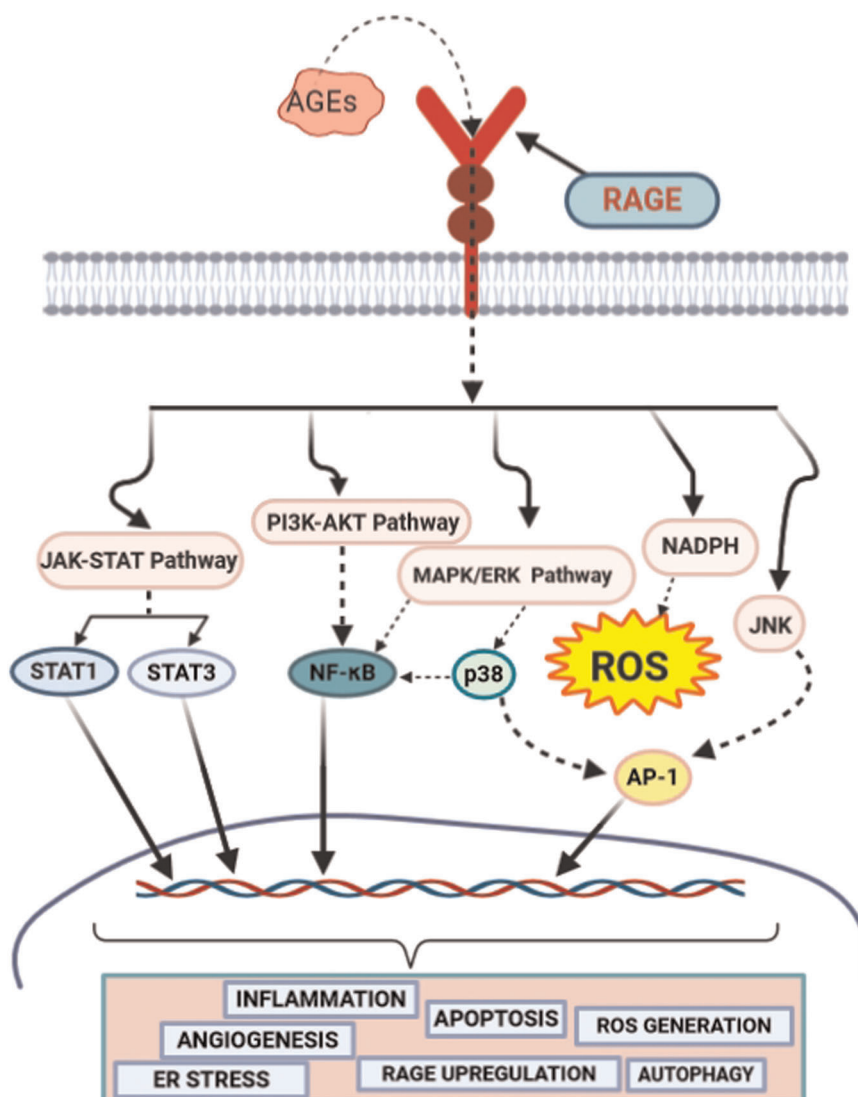


**FIGURE 3** AGEs-RAGE axis signaling. AGEs-RAGE interaction activates different signaling pathways (JAK-STAT, PI3K-AKT, and MAP/ERK pathway) and signaling molecules. Thus, triggering the activation of various transcription factors followed by nuclear translocation and are further responsible for inflammation, upregulation in RAGE expression, autophagy, apoptosis, ER stress, and so forth. Created with BioRender.com. ER, endoplasmic reticulum; ERK, extracellular signal-regulated kinase; JAK, Janus kinase; PI3K, phosphoinositide 3-kinase; RAGE, receptors for advanced glycation end products; STAT, signal transducer and activator of transcription

activated upon RAGE ligand interactions includes the JAK/STAT pathway, MAPK/ERK pathway, Src/RhoA pathway, PI3K/Akt pathway, and activation of PKC and NADPH oxidase.<sup>[81]</sup> Activation of these complex signaling cascades functions through ROS production and activation of transcription factors, mainly NF- $\kappa$ B, AP-1, and Egr-1.<sup>[81]</sup> Activation of NF- $\kappa$ B stimulates the expression and secretion of various inflammatory response molecules like cyclooxygenase-2 (COX-2), interleukin 6 (IL-6), vascular cell adhesion molecule (VCAM), intercellular adhesion molecules (ICAM), and TNF- $\alpha$ , thus regulating AGEs-RAGE mediated inflammatory pathway.<sup>[82]</sup> NF- $\kappa$ B activation also mediates inducible nitric oxide synthase and NADPH oxidase expression leading to the generation of ONOO<sup>-</sup> and oxidative stress.<sup>[12]</sup> AGEs/RAGE axis also contributes to endoplasmic reticulum (ER) stress,<sup>[83]</sup> and NF- $\kappa$ B mediated ROS generation, in turn, impairs mitochondrial function.<sup>[84]</sup> RAGE activation has also been shown to decrease sirtuin 1 (SIRT1) expression, which results in impaired mitochondrial biogenesis.<sup>[85]</sup>

### 3.8 | AGEs and oxidative stress

Oxidative stress can be defined as an imbalance between the origin of free radicals and antioxidants in the defense system. Oxidative stress is a well-recognized player in the pathophysiology of many diseases, including diabetes and cardiovascular disorders. AGEs and oxidative stress have been in a complicated relationship, as generations of both are interlinked. Accumulation of AGEs generates oxidative stress, and the generation of oxidative stress speeds up the generation and accumulation of AGEs. AGEs-RAGE interactions induce a cascade of ROS generation and inflammatory pathways.<sup>[86]</sup> Glycation of enzymes with antioxidant properties are reported to elevate ROS production and cause oxidative damage to cells.<sup>[87]</sup> Antioxidants are known to prevent the activation of NF- $\kappa$ B, TGF- $\beta$ 1, and cell death caused by AGEs induction.<sup>[88]</sup> AGEs formation diminishes the activities of antioxidant enzymes like superoxide dismutase (SOD) and catalases and induces ROS production.<sup>[89]</sup> Overexpression of glyoxalase I (GLO-1) enzyme involved in detoxification of MG had been reported to decrease the levels of GO, MG, and AGEs along with decreasing ROS production in diabetic rats suggesting the correlation between AGEs and oxidative stress.<sup>[90]</sup> Oxidative stress also elevates malondialdehyde (MDA) levels, which can form protein adducts known as ALEs in correspondence to AGEs in rabbit brain.<sup>[91]</sup> AGEs activate Nrf2 dependent antioxidant genes NADPH: quinone oxidoreductase 1 (NQO1) and heme oxygenase-1 (HO-1), providing endogenous protection against oxidative stress in diabetes.<sup>[92]</sup> The complicated relation between AGEs and oxidative stress is yet to be explored for more understanding of the inter-related complications. RAGE activation has been linked with the oxidative liver damage caused by acute systemic injection of lipopolysaccharide.<sup>[93]</sup>

### 3.9 | AGEs, RAGE, and Endoplasmic Reticulum

The ER is the largest membranous organelle in eukaryotic cells. ER serves diverse functions in a cell, like protein synthesis, protein folding and transport, lipid and steroid synthesis, calcium storage, and carbohydrate metabolism. For this, the ER is equipped with unique proteins and enzymes for maintaining a homeostatic environment, which can be disrupted easily by any change in the cellular ambiance resulting in ER stress.<sup>[94]</sup> Any mess in the protein synthesis and folding accumulates misfolded or unfolded protein in the lumen, which activates a series of signaling responses known as unfolded protein response (UPR) to clear this mess. UPR comprises three primary sensors, namely protein kinase RNA-like endoplasmic reticulum kinase (PERK), inositol-requiring enzyme 1 (IRE1), and activating transcription factor 6 (ATF6).<sup>[95]</sup> AGEs, as discussed earlier, being involved in the total disturbance of cellular activities by modifying and inactivating enzymes, proteins, lipids, and nucleic acids, also causes ER stress. Exposure of AGEs to the murine podocytes resulted in apoptosis induced through the ER stress pathway.<sup>[96]</sup> AGEs accumulation leading to the ER stress has also seemed to have roles in hypoxic injuries of kidneys, brain, and heart, pointing out their central role in pathogenesis.<sup>[97,98]</sup> The involvement of AGEs in osteoarthritis has also been linked to ER stress signaling pathways with the activation of RAGE, leading to COX-2 expression and NF- $\kappa$ B pathways in human chondrocytes.<sup>[83]</sup> AGEs precursor, 3-DG, is seen to be involved in ER stress-induced caspase-3 activation independent of RAGE activation in fibroblasts.<sup>[99]</sup> AGEs are reported to be involved in endothelial dysfunction through the apoptosis of endothelial cells via ER stress.<sup>[100]</sup> ER stress generation and autophagy are also seemed to be involved in apoptosis induced by AGEs in mesangial cells.<sup>[101]</sup> AGEs are suggested to play a role in Alzheimer's disease by increasing the amyloid  $\beta$  production and ROS, causing neuronal cell death via ER stress by impairing the neuroprotective ability of Sirt-1.<sup>[102]</sup> Deregulation of calcium homeostasis and initiation of ER stress by an increase in the levels of ER-stress markers like GRP78, ATF4, CHOP, and spliced XBP1 in a time and concentration-dependent manner consequently leads to apoptosis in AGEs treated nucleus pulposus (NP) cells.<sup>[103]</sup> This is clear by all these research that AGEs induced ER stress leads to inflammation and apoptosis, causing severe damage to the tissues in several diseases.

### 3.10 | AGEs, RAGE, and mitochondrial dysfunction

The mitochondria have long been associated with several disorders like Alzheimer's disease, insulin resistance, T2DM, cancer, CVD, infertility, nonalcoholic fatty liver disease (NAFLD), aging, and the list goes on. Many researchers have linked this relation of mitochondria and human disease with mitochondrial dysfunction due to oxidative damage. The mitochondria have been proposed as a crucial source of oxidative stress caused by AGEs.<sup>[104]</sup> AGEs can cause morphological

changes and break cristae and other internal structures via RAGE pathways leading to mitochondrial dysfunction.<sup>[105]</sup> Treatment of  $\beta$  cells with CML-bovine serum albumin (BSA) resulted in increased RAGE expression, depolarization of mitochondrial membrane potential, increased ROS, deletion of mitochondrial DNA, unbalanced mitochondrial dynamics proteins, and decreased ATP content, indicating critical mitochondrial damage that could lead to mitophagy and impaired insulin secretion.<sup>[106]</sup> AGEs treatment of cardiomyocytes resulted in ceramide accumulation and reduced mitochondrial respiration, unraveling the linkage between AGEs, mitochondria, and CVDs.<sup>[107]</sup> HUVECs exhibited energy deficiencies due to decreased mitochondrial respiration and glycolysis when treated with AGEs, which lead to the inhibition of viability and proliferation.<sup>[108]</sup> AGEs treatment also induces apoptosis of osteoblasts, which are linked to the mitochondrial abnormalities through the RAGE pathway.<sup>[109]</sup> Mitochondrial glycation and its consequences ahead are yet to be unraveled for a better understanding of mitochondrial dysfunction and its relation to metabolic diseases.

### 3.11 | AGEs and inflammation

A growing body of evidence suggests that inflammation plays a central role in almost all diseases like diabetes, CVD, cancer, inflammatory bowel diseases, and so forth. And as a result of AGEs accumulation, oxidative stress and inflammation go hand in hand in a vicious cycle.<sup>[110]</sup> As discussed earlier, the interaction of AGEs with RAGE activates several cellular signaling cascades, including inflammation.<sup>[82]</sup> Sterile inflammation or pathogen-free inflammation during aging-related pathologies is mediated by danger associated molecular patterns or DAMPs.<sup>[111]</sup> DAMPs can interact with specific receptors such as RAGE to induce sterile inflammation,<sup>[112]</sup> and AGEs is a sterile danger ligand that can interact with RAGE to induce sterile inflammatory responses.<sup>[113]</sup>

NF- $\kappa$ B acts as the master transcriptional regulator in activating numerous proteins downstream to the AGEs-RAGE axis.<sup>[114]</sup> Activation of NF- $\kappa$ B turns on the secretion of several proinflammatory factors like IL-6, IL-1 $\beta$ , and TNF- $\alpha$ .<sup>[115]</sup> In AGEs-induced HUVECS, the expression of ICAM-1 and VCAM-1 increases along with other proinflammatory cytokines such as IL-6, IL-1 $\beta$ , and TNF- $\alpha$ , indicating the role of AGEs induced inflammatory vascular endothelial dysfunction.<sup>[116]</sup> Streptozotocin-induced diabetic mice on high-AGEs diet exhibited increased serum levels of TNF- $\alpha$  and IL-6 along with significant injury to organs like kidney and heart.<sup>[117]</sup>

### 3.12 | AGEs and heart diseases

AGEs induced collagen crosslinking has always been a matter of concern as it leads to diastolic dysfunction.<sup>[118]</sup> AGEs disrupt cardiomyocytes' relaxation and contracting properties due to the crosslinking of intracellular proteins like sarco-endoplasmic reticulum Ca<sup>2+</sup>-ATPase pump and ryanodine receptor.<sup>[119]</sup> Even reduced LDL uptake due to

the glycation of apolipoprotein B100 is implicated in atherosclerosis.<sup>[120,121]</sup> AGEs/RAGE axis in endothelial cells activate various pathways with detrimental effects like ER stress, inflammation, and oxidative stress, which results in the cytoskeletal rearrangement in cells leading to their enhanced permeability.<sup>[122]</sup> Similarly, AGEs/RAGE signaling in vascular smooth muscle cells (VSMCs) activates MMP-2/9, inflammatory cytokines, and ER stress pathways resulting in proliferation and extracellular matrix degradation, along with impaired autophagy and lysosomal degradation.<sup>[122]</sup>

### 3.13 | AGEs and liver diseases

Several studies demonstrated the involvement of AGEs in liver diseases like fibrosis, cirrhosis, and NASH. In mice fed with high AGEs and a high-fat diet implicated the development of NAFLD with inflammation in the liver.<sup>[123,124]</sup> Elevation in an expression of four hub genes (Cidea, Cidec, Fabp4, and Plin4) involved in the progression of NAFLD was noted in mice on high AGEs diet.<sup>[124]</sup> Increased expression of RAGE pointed out the involvement of the AGEs/RAGE axis in liver injury and inflammation in NAFLD, suggesting AGEs/RAGE pathway as a therapeutic strategy to be considered.<sup>[124]</sup> Several studies implicated the increased concentration of CML in the samples collected from patients with liver diseases, fibrosis, and cirrhosis.<sup>[125]</sup> The involvement of autophagy in hepatic stellate cell activation, which is involved in liver fibrosis through the AGEs/RAGE axis, has also been demonstrated in chronic hepatitis C patients.<sup>[126]</sup> Even involvement of the AGEs/RAGE axis in hepatocellular carcinoma (HCC) has extensively gained attention. The role of RAGE in HCC progression at different levels of proliferation,<sup>[127]</sup> invasion,<sup>[128]</sup> and angiogenesis have attracted intensive interest in the field.

### 3.14 | AGEs and kidney diseases

Renal proximal tubule cells play a major role in AGEs metabolism by absorbing AGEs from glomerular filtrate and catabolizing them.<sup>[129]</sup> These AGEs can interact with RAGE at the cellular surface of proximal tubular epithelial cells (PTECs) and activate a cascade of intracellular signaling pathways.<sup>[130]</sup> AGE/RAGE axis induces ER stress-dependent p21 signaling, leading to premature senescence of PTECs.<sup>[131]</sup> Dicarboxyl stress caused by the formation and accumulation of MG, and its reduced detoxification by GLO-1, during diabetes results in the development of DN.<sup>[132]</sup> In mature podocytes, AGEs activate Notch 1 signaling, which could lead to proteinuria or glomerular disease.<sup>[133]</sup>

### 3.15 | Significance of autophagy in glycation

#### 3.15.1 | Autophagy in general

Autophagy is a self-eating mechanism supported by cellular responses against physiological and pathological stress. It is an

evolutionarily conserved mechanism found in most eukaryotes. It functions as a housekeeping mechanism in normal cells at a basal rate to maintain homeostasis.<sup>[134]</sup> The process includes the digestion or degradation of damaged cellular components, including proteins and cell organelles.<sup>[135]</sup> Autophagy commences to reuse and recycle intracellular energy and protein. It is mostly activated during starvation as a self-preservation process.<sup>[136]</sup> Besides all these positive roles at the basal rate, if left unchecked, autophagy can result in cannibalistic cell death.<sup>[137]</sup> However, autophagy plays an impressive role in cell survival during a broad range of stresses and also in development and differentiation.

### 3.15.2 | Types of autophagy

Autophagy is mainly described in three different forms. These three forms are primarily defined based on the mechanism of the target delivery to the lysosomes.

- Macroautophagy,
- Chaperone mediated autophagy (CMA), and
- Microautophagy.

Macroautophagy (referred to as autophagy in this review) starts with the formation of a double-membrane vesicle known as autophagosomes around the target substrates like damaged proteins and organelles. These autophagosomes then fuse with lysosomes and form autophagolysosomes.

### 3.16 | Selective macroautophagy

Macroautophagy can be highly selective. The cytoplasmic components and organelles are targeted by autophagosomes selectively based on specific molecular markers or specific receptor proteins like ubiquitin and LC-3 interacting regions (LIR; Table 1). Selective autophagy includes mitophagy for mitochondria, ribophagy for ribosomes, and xenophagy for bacteria.

Whereas, CMA includes chaperons, mainly heat shock cognate protein (HSC70), to mediate the transport of the protein to the lysosome. HSC70 recognizes the target proteins by the presence of a specific sequence KFERQ, which is presented to the lysosome membrane specific domain lysosome-associated membrane protein type 2A (LAMP 2A). LAMP 2A acts like a receptor on the lysosomal membrane and mediates internalization by multimerization and degradation of target protein.<sup>[142]</sup> Another type of autophagy described with the discovery of LAMP 2C (RDA receptor) binds RNA and DNA, leading to RN/DN autophagy.<sup>[143,144]</sup> Systemic RNA interference deficient-1 (SIDT2) is another RDA receptor that transports RNA to lysosomes.<sup>[145]</sup> However, several discrepancies are there in the research of SIDT2, so it needs to be explored more.<sup>[146]</sup> In microautophagy, lysosomal membranes invaginate and engulf the cytosolic target substrates for degradation.<sup>[147]</sup>

### 3.17 | Autophagy machinery

The autophagy machinery of mammals is understood based on the identification of almost 30 autophagy-related (ATG) genes in yeasts. The base of the mechanism is conserved as many of the mammalian counterparts of yeast ATG are identified.<sup>[148]</sup>

### 3.18 | Autophagosomes formation

A small cup-shaped structure, phagophore, acts as the origin of autophagosome precursor or pre-autophagosomal structural (PAS). Autophagosome formation is initiated by the inhibition of the mechanistic target of rapamycin complex 1 (mTORC1). It is inhibited under stress conditions like starvation, ER stress, oxidative stress, and hypoxia, or any infectious pathogen attack. The first step in the initiation is the assembly of the unc-51 like autophagy activating kinase (ULK1) complex, which includes ULK1, Atg13, FIP200, and Atg101, at phagophore. ULK1 is inhibited by mTORC1 at a well-fed state; thus, inhibition of mTORC1 activates the ULK1 complex. Autophagosome formation is controlled and coordinated by acetylation and protein phosphorylation. ULK1, once activated, phosphorylates and activates beclin 1. After initiation comes the nucleation process, where another complex comprises several proteins, including Beclin1, gets activated. The complex is called the Beclin1/Class III phosphatidylinositol-3-kinase (PI3K) complex. The complex includes proteins like Beclin1, B-cell leukemia/lymphoma-2 (BCL-2), ambra1, Atg14, UV-irradiation resistance-associated tumor suppressor gene (UVRAG), endophilin B1, Vps15, PI3K, and vacuolar protein sorting 34 (Vps34). Beclin 1 complex activates PI3K and converts phosphoinositol diphosphate (PIP2) to phosphoinositol triphosphate (PIP3) (Figure 4). PIP3 recruits WD repeat domain phosphoinositide-interacting protein (WIPI proteins) to the preautosomal membrane. Along with WIPI comes p62 (ubiquitin cargo binding protein) and NBR1, which acts as a receptor for selective target substrates. Next is the elongation of the membrane, and it is coordinated by microtubule-associated protein 1A/1B-light chain 3 (LC3) proteins and the Atg5-Atg12-Atg16L1 complex that helps in the conjugation of phosphatidylethanolamine for the translocation of LC3-II for elongation to form a mature autophagosome. LC3 conjugation system includes the conversion of LC3 protein to LC3-I, which is again converted to LC3-II, the key players involved in the conjugation system are Atg4, Atg3, Atg7, and Atg10.

### 3.19 | Autophagosome fusion with the lysosome

Once the autophagosome is formed, it fuses to the lysosome to form the autophagolysosome. Autophagosome maturation is regulated by lysosomal membrane proteins (LAMP2) and endosomal marker protein Rab-7 and SNARE proteins.<sup>[149,150]</sup> Small GTPases like RAB7A, RAB2A, ARL84A/B are responsible for controlling autophagosome-lysosome fusion, adaptors, and tethering proteins

**TABLE 1** Receptors for selective autophagy

Selective autophagy type	Receptors	Protein recognized	Reference
Aggrephagy	SQSTM1/p62	Ubiquitin	[138]
	Optineurin		[139]
	NDP52		
	NBR1		[138]
	TOLLIP		[139]
ER-phagy/ reticulophagy	BNIP3	ER membrane	[139]
	FAM134B		
	RTN3		
	SEC62		
	ATL3		
	CCPG1		
Ferritinophagy	NCOA4	Ferritin	[139]
Glycophagy	STBD1	Glycogen	[139]
Lipophagy	ATGL	LC3	[140]
	HSL		
Mitophagy	SQSTM1/p62	Ubiquitin	[138]
	Optineurin	Ubiquitin	[138]
	NDP52	Ubiquitin/ galectin-8	[139]
	TAX1BP1	Ubiquitin	
	NBR1	Ubiquitin	
	TOLLIP	Ubiquitin	
	BNIP3	OMM	[139]
	BNIP3L (NIX)	OMM	[138]
	FUNDC1	OMM	[139]
	BCL-L-13		
	FKBP8		
	NIPSNAP1/2		
	Prohibitin 2	IMM	
Nucleophagy	LaminB1	Lamin-associated domains, nuclear LC3	[141]
	Lamin A/C	UBC9, nuclear LC3	
Pexophagy	SQSTM1/p62	Ubiquitin	[138]
	NBR1		
	PEX14	Peroxisomal membrane, TNKS/TNKS2- ATG9A complex	[141]
Ribophagy	NUFIP1	60S ribosomal subunit	[139]

**TABLE 1** (Continued)

Selective autophagy type	Receptors	Protein recognized	Reference
Xenophagy	SQSTM1/p62	Ubiquitin	[138]
	Optineurin		
	NDP52		[139]
	TAX1BP1V		

(HOPS, EPG-5, ATG14L, TECPR1, GRASP55, BRUCE, RUFY4) tie up autophagosomes to lysosomes. The fusion between autophagosomes with lysosomes is accomplished by SNARE proteins.<sup>[151]</sup> Once fused, the contents in autophagolysosomes get degraded by lysosomal enzymes into amino acids, lipids, or nucleotides and are translocated to the cytoplasm through permeases. These products of degradation are used up for various anabolic reactions by the cell for its sustainability in the stressful condition.<sup>[152]</sup>

### 3.20 | Autophagy in diabetes

#### 3.20.1 | Autophagy in pancreatic $\beta$ -cells

Autophagy is a critically important pathway in normal metabolic functions and survival of insulin-producing  $\beta$ -cells, including insulin homeostasis. Impairment of autophagy in  $\beta$ -cells results in the increased apoptosis and decreased insulin secretion.<sup>[153]</sup> A decrease in proliferation and insulin secretion along with increased apoptosis resulting in reduced  $\beta$ -cells mass was also reported in atg7 knockout mice.<sup>[154]</sup> Atg7 knockout mice also implicated the presence of big inclusion bodies with ubiquitin and overexpressed p62.<sup>[154]</sup> The involvement of the ER stress UPR pathway and decreased mitophagy has also been critically evaluated in  $\beta$ -cells dysfunction.<sup>[155]</sup> ER stress-mediated islets amyloid polypeptide (IAPP) aggregate accumulation leads to  $\beta$ -cells death. IAPP is cosecreted with insulin and plays a critical role in maintaining blood glucose levels, satiation, and body weight. Amyloidogenicity of IAPP has been reported as a reason for  $\beta$ -cells dysfunction during diabetes, and autophagy plays a protective role in the scenario.<sup>[156]</sup>

#### 3.20.2 | Autophagy in skeletal muscle

Skeletal muscle plays a major role in insulin-mediated glucose uptake and, therefore, an important target of insulin resistance in T2D. In skeletal muscle, autophagy is stimulated by exercise, fasting, and atrophies.<sup>[157]</sup> Autophagy deficiency in mice was reported to have impaired GLUT4 expression, less glucose sensitivity/tolerance, and reduced glucose uptake.<sup>[158]</sup> Therefore, impairment in autophagy in skeletal muscle implicates in the progression of insulin resistance in T2D.

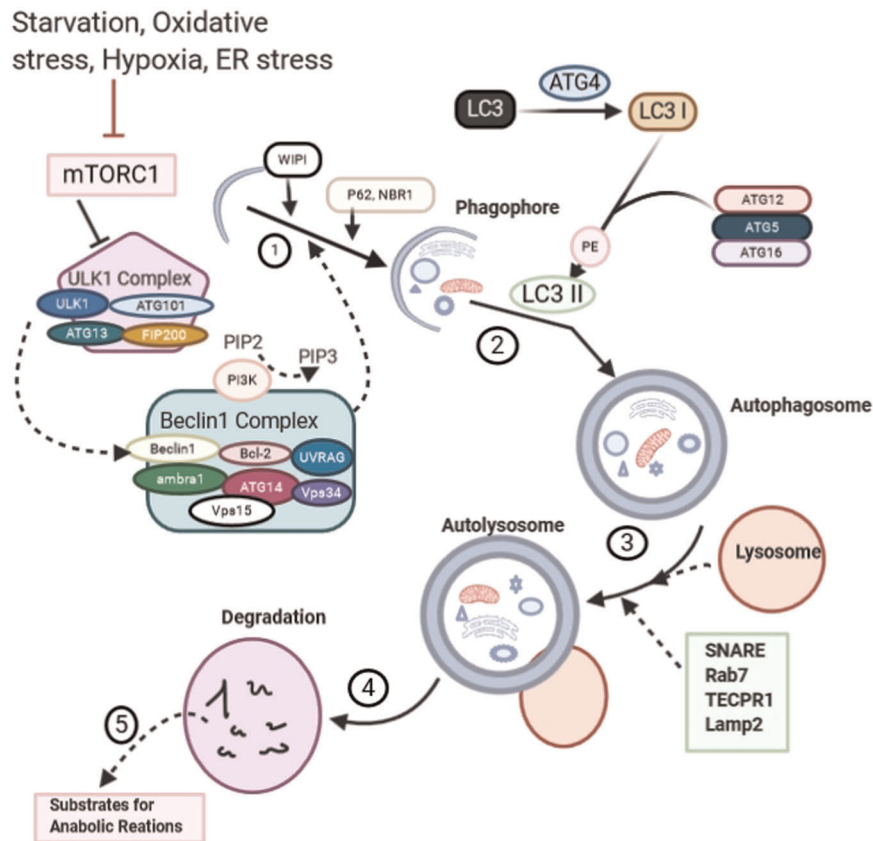


**FIGURE 4** Autophagy signaling transduction. The signaling is initiated by AMPK dependent inhibition of mTORC1, which in turn stimulates ULK1 complex molecules to activate beclin complex molecules, followed by activation of PIP3. (1) Nucleation, PIP3 recruits WIPI and p62 (ubiquitin-binding proteins) and NBR1 proteins to pre autosomal membrane for nucleation of selective substrates. (2) Maturation, where the phagophore expands to form an enclosed structure with the target substrate, is called the autophagosome. (3) Fusion, at this stage, the autophagosome fuses with the lysosome with the help of adaptors and tethering proteins to form an autolysosome. (4) Recycling, this stage involves degradation of the cargo substrates and (5) recycling into metabolites and nutrients. Created with BioRender.com. mTORC1, mechanistic target of rapamycin complex 1; ULK1, unc-51 like autophagy activating kinase; WIPI, WD repeat domain phosphoinositide-interacting protein

### 3.20.3 | Adipose Tissue autophagy

Another major site of insulin-mediated glucose uptake is AT. When compared, autophagy in AT of T2D patients with nondiabetic obese and normal lean individuals, an upregulation of autophagy was observed in T2D.<sup>[159]</sup> Autophagy has been reported to be critically important for the peroxisome proliferator-activated receptor (PPAR- $\gamma$ ) mediated adipocyte differentiation and adipogenesis.<sup>[160]</sup> Atg7 knockout mice were noticed to be lean and had a better metabolic rate with enhanced glucose utilization, insulin sensitivity, and  $\beta$ -oxidation.<sup>[161]</sup>

### 3.20.4 | AGEs and autophagy

Autophagy is an efficient clearance pathway for AGEs, but there is a decline in this pathway with aging.<sup>[162]</sup> Several studies have shown the induction of autophagy in AGEs treated cell lines. However, the area needs to be keenly explored for the facts about its positive or

negative roles. Where autophagy plays as a cytoprotective clearance pathway for the degradation of unwanted or no more wanted cellular components, its hyperactivation could lead to autophagic apoptosis. There are many reports of the protective effects of AGEs induced autophagy, while some reports say that autophagy induced by AGEs is responsible for impaired wound healing in diabetes.<sup>[163]</sup> However, Han et al.<sup>[164]</sup> reviewed the clinical application of autophagy in the clearance of AGEs for diabetic wound healing. However, in diabetic vascular complications, it has been reported that FoXO1 is involved in AGEs induced autophagic apoptosis in endothelial cells.<sup>[165]</sup> AGEs induced autophagy has also been shown to contribute to the pathology of atherosclerosis through ERK and Akt pathway (Figure 5).

Autophagy is suggested to play a protective role against AGEs – induced apoptosis.<sup>[166]</sup> AGEs treatment increases the ratio of LC3B/LC3A in tendon derived stem cells, chondrocytes, and osteoblasts.<sup>[166–168]</sup>

MG based glycative stress involved SIRT1/AMPK signaling pathway mediated ovarian dysfunction in mice via activation of autophagy markers in the ovaries of the polycystic ovarian syndrome.<sup>[169]</sup>

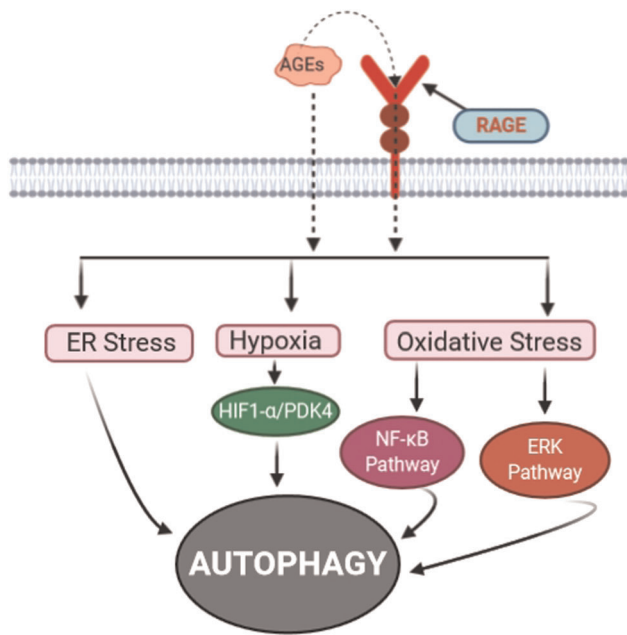


**FIGURE 5** AGEs stimulated Autophagy. AGEs and RAGE axis triggers ER stress, hypoxia, and oxidative stress. These stresses can set in the autophagy signaling transduction pathway. Created with BioRender.com. AGE, advanced glycation end product; ER, endoplasmic reticulum; RAGE, receptors for advanced glycation end products

Another study demonstrated the deleterious effects of MG induced autophagy in the degradation of two cytoprotective proteins, thioredoxin 1 (trx1) and glyoxalase 2 (GLO-2).<sup>[170]</sup> VSMCs calcification induced by AGEs was attenuated through the activation of HIF-1 $\alpha$ /PDK4 induced autophagy pathway.<sup>[171]</sup> However, toxic AGEs in cardiomyocytes suppressed the expression of LC3-II/LC3-I to attenuate the autophagy pathway leading to cell death.<sup>[172]</sup> Mei et al.<sup>[173]</sup> indicated the role of the ROS/ERK pathway in the induction of autophagy in AGEs treated human periodontal ligament cells.

It has also been reported about the involvement of RAF protein kinase and NF- $\kappa$ B in the stimulation of AGEs induced autophagy, indicating the involvement of the RAGE activation pathway.<sup>[174]</sup> The protective role of autophagy in inhibiting kidney aging has also been demonstrated along with the involvement of the RAGE/STAT5 signaling pathway in the inhibition of autophagy in AGEs treated mesangial cells.<sup>[175]</sup> A STAT3 dependent inhibition of autophagy by sRAGE has shown a protective action against ischemia/reperfusion (I/R) injuries in the heart.<sup>[176]</sup> RAGE also plays a critical role in the regulation of autophagy in pancreatic cancer, and inhibition of RAGE along with autophagy alleviated tumor growth and tumorigenesis in mouse models.<sup>[177]</sup> AGEs promote vascular calcification by suppressing autophagy linked with AMPK/mTOR signaling pathway.<sup>[178]</sup> The AGE-RAGE-autophagy axis has also been linked with cancer progression.<sup>[179]</sup>  $\beta$ -Carotene treatment to the H9c2 cells exposed to AGEs reversed the elevation of autophagy, and  $\beta$ -carotene is suggested as a protective measure for AGEs induced cardiac

dysfunction.<sup>[180]</sup> AGEs suppressed autophagic flux in macrophages, thus diminishing the intracellular bactericidal capability during *Staphylococcus aureus* infection.<sup>[181]</sup> Epidermal AGEs have been implicated in the dull appearance of the skin, and activation of autophagy is suggested to be an effective remedy.<sup>[182]</sup> Halofuginone is reported to be protective against AGEs induced damages in H9c2 cells by the succession of autophagy.<sup>[183]</sup>

Inhibition of autophagy in AGEs treated mesangial cells resulted in ROS generation and apoptotic cell death.<sup>[184]</sup> ROS generation and mitochondrial damage induced by AGEs in osteoblasts are shown to activate the autophagy response against apoptosis.<sup>[168]</sup> In podocytes, AGEs inhibited nuclear translocation of TFEB and activated mTOR signaling to inhibit the formation and turnover of autophagosomes.<sup>[185]</sup>

A biphasic effect of autophagy has also been demonstrated in the context of time and concentration of AGEs in human chondrocytes. AGEs were at a low dose for a short period induced autophagy, while the high dose for a prolonged-time period inhibited autophagy.<sup>[186]</sup> AGEs induction increased expression of p62 and the ratio of LC3-II/I in HUVEC.<sup>[187]</sup> Verma and Manna demonstrated the role of p53 in the switching of cellular response between autophagy and apoptosis in different AGEs treated cells.<sup>[188]</sup>

Thus, a clear view about the role of autophagy as a friend or a foe needs thorough understanding and intense research for proficiently targeting this pathway against AGEs and AGEs induced complications during diabetes and aging.

### 3.20.5 | AGEs induced CVDs and autophagy

Several studies have reported the involvement of autophagy in different CVDs like cardiomyopathy, atherosclerosis, I/R, and heart failure.<sup>[189,190]</sup> AGEs-RAGE activation in VSMC induces ROS production, inflammation, ER stress, and hypoxia, all of which lead to cell proliferation and migration, resulting in the development of atherosclerosis lesions.<sup>[191]</sup> In cardiovascular pathophysiology, autophagy may play as a friend or foe under different conditions in different cell lines.<sup>[190]</sup>

Autophagy acts as a friend during ischemia whereas as a foe during the reperfusion process.<sup>[192]</sup> Another study demonstrated the effect of prolonged activation of autophagy in the progression of cardiac hypertrophy to heart failure.<sup>[193]</sup> RAGE/PI3K/Akt/mTOR pathway can activate autophagy in AGEs induced cardiomyocytes.<sup>[194]</sup> The involvement of the RAGE-autophagy axis in heart failure was demonstrated as a novel target for treatment, as RAGE inhibition weakened the autophagic death of cardiomyocytes.<sup>[195]</sup> MG induced autophagic degradation of vascular endothelial growth factor receptor 2 and plays a major role in the impairment of angiogenesis in diabetes.<sup>[196]</sup> Thus, the area needs to be explored more for a better understanding of autophagy as a cytoprotective or cytopathic role in CVDs. And drug development criteria, whether an activation or an inhibition, would differ in accordance to the condition of the patients.

### 3.20.6 | AGEs induced DN and autophagy

Autophagy is suggested to be a novel therapeutic target against DN.<sup>[197]</sup> Aminoguanidine, a well-known antiglycation compound, was reported to restore diabetes-induced modulation in renal lysosomal processing suggested as the initial events of DN.<sup>[198]</sup> Modified lysosomal cathepsin activity results in impairment of tubular cell protein degradation, which leads to the accumulation of abnormal proteins and, hence, diabetic renal hypertrophy.<sup>[199]</sup> AGEs-BSA exposure to HK-2 cells disrupted the autophagy-lysosome pathway via AGE/RAGE interaction and resulted in abnormal protein accumulation.<sup>[190]</sup> Several potential targets against DN have been studied, including the AGEs inhibitor aminoguanidine that unfortunately did not reach the end stage drug development process. However, the prevalence of this serious diabetic complication is increasing worldwide. Therefore, there is an urgent need for novel therapeutic targets against DN, and autophagy is a nice one to be considered.

### 3.21 | Translational significance

As discussed earlier AGEs and their adverse effects indicate their critical involvement in various pathophysiological conditions. The development of a potential antiglycation agent would be effective for the cure of many diseases. Till now there is no drug available in the market and researchers are in search of a potential molecular target against AGEs. The arena of autophagy research is a promising breakthrough. Involvement of autophagy is implicated in various disease models. A better understanding of how autophagy is involved in AGEs induced complications will be a new perspective on diabetes and related diseases. Modulation of autophagy pathways with activators, inhibitors, or gene manipulation could be a useful approach against diseases. The effect of autophagy on different conditions is surprisingly contradictory. Moreover, autophagy and its role in diseases have still not been explored. They are thus widening a new horizon in the field of drug development.

## 4 | CONCLUSION

The purpose of this review is to help the readers understand different adverse effects of AGEs and the link between the AGEs related signaling pathways and autophagy. Autophagy plays a pivotal role in maintaining homeostasis in the cellular environment. Most of the studies in this review suggest the role of autophagy as a protective measure against AGEs induced damage to the cells. It is reasonable to target autophagy as a defensive tool against AGEs and related diabetic complications. It is important for the researchers to understand and critically evaluate the connection between AGEs and autophagy. And intense research is needed to understand the basic biology of AGEs induced autophagy for the development of autophagy based therapies.

## ACKNOWLEDGMENTS

Sruthi C. R. is thankful to the University Grants Commission (UGC, New Delhi) for the financial support to conduct research on the role of Advanced Glycation End Products in the development of metabolic syndrome.

## CONFLICT OF INTERESTS

The authors declare that there are no conflict of interests.

## ORCID

K. G. Raghu  <http://orcid.org/0000-0002-1341-5470>

## REFERENCES

- [1] X. Luo, J. Wu, S. Jing, L. J. Yan, *Aging Dis.* **2016**, 7(1), 90. <https://doi.org/10.14336/AD.2015.0702>
- [2] A. Gugliucci, *Mechanisms Linking Aging, Diseases and Biological Age Estimation*, CRC Press, Boca Raton, FL **2017**, p. 68. <https://doi.org/10.1201/9781315371382-9>
- [3] J. D. Méndez, J. Xie, M. Aguilar-Hernández, V. Méndez-Valenzuela, *Mol. Cell. Biochem.* **2010**, 341(1-2), 33. <https://doi.org/10.1007/s11010-010-0434-5>
- [4] T. H. Fleming, P. M. Humpert, P. P. Nawroth, A. Bierhaus, *Gerontology* **2010**, 57(5), 435. <https://doi.org/10.1159/000322087>
- [5] J. Uribarri, S. Woodruff, S. Goodman, W. Cai, X. Chen, R. Pyzik, A. Yong, G. E. Striker, H. Vlassara, *J. Am. Diet. Assoc.* **2010**, 110(6), 911. <https://doi.org/10.1016/j.jada.2010.03.018>
- [6] C. Cerami, H. Founds, I. Nicholl, T. Mitsushashi, D. Giordano, S. Vanpatten, A. Lee, Y. Al-Abed, H. Vlassara, R. Bucala, A. Cerami, *Proc. Natl. Acad. Sci. U. S. A.* **1997**, 94, 13915.
- [7] W. T. Cade, *Phys. Ther.* **2008**, 88(11), 1322. <https://doi.org/10.2522/ptj.20080008>
- [8] G. Sorci, F. Riuzzi, I. Giambanco, R. Donato, *Biochim. Biophys. Acta.-Mol. Cell. Res.* **2013**, 1833(1), 101. <https://doi.org/10.1016/j.bbamcr.2012.10.021>
- [9] L. C. Maillard, *Compte-Rendu l'Academie des Sci.* **1912**, 154, 66. <https://ci.nii.ac.jp/naid/20000509994>
- [10] E. Hodge, *J. Agric. Food Chem.* **1953**, 46, 2599. <https://ci.nii.ac.jp/naid/10008765425>
- [11] J. Gerrard, *Aust. J. Chem.* **2005**, 58(10), 756. [https://doi.org/10.1071/ch0505\\_br](https://doi.org/10.1071/ch0505_br)
- [12] A. Negre-Salvayre, R. Salvayre, N. Augé, R. Pamplona, M. Portero-Otín, *Antioxid. Redox Signal.* **2009**, 11(12), 3071. <https://doi.org/10.1089/ars.2009.2484>
- [13] A. Lapolla, P. Traldi, D. Fedele, *Clin. Biochem.* **2005**, 38(2), 103. <https://doi.org/10.1016/j.clinbiochem.2004.09.007>
- [14] G. Vistoli, D. De, A. Cipak, N. Zarkovic, M. Carini, G. Aldini, *Free Radic. Res.* **2013**, 47(S1), 3. <https://doi.org/10.3109/10715762.2013.815348>
- [15] M. Lorenzi, *Exp. Diabetes Res.* **2007**, 2007, 61038. <https://doi.org/10.1155/2007/61038>
- [16] I. D. Nicholl, R. Bucala, *Cell Mol. Biol. (Noisy-le-grand)* **1998**, 44(7), 1025. <https://europepmc.org/article/med/9846884>
- [17] I. D. Nicholl, A. W. Stitt, J. E. Moore, A. J. Ritchie, D. B. Archer, R. Bucala, *Mol. Med.* **1998**, 4(9), 594. <https://doi.org/10.1007/bf03401759>
- [18] M. Peppia, J. Uribarri, H. Vlassara, *Cardiovasc. Toxicol.* **2002**, 2, 275. <https://link.springer.com/article/10.1385/CT:2:4:275>
- [19] C. Cerami, H. Founds, I. Nicholl, T. Mitsushashi, D. Giordano, S. Vanpatten, A. Lee, Y. Al-Abed, H. Vlassara, R. Bucala, A. Cerami, *Proc. Natl. Acad. Sci. U. S. A.* **1997**, 94(25), 13915. <https://doi.org/10.1073/pnas.94.25.13915>

- [20] T. Goldberg, W. Cai, M. Peppas, V. Dardaine, B. S. Baliga, J. Uribarri, H. Vlassara, *J. Am. Diet. Assoc.* **2004**, *104*, 1287. <https://doi.org/10.1016/j.jada.2004.05.214>
- [21] J. Uribarri, M. D. del Castillo, M. P. de la Maza, R. Filip, A. Gugliucci, C. Luevano-Contreras, M. H. Macias-Cervantes, D. H. Markowicz Bastos, A. Medrano, T. Menini, M. Portero-Otin, A. Rojas, G. R. Sampaio, K. Wrobel, K. Wrobel, M. E. Garay-Sevilla, *Adv. Nutr.* **2015**, *6*(4), 461. <https://doi.org/10.3945/an.115.008433>
- [22] C. H. Wu, S. M. Huang, J. A. Lin, G. C. Yen, *Food Funct.* **2011**, *2*(5), 224. <https://doi.org/10.1039/c1fo10026b>
- [23] S. Geissler, M. Hellwig, M. Zwarg, F. Markwardt, T. Henle, M. Brandsch, *J. Agric. Food Chem.* **2010**, *58*(4), 2543. <https://doi.org/10.1021/jf903791u>
- [24] M. Hellwig, S. Geissler, A. Peto, I. Knütter, M. Brandsch, T. Henle, *J. Agric. Food Chem.* **2009**, *57*(14), 6474. <https://doi.org/10.1021/jf901224p>
- [25] M. Hellwig, R. Matthes, A. Peto, J. Löbner, T. Henle, *Amino Acids* **2014**, *46*, 289. <https://doi.org/10.1007/s00726-013-1501-5>
- [26] T. Koschinsky, C. J. He, T. Mitsuhashi, R. Bucala, C. Liu, C. Buenting, K. Heitmann, H. Vlassara, *Proc. Natl. Acad. Sci. U. S. A.* **1997**, *94*(12), 6474. <https://doi.org/10.1073/pnas.94.12.6474>
- [27] C. He, J. Sabol, T. Mitsuhashi, H. Vlassara, *Diabetes* **2000**, *48*(6), 1308. <https://doi.org/10.2337/diabetes.48.6.1308>
- [28] J. O'Brien, P. A. Morrissey, *Crit. Rev. Food Sci. Nutr.* **1989**, *28*(3), 211. <https://doi.org/10.1080/10408398909527499>
- [29] P. Ulrich, A. Cerami, *Recent Prog. Horm. Res.* **2001**, *56*, 1.
- [30] T. L. Willett, R. Kandel, J. N. A. De Croos, N. C. Avery, M. D. Grynblas, *Osteoarthritis Cartilage* **2012**, *20*(7), 736. <https://doi.org/10.1016/j.joca.2012.03.012>
- [31] L. J. Sparvero, D. Asafu-Adjei, R. Kang, D. Tang, N. Amin, J. Im, R. Rutledge, B. Lin, A. A. Amoscatto, H. J. Zeh, M. T. Lotze, *J. Transl. Med.* **2009**, *7*(1), 1. <https://doi.org/10.1186/1479-5876-7-17>
- [32] A. R. Saltiel, C. R. Kahn, *Nature* **2001**, *414*(6865), 799. <https://doi.org/10.1038/414799a>
- [33] F. P. M. O'Harte, P. Højrup, C. R. Barnett, P. R. Flatt, *Peptides* **1996**, *17*(8), 1323. [https://doi.org/10.1016/S0196-9781\(96\)00231-8](https://doi.org/10.1016/S0196-9781(96)00231-8)
- [34] S. J. Hunter, A. C. Boyd, F. P. M. O'Harte, A. M. McKillop, M. I. Wiggam, M. H. Mooney, J. T. McCluskey, J. R. Lindsay, C. N. Ennis, R. Gamble, B. Sheridan, C. R. Barnett, H. McNulty, P. M. Bell, P. R. Flatt, *Diabetes* **2003**, *52*(2), 492.
- [35] J. R. Lindsay, A. M. McKillop, M. H. Mooney, F. P. M. O'Harte, P. M. Bell, P. R. Flatt, *Diabetologia* **2003**, *46*(4), 475. <https://doi.org/10.1007/s00125-003-1059-y>
- [36] A. M. McKillop, Y. H. A. Abdel-Wahab, M. H. Mooney, F. P. M. O'Harte, P. R. Flatt, *Diabetes Metab.* **2002**, *28*, 3561. <https://europepmc.org/article/med/12688635>
- [37] L. Shahriyari, G. Riazi, M. R. Lornejad, M. Ghezlou, B. Bigdeli, B. Delavari, F. Mamashli, S. Abbasi, J. Davoodi, A. A. Saboury, *Arch. Biochem. Biophys.* **2018**, *647*, 54. <https://doi.org/10.1016/j.abb.2018.02.004>
- [38] L. Ma, C. Yang, L. Huang, Y. Chen, Y. Li, C. Cheng, B. Cheng, L. Zheng, K. Huang, *ACS Chem. Biol.* **2019**, *14*(3), 486. <https://doi.org/10.1021/acscchembio.8b01128>
- [39] S. Rahbar, *Ann. NY Acad. Sci.* **2005**, *1043*, 9. <https://doi.org/10.1196/annals.1333.002>
- [40] M. Panush Cohen, V. Y. Wu, *Methods Enzymol.* **1994**, *231*(C), 65. [https://doi.org/10.1016/0076-6879\(94\)31007-6](https://doi.org/10.1016/0076-6879(94)31007-6)
- [41] M. Massi-Benedetti, *Curr. Med. Res. Opin.* **2006**, *22*(Suppl. 2), S5. <https://doi.org/10.1185/030079906X112714>
- [42] M. de Jong, M. Woodward, S. A. E. Peters, *Diabetes Care* **2020**, *43*(9), 2050. <https://doi.org/10.2337/dc19-2363>
- [43] H. Jin, *Exp. Ther. Med.* **2019**, *19*(2), 1281. <https://doi.org/10.3892/etm.2019.8336>
- [44] T. P. Peters Jr., *All About Albumin: Biochemistry, Genetics, and Medical Applications*, Academic Press, **1995**.
- [45] N. Iberg, R. Flückiger, *J. Biol. Chem.* **1986**, *261*(29), 13542. <https://www.jbc.org/content/261/29/13542.short>
- [46] M. P. Cohen, N. Masson, E. Hud, F. Ziyadeh, D. C. Han, R. S. Clements, *Exp. Nephrol.* **2000**, *8*(3), 135. <https://doi.org/10.1159/000020661>
- [47] S. Chen, M. P. Cohen, F. N. Ziyadeh, *Kidney Int. Suppl.* **2000**, *58*(77), S40. <https://doi.org/10.1046/j.1523-1755.2000.07707.x>
- [48] N. A. Hasan, *Saudi. Med. J.* **2009**, *30*(10), 1263.
- [49] D. A. Rubenstein, W. Yin, *Platelets* **2009**, *20*(3), 206. <https://doi.org/10.1080/09537100902795492>
- [50] M. P. Cohen, E. Shea, S. Chen, C. W. Shearman, *J. Lab. Clin. Med.* **2003**, *141*(4), 242. <https://doi.org/10.1067/mlc.2003.27>
- [51] T. Yajima, K. Yajima, M. Hayashi, H. Takahashi, K. Yasuda, *Diabetes Res. Clin. Pract.* **2017**, *130*, 148. <https://doi.org/10.1016/j.diabres.2017.05.020>
- [52] J. E. Jun, K. Y. Hur, Y. B. Lee, S. E. Lee, S. M. Jin, M. K. Lee, J. H. Kim, *Diabetes Metab.* **2018**, *44*(2), 178. <https://doi.org/10.1016/j.diabet.2017.08.003>
- [53] N. Wang, Z. Xu, P. Han, T. Li, *Diabetes Metab. Res. Rev.* **2017**, *33*(2), e2843. <https://doi.org/10.1002/dmrr.2843>
- [54] J. S. Flier, L. H. Underhill, M. Brownlee, A. Cerami, H. Vlassara, *N. Engl. J. Med.* **1988**, *318*(20), 1315. <https://doi.org/10.1056/NEJM198805193182007>
- [55] M. J. C. Kent, N. D. Light, A. J. Bailey, *Biochem. J.* **1985**, *225*(3), 745. <https://portlandpress.com/biochemj/article-abstract/225/3/745/19375>
- [56] D. Kitzman, *Eur. Heart J.* **2003**, *24*(5), 408. [https://doi.org/10.1016/s0195-668x\(03\)95162-1](https://doi.org/10.1016/s0195-668x(03)95162-1)
- [57] I. Talior-Volodarsky, P. D. Arora, Y. Wang, C. Zeltz, K. A. Connelly, D. Gullberg, C. A. McCulloch, *J. Cell. Physiol.* **2015**, *230*(2), 327. <https://doi.org/10.1002/jcp.24708>
- [58] R. Navab, D. Strumpf, C. To, E. Pasko, K. S. Kim, C. J. Park, J. Hai, J. Liu, J. Jonkman, M. Barczyk, B. Bandarchi, Y. H. Wang, K. Venkat, E. Ibrahimov, N. A. Pham, C. Ng, N. Radulovich, C. Q. Zhu, M. Pintilie, D. Wang, A. Lu, I. Jurisica, G. C. Walker, D. Gullberg, M. S. Tsao, *Oncogene* **2016**, *35*(15), 1899. <https://doi.org/10.1038/onc.2015.254>
- [59] G. B. Sajithlal, P. Chithra, G. Chandrakasan, *Biochim. Biophys. Acta, Mol. Basis Dis.* **1998**, *1407*(3), 215. [https://doi.org/10.1016/S0925-4439\(98\)00043-X](https://doi.org/10.1016/S0925-4439(98)00043-X)
- [60] A. Perrone, A. Giovino, J. Benny, F. Martinelli, *Oxid. Med. Cell Longev.* **2020**, *2020*, 3818196. <https://doi.org/10.1155/2020/3818196>
- [61] M. Sun, Y. Li, W. Bu, J. Zhao, J. Zhu, L. Gu, P. Zhang, Z. Fang, *Evid. Based Complement Alternat. Med.* **2017**, *2017*, 2942830. <https://doi.org/10.1155/2017/2942830>
- [62] G. Fritz, *Trends Biochem. Sci.* **2011**, *36*(12), 625. <https://doi.org/10.1016/j.tibs.2011.08.008>
- [63] M. Neeper, A. Marie Schmidt, J. Brett, S. D. Yan, F. Wang, Y. C. Pan, K. Elliston, D. Stern, A. Shaw, *J. Biol. Chem.* **1992**, *267*(21), 14998. <https://www.jbc.org/content/267/21/14998.short>
- [64] R. Ramasamy, S. F. Yan, A. M. Schmidt, *Amino Acids* **2012**, *42*(4), 1151. <https://doi.org/10.1007/s00726-010-0773-2>
- [65] J. Brett, A. M. Schmidt, S. D. Yan, Y. S. Zou, E. Weidman, D. Pinsky, R. Nowygrod, M. Neeper, C. Przysocki, A. Shaw, *Am. J. Pathol.* **1993**, *143*(6), 1699. <https://www.ncbi.nlm.nih.gov/pmc/articles/PMC1887265/>
- [66] N. Demling, C. Ehrhardt, M. Kasper, M. Laue, L. Knels, E. P. Rieber, *Cell Tissue Res.* **2006**, *323*(3), 475. <https://doi.org/10.1007/s00441-005-0069-0>
- [67] K. Narumi, R. Miyakawa, R. Ueda, H. Hashimoto, Y. Yamamoto, T. Yoshida, K. Aoki, *J. Immunol.* **2015**, *194*(11), 5539. <https://doi.org/10.4049/jimmunol.1402301>

- [68] A. M. Schmidt, *Arterioscler. Thromb. Vasc. Biol.* **2017**, 37(4), 613. <https://doi.org/10.1161/ATVBAHA.117.307263>
- [69] S. Bongarzone, V. Savickas, F. Luzi, A. D. Gee, *Perspective. ACS Publ.* **2017**, 60(17), 7213. <https://doi.org/10.1021/acs.jmedchem.7b00058>
- [70] L. Yatime, G. R. Andersen, *FEBS J.* **2013**, 280(24), 6556. <https://doi.org/10.1111/febs.12556>
- [71] J. Jules, D. Maiguel, B. I. Hudson, *PLOS One* **2013**, 8(11), e78267. <https://doi.org/10.1371/journal.pone.0078267>
- [72] A. Raucci, S. Cugusi, A. Antonelli, S. M. Barabino, L. Monti, A. Bierhaus, K. Reiss, P. Saftig, M. E. Bianchi, *FASEB J.* **2008**, 22(10), 3716. <https://doi.org/10.1096/fj.08-109033>
- [73] M. I. A. Oliveira, E. M. Souza, F. O. Pedrosa, R. R. Réa, A. S. C. Alves, G. Picheth, F. G. M. Rego, *J. Bras. Patol. e Med. Lab.* **2013**, 49(2), 97. <https://doi.org/10.1590/S1676-24442013000200004>
- [74] R. Ramasamy, S. F. Yan, A. M. Schmidt, *Ann. N. Y. Acad. Sci.* **2011**, 1243(1), 88. <https://doi.org/10.1111/j.1749-6632.2011.06320.x>
- [75] S. F. Yan, R. Ramasamy, A. M. Schmidt, *Circ. Res.* **2010**, 106(5), 842. <https://doi.org/10.1161/CIRCRESAHA.109.212217>
- [76] J. Chaudhuri, Y. Bains, S. Guha, A. Kahn, D. Hall, N. Bose, A. Gugliucci, P. Kapahi, *Cell Metab.* **2018**, 28(3), 337. <https://doi.org/10.1016/j.cmet.2018.08.014>
- [77] A. M. Kay, C. L. Simpson, J. A. Stewart, *J. Diabetes Res.* **2016**, 2016, 1. <https://doi.org/10.1155/2016/6809703>
- [78] S.-I. Yamagishi, H. Yonekura, Y. Yamamoto, K. Katsuno, F. Sato, I. Mita, H. Ooka, N. Satozawa, T. Kawakami, M. Nomura, H. Yamamoto, *J. Biol. Chem.* **1997**, 272(13), 8723. <http://www.jbc.stanford.edu/jbc/>
- [79] T. Miyata, O. Hori, J. Zhang, S. D. Yan, L. Ferran, Y. Iida, A. M. Schmidt, *J. Clin. Invest.* **1996**, 98(5), 1088. <https://doi.org/10.1172/JCI118889>
- [80] D. T. Connolly, *J. Cell. Biochem.* **1991**, 47(3), 219. <https://doi.org/10.1002/jcb.240470306>
- [81] K. Asadipooya, E. M. Uy, *J. Endocr. Soc.* **2019**, 3(10), 1799. <https://doi.org/10.1210/js.2019-00160>
- [82] J. Xie, J. D. Méndez, V. Méndez-Valenzuela, M. M. Aguilar-Hernández, *Cell. Signal.* **2013**, 25(11), 2185. <https://doi.org/10.1016/j.cellsig.2013.06.013>
- [83] Z. Rasheed, T. M. Haqqi, *Biochim. Biophys. Acta, Mol. Cell Res.* **2012**, 1823(12), 2179. <https://doi.org/10.1016/j.bbamcr.2012.08.021>
- [84] Y. Yu, L. Wang, F. Delguste, A. Durand, A. Guilbaud, C. Rousselin, A. M. Schmidt, F. Tessier, E. Boulanger, R. Nevriere, *Free Radic. Biol. Med.* **2017**, 112, 397. <https://doi.org/10.1016/j.freeradbiomed.2017.08.012>
- [85] T. Teissier, É. Boulanger, *Biogerontology* **2019**, 20(3), 279. <https://doi.org/10.1007/s10522-019-09808-3>
- [86] S. J. Yoon, Y. W. Yoon, B. K. Lee, H. M. Kwon, K. C. Hwang, M. Kim, W. Chang, B. K. Hong, Y. H. Lee, S. J. Park, P. K. Min, S. J. Rim, *Exp. Mol. Med.* **2009**, 41(11), 802. <https://doi.org/10.3858/emmm.2009.41.11.086>
- [87] J. Fujii, T. Myint, A. Okado, H. Kaneto, N. Taniguchi, *Nephrol., Dial., Transplant.* **1996**, 11(suppl 5), 34. <https://academic.oup.com/ndt/article/11/suppl5/34/1857001>
- [88] M. A. Lal, H. Brismar, A. C. Eklöf, A. Aperia, *Kidney Int.* **2002**, 61(6), 2006. <https://doi.org/10.1046/j.1523-1755.2002.00367.x>
- [89] J. M. Jiang, Z. Wang, D. D. Li, *Biomed. Environ. Sci.* **2004**, 17(1), 79. <https://europepmc.org/article/med/15202867>
- [90] O. Brouwers, P. M. Niessen, I. Ferreira, T. Miyata, P. G. Scheffer, T. Teerlink, P. Schrauwen, M. Brownlee, C. D. Stehouwer, C. G. Schalkwijk, *J. Biol. Chem.* **2011**, 286(2), P1374. <https://doi.org/10.1074/jbc.M110.144097>
- [91] K. Kowalczyk, M. Stryjecka-Zimmer, *Ann. Univ. Mariae Curie-Skłodowska Sect D Med.* **2002**, 57(2), 160. <https://europepmc.org/article/med/12898834>
- [92] M. He, R. C. M. Siow, D. Sugden, L. Gao, X. Cheng, G. E. Mann, *Nutr., Metab. Cardiovasc. Dis.* **2011**, 21(4), 277. <https://doi.org/10.1016/j.numecd.2009.12.008>
- [93] C. Tiefensee Ribeiro, J. Gasparotto, A. A. Teixeira, L. V. C. Portela, V. N. L. Flores, J. C. F. Moreira, D. P. Gelain, *J. Biochem.* **2018**, 163(6), 515. <https://doi.org/10.1093/jb/mvy013>
- [94] C. Piperi, C. Adamopoulos, G. Dalagiorgou, E. Diamanti-Kandarakis, A. G. Papavassiliou, *J. Clin. Endocrinol. Metab.* **2012**, 97(7), 2231. <https://doi.org/10.1210/jc.2011-3408>
- [95] R. Iurlaro, C. Muñoz-Pinedo, *FEBS J.* **2016**, 283(14), 2640. <https://doi.org/10.1111/febs.13598>
- [96] G. Rong, X. Tang, T. Guo, N. Duan, Y. Wang, L. Yang, J. Zhang, X. Liang, *J. Physiol. Biochem.* **2015**, 71(3), 455. <https://doi.org/10.1007/s13105-015-0424-x>
- [97] W. Prachasilchai, H. Sonoda, N. Yokota-Ikeda, K. Ito, T. Kudo, K. Imaizumi, M. Ikeda, *J. Pharmacol. Sci.* **2009**, 109(2), 311. <https://doi.org/10.1254/jphs.082725C>
- [98] T. Kumagai, M. Nangaku, I. Kojima, R. Nagai, J. R. Ingelfinger, T. Miyata, T. Fujita, R. Inagi, *Am. J. Physiol. Ren. Physiol.* **2009**, 296(4), F912. <https://doi.org/10.1152/ajprenal.90575.2008>
- [99] D. T. Loughlin, C. M. Artlett, *PLOS One* **2010**, 5(6), e11093. <https://doi.org/10.1371/journal.pone.0011093>
- [100] C. Adamopoulos, E. Farmaki, E. Spilioti, H. Kiaris, C. Piperi, A. G. Papavassiliou, *Clin. Chem. Lab. Med.* **2014**, 52(1), 151. <https://doi.org/10.1515/cclm-2012-0826>
- [101] C. K. Chiang, C. C. Wang, T. F. Lu, K. H. Huang, M. L. Sheu, S. H. Liu, K. Y. Hung, *Sci. Rep.* **2016**, 6, 34167. <https://doi.org/10.1038/srep34167>
- [102] S. Y. Ko, H. A. Ko, K. H. Chu, T. M. Shieh, T. C. Chi, H. I. Chen, W. C. Chang, S. S. Chang, *PLOS One* **2015**, 10(11), e0143345. <https://doi.org/10.1371/journal.pone.0143345>
- [103] R. Luo, Y. Song, Z. Liao, H. Yin, S. Zhan, K. Wang, S. Li, G. Li, L. Ma, S. Lu, Y. Zhang, C. Yang, *FEBS J.* **2019**, 286(21), 4356. <https://doi.org/10.1111/febs.14972>
- [104] L. Shi, X. Yu, H. Yang, X. Wu, *PLOS One* **2013**, 8(6), e66781. <https://doi.org/10.1371/journal.pone.0066781>
- [105] X. Wang, S. Yu, C. Y. Wang, Y. Wang, H. X. Liu, Y. Cui, L. D. Zhang, *Vitr. Cell Dev. Biol.- Anim.* **2014**, 51(2), 204. <https://doi.org/10.1007/s11626-014-9823-5>
- [106] M. C. Lo, M. H. Chen, W. S. Lee, C. I. Lu, C. R. Chang, S. H. Kao, H. M. Lee, *Am. J. Physiol.-Endocrinol. Metab.* **2015**, 309(10), 829. <https://doi.org/10.1152/ajpendo.00151.2015>
- [107] M. B. Nelson, A. C. Swensen, D. R. Winden, J. S. Bodine, B. T. Bikman, P. R. Reynolds, *Am. J. Physiol.- Hear Circ. Physiol.* **2015**, 309(1), H63. <https://doi.org/10.1152/ajpheart.00043.2015>
- [108] Y. Li, Y. Chang, N. Ye, Y. Chen, N. Zhang, Y. Sun, *Mol. Med. Rep.* **2017**, 15(5), 2673. <https://doi.org/10.3892/mmr.2017.6314>
- [109] Y. X. Mao, W. J. Cai, X. Y. Sun, P. P. Dai, X. M. Li, Q. Wang, X. L. Huang, B. He, P. P. Wang, G. Wu, J. F. Ma, S. B. Huang, *Cell Death Dis.* **2018**, 9(6), 674. <https://doi.org/10.1038/s41419-018-0718-3>
- [110] L. Massaccesi, B. Bonomelli, M. G. Marazzi, L. Drago, M. M. C. Romanelli, D. Erba, N. Papini, A. Barassi, G. Goi, E. Galliera, *Dis. Markers* **2017**, 2017, 1. <https://doi.org/10.1155/2017/6140896>
- [111] N. Feldman, A. Rotter-Maskowitz, E. Okun, *Ageing Res. Rev.* **2015**, 24(Pt A), 29. <https://doi.org/10.1016/j.arr.2015.01.003>
- [112] J. Zindel, P. Kubes, *Annu. Rev. Pathol.: Mech. Dis.* **2020**, 15(1), 493. <https://doi.org/10.1146/annurev-pathmechdis-012419-032847>
- [113] W. Yu, M. Tao, Y. Zhao, X. Hu, M. Wang, *Molecules* **2018**, 23(6), 1447. <https://doi.org/10.3390/molecules23061447>
- [114] R. Banarjee, A. Sharma, S. Bai, A. Deshmukh, M. Kulkarni, *J. Proteomics* **2018**, 187, 69. <https://doi.org/10.1016/j.jprot.2018.06.009>

- [115] R. Hu, M. Wang, S. Ni, M. Wang, L. Y. Liu, H. Y. You, X. H. Wu, Y. J. Wang, L. Lu, L. B. Wei, *Eur. J. Pharmacol.* **2020**, *867*, 172797. <https://doi.org/10.1016/j.ejphar.2019.172797>
- [116] M. S. Hayden, S. Ghosh, *Cell* **2008**, *132*(3), 344. <https://doi.org/10.1016/j.cell.2008.01.020>
- [117] X. Lv, G. H. Lv, G. Y. Dai, H. M. Sun, H. Q. Xu, *Chin. J. Nat. Med.* **2016**, *14*(11), 844. [https://doi.org/10.1016/S1875-5364\(16\)30101-7](https://doi.org/10.1016/S1875-5364(16)30101-7)
- [118] D. Deluyker, V. Ferferieva, J. P. Noben, Q. Swennen, A. Bronckaers, I. Lambrechts, J. M. Rigo, V. Bito, *Int. J. Cardiol.* **2016**, *210*, 100. <https://doi.org/10.1016/j.ijcard.2016.02.095>
- [119] K. R. Bidasee, Y. Zhang, C. H. Shao, M. Wang, K. P. Patel, U. D. Dincer, H. R. Besch Jr, *Diabetes* **2004**, *53*(2), 463. <https://diabetes.diabetesjournals.org/content/53/2/463.short>
- [120] S.-I. Yamagishi, T. Matsui, *Ann. Vasc. Dis.* **2018**, *11*(3), 1. <https://doi.org/10.3400/avd.ra.18-00070>
- [121] S. L. Fishman, H. Sonmez, C. Basman, V. Singh, L. Poretsky, *Mol. Med.* **2018**, *24*(1), 59. <https://doi.org/10.1186/s10020-018-0060-3>
- [122] M. Kosmopoulos, D. Drekolias, P. D. Zavras, C. Piperi, A. G. Papavassiliou, *Biochim. Biophys. Acta, Mol. Basis Dis.* **2019**, *1865*(3), 611. <https://doi.org/10.1016/j.bbadis.2019.01.006>
- [123] W. N. Sayej, P. R. Knight III, W. A. Guo, B. Mullan, P. J. Ohtake, B. A. Davidson, A. Khan, R. D. Baker, S. S. Baker, *BioMed Res. Int.* **2016**, *2016*, 1. <https://doi.org/10.1155/2016/7867852>
- [124] J. Wang, H. Liu, G. Xie, W. Cai, J. Xu, *Mol. Med. Rep.* **2020**, *21*(2), 685. <https://doi.org/10.3892/mmr.2019.10872>
- [125] E. Yagmur, F. Tacke, C. Weiss, B. Lahme, M. P. Manns, P. Kiefer, C. Trautwein, A. M. Gressner, *Clin. Biochem.* **2006**, *39*(1), 39. <https://doi.org/10.1016/j.clinbiochem.2005.07.016>
- [126] Y. L. He, J. Q. Zhu, Y. Q. Huang, H. Gao, Y. R. Zhao, *Acta Diabetol.* **2015**, *52*(5), 959. <https://doi.org/10.1007/s00592-015-0763-7>
- [127] K. Hiwatashi, S. Ueno, K. Abeyama, F. Kubo, M. Sakoda, I. Maruyama, M. Hamanoue, S. Natsugoe, T. Aikou, *Ann. Surg. Oncol.* **2008**, *15*(3), 923. <https://doi.org/10.1245/s10434-007-9698-8>
- [128] Y. Yang, L. H. Zhao, B. Huang, R. Y. Wang, S. X. Yuan, Q. F. Tao, Y. Xu, H. Y. Sun, C. Lin, W. P. Zhou, *Mol. Carcinog.* **2015**, *54*(12), 1584. <https://doi.org/10.1002/mc.22231>
- [129] X. Zhou, B. Wang, L. Zhu, S. Hao, *Organogenesis* **2012**, *8*(1), 18. <https://doi.org/10.4161/org.19332>
- [130] S. Arsov, R. Graaff, W. Van Oeveren, B. Stegmayr, A. Sikole, G. Rakhorst, A. J. Smit, *Chem. Lab. Med.* **2014**, *52*(1), 11. <https://doi.org/10.1515/cclm-2012-0832>
- [131] A. E. M. Stinghen, Z. A. Massy, H. Vlassara, G. E. Striker, A. Boullier, *J. Am. Soc. Nephrol.* **2016**, *27*(2), 354. <https://doi.org/10.1681/ASN.2014101047>
- [132] A. Dimitropoulos, C. J. Rosado, M. C. Thomas, *J. Nephrol.* **2020**, *33*, 909. <https://doi.org/10.1007/s40620-020-00718-z>
- [133] R. Nishad, P. Meshram, A. K. Singh, G. B. Reddy, A. K. Pasupulati, *BMJ Open Diabetes Res. Care* **2020**, *8*(1), e001203. <https://doi.org/10.1136/bmjdr-2020-001203>
- [134] B. Levine, D. J. Klionsky, *Dev. Cell* **2004**, *6*(4), 463. [https://doi.org/10.1016/S1534-5807\(04\)00099-1](https://doi.org/10.1016/S1534-5807(04)00099-1)
- [135] N. Mizushima, B. Levine, A. M. Cuervo, D. J. Klionsky, *Nature* **2008**, *451*(7182), 1069. <https://doi.org/10.1038/nature06639>
- [136] M. C. Maiuri, E. Zalckvar, A. Kimchi, G. Kroemer, *Nat. Rev. Mol. Cell Biol.* **2007**, *8*(9), 741. <https://doi.org/10.1038/nrm2239>
- [137] A. Bergmann, *Cell* **2007**, *131*(6), 1032. <https://doi.org/10.1016/j.cell.2007.11.027>
- [138] K. Mao, *Autophagy: Cancer, Other Pathologies, Inflammation, Immunity, Infection, and Aging*, 10, Academic Press, London, UK **2020**, 85.98 <https://doi.org/10.1016/B978-0-12-805421-5.00002-1>
- [139] V. Kirkin, V. V. Rogov, *Mol. Cell* **2019**, *76*(2), 268. <https://doi.org/10.1016/j.molcel.2019.09.005>
- [140] N. Martinez-Lopez, M. Garcia-Macia, S. Sahu, D. Athonvarangkul, E. Liebling, P. Merlo, F. Cecconi, G. J. Schwartz, R. Singh, *Cell Metab.* **2016**, *23*(1), 113. <https://doi.org/10.1016/j.cmet.2015.10.008>
- [141] A. Abdrakhmanov, V. Gogvadze, B. Zhivotovsky, *Trends Biochem. Sci.* **2020**, *45*(4), 347. <https://doi.org/10.1016/j.tibs.2019.11.006>
- [142] S. Kaushik, A. M. Cuervo, *Trends Cell Biol.* **2012**, *22*(8), 407. <https://doi.org/10.1016/j.tcb.2012.05.006>
- [143] Y. Fujiwara, H. Kikuchi, S. Aizawa, A. Furuta, Y. Hatanaka, C. Konya, K. Uchida, K. Wada, T. Kabuta, *Autophagy* **2013**, *9*(8), 1167. <https://doi.org/10.4161/auto.24880>
- [144] Y. Fujiwara, A. Furuta, H. Kikuchi, S. Aizawa, Y. Hatanaka, C. Konya, K. Uchida, A. Yoshimura, Y. Tamai, K. Wada, T. Kabuta, *Autophagy* **2013**, *9*(3), 403. <https://doi.org/10.4161/auto.23002>
- [145] S. Aizawa, V. R. Contu, Y. Fujiwara, K. Hase, H. Kikuchi, C. Kabuta, K. Wada, T. Kabuta, *Autophagy* **2017**, *13*(1), 218. <https://doi.org/10.1080/15548627.2016.1248019>
- [146] J. Gao, C. Yu, Q. Xiong, Y. Zhang, L. Wang, *Int. J. Clin. Exp. Pathol.* **2015**, *8*(12), 15622. <https://www.ncbi.nlm.nih.gov/pmc/articles/PMC4730044/>
- [147] W.-W. Li, J. Li, Bao Jin-Ku, *Springer.* **2012**, *69*(7), 1125-1136. <https://doi.org/10.1007/s00018-011-0865-5>
- [148] Z. Xie, D. J. Klionsky, *Nat. Cell Biol.* **2007**, *9*(10), 1102. <https://doi.org/10.1038/ncb1007-1102>
- [149] S. Kimura, T. Noda, T. Yoshimori, *Autophagy* **2007**, *3*(5), 452. <https://doi.org/10.4161/auto.4451>
- [150] S. Jager, *J. Cell Sci.* **2004**, *117*(20), 4837. <https://doi.org/10.1242/jcs.01370>
- [151] P. Lőrincz, G. Juhász, *J. Mol. Biol.* **2020**, *432*(8), 2462. <https://www.sciencedirect.com/science/article/pii/S0022283619306242>
- [152] P. Boya, *Antioxid. Redox Signal.* **2012**, *17*(5), 766. <https://doi.org/10.1089/ars.2011.4405>
- [153] H. L. Hayes, B. S. Peterson, J. M. Haldeman, C. B. Newgard, H. E. Hohmeier, S. B. Stephens, *PLOS One* **2017**, *12*(2), e0172567. <https://doi.org/10.1371/journal.pone.0172567>
- [154] H. S. Jung, K. W. Chung, J. Won Kim, J. Kim, M. Komatsu, K. Tanaka, Y. H. Nguyen, T. M. Kang, K. H. Yoon, J. W. Kim, Y. T. Jeong, M. S. Han, M. K. Lee, K. W. Kim, J. Shin, M. S. Lee, *Cell Metab.* **2008**, *8*(4), 318. <https://doi.org/10.1016/j.cmet.2008.08.013>
- [155] M. Rocha, N. Apostolova, R. Diaz-Rua, J. Muntane, V. M. Victor, *Trends Endocrinol. Metab.* **2020**, *31*, 725. <https://doi.org/10.1016/j.tem.2020.03.004>
- [156] S. Morita, S. Sakagashira, Y. Shimajiri, N. L. Eberhardt, T. Kondo, T. Kondo, T. Sanke, *J. Diabetes Investig.* **2011**, *2*(1), 48. <https://doi.org/10.1111/j.2040-1124.2010.00065.x>
- [157] P. Grumati, L. Coletto, A. Schiavinato, S. Castagnaro, E. Bertaggia, M. Sandri, P. Bonaldo, *Autophagy* **2011**, *7*(12), 1415. <https://doi.org/10.4161/auto.7.12.17877>
- [158] C. He, M. C. Bassik, V. Moresi, K. Sun, Y. Wei, Z. Zou, Z. An, J. Loh, J. Fisher, Q. Sun, S. Korsmeyer, M. Packer, H. I. May, J. A. Hill, H. W. Virgin, C. Gilpin, G. Xiao, R. Bassel-Duby, P. E. Scherer, B. Levine, *Nature* **2012**, *481*(7382), 511. <https://doi.org/10.1038/nature10758>
- [159] J. Kosacka, M. Kern, N. Klötting, S. Paeschke, A. Rudich, Y. Haim, M. Gericke, H. Serke, M. Stumvoll, I. Bechmann, M. Nowicki, M. Blüher, *Mol. Cell. Endocrinol.* **2015**, *409*, 21. <https://doi.org/10.1016/j.mce.2015.03.015>
- [160] Y. Zhang, X. Zeng, S. Jin, *Pharmacol. Res.* **2012**, *66*(6), 505. <https://doi.org/10.1016/j.phrs.2012.09.004>
- [161] R. Baerga, Y. Zhang, P. H. Chen, S. Goldman, S. Jin, *Autophagy* **2009**, *5*(8), 1118. <https://doi.org/10.4161/auto.5.8.9991>
- [162] S. Rowan, E. Bejarano, A. Taylor, *Biochim. Biophys. Acta, Mol. Basis Dis.* **2018**, *1864*(12), 3631. <https://doi.org/10.1016/j.bbadis.2018.08.036>

- [163] Y. Guo, C. Lin, P. Xu, S. Wu, X. Fu, W. Xia, M. Yao, *Sci. Rep.* **2016**, *6*, 36416. <https://doi.org/10.1038/srep36416>
- [164] Y. Han, T. Sun, R. Tao, Y. Han, J. Liu, *Eur. J. Med. Res.* **2017**, *22*(1), 11. <https://doi.org/10.1186/s40001-017-0253-1>
- [165] H. Zhang, S. Ge, K. He, X. Zhao, Y. Wu, Y. Shao, X. Wu, *Cardiovasc. Res.* **2019**, *115*(14), 2008. <https://doi.org/10.1093/cvr/cvz014>
- [166] W. Huang, P. Ao, J. Li, T. Wu, L. Xu, Z. Deng, W. Chen, C. Yin, X. Cheng, *Biomed Res. Int.* **2017**, *2017*, 6341919. <https://doi.org/10.1155/2017/6341919>
- [167] L. Xu, K. Xu, Z. Wu, Z. Chen, Y. He, C. Ma, S. A. A. Moqbel, J. Ran, C. Zhang, L. Wu, Y. Xiong, *J. Cell. Mol. Med.* **2020**, *24*(3), 2240. <https://doi.org/10.1111/jcmm.14901>
- [168] L. Yang, H. Meng, M. Yang, *J. Mol. Endocrinol.* **2016**, *56*(4), 291. <https://doi.org/10.1530/JME-15-0267>
- [169] G. Di Emidio, M. Placidi, F. Rea, G. Rossi, S. Falone, L. Cristiano, S. Nottola, A. M. D'Alessandro, F. Amicarelli, M. G. Palmerini, C. Tatone, *Cells* **2020**, *9*(1), 209. <https://doi.org/10.3390/cells9010209>
- [170] A. L. Dafre, A. E. Schmitz, P. Maherb, *Free Radic. Biol. Med.* **2020**, *108*, 270. <https://www.sciencedirect.com/science/article/pii/S0891584917301788>
- [171] R. Yang, Y. Zhu, Y. Wang, W. Ma, X. Han, X. Wang, N. Liu, *Biochem. Biophys. Res. Commun.* **2019**, *517*(3), 470. <https://www.sciencedirect.com/science/article/pii/S0006291X19314688>
- [172] T. Takata, A. Sakasai-Sakai, T. Ueda, M. Takeuchi, *Sci. Rep.* **2019**, *9*(1), 1. <https://doi.org/10.1038/s41598-019-39202-5>
- [173] Y. M. Mei, L. Li, X. Q. Wang, M. Zhang, L. F. Zhu, Y. W. Fu, Y. Xu, *J. Cell. Biochem.* **2020**, *121*(8-9), 3764. <https://doi.org/10.1002/jcb.29499>
- [174] N. Verma, S. K. Manna, *J. Biol. Chem.* **2015**, *291*(3), P1481. <https://doi.org/10.1074/jbc.M115.667576>
- [175] M. Shi, S. Yang, X. Zhu, D. Sun, D. Sun, X. Jiang, C. Zhang, L. Wang, *Cell. Signal.* **2019**, *62*, 109334. <https://doi.org/10.1016/j.cellsig.2019.05.019>
- [176] M. Dang, X. Zeng, B. Chen, H. Wang, H. Li, Y. Liu, X. Zhang, X. Cao, F. Du, C. Guo, *Free Radic. Biol. Med.* **2019**, *130*, 107. <https://doi.org/10.1016/j.freeradbiomed.2018.10.437>
- [177] E. A. Guzmán, T. P. Pitts, M. C. Diaz, A. E. Wright, *Invest. New Drugs* **2019**, *37*(2), 262. <https://doi.org/10.1007/s10637-018-0635-4>
- [178] Y. Liu, J. Li, Y. Han, Y. Chen, L. Liu, J. Lang, C. Yang, H. Luo, J. Ning, *Mol. Cell. Biochem.* **2020**, *471*(1-2), 91. <https://doi.org/10.1007/s11010-020-03769-9>
- [179] B. N. Waghela, F. U. Vaidya, K. Ranjan, A. S. Chhipa, B. S. Tiwari, C. Pathak, *Mol. Cell. Biochem.* **2020**, *1*<https://doi.org/10.1007/s11010-020-03928-y>
- [180] G. Zhao, X. Zhang, H. Wang, Z. Chen, *Ann. Transl. Med.* **2020**, *8*(10), 647. <https://doi.org/10.21037/atm-20-3768>
- [181] X. Xie, C. Yang, C. Duan, H. Chen, T. Zeng, S. Huang, H. Li, M. Ren, W. J. Lin, L. Yan, *Eur. J. Immunol.* **2020**, *50*(8), 1174. <https://doi.org/10.1002/eji.201948477>
- [182] T. Laughlin, Y. Tan, B. Jarrold, J. Chen, L. Li, B. Fang, W. Zhao, M. Tamura, A. Matsubara, G. Deng, X. Wang, T. Hakozaiki, *J. Eur. Acad. Dermatol. Venereol.* **2020**, *34*(S3), 12. <https://doi.org/10.1111/jdv.16453>
- [183] Y. H. Li, W. L. Zhang, H. Y. Zhou, D. W. Yu, X. N. Sun, Q. Hu, *Mol. Med. Rep.* **2019**, *20*(4), 3131. <https://doi.org/10.3892/mmr.2019.10554>
- [184] L. Xu, Q. Fan, X. Wang, X. Zhao, L. Wang, *Cell Death Dis.* **2016**, *7*(11), e2445. <https://doi.org/10.1038/cddis.2016.322>
- [185] X. Zhao, Y. Chen, X. Tan, L. Zhang, H. Zhang, Z. Li, S. Liu, R. Li, T. Lin, R. Liao, Q. Zhang, W. Dong, W. Shi, X. Liang, *J. Pathol.* **2018**, *245*(2), 235. <https://doi.org/10.1002/path.5077>
- [186] Z. J. Wang, H.B.in Zhang, C. Chen, H. Huang, J. X. Liang, *Cell Biol. Int.* **2018**, *42*(7), 841. <https://doi.org/10.1002/cbin.10951>
- [187] Y. Li, Y. Chang, N. Ye, D. Dai, Y. Chen, N. Zhang, G. Sun, Y. Sun, *Int. J. Mol. Sci.* **2017**, *18*(2), 436. <https://doi.org/10.3390/ijms18020436>
- [188] N. Verma, S. K. Manna, *J. Cell. Physiol.* **2017**, *232*(12), 3598. <https://doi.org/10.1002/jcp.25828>
- [189] W. Martinet, G. R. Y. De Meyer, *Circ. Res.* **2009**, *104*(3), 304. <https://doi.org/10.1161/CIRCRESAHA.108.188318>
- [190] H. Liu, Y. Cao, T. Tong, J. Shi, Y. Zhang, Y. Yang, C. Liu, *Chin. Med. J. (Engl)*. **2015**, *128*(1), 69. <https://doi.org/10.4103/0366-6999.147815>
- [191] M. Xie, Y. Kong, W. Tan, H. May, P. K. Battiprolu, Z. Pedrozo, Z. V. Wang, C. Morales, X. Luo, G. Cho, N. Jiang, M. E. Jessen, J. J. Warner, S. Lavandero, T. G. Gillette, A. T. Turer, J. A. Hill, *Circulation* **2014**, *129*(10), 1139. <https://doi.org/10.1161/CIRCULATIONAHA.113.002416>
- [192] V. L. Bodiga, S. R. Eda, S. Bodiga, *Heart. Fail. Rev.* **2014**, *19*(1), 49. <https://doi.org/10.1007/s10741-013-9374-y>
- [193] P. Yu, Y. Zhang, C. Li, Y. Li, S. Jiang, X. Zhang, Z. Ding, F. Tu, J. Wu, X. Gao, L. Li, *J. Cell. Mol. Med.* **2015**, *19*(7), 1710. <https://doi.org/10.1111/jcmm.12547>
- [194] X. Hou, Z. Hu, H. Xu, J. Xu, S. Zhang, Y. Zhong, X. He, N. Wang, *Cardiovasc. Diabetol.* **2014**, *13*(1), 78. <https://doi.org/10.1186/1475-2840-13-78>
- [195] W. Gao, Z. Zhou, B. Liang, Y. Huang, Z. Yang, Y. Chen, L. Zhang, C. Yan, J. Wang, L. Lu, Z. Wen, S. Xian, L. Wang, *Front. Physiol.* **2018**, *9*, 1333. <https://doi.org/10.3389/fphys.2018.01333>
- [196] H. Liu, S. Yu, H. Zhang, J. Xu, *PLoS One* **2012**, *7*(10), <https://doi.org/10.1371/journal.pone.0046720>
- [197] Y. Tanaka, S. Kume, M. Kitada, K. Kanasaki, T. Uzu, H. Maegawa, D. Koya, *Exp. Diabetes. Res.* **2012**, *2012*, 1. <https://doi.org/10.1155/2012/628978>
- [198] T. M. Osicka, Z. Kiriazis, L. M. Pratt, G. Jerums, W. D. Comper, *Diabetologia* **2001**, *44*(2), 230. <https://doi.org/10.1007/s001250051604>
- [199] P. Shechter, G. Boner, R. Rabkin, P. Shechter, P. Rabkin, *J. Am. Soc. Nephrol.* **1994**, *4*(8), 1582. <https://jasn.asnjournals.org/content/4/8/1582.short>

**How to cite this article:** Sruthi CR, Raghu KG. Advanced glycation end products and their adverse effects: The role of autophagy. *J Biochem Mol Toxicol.* 2021;e22710. <https://doi.org/10.1002/jbt.22710>